GEOCHEMISTRY OF HYDROTHERMAL VENT FLUIDS FROM THE NORTHERN JUAN DE FUCA RIDGE

by
Anna M. Cruse
B.S., University of Missouri–Columbia, 1994
M.S., University of Missouri–Columbia, 1997

Submitted in partial fulfillment of the requirements for the degree of

Doctor of Philosophy

at the

MASSACHUSETTS INSTITUTE OF TECHNOLOGY

and the

WOODS HOLE OCEANOGRAPHIC INSTITUTION

February, 2003

Signature of Author

_____

Joint Program in Oceanography/Applied Ocean Science and Engineering
Massachusetts Institute of Technology
and Woods Hole Oceanographic Institution
February, 2003

Certified by

_____

Jeffrey S. Seewald
Thesis Supervisor

Accepted by

_____

Philip M. Gschwend
Chair, Joint Committee for Chemical Oceanography
Woods Hole Oceanographic Institution

GEOCHEMISTRY OF HYDROTHERMAL VENT FLUIDS FROM THE NORTHERN JUAN DE FUCA RIDGE

by

Anna M. Cruse

Submitted on November 12, 2002, in partial fulfillment of the requirements for the degree of Doctor of Philosophy at the Massachusetts Institute of Technology and the Woods Hole Oceanographic Institution

ABSTRACT

The presence of aqueous organic compounds derived from sedimentary organic matter has the potential to influence a range of chemical processes in hydrothermal vent environments. For example, hydrothermal alteration experiments indicate that alteration of organic-rich sediments leads to up to an order of magnitude more metals in solution than alteration of organic-poor basalt. This result is in contrast to traditional models for the evolution of vent fluids at sediment-covered mid-ocean ridge axis environments, and indicates the fundamental importance of including the effects of organic compounds in models of crustal alteration processes. However, in order to rigorously constrain their role in crustal alteration processes, quantitative information on the abundances and distributions of organic compounds in hydrothermal vent fluids is required. This thesis was undertaken to provide quantitative information on the distributions and stable carbon isotopic compositions of several low-molecular weight organic compounds (C_1-C_4 alkanes, C_2-C_3 alkenes, benzene and toluene) in fluids collected in July, 2000, at three sites on the northern Juan de Fuca Ridge: the Dead Dog and ODP Mound fields, which are located at Middle Valley, and the Main Endeavour Field, located on the Endeavour segment.

At Middle Valley, the ridge axis is covered by up to 1.5 km of hemipelagic sediment containing up to 0.5 wt. % organic carbon. The Main Endeavour Field (MEF) is located approximately 70 km south of Middle Valley in a sediment-free ridge-crest environment, but previously measured high concentrations of NH_3 and isotopically light CH_4 relative to other bare-rock sites suggest that the chemical composition of these fluids is affected by sub-seafloor alteration of sedimentary material (LILLEY et al., 1993). Differences in the absolute and relative concentrations of NH_3 and organic compounds and the stable carbon isotopic compositions of the C_1-C_3 organic compounds suggest that the three fields represent a continuum in terms of the extent of secondary alteration of the aqueous organic compounds, with the Dead Dog fluids the least altered, the MEF fluids the most altered and ODP Mound fluids in an intermediate state. At the two Middle Valley sites, the greater extent of alteration in the ODP Mound fluids as compared to the Dead Dog fluids is due either to higher temperatures in the subsurface reaction zone, or a greater residence time of the fluids at high temperatures. Higher reaction zone

temperatures at the ODP Mound field than at the Dead Dog field are consistent with differences in endmember Cl concentrations between the two fields. The greater extent of alteration in the MEF fluids is caused by relatively oxidizing conditions in the subsurface reaction zone that promote faster reaction kinetics.

Temperatures in the subsurface reaction zones calculated by assuming equilibrium among aqueous alkanes, alkenes and hydrogen are consistent with other inorganic indicators (Cl and Si concentrations) of temperature, indicating that metastable equilibrium among these compounds may be attained in natural systems. Isotopic equilibration among CH_4 and CO_2 appears to have been attained in ODP Mound fluids due to the high temperatures in the subsurface reaction zone and the approach to chemical equilibrium from excess methane. However, isotopic equilibrium between CH_4 and CO_2 was not attained in the MEF fluids, due to a short residence time of the fluids in the crust following late-stage addition of magmatic-derived CO_2 to the fluids.

Time series analysis indicate that Middle Valley fluid compositions are generally characterized by stable concentrations over the last decade. However, decreases in Br concentrations in Dead Dog fluids from 1990 to 2000 suggest that either a greater proportion of the fluids interact with basalt rather than sediments or that the sediment with which hydrothermal fluids interact is becoming exhausted. In contrast, the concentrations of H_2 and H_2S and the $\delta^{34}S$ of H_2S are quite different in fluids sampled from vents of differing ages at the ODP Mound field, despite their close spatial proximity. The observed variations are caused by the reaction of hydrogen-rich fluids within the ODP Mound massive sulfide to reduce pyrite to pyrrhotite during upflow. The replacement of pyrite by pyrrhotite is opposite to the reaction predicted during the weathering of sulfide minerals weather on the seafloor and reflects the real-time equilibration of the reduced fluids with mound mineralogy due to the very young age (< 2 years) venting from Spire vent. The presence of aqueous organic compounds therefore affects not only the inorganic chemical speciation in vent fluids, but can also control the mineralogy of associated sulfide deposits. These results also indicate that vent fluid compositions do not necessarily reflect conditions in the deep subsurface, but can be altered by reactions occurring in the shallow subsurface

REFERENCES

LILLEY M. D., BUTTERFIELD D. A., OLSON E. J., LUPTON J. E., MACKO S. A., and MCDUFF R. E. (1993) Anomalous CH_4 and NH_4^+ concentrations at an unsedimented mid-ocean-ridge hydrothermal system. *Nature* **364**(6432), 45-47.

ACKNOWLEDGEMENTS

I would like to first thank my advisor, Jeff Seewald, for introducing me to the field of hydrothermal vent research. When I first sent in my application to the Joint Program, little did I know that my doctoral research would take me to the bottom of the ocean in *DSV Alvin*. As an advisor, Jeff was able to strike the perfect balance between knowing when to let me run with an idea, and knowing when to step in and save me from myself. I have benefited immeasurably from his expectations and high scientific ideals, and thank him for his support and guidance. I would also like to thank my committee, Meg Tivey, Tim Eglinton and Tina Voelker, for their support. Each of them brought a unique scientific perspective to this research, and this thesis has benefited greatly from their insights. I would also like to thank Meg in particular for being a wonderful role model as to how one actually balances the demands of scientific and family life–and for being right about the timing of key events in January, 1999. Thank you to Lary Ball for his assistance with the ICP-MS and to Leah Houghton and Carl Johnson for their assistance with the IRM-GCMS analysis. I would also like to thank Robert Zierenberg, of the University of California at Davis, for assistance with the sulfur isotope measurements and for the insightful discussions of the Middle Valley system.

I would also like to acknowledge the captain and crew of the *R/V Atlantis* and the pilots of *DSV Alvin*. Their efforts and expertise combined to provide us with a highly successful cruise in July, 2000. Tom McCollom, Peter Saccocia, Karen Hurley, Hallie Marbet and Dane Percy provided invaluable assistance in the collection and processing of the fluid samples at sea.

Thank you to my family and friends for all of their support. Ann Pearson, Liz Kujawinski, Ana Lima, Carrie Tuit and Tracy Quan all provided shoulders, advice and humor at the critical times. A special thank you goes to Tim Lyons, my master's advisor at the University of Missouri, for first helping me start down this path, and for continuing to offer his friendship. I consider myself especially fortunate to have found a friend like Joanna Wilson to share the joys and trials of both our scientific careers and motherhood. She and her husband, Andrew McArthur, and their son, Galen, have been invaluable sources of support, love and joy. To my parents, thank you for all you have done this past year, for always pushing me to reach any goal, and for your example of how to live. Thank you to my brothers and sister for their love and support—and for not giving me *too* much grief for being in school for how many years.

Finally, everything I have achieved is a tribute to the unwavering love and support of my husband, Steve, and my daughter, Maia. Thank you for your sacrifices, your understanding, your enthusiasm, and most important, the unbounded joy you bring into my life.

This research was supported by grants to Jeffrey Seewald from the Petroleum Research Fund (32310-AC2), administered by the American Chemical Society, the National Science Foundation (OCE-9618179, OCE-9906752, OCE-0136954) and the WHOI Green Technology Fund.

TABLE OF CONTENTS

LIST OF TABLES

LIST OF FIGURES

CHAPTER 1. INTRODUCTION

Convective circulation of seawater through the oceanic crust at mid-ocean ridges is a major mechanism by which heat and material is transferred from the interior of the Earth. During convection at mid-ocean ridges, seawater is heated and reacts with basaltic rocks and overlying sediments, if present, resulting in a fluid that is hot, acidic, reducing, enriched in the alkali and alkaline earth metals and transition metals, depleted in SO_4 and Mg, and either enriched or depleted in Cl, compared to the original seawater (EDMOND et al., 1979; VON DAMM, 1995). In the twenty-five years since the first report of the chemical composition of hydrothermal vent fluids sampled at the Galapagos Ridge (CORLISS et al., 1979), the concentrations of over 30 different chemical species have been analyzed in fluids from over 40 locations around the globe have been measured (e.g., BOTZ et al., 1999; BUTTERFIELD, 2000; KELLEY et al., 2001; VON DAMM, 1995). In comparison to the inorganic compounds, measurements of aqueous low molecular weight aqueous hydrocarbons has been very few, and predominantly confined to methane (Table 1-1). Other efforts at the quantitation of aqueous organic compounds, many of which are volatile or semi-volatile, have been hampered by the use of non-gas tight fluid samplers (e.g., WELHAN and LUPTON, 1987). Also, investigations of the altered sediments from environments such as Middle Valley and Guaymas Basin, Gulf of California, indicate that thermal maturation of organic matter results in the generation of number organic compounds such as C_{6+} *n*-alkanes, alkenones, aromatic and polyaromatic hydrocarbons, biomarker compounds and organic acids that may be transported in solution (KAWKA and SIMONEIT, 1990; KVENVOLDEN et al., 1990; KVENVOLDEN et al., 1986; RUSHDI and SIMONEIT, 2002; SIMONEIT, 1984, 1993; SIMONEIT, 1994; SIMONEIT et al., 1990; SIMONEIT and GALIMOV, 1984; SIMONEIT et al., 1992; SIMONEIT et al., 1988; SIMONEIT and KVENVOLDEN, 1994; SIMONEIT et al., 1994; WHELAN et al., 1988).

Organic compounds can play a key role in subsurface processes. For example, Crossy et al. (1984) have demonstrated that the generation of organic acids is key in the development of secondary porosity in aquifers. The presence of organic compounds in

hot fluids may play a key role in the formation of some economic-grade ore deposits (DISNAR and SUREAU, 1990, and references therein). Organic compounds present in hydrothermal vent fluids represent important energy sources for both the surface-dwelling vent fauna as well as for any subsurface microbial communities that might exist (SUMMIT and BAROSS, 2001).

An underlying goal in the study of hydrothermal vent fluids is to understand the conditions under which crustal alteration processes occur in subsurface environments that cannot be directly observed. Inorganic compounds such as Cl or Si have often been utilized as geochemical indicators of subsurface reaction conditions. Aqueous organic species also respond systematically to environmental variables and key reactions that can control their abundances have been identified in laboratory experiments. However, the lack of fundamental data on the abundance of many organic compounds in hydrothermal vent fluids precludes the assessment of the mechanisms that control their abundances in nature, and therefore, the role that they may play in crustal alteration processes, transport of transition metals, ore deposit formation, and the maintenance of subsurface microbial populations.

In this thesis, the first step toward addressing such issues has been taken by quantifying the concentration and isotopic composition of several organic compounds in vent fluids collected from two vent sites on the northern Juan de Fuca Ridge: Middle Valley and the Main Endeavour field (MEF; Fig. 1-1). At Middle Valley, the ridge axis is covered by up to 1.5 kilometers of hemipelagic and turbiditic sediment (GOODFELLOW and BLAISE, 1988) that represents a source of organic compounds to the vent fluids. In contrast, the MEF is located on sediment-free basaltic rocks (DELANEY et al., 1992). However, previous measurements of methane and ammonia concentrations, and the stable carbon and nitrogen compositions of these compounds, suggest that fluids at the MEF do interact with a sediment source that as yet remains unconstrained in terms of both its location and composition (LILLEY et al., 1993). These two sites vary in terms of physical conditions such as temperature and pressure, as well as the relative amounts of basalt versus sediment interaction with circulating hydrothermal fluids, providing an

ideal setting to compare and contrast different mechanisms by which organic compounds react in mid-ocean ridge settings.

1.1. Hydrothermal Circulation Processes

Hydrothermal vents are a pervasive phenomenon associated with the generation of new oceanic crust at mid-ocean ridges. After formation, the crust cools as it moves away from the ridge axis. Cracks that form during cooling allow seawater to percolate into the crust resulting in the development of hydrothermal circulation systems. Hydrothermal circulation can be divided into three zones: recharge, reaction zone and discharge (ALT, 1995; Fig. 1-2), during which different characteristic chemical reactions occur. The following discussion has been taken largely from Alt (1995).

During recharge, large volumes of seawater percolate downward through the porous and permeable volcanic upper section, with only a small portion entering the underlying sheeted dikes. During the initial stages of circulation, low-temperature oxidation and fixation of the alkali metals from result in the formation of various alteration minerals such as celadonite, smectite, and Fe-oxyhyroxides. Reaction of seawater with the crust at temperatures as low as 50° causes the near quantitative removal of Mg from seawater, which, together with OH^-, precipitates as smectite and chlorite (BISCHOFF and DICKSON, 1975; MOTTL and HOLLAND, 1978; SEYFRIED and BISCHOFF, 1981b). This results in the dramatic pH shift of the fluid from ~8 in seawater to values typically between 3 and 5.5 (as measured at 25°C) in hydrothermal fluids. Fixation of Mg in the crust also releases Ca to solution (SEYFRIED and BISCHOFF, 1979, 1981a). Increased concentrations of Ca, combined with the retrograde solubility of anhydrite, results in the removal of virtually all of the sulfate from seawater as anhydrite precipitates from heated fluids during recharge (SEYFRIED, 1987). At this point, the initially cool, alkaline and oxidizing seawater has become a hot, acidic and reduced fluid.

In subsurface "reaction zones", which are traditionally envisioned as the hottest portions of the hydrothermal system, the acidic, reducing fluids interact with basalt at temperatures above ~350°C (Fig. 1-2). This results in the leaching of transition metals, sulfur and a host of other elements (alkali metals, alkaline earths, Si) from the basalt.

Volatile compounds such as CO_2, and ^3He can also be gained by the fluid from magma degassing in the deepest portion of the hydrothermal circulation cell. Precipitation of the leached metals and sulfur as sulfide minerals in response to the large contrast in temperature and acidity between hydrothermal fluids and seawater forms the smoke observed at high-temperature vents.

As the hydrothermal fluid is heated, it undergoes dramatic changes in its physical properties: the dielectric constant and density decrease, the coefficient of thermal expansion and heat capacity reach maxima and viscosity reaches a minimum as the temperature and pressure conditions approach the critical point for seawater (NORTON, 1984). These combine to provide maximum buoyancy forces, and the hydrothermal fluid rises to the seafloor. During upflow, quartz and epidote minerals may be deposited, resulting in a loss of Si and Ca from the fluid. The hydrothermal fluids can also entrain cooler seawater in the upper portions of the crust, which cools the hydrothermal fluid and results in the deposition of metal sulfides in the subsurface rather than at the seafloor.

1.2. PROCESSES OF ORGANIC MATTER ALTERATION

In traditional models for organic matter maturation in sedimentary basins, the generation of organic species and their resulting isotopic composition are controlled entirely by kinetic factors such as the composition of the initial products, residence time of products in the source region, and relative rates of competing production and consumption reactions (ABBOTT et al., 1985; BERNER et al., 1995; HUNT, 1996; LEWAN, 1983; LORANT et al., 1998; TISSOT and WELTE, 1984). In these models, geologic time and temperature can be regarded as interchangeable variables (CONNAN, 1974; HUNT, 1996; TISSOT and WELTE, 1984), although others have challenged this assumption (PRICE, 1983, 1985, 1993). In traditional models for the alteration of longer-chained hydrocarbons, degradation is hypothesized to occur via thermal cracking (HUNT, 1996; TISSOT and WELTE, 1984; WAPLES, 1984). Thermal cracking refers to the homolytic cleavage of C-C bonds caused by greater bond vibration frequencies in response to increasing temperature. A greater extent of alteration of organic compounds by this

mechanism will also be favored by longer reaction times at a given temperature since longer times will increase the possibility of bond cleavage.

Recent theoretical work suggests that metastable thermodynamic equilibrium among organic compounds, inorganic minerals and water may regulate the abundances of compounds such as carbon dioxide, hydrocarbons and organic acids (HELGESON et al., 1993; SHOCK, 1988, 1990). Of the myriad laboratory experiments that have attempted to constrain the stability of organic compounds at elevated temperatures and pressures, many have not been conducted in such a way that key variables such as pH or redox conditions have been measured or buffered, or under geologically realistic conditions (ELLIOT et al., 1994; KATRITZKY et al., 1990; SISKIN and KATRITZKY, 1991). In experiments conducted with water and inorganic minerals at temperatures and pressures that are attained within the crust, Seewald (1994; 1997) demonstrated that alkanes and alkenes rapidly reacted readily so as to attain concentrations in equilibrium with dissolved H_2 at the temperature and pressure of the system. Similarly, McCollom et al. (2001) demonstrated the attainment of thermodynamic equilibrium among species where the reactions involved the breaking of C-C bonds in an experimental investigation of the thermal stability of monocyclic aromatic compounds. In these studies, the rate at which equilibrium was attained was a function of the redox state within the system, which was controlled by the mineral buffers that were used. As an alternative to thermal cracking reactions, Seewald (2001) has developed a model whereby the distributions of aqueous low molecular weight hydrocarbons are controlled by a stepwise oxidation reaction mechanism in which alkanes undergo oxidation and hydration reactions with alkenes, alcohols, ketones and organic acids produced as reaction intermediaries. The participation of H_2O and mineral-derived H_2 as reactants within this scheme point to the likely pervasive interactions between organic and inorganic constituents that should not be neglected in models of crustal alteration in hydrothermal environments.

1.3. ORGANIZATION OF THIS THESIS

The results from this thesis are organized into four chapters that describe the effects of organic carbon on the mobilization of metals into high-temperature fluids,

compare and contrast the organic geochemistry of vent fluids from Middle Valley and the Main Endeavour field, and investigate the temporal variability of vent fluid compositions at Middle Valley.

Chapter 2. The role of organic matter in the mobilization of metals in high-temperature fluids.

Fluids from sediment-covered mid-ocean ridge hydrothermal systems are characterized by metal concentrations that are lower than those determined in fluids from bare-rock hydrothermal systems (Table 2-1). In early models of crustal alteration processes, this difference was attributed to the buffering of pH by different reactions during basalt versus sediment alteration (BOWERS et al., 1985; SCOTT, 1985; VON DAMM et al., 1985b). Chapter 2 presents experimental work comparing the results of hydrothermal alteration experiments utilizing basalt, organic-rich sediment from Guaymas Basin and organic-lean sediment from Middle Valley. These experiments demonstrated a trend opposite to that predicted from these early models: at a given temperature and pressure, alteration of organic-rich sediments released greater concentrations of metals to fluids as compared to organic-free basaltic rocks. Thermodynamic modeling indicated that this is due to the generation of acidity from calcite precipitation, which is caused by the release of CO_2 from organic matter and release of Ca from the formation of anorthite from albite. The overall reaction mechanism is:

$$2\,Na^+ + 4\,\underset{\text{quartz}}{SiO_2} + H_2CO_3 + \underset{\text{albite}}{CaAl_2Si_2O_8} = \underset{\text{calcite}}{CaCO_3} + 2\,\underset{\text{anorthite}}{NaAlSi_3O_8} + 2\,H^+ \qquad (1)$$

In contrast, the alteration of organic-free basaltic rocks Ca is fixed in hydrous alteration minerals such as epidote:

$$Na^+ + 2\,\underset{\text{albite}}{CaAl_2Si_2O_8} + 2\,\underset{\text{quartz}}{SiO_2} + H_2O = \underset{\text{anorthite}}{NaAlSi_3O_8} + \underset{\text{clinozoisite}}{Ca_2Al_3Si_3O_{12}(OH)} + H^+, \qquad (2)$$

a reaction which results in higher fluid pH at a given temperature and pressure than Reaction 1. Consequently, the lower metal abundances observed in natural fluids from sedimented systems is a function of their lower temperature as compared to bare-rock systems, not to the reaction mechanism by which organic carbon-bearing sediments are

altered. The results from this chapter provide evidence that organic compounds can be powerful controls on the potential composition of vent fluid chemistry, and need to be considered in chemical models of ridge crest systems. To do this, the organic compounds in hydrothermal vent fluids need to be identified and quantified, which was a main objective of this thesis.

Chapter 3. Organic geochemistry of Middle Valley vent fluids.

Middle Valley is a sedimented ridge crest environment, where circulating hydrothermal fluids interact with a large source of sediment-derived organic compounds as well as basaltic rocks. In Chapter 3, the aqueous abundances of several low-molecular weight organic compounds and their stable carbon isotopic composition are reported from two areas of venting at Middle Valley, the Dead Dog and ODP Mound fields (Fig. 1-3), and utilized to provide insight into subsurface reaction zone conditions at the vent fields. At the Dead Dog fields, fluids with maximum measured exit temperatures of 270°C vent through anhydrite chimneys found atop mounds of sulfide mineral rubble (AMES et al., 1993). To the south of the Dead Dog field, venting of fluids at temperatures estimated to be in the vicinity of 400°C resulted in the formation of the Bent Hill massive sulfide deposit, which contains an estimated 8 million tons of ore (ZIERENBERG et al., 1998). Although high temperature venting has ceased, ~270°C fluids do vent from small spires and chimneys near the ODP Mound, a smaller massive sulfide deposit located ~300 m south of Bent Hill. The ODP Mound vent field has apparently undergone rapid changes on time scales of only 1-2 years, with several new small spires and chimneys having formed across the surface of the mound as a result of puncturing of a hydrologic seal in the subsurface during ODP Leg 169 drilling operations.

Chloride systematics in vent fluids indicate that the ODP Mound field is characterized by subsurface reaction zone temperatures that are hotter than those at the Dead Dog field. Temperatures calculated from the relative abundances of C_2-C_3 alkanes and alkenes are consistent with temperatures required to produce the observed Cl concentrations and suggest that equilibrium between these organic compounds occurs in nature. The abundances and isotopic compositions of C_1-C_4 alkanes, benzene and toluene

indicate that the aqueous organic compounds have undergone a greater extent of alteration in the ODP Mound vent fluids in response to the hotter subsurface temperatures or longer reaction times. Abiotic oxidation of methane and other organic compounds is a key process influencing the concentration and isotopic composition of carbon dioxide in the Middle Valley vent fluids. Chemical and isotopic equilibrium between methane and carbon dioxide has likely occurred in the subsurface reaction zones of these two vent fields, driven by an approach to equilibrium from excess methane. Oxidation of organic compounds is also hypothesized to lead to the very high aqueous H_2 concentrations observed in the ODP Mound fluids. That the sediments from Middle Valley contain relatively low levels of organic carbon relative to the sediments that overlie other mid-ocean ridges such as at Guaymas Basin, Gulf of California, yet can still affect the concentrations of such inorganic species as CO_2 and H_2, indicates the importance of further investigation of organic compounds in other hydrothermal systems and their inclusion in models of crustal alteration.

Chapter 4. Temporal variability of fluid compositions at Middle Valley.

Vent fluid compositions in some locations such at the MEF, northern Juan de Fuca Ridge, and 21°N, on the East Pacific Rise, have exhibited stability at time scales of up to six years (BUTTERFIELD et al., 1994b; CAMPBELL et al., 1988). Large changes observed in fluid compositions at the Main Endeavour field from 1999 and 2000 following seismic activity indicate the sensitivity of the fluid chemistry to changes in subsurface conditions (SEEWALD et al., 2002; SEYFRIED et al., 2002). The temporal variability of vent fluid compositions at Middle Valley can be investigated at the yearly and decadal scales. Fluid chemistries from active vents in the Dead Dog field were sampled in 1990 and 1991 by Butterfield et al. (1994a). Heineken Hollow, Dead Dog Mound, Inspired Mounds and Chowder Hill vents were sampled in both that study and this thesis, providing a ten-year interval over which to compare changes in the major ion chemistry. Lone Star vent was sampled by Butterfield et al. (1994a) at the ODP Mound in 1990, but was not sampled as part of this thesis, precluding an assessment of the temporal variability of vent fluid compositions at the scale of individual vents. However,

comparison of the fluid chemistry of Lone Star vent in 1990, with Shiner Bock vent in 2000, allows an assessment of the temporal variability on the scale of the entire ODP Mound vent field. During the ten-year interval between 1990 and 2000, the concentrations of the major and minor inorganic ion concentrations were stable, indicating that the chemistry of the rocks regulating fluid compositions has remained largely unchanged over the last decade.

Temporal variability can also be assessed at shorter time scales at the ODP Mound field. Drilling during ODP Leg 169 breached a hydrologic seal in the subsurface, which lead to the establishment of venting from several drillholes. This also resulted in the development of venting from several small vents and spires on the eastern edge of the ODP Mound, which were not observed in 1998 (Zierenberg, pers. comm.). One of these vents, Spire, was sampled as part of this thesis. Abiotic methane oxidation at the ODP Mound field results in aqueous hydrogen concentrations in fluids from Shiner Bock and OPD Hole 1035H that are among the highest yet measured. These high concentrations are not observed in fluids sampled from Spire vent, located only ~30 meters from Shiner Bock and 1035H. Thermodynamic modeling indicates that, at Spire vent, hydrogen concentrations derived from methane oxidation are titrated by reaction of the fluids with fresh pyrite in the mound to form pyrrhotite. This also results in the generation of elevated concentrations of H_2S that are depleted in $\delta^{34}S$ as compared to Shiner Bock and 1035H. The fluids from Spire vent are thus undergoing real-time equilibration with the mound mineralogy. The results from this chapter also indicate that fluid compositions can undergo dramatic changes during upflow, and that the observed vent fluid compositions may not necessarily reflect conditions in the deepest subsurface reaction zones.

Chapter 5. A comparison of the organic geochemistry of Middle Valley and Main Endeavour Field fluids.

The Main Endeavour field (Fig. 1-4), is located on sediment-free basalt, yet previously reported vent fluid chemistries point to an interaction of the fluids with an organic carbon-bearing sediment. In Chapter 5, the chemistry of hydrothermal vent

fluids collected at the Main Endeavour Field are compared to those from Middle Valley in order to constrain the relative importance of sediment alteration versus other processes (e.g., mantle degassing; abiotic synthesis) as sources for organic compounds. The relationship between alkane abundances and stable carbon isotopic composition among the three vent areas is consistent with a greater extent of secondary alteration of the aqueous organic compounds in MEF fluids as compared to Middle Valley fluids. The stable carbon isotopic compositions of ethane and propane suggest that stepwise oxidation of low-molecular weight organic compounds is occurring. The redox condition of the Main Endeavour field subsurface reaction zone is more oxidizing than that at the ODP Mound field, due to the regulation of fluid chemistry by reaction with basalt, and leads to the observed greater extent of secondary alteration of the aqueous organic compounds. Thermodynamic modeling of the abundances of C_1-C_3 alkanes and CO_2 and the presence of benzene with stable carbon isotopic compositions that are identical to that in Middle Valley fluids provide evidence that the source of organic compounds is sedimentary organic matter rather than abiotic synthesis. For a given year, measured NH_3 and CH_4 concentrations, which are both derived predominantly from sediment-fluid rather than basalt-fluid interactions, are very similar in all vents. This points to a source of the organic compounds on the spatial scale of the entire field, rather than local to individual vents. Time series analysis of the organic compounds is available over a one year period from 1999 to 2000. When concentrations are normalized to temporal variations in Cl caused by seismic activity in July of 1999, increases of 4% to 15% are observed. This suggests that the decreases in methane concentration observed between pre-1988 and 1999-2000 vent fluids were caused by an earthquake-induced change in subsurface hydrology rather than an exhaustion of the sediment source. However, the amount of change between 1999 and 2000 is not large enough to unequivocally exlude the second possibility.

Unlike Middle Valley, carbon dioxide and methane are not in chemical or isotopic equilibrium. In the fluids that interact with sediments, the ~1 mmol/kg fluid methane most likely does form some CO_2 via methane oxidation, as was observed in Middle

Valley. However, the amount and isotopic composition of CO_2 in MEF fluids indicate that it is derived predominantly from magma degassing into fluids that react with basalt. The lack of chemical and isotopic equilibrium between methane and carbon dioxide in MEF fluids arises from short residence times of fluids in the subsurface reaction zone following late-stage addition of carbon dioxide to the fluids.

Table 1-1. Endmember concentrations of low molecular weight hydrocarbons in mid-ocean ridge hydrothermal vent fluids.

Location*	Temp °C	Cl mmol/kg	CH_4 mmol/kg	C_2H_6 µmol/kg	C_3H_8 µmol/kg	iso-C_4H_{10} µmol/kg	n-C_4H_{10} µmol/kg	$C_1/(C_2+C_3)$	Ref
MAR									
¤Rainbow	360	>750	2.2						1
Broken Spur	356-360	469	0.06						2
Lucky Strike	185-324	417-514	0.3-0.8						3
Menez Gwen	275-284	357-381	1.5-2.1						3
Snakepit	345	559	0.06						4
¤Lost City	40-75	546-549	0.13-0.28						5
EPR									
11°N		327-681	0.06-1.1						6
13°N	317-381	712-763	0.03-0.18						6-8
21°N	273-355	489-579	0.05-0.09						9-14
17-19°S	>210-340	190-871	0.008-0.13	0.06-0.2	0.007				15
‡Guaymas	100-315	581-637	54						11, 12, 14
JdFR									
Middle Valley									
‡Dead Dog	187-281	546-586	18.5-21.6	194-232	49.9-57.5	5.00-6.15	5.58-6.24	70.5-76.1	16
‡ODP Mound	263-272	432-449	5.85-7.07	23.2-24.3	4.48-4.63	0.34-0.36	0.87-1.06	211-245	16
Endeavour Segement									
Main Endeavour	120-370	31.8-505	1.7-3.4	1.6-28	0.06-0.1				17-20
Cleft Segment									
Plume	224	1090	0.08	0.2	0.05	0.004	0.006		21, 22
KR									
Kolbeinsey†	>100-131		0.06	0.29	0.46			73.3	23
Grimsey†	200-250	274	0.02	0.28	0.02		0.02	78.5	22,24

*MAR: Mid-Atlantic Ridge; EPR: East Pacific Rise; JdFR: Juan de Fuca Ridge; KR: Kolbeinsey Ridge

References: [1]Donval et al. (1997); [2]James et al. (1995) [3]Charlou et al. (2000); [4]Jean-Baptiste et al. (1991); [5]Kelley et al. (2001); [6]Kim et al. (1984); [7]Merlivat et al. (1987); [8]Michard et al. (1984); [9]Lilley et al. (1983); [10]Welhan and Craig (1983); [11]Seewald et al. (1998); [12]Von Damm (1983); [13]Von Damm et al. (1985a); [14]Von Damm et al. (1985b); [15]Charlou et al. (1996)[16]Chapter 3, this thesis; [17]Butterfield et al. (1994b); [18]Lilley et al. (1993); [19]Seewald et al. (2002); [20]Chapter 4, this thesis; [21]Evans et al. (1988); [22]Von Damm and Bischoff (1987); [23]Botz et al. (1999); [24]Hannington et al. (2001).

†endmember hydrocarbon concentrations calculated only for water samples and not gas bubble samples.

¤located on ultramafic rocks where the methane is believed to be derived from serpentinization processes

‡sedimented ridge axis

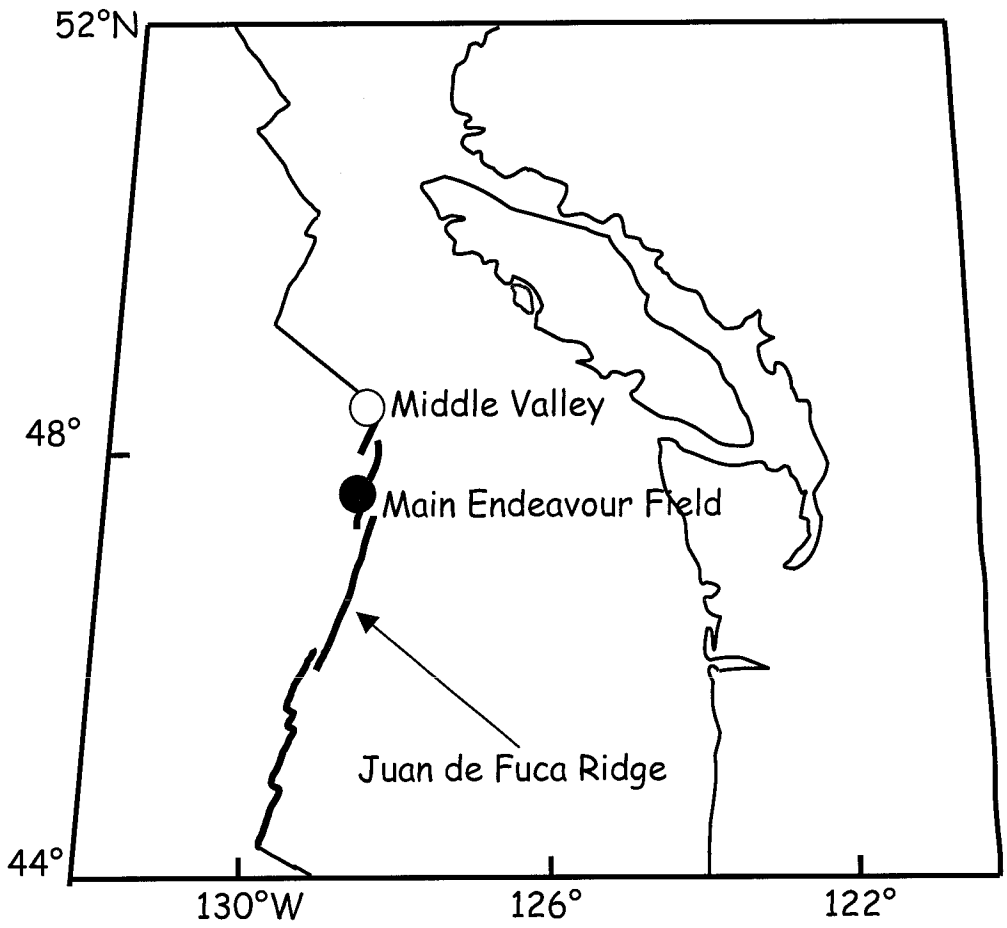

Figure 1-1. Location map of vent fields sampled in this thesis. Map redrawn from Shipboard Scientific Party (1998).

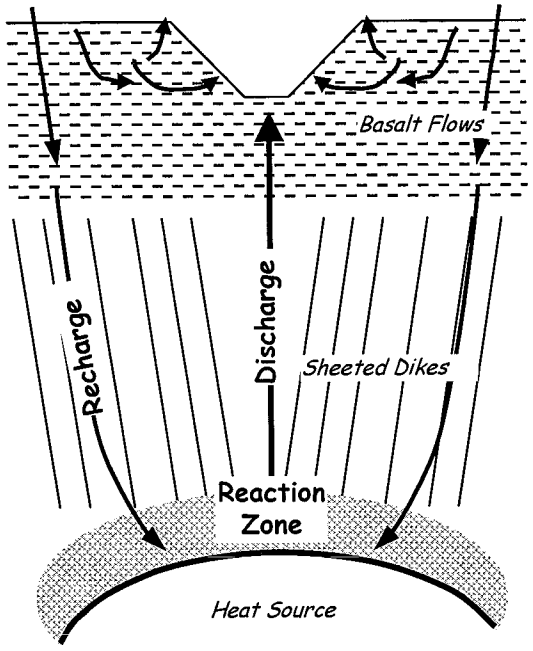

Figure 1-2. Schematic drawing showing the conceptual divisions of fluid flow regimes in mid-ocean ridge systems. Redrawn from Alt (1995).

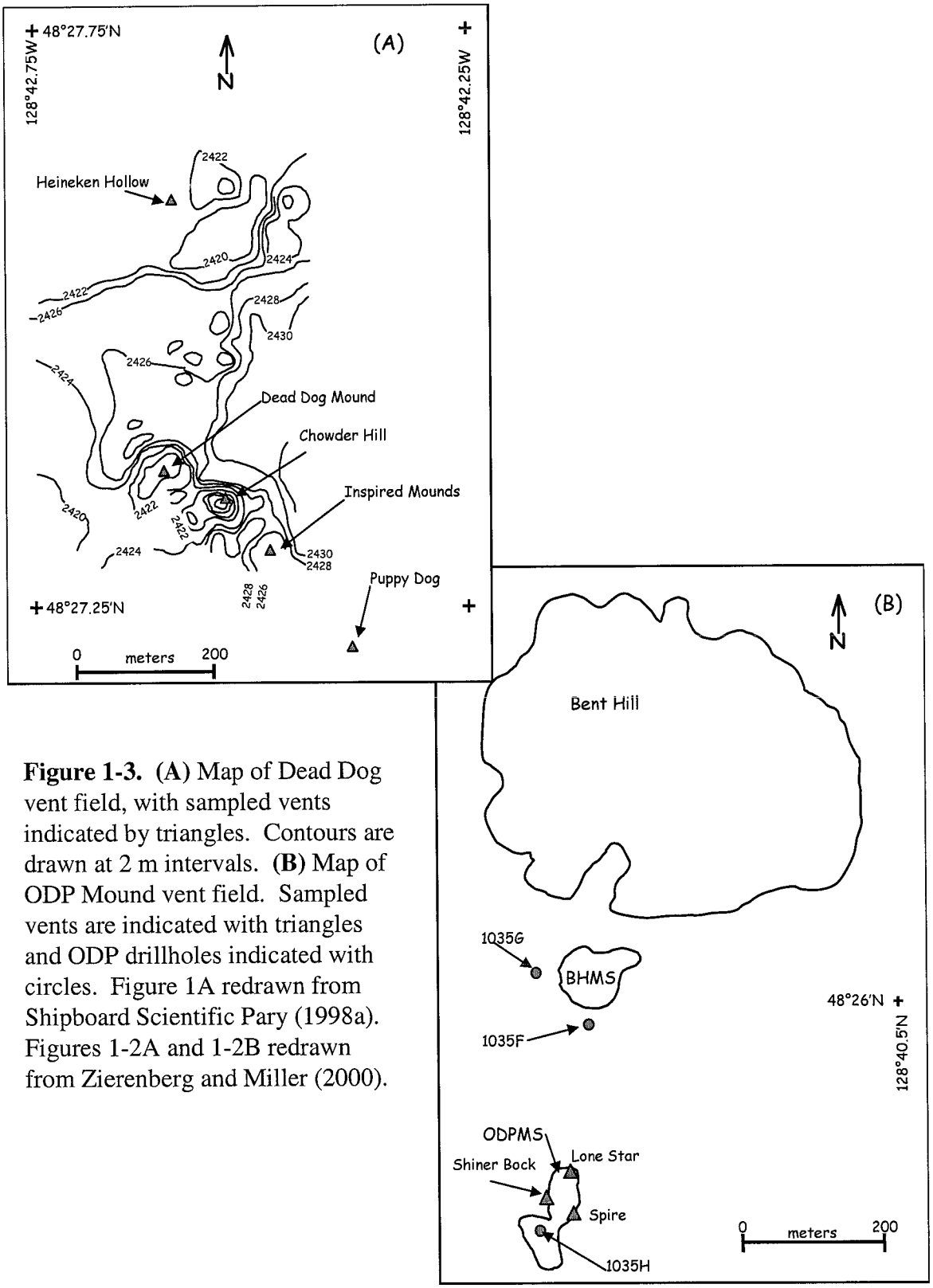

Figure 1-3. **(A)** Map of Dead Dog vent field, with sampled vents indicated by triangles. Contours are drawn at 2 m intervals. **(B)** Map of ODP Mound vent field. Sampled vents are indicated with triangles and ODP drillholes indicated with circles. Figure 1A redrawn from Shipboard Scientific Pary (1998a). Figures 1-2A and 1-2B redrawn from Zierenberg and Miller (2000).

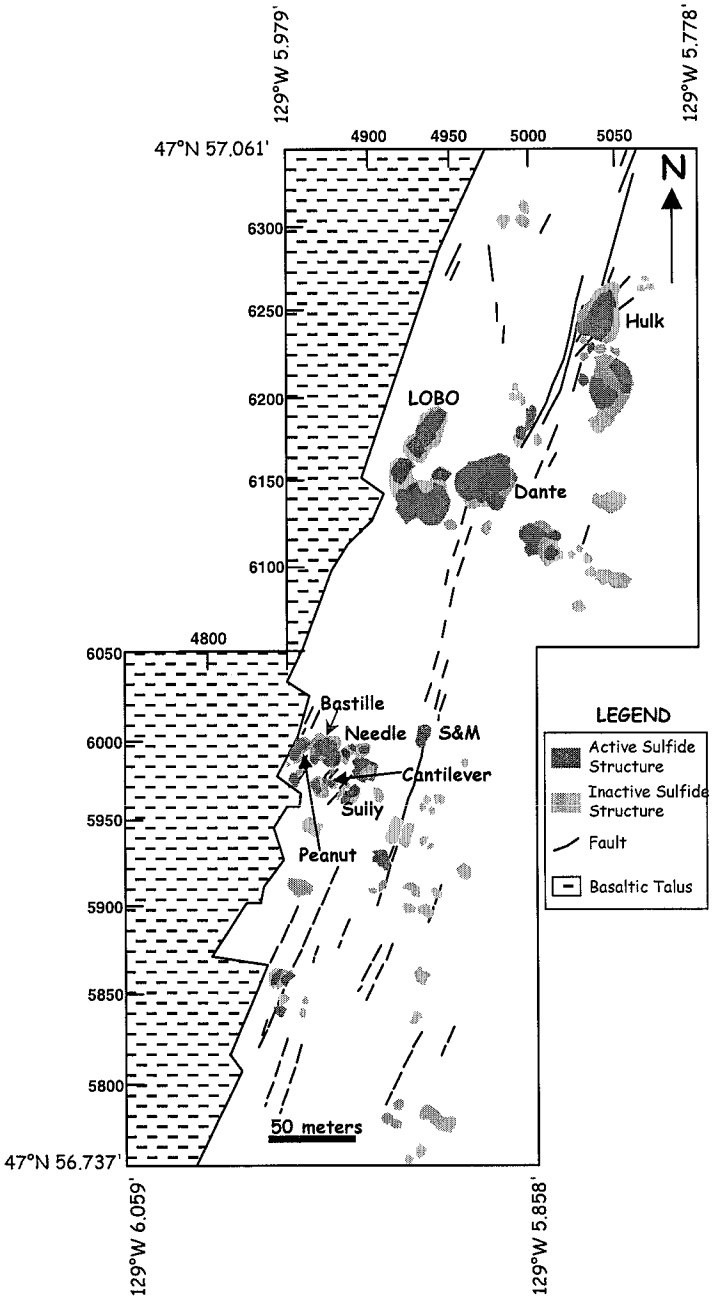

Figure 1-4. Map of the Main Endeavour Field showing vents sampled in this study, redrawn from Seewald et al. (2002).

1.4. REFERENCES

ABBOTT G. D., LEWIS C. A., and MAXWELL J. R. (1985) The kinetics of specific organic reactions in the zone of catagenesis. *Philos. Trans. R. Soc. London, A* **A 315**, 107-122.

ALT J. C. (1995) Subseafloor processes in mid-ocean ridge hydrothermal systems. In *Seafloor Hydrothermal Systems: Physical, Chemical, Biological, and Geological Interactions*, Geophysical Monograph **91** (ed. S. E. Humphris, R. A. Zierenberg, L. S. Mullineaux, and R. E. Thomson), pp. 85-114.

AMES D. E., FRANKLIN J. M., and HANNINGTON M. H. (1993) Mineralogy and geochemistry of active and inactive chimneys and massive sulfide, Middle Valley, northern Juan de Fuca Ridge: An evolving hydrothermal system. *Can. Mineral.* **31**, 997-1024.

BERNER U., FABER E., SCHEEDER G., and PANTEN D. (1995) Primary cracking of algal and landplant kerogens: kinetic models of isotope variations in methane, ethane and propane. *Chem. Geol.* **126**, 233-245.

BISCHOFF J. L. and DICKSON F. W. (1975) Seawater-basalt interaction at 200°C and 500 bars: Implications for the origin of sea-floor heavy-metal deposits and the regulation of seawater chemistry. *Earth Planet. Sci. Lett.* **25**, 385-397.

BOTZ R., WINCKLER G., BAYER R., SCHMITT M., SCHMIDT M., GARBE-SCHÖNBERG D., STOFFERS P., and KRISTJANSSON J. K. (1999) Origin of trace gases in submarine hydrothermal vents of the Kolbeinsey Ridge, north Iceland. *Earth Planet. Sci. Lett.* **171**, 83-93.

BOWERS T. S., VON DAMM K. L., and EDMOND J. M. (1985) Chemical evolution of mid-ocean ridge hot springs. *Geochim. Cosmochim. Acta* **49**, 2239-2252.

BUTTERFIELD D. A. (2000) Deep Ocean Hydrothermal Vents. In *Encyclopedia of Volcanoes* (ed. H. Sigurdsson, B. F. Houghton, S. R. McNutt, H. Rymer, and J. Stix), pp. 857-875. Academic Press.

BUTTERFIELD D. A., MCDUFF R. E., FRANKLIN J., and WHEAT C. G. (1994a) Geochemistry of hydrothermal vent fluids from Middle Valley, Juan de Fuca Ridge. In *Proc. ODP, Sci. Results* **139** (ed. M. J. Mottl, E. E. Davis, A. T. Fisher, and J. F. Slack), pp. 395-410.

BUTTERFIELD D. A., MCDUFF R. E., MOTTL M. J., LILLEY M. D., LUPTON J. E., and MASSOTH G. J. (1994b) Gradients in the composition of hydrothermal fluids from the Endeavour segment vent field: Phase separation and brine loss. *J. Geophys. Res.* **99**, 9561-9583.

CAMPBELL A. C., BOWERS T. S., and EDMOND J. M. (1988) A time-series of vent fluid compositions from 21°N, EPR (1979, 1981 and 1985) and the Guaymas Basin, Gulf of California (1982, 1985). *J. Geophys. Res.* **99**, 9561-9583.

CHARLOU J. L., DONVAL J. P., DOUVILLE E., JEAN-BAPTISTE P., RADFORD-KNOERY J., FOUQUET Y., DAPOIGNY A., and STIEVENARD M. (2000) Compared geochemical signatures and the

evolution of Menez Gwen (37°50'N) and Lucky Strike (37°17'N) hydrothermal fluids, south of the Azores triple junction on the Mid-Atlantic Ridge. *Chem. Geol.* **171**, 49-75.

CHARLOU J. L., FOUQUET Y., DONVAL J. P., and AUZENDE J. M. (1996) Mineral and gas chemistry of hydrothermal fluids on an ultrafast spreading ridge: East Pacific Rise, 17° to 19°S (Naudur cruise, 1993) phase separation processes controlled by volcanic and tectonic activity. *J. Geophys. Res.* **101**, 15889-15919.

CONNAN J. (1974) Time-temperature relations in oil genesis. *AAPG Bull.* **58**, 2516-2521.

CORLISS J. B., DYMOND J., GORDON L. I., EDMOND J. M., VON HERZEN R. P., BALLARD R. D., GREEN K., WILLIAMS D., BAINBRIDGE A., CRANE K., and VAN ANDEL T. H. (1979) Submarine thermal springs on the Galapagos Rift. *Science* **203**, 1073-1083.

CROSSEY L. J., FROST B. R., and SURDAM R. C. (1984) Secondary porosity in laumontite-bearing sandstones. In *Clastic Diagenesis* (ed. D. A. McDonald and R. C. Surdam), pp. 225-237. American Association of Petroleum Geologists.

DELANEY J. R., ROBIGOU V., MCDUFF R. E., and TIVEY M. K. (1992) Geology of a vigorous hydrothermal system on the Endeavour Segment, Juan de Fuca Ridge. *J. Geophys. Res.* **97**, 19,663-19, 682.

DISNAR J. R. and SUREAU J. F. (1990) Organic matter in ore genesis: Progress and perspectives. *Org. Geochem.* **16**, 577-599.

DONVAL J. P. and AL. E. (1997) High H_2 and CH_4 content in hydrothermal fluids from Rainbow site newly sampled at 36°14' on the AMAR segment, Mid-Atlantic Rigde (diving FLORES cruise, July 1997). Comparison with other MAR sites. *Eos* **78**, 832.

EDMOND J. M., MEASURES C. I., MCDUFF R. E., CHAN L. H., COLLIER R., GRANT B., GORDON L. I., and CORLISS J. B. (1979) Ridge crest hydrothermal activity and the balance of the major and minor elements in the ocean; the Galapagos data. *Earth Planet. Sci. Lett.* **46**, 1-18.

ELLIOT D. C., SEALOCK L. J., JR. , and BAKER E. G. (1994) Chemical processing in high-pressure aqueous environments. 3. Batch reactor process development experiments for organic destruction. *Ind. Eng. Chem. Res.* **33**, 558-565.

EVANS W. C., WHITE L. D., and RAPP J. B. (1988) Geochemistry of some gases in hydrothermal fluids from the southern Juan de Fuca Ridge. *J. Geophys. Res.* **93**, 15,305-15,313.

GOODFELLOW W. D. and BLAISE B. (1988) Sulfide formation and hydrothermal alteration of hemipelagic sediment in Middle Valley, northern Juan de Fuca Ridge. *Can. Mineral.* **26**, 675-696.

HANNINGTON M., HERZIG P., SCHOLTEN J., BOTZ R., GARBE-SCHÖNBERG D., JONASSON I. R., ROEST W., and SHIPBOARD SCIENTIFIC PARTY. (2001) First observations of high-

temperature submarine hydrothermal vents and massive anhydrite deposits off the north coast of Iceland. *Mar. Geol.* **177**, 199-220.

HELGESON H. C., KNOX A. M., OWENS C. E., and SHOCK E. L. (1993) Petroleum, oil field waters, and authigenic mineral assemblages: Are they in metastable equilibrium in hydrocarbon reservoirs? *Geochim. Cosmochim. Acta* **57**, 3295-3339.

HUNT J. M. (1996) *Petroleum Geochemistry and Geochemistry*. W. H. Freeman.

JAMES R. H., ELDERFIELD H., and PALMER M. R. (1995) The chemistry of hydrothermal fluids from the Broken Spur site, 29°N Mid-Atlantic Ridge. *Geochim. Cosmochim. Acta* **59**, 651-659.

JEAN-BAPTISTE P., CHARLOU J. L., STIEVENARD M., DONVAL J. P., BOUGAULT H., and MEVEL C. (1991) Helium and methane measurements in hydrothermal fluids from the mid-Atlantic ridge: the Snake Pit site at 23°N. *Earth Planet. Sci. Lett.* **106**, 17-28.

KATRITZKY A. R., BALASUBRAMANIAN M., and SISKIN M. (1990) Aqueous high-temperature chemistry of carbo- and heterocycles. 2. Monosubstituted benzenes: benzyl alcohol, benzaldehyde, and benzoic acid. *Energy Fuels* **4**, 499-505.

KAWKA O. E. and SIMONEIT B. R. T. (1990) Polycyclic aromatic hydrocarbons in hydrothermal petroleums from the Guaymas Basin spreading center. *Appl. Geochem.* **5**, 17-27.

KELLEY D. S., KARSON J. A., BLACKMAN D. A., FRÜH-GREEN G. L., BUTTERFIELD D. A., LILLEY M. D., OLSON E. J., SCHRENK M. O., ROE K. K., LEBON G. T., RIVIZZIGNO P., and AT3-60 SHIPBOARD PARTY. (2001) An off-axis hydrothermal vent field near the Mid-Atlantic Ridge at 30°N. *Nature* **412**, 145-149.

KIM K.-R., WELHAN J. A., and CRAIG H. (1984) The hydrothermal vent fields at 13°N and 11°N on the East Pacific Rise: *Alvin* 1984 results. *Eos* **65**, 973.

KVENVOLDEN K. A., RAPP J. B., and HOSTETTLER F. D. (1990) Hydrocarbon geochemistry of hydrothermally generated petroleum from Escanaba Trough, offshore California, U.S.A. *Appl. Geochem.* **5**.

KVENVOLDEN K. A., RAPP J. B., HOSTETTLER F. D., MORTON J. L., KING J. D., and CLAYPOOL G. E. (1986) Petroleum associated with polymetallic sulfide in sediment from Gorda Ridge. *Science* **234**, 1231-1234.

LEWAN M. D. (1983) Effects of thermal maturation on stable organic carbon isotopes as determined by hydrous pyrolysis of Woodford Shale. *Geochim. Cosmochim. Acta* **47**, 1471-1479.

LILLEY M. D., BAROSS J. A., and GORDON L. I. (1983) Reduced gases and bacteria in hydrothermal fluids: The Galapagos spreading center and 21°N East Pacific Rise. In *Hydrothermal Processes at Seafloor Spreading Centers* (ed. P. A. Rona, K. Boström, L. Laubier, and K. L. Smith), pp. 411-449. Plenum.

LILLEY M. D., BUTTERFIELD D. A., OLSON E. J., LUPTON J. E., MACKO S. A., and MCDUFF R. E. (1993) Anomalous CH_4 and NH_4^+ concentrations at an unsedimented mid-ocean-ridge hydrothermal system. *Nature* **364**, 45-47.

LORANT F., PRINZHOFER A., BEHAR F., and HUC A.-Y. (1998) Carbon isotopic and molecular constraints on the formation and the expulsion of thermogenic hydrocarbon gases. *Chem. Geol.* **147**, 249-264.

MCCOLLOM T. M., SEEWALD J. S., and SIMONEIT B. R. T. (2001) Reactivity of monocyclic aromatic compounds under hydrothermal conditions. *Geochim. Cosmochim. Acta* **65**, 455-468.

MERLIVAT L., PINEAU F., and JAVOY M. (1987) Hydrothermal vent waters at 13°N on the East Pacific Rise: Isotopic composition and gas concentration. *Earth Planet. Sci. Lett.* **84**, 100-108.

MICHARD G., ALBARÈDE F., MICHARD A., MINSTER J.-F., CHARLOU J.-L., and TAN N. (1984) Chemistry of solutions from the 13°N East Pacific Rise hydrothermal site. *Earth Planet. Sci. Lett.* **67**, 297-307.

MOTTL M. J. and HOLLAND H. D. (1978) Chemical exchange during hydrothermal alteration of basalt by seawater-I. Experimental results for major and minor components of seawater. *Geochim. Cosmochim. Acta* **42**, 1103-1115.

NORTON D. (1984) Theory of hydrothermal systems. *Ann. Rev. Earth Planet. Sci.* **12**, 155-177.

PRICE L. C. (1983) Geologic time as a parameter in organic metamorphism and vitrinite reflectance as an absolute paleogeothermometer. *J. Petrol. Geol.* **6**, 5-38.

PRICE L. C. (1985) Geologic time as a parameter in organic metamorphism and vitrinite reflectance as an absolute paleogeothermometer: Reply. *J. Petrol. Geol.* **8**, 233-240.

PRICE L. C. (1993) Thermal stability of hydrocarbons in nature: Limits, evidence, characteristics, and possible controls. *Geochim. Cosmochim. Acta* **57**, 3261-3280.

RUSHDI A. I. and SIMONEIT B. R. T. (2002) Hydrothermal alteration of organic matter in sediments of the Northeastern Pacific Ocean: Part 1. Middle Valley, Juan de Fuca Ridge. *Appl. Geochem.* **17**, 1401-1428.

SCOTT S. D. (1985) Seafloor polymetallic sulfide deposits: Modern and ancient. *Marine Mining* **5**, 191-212.

SEEWALD J. S. (1994) Evidence for metastable equilibrium between hydrocarbons under hydrothermal conditions. *Nature* **370**, 285-287.

SEEWALD J. S. (1997) Mineral redox buffers and the stability of organic compounds under hydrothermal conditions. In *Aqueous Chemistry and Geochemistry of Oxides, Oxyhydroxides, and Related Materials*, Materials Research Society Symposium

Proceedings **432** (ed. J. A. Voight, T. E. Wood, B. E. Bunker, W. H. Casey, and L. J. Crossey), pp. 317-331.

SEEWALD J. S. (2001) Aqueous geochemistry of low molecular weight hydrocarbons at elevated temperatures and pressures: Constraints from mineral buffered laboratory experiments. *Geochim. Cosmochim. Acta* **65**, 1641-1664.

SEEWALD J. S., CRUSE A. M., LILLEY M. D., and OLSON E. J. (1998) Hot-spring fluid chemistry at Guaymas Basin, Gulf of California: Temporal variations and volatile content. *Eos* **79**, F47.

SEEWALD J. S., CRUSE A. M., and SACCOCIA P. (2002) Aqeous volatiles in hydrothermal fluids from the Main Endeavour Field, northern Juan de Fuca Ridge: Temporal variability following earthquake activity. *submitted to Earth and Planetary Science Letters.*

SEYFRIED W. E., JR. (1987) Experimental and theoretical constraints on hydrothermal alteration processes at mid-ocean ridges. *Ann. Rev. Earth Planet. Sci.* **15**, 317-335.

SEYFRIED W. E., JR. and BISCHOFF J. L. (1979) Low-temperature basalt alteration by seawater: an experimental study at 70°C and 150°C. *Geochim. Cosmochim. Acta* **43**, 1937-1947.

SEYFRIED W. E., JR. and BISCHOFF J. L. (1981a) Experimental seawater-basalt interaction at 300°C, 500 bars, chemical exchange, secondary mineral formation and implications for the transport of heavy meatals. *Geochim. Cosmochim. Acta* **45**, 135-147.

SEYFRIED W. E., JR. and BISCHOFF J. L. (1981b) Experimental seawater-basalt interaction at 300°C, 500 bars: Chemical exchange, secondary mineral formation and implications for the transport of heavy metals. *Geochimica et Cosmochimica Acta* **45**, 135-149.

SEYFRIED W. E., JR., SEEWALD J. S., BERNDT M. E., DING K., and FOUSTOUKOS D. (2002) Chemistry of hydrothermal vent fluids from the Main Endeavour Field, Northern Juan de Fuca Ridge: Geochemical controls in the aftermath of June 1999 seismic events. *submitted to Journal of Geophysical Research.*

SHOCK E. L. (1988) Organic acid metastability in sedimentary basins. *Geology* **16**, 886-890.

SHOCK E. L. (1990) Do amino acids equilibratein hydrothermal fluids? *Geochim. Cosmochim. Acta* **54**, 1185-1189.

SIMONEIT B. R. T. (1984) Hydrothermal effects on organic matter: high verus low temperature components. *Org. Geochem.* **6**, 857-864.

SIMONEIT B. R. T. (1993) Aqueous high-temperature and high-pressure organic geochemistry of hydrothermal vent systems. *Geochim. Cosmochim. Acta* **57**, 3231-3243.

SIMONEIT B. R. T. (1994) Lipid/bitumen maturation by hydrothermal activity in sediments of Middle Valley, Leg 139. In *Proc. ODP, Sci. Results* (ed. M. J. Mottl, E. E. Davis, A. T. Fisher, and J. F. Slack), pp. 447-464. Ocean Drilling Program.

SIMONEIT B. R. T., BRAULT M., and SALIOT A. (1990) Hydrocarbons associated with hydrothermal minerals, vent waters and talus on the East Pacific.

SIMONEIT B. R. T. and GALIMOV E. M. (1984) Geochemistry of interstitial gases in Quaternary sediments of the Gulf of California. *Chem. Geol.* **43**, 151-166.

SIMONEIT B. R. T., GOODFELLOW W. D., and FRANKLIN J. M. (1992) Hydrothermal petroleum at the seafloor and organic matter alteration in sediments of Middle Valley, Northern Juan de Fuca Ridge. *Appl. Geochem.* **7**, 257-264.

SIMONEIT B. R. T., KAWKA O. E., and BRAULT M. (1988) Origin of gases and condensates in the Guaymas Basin hydrothermal system (Gulf of California). *Chem. Geol.* **71**, 169-182.

SIMONEIT B. R. T. and KVENVOLDEN K. A. (1994) Comparison of ^{14}C ages of hydrothermal petroluems. *Org. Geochem.* **21**, 525-529.

SIMONEIT B. R. T., PRAHL F. G., LEIF R. N., and MAO S.-Z. (1994) Alkenones in sediments of Middle Valley, Leg 139. In *Proc. ODP, Sci. Results* **139** (ed. M. J. Mottl, E. E. Davis, A. T. Fisher, and J. F. Slack), pp. 479-484.

SISKIN M. and KATRITZKY A. R. (1991) Reactivity of organic compounds in hot water: Geochemical and technological implications. *Science* **254**, 231-237.

SUMMIT M. and BAROSS J. A. (2001) A novel microbial habitat in the mid-ocean ridge seafloor. *Proc. Natl. Acad. Sci. U. S. A.* **98**, 2158-2163.

TISSOT B. and WELTE D. H. (1984) *Petroleum Formation and Occurrence*. Verlag.

VON DAMM K. L. (1983) Chemistry of Submarine Hydrothermal Solutions at 21°N, East Pacific Rise and Guaymas Basin, Gulf of California. PhD., MIT/WHOI, WHOI-84-3. 240 p.

VON DAMM K. L. (1995) Controls on the chemistry and temporal variability of seafloor hydrothermal fluids. In *Seafloor Hydrothermal Systems: Physical, Chemical, Biological, and Geological Interactions*, Geophysical Monograph **91** (ed. S. E. Humphris, R. A. Zierenberg, L. S. Mullineaux, and R. E. Thomson), pp. 222-247.

VON DAMM K. L. and BISCHOFF J. L. (1987) Chemistry of hydrothermal solutions from the southern Juan de Fuca Ridge. *J. Geophys. Res.* **92**, 11,334-11,346.

VON DAMM K. L., EDMOND J. M., GRANT B., MEASURES C. I., WALDEN B., and WEISS R. F. (1985a) Chemistry of submarine hydrothermal solutions at 21°N, East Pacific Rise. *Geochim. Cosmochim. Acta* **49**, 2197-2220.

VON DAMM K. L., EDMOND J. M., MEASURES C. I., and GRANT B. (1985b) Chemistry of submarine hydrothermal solutions at Guaymas Basin, Gulf of California. *Geochim. Cosmochim. Acta* **49**, 2221-2237.

WAPLES D. W. (1984) Thermal models for oil generation. In *Advances in Petroleum Geochemistry* **1** (ed. J. Brooks and D. Welte), pp. 7-67.

WELHAN J. A. and CRAIG H. (1983) Methane, hydrogen and helium in hydrothermal fluids at 21°N on the East Pacific Rise. In *Hydrothermal Processes at Seafloor Spreading Centers* (ed. P. A. Rona, K. Boström, and L. Laubier), pp. 391-409. Plenum.

WELHAN J. A. and LUPTON J. E. (1987) Light hydrocarbon gases in Guaymas Basin hydrothermal fluids: Thermogenic versus Abiogenic Origin. *AAPG Bull.* **71**, 215-223.

WHELAN J. K., SIMONEIT B. R. T., and TARAFA M. E. (1988) C_1-C_8 hydrocarbons in sediments from Guaymas Basin, Gulf of California--Comparison to Peru Margin, Japan Trench and California Borderlands. *Org. Geochem.* **12**, 171-194.

ZIERENBERG R. A., FOUQUET Y., MILLER D. J., BAHR J. M., BAKER P. A., BJERKGÅRD T., BRUNNER C. A., GOODFELLOW W. D., GRÖSCHEL-BECKER H. M., GUÈRIN G., ISHIBASHI J., ITURRINO G., JAMES R. H., LACKSCHEWITZ K. S., MARQUEZ L. L., NEHLING P., PETER J. M., RIGSBY C. A., SCHULTHEISS P., III W. C. S., SIMONEIT B. R. T., SUMMIT M., TEAGLE D. A. H., URBAT M., and ZUFFA G. G. (1998) The deep structure of a sea-floor hydrothermal deposit. *Nature* **392**, 485-488.

CHAPTER 2. METAL MOBILITY IN SEDIMENT-COVERED RIDGE-CREST HYDROTHERMAL SYSTEMS: EXPERIMENTAL AND THEORETICAL CONSTRAINTS

(Previously published as: CRUSE A. M. and SEEWALD J. S. (2001) Controls on metal transport in sediment-covered ridge-crest hydrothermal systems: Experimental and theoretical constraints. *Geochim. Cosmochim Acta*, **65**, 3233-3247.

ABSTRACT

The presence of sedimentary organic matter blanketing mid-ocean ridge crests has a potentially strong impact on metal transport in hydrothermal vent fluids. To constrain the role of organic matter in metal mobility during hydrothermal sediment alteration, we reacted organic-rich diatomaceous ooze from Guaymas Basin, Gulf of California, and organic-poor hemipelagic mud from Middle Valley, northern Juan de Fuca ridge, with seawater and a Na-Ca-K-Cl fluid of seawater chlorinity, at 275-400°C, 350-500 bars and initial fluid-sediment mass ratios ranging from 1.6-9.8. Reaction of these fluids with both sediment types released CO_2 and high concentrations of ore-forming metals (Fe, Mn, Zn, Pb) to solution. Relatively low concentrations of Cu were observed in solution and likely reflect the reducing conditions that resulted from the presence of sedimentary organic matter. Both the concentrations of CO_2 and dissolved metals were lower in fluids reacted with Middle Valley sediment as compared to aqueous concentrations in fluids reacted with Guaymas Basin sediment. During alteration of both sediment types, metal concentrations varied strongly as a function of temperature, increasing by up to an order of magnitude over the 75°C range of each experiment. Major element fluid chemistry and observed alteration assemblages suggest that during hydrothermal alteration of organic-lean sediment from Middle Valley a feldspar-quartz-illite mineral assemblage buffered in situ pH. In contrast, data from the experimental alteration of organic-rich Guaymas Basin sediment suggest that a calcite-plagioclase-quartz assemblage regulated in situ pH. Fluid speciation calculations suggest that in situ pH during Guaymas Basin sediment alteration was lower than during alteration of Middle Valley sediment, and accounts for the substantially greater metal mobility at a given temperature and pressure during the former experiment. Comparison of our results with the results of basalt alteration experiments indicate that except for Cu, hydrothermal sediment alteration results in equal or greater concentrations of ore-forming metals at a given temperature and pressure. Accordingly, the presence of ore-forming metals in fluids currently venting from sediment-covered hydrothermal systems at concentrations substantially lower than in fluids from bare-rock systems may reflect chemical re-equilibration during subsurface

cooling within the sediment pile.

2.1. INTRODUCTION

Convective circulation of seawater-derived hydrothermal fluids is a consequence of the high heat flux associated with crustal generation at oceanic spreading centers. Hydrothermal activity in ridge-crest environments characterized by low sedimentation rates involves the chemical interaction of seawater with rocks of basaltic composition, while in regions of high sedimentation, hydrothermal fluids also react with sediments that blanket the spreading axis. Relative to seawater, vent fluids from both environments are enriched in transition metals (e.g., Fe, Mn, Zn, Cu) that may precipitate at the seafloor to form massive sulfide deposits (LONSDALE et al., 1980; FRANKLIN et al., 1981; KOSKI et al., 1985, 1988; GOODFELLOW and BLAISE, 1988; PETER and SCOTT, 1988; FRANKLIN, 1993; HANNINGTON et al., 1995). In general, fluids currently venting at sedimented hydrothermal systems contain lower concentrations of metals relative to fluids from unsedimented systems (Table 2-1). Nonetheless, large massive sulfide deposits have formed at sediment-covered hydrothermal systems such as Middle Valley, northern Juan de Fuca Ridge, where an estimated minimum 8 million tons of massive sulfide have accumulated largely on the seafloor near Bent Hill (SHIPBOARD SCIENTIFIC PARTY, 1997; JAMES et al., 1998; ZIERENBERG et al., 1998). At Guaymas Basin, Gulf of California, and Escanaba Trough, southern Juan de Fuca Ridge, large sulfide deposits are absent at the seafloor, but it has been postulated that an ore deposit may be forming at basalt-sediment interfaces as metals precipitate from fluids generated during seawater-basalt interaction prior to ascent through the sediment pile (BOWERS et al., 1985; SCOTT, 1985; VON DAMM et al., 1985b; JAMES et al., 1999).

Evaluating ore formation at or below the seafloor at sediment-covered spreading centers requires information regarding factors that regulate metal mobility in hot aqueous fluids. In particular, it is necessary to constrain the relative roles of fluid-basalt and fluid-sediment chemical interaction during metal transport and deposition. Sediments are compositionally and mineralogically more variable than fresh oceanic basalt. Organic

matter is absent in basalt, but is present in sediments at varying levels and likely plays an integral role in ore formation (DISNAR and SUREAU, 1990, and references therein). Additionally, the extent to which fluids will interact with sediment or basalt at a particular site will also be a function of fluid flow pathways and velocities. This study was conducted to investigate the mobilization of metals during hydrothermal alteration of organic-rich sediment from Guaymas Basin and relatively organic-lean sediment from Middle Valley. Laboratory hydrothermal experiments have been effective in constraining organic and inorganic sediment alteration processes (BISCHOFF et al., 1981; THORNTON and SEYFRIED, 1987; SEEWALD et al., 1990, 1994; VON DAMM, 1991). Large uncertainties, however, are associated with reported data for aqueous transition metal concentrations during these experiments due to sampling artifacts. Specifically, results of basalt alteration experiments have demonstrated that unless extreme care is taken to preclude precipitation during sampling, measured transition metal concentrations may be substantially lower than in situ values (SEEWALD and SEYFRIED, 1990). Presented here are the results of sediment alteration experiments conducted at 275-400°C and 350-500 bars during which the concentrations of selected inorganic and organic aqueous species were monitored as a function of time. A rapid sampling technique was utilized to prevent precipitation of transition metals during extraction of fluids for analysis.

2.2. PROCEDURES

2.2.1. Experimental Equipment

Flexible cell hydrothermal equipment consisting of a deformable gold-titanium reaction cell was used for all experiments (SEYFRIED et al., 1987). This equipment allows fluid samples to be withdrawn from the reaction cell at the temperature and pressure of an experiment as a function of time, avoiding ambiguities arising from retrograde reactions during a prolonged quench process. An internal Ti filter ensures the recovery of particle-free fluids. Prior to an experiment, all Ti pieces in contact with the fluid were heated in air at 400°C to form a chemically-inert oxide layer.

2.2.2. Experimental Conditions

Experiments were conducted using unaltered sediment from Middle Valley and Guaymas Basin. The Middle Valley sediment is Upper Pleistocene in age and was recovered from a depth of 19.5 meters below the seafloor during ODP Leg 139 (sample no. 855A-3R-2, 137-140 cm interval; DAVIS et al., 1992). The sediment is fine-grained, gray, and composed of quartz, albitic feldspar, K-feldspar, chlorite, smectite, and calcite, with 0.44 wt.% total organic carbon (TOC) and 0.21 wt. % total inorganic carbon (TIC). Guaymas Basin surficial sediment was collected by piston core in the Southern Trough. The sediment is fine-grained, olive green in color and composed of abundant diatoms, quartz, plagioclase feldspar, K-feldspar, clays, calcite, bacteriogenic pyrite, 2.5 wt. % TOC, and 0.36 wt. % TIC. Both sediments were stored frozen at –30°C with their original pore fluids prior to use in the experiments.

Previous experimental studies have demonstrated that during the initial stages of seawater-sediment or seawater-basalt alteration at temperatures greater than 200°C, Mg and SO_4 are rapidly removed from the fluid by precipitation of Mg-rich alteration products (smectite, mixed-layer chlorite/smectite) and anhydrite, respectively (THORNTON and SEYFRIED, 1987; SEEWALD et al., 1990). Therefore, sediment alteration in the deepest and hottest parts of a hydrothermal system likely involves Mg- and SO_4-depleted fluids. In order to model sediment alteration in this part of the system, the Middle Valley experiments were conducted with Mg- and SO_4-free Na-Ca-K-Cl fluids of seawater chlorinity (Tables 2-2 and 2-3). The original sediment pore fluids were removed by repeated dilution with the experimental fluid, followed by centrifugation and decantation.

Two experiments were conducted with Middle Valley sediments, MV and MVCAL. Experiment MV initially contained 4.37 g of sediment (dry weight) and 42.7 g of Na-Ca-K-Cl fluid, resulting in an initial fluid:sediment mass ratio of 9.8 (Table 2-2). Excess calcite was added to experiment MVCAL to allow estimation of in situ pH by fixing the total ionizable H^+ concentration to calcite solubility in the fluid speciation calculations as described below. This experiment initially contained 4.16 g of sediment (dry weight), 1.96 g reagent-grade calcite and 35.7 g of an Na-Ca-K-Cl fluid, resulting in

an initial fluid:sediment mass ratio of 8.0 (Table 2-3). Initially, both Middle Valley experiments were conducted at 275°C and 350 bars. During experiment MV, the temperature was raised to 325°C at 477 hours and to 350°C at 1017 hours. The temperature was lowered to 325°C at 1686 hours to examine the reversibility of chemical reactions. During experiment MVCAL, the temperature was raised to 325°C at 404 hours and to 350°C at 812.

The Guaymas Basin sediment alteration experiment (GB) initially contained 54.6 g of original pore fluid with a composition similar to seawater and 35.0 g of sediment, resulting in a fluid:sediment mass ratio of 1.6 (Table 2-4). The initial conditions were 325°C and 500 bars; after 414 hours, the temperature was raised to 400°C and the pressure was lowered to 400 bars. The stable isotope systematics of carbon and sulfur species during this experiment have been previously discussed (experiment SED-SW in SEEWALD et al., 1994). Transition metal data from this experiment are reported here for the first time.

2.2.3. Analytical Procedures

Because dissolved metal concentrations are highly sensitive to temperature-dependent precipitation of metal sulfides, we used a rapid sampling technique identical to that described in SEEWALD and SEYFRIED (1990) to extract fluid samples from the reaction cell for metal analysis. A small Ti tube (0.82 ml internal volume) with a Ti valve attached at one end was connected to the reaction cell sampling valve. The sampling valve on the cell was then opened rapidly, allowing fluid to instantaneously fill the attached tube. Two aliquots of fluid were extracted in this manner. The first aliquot served only to flush the sampling lines and was discarded. The second aliquot was extracted into an acid-cleaned Ti tube. The tube was then rinsed with 50% aqua regia and Milli-Q water to recover any metals that may have precipitated upon cooling.

Transition metal concentrations in fluids from experiment GB were measured using DC-plasma emission spectrometry. Analytical uncertainties (2σ) are 2% of the measured concentrations. Dissolved transition metals in the Middle Valley experiments

were analyzed using a high-resolution inductively-coupled plasma mass spectrometer (ICP-MS). Prior to analysis, chloride was removed from the acidified samples by evaporation, followed by dissolution of the resultant precipitate in 50% trace-metal grade HNO_3. This process was repeated three times. After the final evaporation, samples were brought to volume in 2% trace-metal grade HNO_3 for analysis. Analytical uncertainties (2σ) for metals analyzed by ICP-MS are $\leq$ 8 % of the reported concentrations for iron and $\leq$ 3 % for the other transition metals.

Fluid samples for dissolved gas and major ion analysis were removed from the reaction cell directly into gas-tight glass syringes with Teflon plungers. Fluids were analyzed for dissolved Na, Ca, K and NH_3 using DC plasma emission spectroscopy or ion chromatography. Dissolved Cl concentrations were measured by ion chromatography. Aqueous ΣH_2S concentrations were determined gravimetrically following precipitation as Ag_2S in a 5 wt. % $AgNO_3$ solution. Dissolved H_2 concentrations were determined by gas chromatography following a headspace extraction. Dissolved CO_2 and CH_4 concentrations were determined using a gas chromatograph equipped with a purge and trap apparatus. Dissolved acetate concentrations were measured by ion chromatography but were below detection (<1 mmol/kg) in all experiments. Analytical uncertainties (2σ) are $\leq$ 5% of the reported concentrations for all dissolved species, except for H_2, CO_2, which have estimated uncertainties $\leq$ 10%, and ΣH_2S which has an estimated uncertainty of $\leq$ 15%.

2.3. RESULTS

2.3.1. Solid Alteration Products

Albitic feldspar, quartz, amphibole, clay minerals (chlorite, kaolinite, smectite, and illite) and trace amounts of K-feldspar were identified in the altered sediment at the termination of experiment MV using XRD. No calcite remained in the altered sediment from experiment MV, but was detected in the MVCAL alteration products by

effervescence after treatment with dilute HCl. XRD and optical microscopy were used to identify albite, pyrrhotite, and quartz as the dominant alteration phases in experiment GB. As discussed below, changes in fluid chemistry during this experiment indicate quantitative fixation of Mg into the sediments during alteration. This process has been observed in natural hydrothermally-altered sediments from Guaymas Basin (KOSKI et al., 1985; PETER and SCOTT, 1988), Middle Valley (GOODFELLOW and BLAISE, 1988) as well as Escanaba Trough (GERMAN et al., 1995). The absolute amount of this mineral formed during experiment GB, however, was small due to the low fluid:sediment mass ratio employed, precluding detection by XRD analysis due to the high detection limits. However, a fine-grained alteration product coating the surfaces of many minerals was observed using optical microscopy. Previous seawater-sediment alteration experiments conducted at higher fluid:sediment mass ratios suggest that this product is smectite and/or mixed-layer smectite-chlorite (THORNTON and SEYFRIED, 1987; SEEWALD et al., 1990). The presence of a minor carbonate phase among the GB experiment alteration products was also indicated by effervescence following treatment with dilute HCl.

2.3.2. Fluid Chemistry

Alteration of organic and inorganic sedimentary components produced large and rapid changes in fluid chemistry in all experiments (Figs. 2-1 to 2-3; Tables 2-2 to 2-4). Dissolved Na concentrations decreased during experiments MC and MVCAL at 275 and 325°C, but remained constant following the increase in temperature from 325 to 350°C (Figs. 2-1 and 2-2). The initial Na decreases were accompanied by an increase in dissolved Ca. Reaction at 350°C in both experiments resulted in Ca concentrations that were constant within the analytical uncertainty (Fig. 2-1 and 2-2). Na concentrations during experiment GB at 325°C decreased for the first 200 hours and then remained constant. Increasing temperature to 400°C initially resulted in a decreased Na concentration that subsequently increased with continued reaction (Fig. 2-3). In contrast to Na, aqueous Ca initially increased during Guaymas Basin sediment alteration at 325°C. Increasing temperature to 400°C resulted in an initial increase in dissolved Ca, followed

by a decrease (Fig. 2-3). Dissolved concentrations of K increased continuously at all temperatures during all experiments, but remained unchanged when the temperature was lowered from 350 to 325°C during experiment MV (Figs. 2-1 to 2-3). NH_3 concentrations were at or below the detection limit of approximately 10 mmol/kg during experiments MV and MVCAL. During experiment GB, aqueous NH_3 increased from 50.4 to 55.3 mmol/kg at 325°C and to 88.5 mmol/kg at 400°C (Table 2-4).

CO_2 concentrations initially increased to approximately 40 mmol/kg at 275°C during experiment MV (Fig. 2-1). Concentrations increased to approximately 58 mmol/kg when the temperature was increased to 325°C and remained unchanged when the temperature was subsequently increased to 350°C. During experiment MVCAL, aqueous CO_2 also increased when temperature was increased, although continued reaction at 350°C resulted in decreased concentrations (Fig. 2-2). Dissolved CO_2 concentrations in experiment GB increased to 388 mmol/kg during the first 100 hours, and continued to increase with increasing reaction. When the temperature was raised to 400°C, dissolved CO_2 initially increased to a maximum concentration of 570 mmol/kg, but subsequently decreased to 65 mmol/kg (Fig. 2-3). Dissolved H_2 concentrations increased with increasing temperature during all experiments (Tables 2-2 to 2-4), attaining maximum concentrations of 0.4, 0.8, and 6.9 mmol/kg in MV, MVCAL, and GB, respectively. Dissolved CH_4 also increased with increasing temperature during experiments MV and MVCAL (Tables 2-2 and 2-3; Figs. 2-1 and 2-2). In experiment GB, aqueous CH_4 increased at both 325 and 400°C, but concentrations subsequently decreased with continued reaction at 400°C (Table 2-4; Fig. 2-3). ΣH_2S concentrations remained between approximately 2-3 mmol/kg fluid during the 275° and 325°C phases of experiment MVCAL, but increased to a maximum of 6.5 mmol/kg at 350°C (Table 2-3). Due to sample size limitations, the analytical detection limit for ΣH_2S during experiment MV was approximately twice that during experiment MVCAL (Table 2-2). Therefore, ΣH_2S concentrations were measured in only one sample from the 350°C phase of MV, although the presence of H_2S in all samples was confirmed by its diagnostic odor. The

maximum concentration of 6.7 mmol/kg ΣH_2S measured in experiment MV is in close agreement with that measured in experiment MVCAL (Tables 2-2 and 2-3). During experiment GB, dissolved ΣH_2S concentrations initially peaked at 14.9 mmol/kg at 325°C, but subsequently dropped to between 8.7 and 9.0 mmol/kg with increasing reaction time. When the temperature was increased to 400°C, ΣH_2S increased to 14 mmol/kg (Table 2-4).

Dissolved SO_4 in experiment GB immediately dropped from an initial value of 37.3 mmol/kg to $\leq$ 0.19 mmol/kg upon heating during the first 96 hours (Table 2-4). Similarly, dissolved Mg was also rapidly depleted, dropping from an initial value of 58.2 mmol/kg to $\leq$ 0.4 mmol/kg (Table 2-4).

Transition metal concentrations in the three experiments varied strongly as a function of temperature and sediment composition (Tables 2-2 to 2-4, Fig. 2-4). In general, the concentrations of Fe, Mn, and Zn in the final sample at each temperature increased by up to an order of magnitude with increasing temperature (Fig. 2-4). For example, dissolved Zn increased from 9.8 μmol/kg at 275°C to a maximum of 104 μmol/kg in experiment MV and from 62.9 mmol/kg at 325°C to 1062 μmol/kg at 400°C in experiment GB. Lead concentrations, which were measured only in experiments MV and MVCAL, also increased greatly with increasing temperature, attaining a maximum of 10.5 μmol/kg at 350°C (Tables 2-2 and 2-3, Fig. 2-4). In contrast, dissolved Cu concentrations during experiments MV and MVCAL remained consistently low, near 1 μmol/kg, while those in experiment GB were consistently below the higher detection limits (~10 μmol/kg) characteristic of the DC-plasma emission spectroscopy used for this experiment. At a given temperature, alteration of organic-rich sediment from Guaymas Basin resulted in dissolved Fe, Mn, and Zn concentrations that were up to two orders of magnitude greater than in fluids derived from alteration of organic-poor Middle Valley sediment. For example, at 325°C, Mn concentrations in experiment MV were only 97.2 μmol/kg fluid as compared to 750 μmol/kg fluid in experiment GB.

At the end of experiment MV, temperature was lowered from 350°C to 325°C.

Concentrations of all metals decreased and showed reasonable agreement with the concentrations measured during the earlier 325°C phase of the experiment (Tables 2-2 to 2-4; Fig. 2-4).

2.4. DISCUSSION

2.4.1. Reaction Mechanisms

The reversibility of aqueous Mn, Fe, Zn, and Cu concentrations upon the return to 325°C during the final phase of experiment MV (Fig. 2-4) indicates that the abundances of these species were controlled by the solubility of metal-bearing minerals during hydrothermal sediment alteration. For the chalcophile elements (Fe, Zn, Cu, Pb) aqueous mobility in sulfur-bearing systems is likely regulated by sulfide phases. The solubility of carbonates and oxides may also be important, especially for non-chalcophile elements such as Mn. Although variations in the specific mineral assemblage present in each experiment influences the solubility of an individual metal, the uniformly greater concentrations of *all* metals in the Guaymas Basin fluids relative to the Middle Valley fluids suggest that there are significant differences in the composition of fluids causing mineral dissolution. The aqueous activities of H^+, H_2S, and CO_2 strongly influence the solubility of metal carbonates and sulfides. In general, increasing H^+ activity enhances the solubility of carbonates and sulfides at constant H_2S and CO_2 activity, while at constant pH, increasing aqueous H_2S and CO_2 activities decrease the solubility of sulfides and carbonates, respectively. Accordingly, higher concentrations of H_2S and CO_2 associated with greater metal mobility during alteration of Guaymas Basin sediment relative to Middle Valley sediment suggests that the large differences in aqueous metal concentrations during these experiments reflect in situ pH variations.

In situ pH during hydrothermal sediment alteration is controlled by the relative abundance and reactivity of organic and inorganic sedimentary components that participate in pH-dependent alteration processes. During alteration of organic-lean Middle Valley sediment, pH is likely to be controlled by the stability of aluminosilicates

such as feldspars and illite, a common alteration product observed both in this study as well as in the natural system (LEYBOURNE and GOODFELLOW, 1994) according to reactions of the type:

$$4\ NaAlSi_3O_8 + 3\ KAlSi_3O_8 + 4\ H^+ = K_3Al_4(OH)_4Si_5Al_3O_{20} + 4\ Na^+ + 16\ SiO_2. \quad (1)$$

albite K-feldspar illite quartz

Rapid and large changes in measured Na and K concentrations following changes in temperature indicate rapid reaction kinetics for Na- and K- bearing minerals during the experiments. The subsequent approach, in most cases, to near steady concentrations with continued reaction at a given temperature (Figs. 2-1 to 2-3) suggests that a state of thermodynamic equilibrium with respect to Reaction (1) may have been approached. Because large amounts of Na fixation are required to change the absolute activity of aqueous Na, equilibration of Na-rich fluids of seawater chlorinity according to reaction (1) will effectively fix pH at a constant value for a given temperature. For example, the 42 mmol/kg decrease during the 275°C phase of experiment MV was the largest constant-temperature decrease observed during the Middle Valley experiments, but represents only a 9 % decrease in absolute abundance that corresponds to a similar decrease in aqueous activity.

Owing to the strong pH dependence of carbonate mineral solubility:

$$Ca^{2+} + CO_2 + H_2O = CaCO_3 + 2H^+, \quad (2)$$

calcite

extensive dissolution of detrital and added calcite occurred during the Middle Valley experiments to maintain saturation at pH values controlled by the aluminosilicate assemblage. Almost identical aqueous CO_2 and Ca concentrations were observed during experiments MV and MVCAL at 275°C suggesting similar H^+ activity. Upon increasing temperature to 325 and 350°C, exhaustion of the detrital carbonate reservoir during experiment MV resulted in lower CO_2 concentrations relative to experiment MVCAL which contained added calcite. During the 325 and 350°C phases of each experiment, dissolved Na concentrations in experiment MVCAL were slightly lower than those observed in experiment MV (Tables 2-2 and 2-3), consistent with enhanced albitization

due to H^+ consumption (reaction 1) by calcite dissolution (reaction 2). Maintenance of equilibrium according to reaction (1), however, kept in situ pH at similar values during both experiments.

Fluid-sediment interaction during the initial stages of experiment GB was characterized by substantially different reactions than the Middle Valley experiments due to the presence of Mg and SO_4 in the starting fluid and more abundant sedimentary organic matter. Rapid anhydrite ($CaSO_4$) precipitation during early stage alteration at 325°C resulted in complete removal of SO_4 from solution (SEEWALD et al., 1994). In addition, fixation of Mg as the $Mg(OH)_2$ component of Mg-rich aluminosilicates resulted in the almost quantitative removal of aqueous Mg (SEEWALD et al., 1994). Formation of Mg-rich alteration phases represents an effective mechanism for generating acidity, provided high Mg activity is maintained in solution (Thornton and Seyfried, 1987; Seewald et al., 1990, 1994). This was not the case for experiment GB during which complete Mg removal occurred within the first 98 h of reaction at 325°C (Table 2-4). Accordingly, reaction of other sedimentary components is responsible for regulating in situ pH at sufficiently low values to attain the observed aqueous concentrations of transition metals during later stage reaction. Although K-bearing minerals underwent extensive alteration during Guaymas Basin sediment alteration, the absence of illite in the alteration products and substantially greater metal mobility suggests that alkali feldspar-illite-quartz equilibria (e.g., Reaction 1) was not responsible for regulating pH following early stage Mg-removal.

Previous studies have demonstrated that H^+ activity during organic-rich sediment alteration is strongly influenced by pH-dependent reactions involving sedimentary organic matter (THORNTON and SEYFRIED, 1987; SEEWALD et al., 1990, 1994). In particular, thermal maturation of organic material releases large quantities of CO_2 to solution as a result of decarboxylation and oxidation reactions. This CO_2 can induce calcite precipitation and the generation of acidity according to reaction (2). Decreased calcite solubility in response to increased aqueous CO_2 is contrary to the effects in pure water-carbonate systems where increasing P_{CO2} increases calcite solubility (Stumm and

Morgan, 1996). However, in the complex chemical environment that characterizes high-temperature sediment alteration, pH is not dominated solely by carbonate equilibria due to numerous reactions involving aluminosilicates and protonation of organically derived species such as carboxylic acid anions and ammonia.

The generation of acidity by calcite precipitation is also enhanced by the presence of a continuous source of Ca during sediment alteration. Extensive Na fixation and the presence of abundant albite in the alteration products from the experiments suggests that albitization of plagioclase released Ca^{2+} to solution according to the reaction:

$$2\,Na^{+} + 4\,SiO_2 + CaAl_2Si_2O_8 = 2\,NaAlSi_3O_8 + Ca^{2+}, \qquad (3)$$

quartz anorthite albite

where anorthite and albite represent the endmember components of plagioclase feldspar solid solution. The generation of acidity associated with the cycling of aluminosilicate-derived Ca and organically derived carbon into calcite can be represented by the overall reaction:

$$2\,Na^{+} + 4\,SiO_2 + H_2CO_3 + CaAl_2Si_2O_8 = CaCO_3 + 2\,NaAlSi_3O_8 + 2\,H^{+}. \qquad (4)$$

quartz anorthite calcite albite

Equation (4) represents an effective mechanism to generate low in situ pH if a large and continuous source of organically derived CO_2 is available. Accordingly, despite the likelihood that experiment MVCAL may have equilibrated according to Reaction (4) as well as Reaction (1) due to the addition of calcite, the absence of sufficient sedimentary organic matter to generate CO_2 precluded production of acidity by this mechanism. While weak acids such as NH_4^{+} and acetic acid could also buffer pH under the appropriate conditions, this was not the case during the experiments because the buffer capacity of these aqueous species at the observed concentrations was far exceeded by the buffer capacity of the sedimentary mineral assemblages.

2.4.2. In situ pH

Determination of in situ pH during the experiments provides important constraints on sediment alteration processes and metal transport. Measured pH at 25°C, however,

does not accurately reflect H^+ activity at the temperature and pressure of an experiment due to large changes in the dissociation constants of protonated species such as NH_4^+, H_2CO_3, HCO_3^-, H_2S, HCl, and organic acids as a function of temperature and pressure. Additionally, measured pH values are sensitive to metal sulfide precipitation and degassing of acid volatiles such as CO_2 and H_2S as fluids equilibrate at ambient laboratory temperature and pressure. Determination of in situ pH during the experiments was accomplished by calculating the thermodynamically stable distribution of aqueous species at the conditions of each experiment using the computer code EQ3NR (WOLERY, 1992) with a thermodynamic dataset based on the SUPCRT92 compilation of Johnson et al (1992). Total measured concentrations of Na, K, Ca, Cl, NH_3 and CO_2 were used as input parameters for the fluid speciation calculations. Although measured pH (25°C) can be utilized as an input constraint on total ionizable H^+, we chose not to use this approach because of the significant errors associated with this measurement as detailed above. Total ionizable H^+ was controlled during fluid speciation calculations by assuming the experiments were saturated with calcite and constraining in situ H^+ activity to calcite solubility limits. The assumption of calcite saturation is valid for experiments MVCAL and GB in which calcite was present at the termination of each experiment but is less valid for experiment MV since calcite was not identified in the alteration products. However, the similarity of dissolved Ca and CO_2 concentrations from experiments MV and MVCAL at 275°C suggests that fluids in experiment MV were initially saturated with calcite. Calculations based on this assumption are nonetheless useful since they provide constraints on the upper limit for in situ pH during experiment MV. An alternative approach would have been to assume equilibrium with a mineral assemblage represented by Reaction (1). The absence of thermodynamic data for illite at the temperature and pressure of these experiments currently precludes this approach.

Calculated in situ pH values increased with increasing temperature and were considerably lower during experiment GB relative to experiments MV and MVCAL (Fig. 2-5). For example, at 325°C, calculated in situ pH values were 5.2 and 5.8 for experiments GB and MVCAL, respectively (Fig. 2-5). The 0.6 difference in pH is an

order of magnitude greater than the difference of 0.04 pH units based on error in the analytical measurements. The error associated with the thermodynamic data is difficult to quantify due to the large number of species included in the chemical models, each of which has its own associated error. However, since the same thermodynamic dataset was used for all calculations, the associated errors will affect the speciation results uniformly and have little effect on the calculated pH differences. A pH difference of 0.6 units is significant with respect to the aqueous mobility of metals because the equilibrium activities of divalent metal ions in equilibrium with minerals such as sulfides will vary as the square of H^+ activity according to the general reaction:

$$MeS_{(s)} + 2\ H^+ = Me^{2+} + H_2S_{(aq)}, \qquad (5)$$

where Me represents a divalent metal. Thus, a 0.6 log unit increase in H^+ activity should result in a 1.2 log unit increase in aqueous metal activities at constant H_2S activity. Dissolved metal concentrations at 325°C during experiment GB were 0.2 to 1.2 log units higher than during experiments MV and MVCAL, values that are consistent with the in situ pH estimates and measured H_2S concentrations.

Calculated pH values for both Middle Valley experiments were identical at 275°C but showed increasing divergence with increasing temperature (Fig. 2-5). Because our assumption of calcite saturation is likely not valid during experiment MV at 325 and 350°C, the relatively high calculated in situ pH values may be an artifact of this assumption and not representative of actual fluid composition. Generally similar concentrations of Fe, Zn, Cu, and Pb during experiments MV and MVCAL suggest similar in situ pH values.

In contrast to Fe, Zn, Cu, and Pb, aqueous Mn concentrations were significantly higher during experiment MV relative to MVCAL. This difference may be attributable to the addition of calcite in the latter experiment. Although our fluid speciation calculations indicate substantial undersaturation with respect to rhodochrosite ($MnCO_3$), Mn readily substitutes for Ca as a trace component to form manganiferous calcite (DEER et al., 1965; CAPOBIANCO and NAVROTSKY, 1987). Accordingly, recrystallization of excess calcite (2 g calcite added to 4.2 g sediment) during experiment MVCAL may have created a sink

for Mn that regulated its abundance in solution. Due to the absence of calcite during experiment MV, Mn concentrations were likely regulated by clay minerals which have been shown to be important sinks for Mn in hydrothermally altered portions of the oceanic crust (ALT et al. 1989).

2.4.3. Comparison with Basalt Alteration Experiments

Sediments and basaltic rocks coexist at sediment-covered spreading centers and represent potential sources of metals that can be mobilized during reaction with hydrothermal fluids. There have been numerous laboratory studies of metal mobility during seawater-basalt interaction under hydrothermal conditions (BISCHOFF and DICKSON, 1975; MOTTL et al., 1979; SEYFRIED and BISCHOFF, 1981; SEYFRIED and MOTTL, 1982; SEYFRIED and JANECKY, 1985; SEYFRIED, 1987; SEEWALD and SEYFRIED, 1990). Except for the experiments of Seewald and Seyfried (1990), fluid sampling techniques were not optimized to minimize precipitation of metals during extraction of fluids from the reaction cell. Accordingly, there is significant uncertainty associated with dissolved metal concentrations reported for these experiments, especially for Fe, Zn, and Cu which are more prone to sampling related artifacts than Mn (SEEWALD and SEYFRIED, 1990). Comparison of our results with those of Seewald and Seyfried (1990) indicates that hydrothermal alteration of Middle Valley and Guaymas Basin sediment produces aqueous Mn, Fe, and Zn concentrations that are generally greater than values observed during basalt alteration at the same temperature and similar pressures (Fig. 2-4). As is the case during hydrothermal sediment alteration, temperature plays a key role in reactions responsible for metal mobilization during basalt alteration as evidenced by the 1 to 2 orders of magnitude increase in metal mobility associated with an increase in temperature from 300 to 400°C (Fig. 2-4).

Greater mobility of Mn, Fe, and Zn during hydrothermal sediment alteration relative to basalt alteration for a given temperature and pressure likely reflects differences in reaction mechanisms responsible for regulating in situ pH. Experimental and theoretical investigations have demonstrated that during interaction of Na-K-Ca-Cl fluids

and basalt, fixation of Ca^{2+} in hydrous phases such as epidote regulates in situ pH. This process can be represented in general by the overall reaction:

$$Na^+ + 2\ CaAl_2Si_2O_8 + 2\ SiO_2 + H_2O = NaAlSi_3O_8 + Ca_2Al_3Si_3O_{12}(OH) + H^+, \quad (6)$$

anorthite quartz albite clinozoisite

where anorthite, albite, and clinozoisite represent endmember components of plagioclase and epidote solid solutions. Reaction (6) is analogous to reaction (4) in that Ca released during the albitization of plagioclase is fixed in a calcic alteration phase. However, during organic-rich sediment alteration, calcite represents the dominant stable calcic phase due to the release of abundant CO_2 from organic matter decomposition. Substantially higher aqueous metal mobility was observed during Guaymas Basin sediment alteration relative to basalt alteration, suggesting that plagioclase-calcite equilibria constrains the pH at a lower value than plagioclase-epidote equilibria. Similarly, moderately higher aqueous metal concentrations during Middle Valley sediment alteration indicates feldspar-illite equilibria may regulate pH at values slightly lower than plagioclase-epidote equilibria.

Comparison of aqueous Cu mobility during hydrothermal sediment and basalt alteration is hampered by the high uncertainty associated with the analytical method used to measure Cu concentrations in fluids from experiment GB and the basalt alteration experiment of Seewald and Seyfried (1990). Except for the reported Cu concentration at 400°C during the basalt alteration experiment, Cu concentrations measured at 300 and 350°C during basalt alteration and all temperatures during experiment GB were very close to or below the detection limit of the DC-plasma emission spectrometer used for the analyses. Examination of Figure 2-4 reveals that, in contrast to data for the abundance of other metals, basalt alteration at 400°C was characterized by higher aqueous concentrations of Cu relative to Guaymas Basin sediment alteration at the same temperature (Fig. 2-4).

Relatively low Cu during Guaymas Basin sediment alteration is consistent with the results of Seyfried and Ding (1993) who demonstrated that in addition to pH, Cu mobility in subseafloor hydrothermal systems is strongly dependent on the redox state of

the chemical system. In particular, greatly enhanced Cu mobility was observed under relatively oxidizing conditions during equilibration of Cu- and Fe-sulfide phases with Na-K-Cl fluids of seawater chlorinity at 400°C and 500 bars. Aqueous H_2 concentrations are an excellent indicator of redox at the temperatures of our experiments due to the rapid rate of equilibration for the reaction:

$$H_2O_{(l)} = H_{2(aq)} + \frac{1}{2} O_{2(g)}. \quad (7)$$

Values of fO_2 for the sediment and basalt experiments were calculated from measured aqueous H_2 and thermodynamic data included in the compilation of Johnson et al. (1992) for Reaction (7) (Fig. 2-6). These calculations reveal that basalt alteration resulted in higher oxygen fugacties during Middle Valley sediment alteration, which in turn were higher than during Guaymas Basin sediment alteration. The extremely reducing conditions during experiment GB reflect the high reactivity of reduced carbon species in the abundant sedimentary organic matter (THORNTON and SEYFRIED, 1987; SEEWALD et al., 1990, 1994) and are consistent with low Cu mobility during this experiment, the relatively low in situ pH notwithstanding. Thus, in addition to participating in reactions that regulate pH, sedimentary organic matter may influence the mobility of redox sensitive metals such as Cu by regulating redox conditions.

2.4.4. Comparison with Hydrothermal Vent Fluids

Hydrothermal fluids venting from sediments that overly young oceanic crust have been observed and sampled at Middle Valley, northern Juan de Fuca Ridge (BUTTERFIELD et al., 1994a), Escanaba Trough, Gorda Ridge (CAMPBELL et al., 1994), and Guaymas Basin, Gulf of California (VON DAMM et al., 1985b; CAMPBELL et al., 1988a; SEEWALD et al., 1998). A common feature of these systems is the intrusion of basaltic dikes and sills into overlying sediments to create a series of alternating lithologies characterized by vastly different physical and chemical properties. Sediments at Middle Valley and Escanaba Trough are composed of turbiditic and hemipelagic sediments derived from the North American continental margin with a small component of biological detritus produced in the surface waters (GOODFELLOW and BLAISE, 1988; DAVIS et al., 1992). In

contrast, higher biological productivity in the surface waters at Guaymas Basin results in a substantially higher biogenic component relative to continentally-derived hemipelagic and turbiditic material (KOSKI et al., 1985; VON DAMM et al., 1985b).

Relative to seawater, vent fluids from sediment-covered spreading centers are depleted in Na, SO_4, and Mg and enriched in K, Ca, metals, alkali and alkaline earth trace elements, H_2S, and SiO_2 (VON DAMM et al., 1985b; CAMPBELL et al., 1988a; BUTTERFIELD et al., 1994a; CAMPBELL et al., 1994; SEEWALD et al., 1998). High concentrations of NH_3 in these fluids provide strong evidence for direct interaction with organic-bearing sediments. Comparison of the results from our sediment alteration experiments demonstrates that these general trends are reproduced during reaction with sediment. Careful examination of the data, however, reveals some important differences with respect to the extent of chemical enrichment or depletion. For example, NH_3 concentrations in vent fluids from Guaymas Basin are 3 to 8 times lower than those in the experimental fluids (Table 2-4; VON DAMM et al., 1985b; SEEWALD et al., 1998). At Middle Valley, Ca concentrations are 1.2 to 2.5 times higher and K concentrations are 1.5 to 4.8 times lower than those produced during our experiments (Table 2-2; BUTTERFIELD et al., 1994a). These discrepancies may reflect differences in fluid:sediment mass ratios during our experiments relative to natural systems. The Guaymas Basin experiment was conducted at a maximum fluid:sediment mass ratio of only 1.6. Estimates of fluid:sediment ratios for the Guaymas Basin system assuming complete mobilization of sedimentary N as aqueous NH_3 during hydrothermal alteration range from 9.2 to 13.4 (SEEWALD et al., 1994). Degradation of sedimentary organic matter during experiment GB would have resulted in lower aqueous concentrations of NH_3 had the experiment been conducted at a higher fluid:sediment mass ratio. A fluid:sediment mass ratio of 15.3 is calculated for Middle Valley assuming that complete mobilization of the approximately 0.06 wt. % N in the unaltered sediments (GOODFELLOW and PETER, 1994) resulted in the 2.3 mmol/kg NH_3 measured in the vent fluids (BUTTERFIELD et al., 1994a). Therefore, it appears likely that fluid:sediment ratios for the Middle Valley system are slightly higher than those utilized in the experiment and may account for the lower K observed in Middle

Valley vent fluids relative to the experiments (Table 2-2; BUTTERFIELD et al., 1994a).

Results of hydrothermal experiments conducted at fluid:sediment ratios of 4 to 80 with Middle Valley sediment similar to that used in the experiments presented here (SEEWALD et al., 2000) suggest that variations in fluid:sediment mass ratio cannot account for substantially higher Ca concentrations in Middle Valley vent fluids (40 to 81 mmol/kg; Butterfield et al., 1994a) relative to the experimental fluids (29 to 33 mmol/kg; Table 2-2). High Ca concentrations in Middle Valley vent fluids may be generated by hydrothermal alteration of basalt glass at low fluid:rock ratios, a process that has been shown to generate substantially higher Ca concentrations than alteration of crystalline basalt (MOTTL and HOLLAND, 1978; SEYFRIED, 1987, SEEWALD and SEYFRIED, 1990). Alternatively, high Ca concentrations may reflect the combined effects of fluid-basalt and fluid-sediment reactions that cannot be reproduced by closed-system laboratory experiments containing only sediment or basalt. For example, organically derived species such as CO_2 that are released to solution during sediment alteration in recharge zones may influence subsequent basalt alteration in high temperature reaction zones.

Early models for the formation of hydrothermal fluids at sediment-covered spreading centers involve the reaction of seawater-derived fluids with basaltic crust to produce a metal-rich fluid which subsequently entered the sediment pile where it underwent further reactions before venting at the seafloor (SCOTT 1985; VON DAMM et al., 1985b). Arguments in favor of extensive fluid-basalt chemical interaction at sediment-covered spreading centers have been based on the observation that vent fluids are characterized by: 1) almost complete removal of Mg and SO_4; 2) high reduced sulfur content; 3) Ca enrichments; 4) high ^3He content; 5) basaltic $^{87}Sr/^{86}Sr$ ratios of vent fluids; and 6) basaltic Pb isotopic composition. However, experiments indicate that items 1 through 3 are not exclusive features of seawater-basalt interaction and readily occur during seawater-sediment interaction (this study; THORNTON and SEYFRIED, 1987; SEEWALD et al., 1990, 1994; VON DAMM 1991). Other studies suggest that the geochemical processes responsible for the addition of magmatic volatiles and metals to hydrothermal vent fluids are not identical and that He isotopes may not be a good tracer

of water-rock interaction (STUART et al., 1994, 1999). Analysis of the Pb and Sr isotopic composition of vent fluids and alteration minerals provides the most unambiguous indication of interaction between hydrothermal fluids and basaltic rocks and sediments. These data indicate that Pb and Sr at Middle Valley are derived primarily from reaction with basaltic rocks with a small but significant sedimentary contribution (GOODFELLOW and FRANKLIN, 1993; STUART et al., 1999; BJERKGÅRD et al., 2000). At Guaymas Basin, a fraction of Pb is derived from basalt alteration, but this input is reduced in importance relative to reaction with overlying sediments (CHEN et al., 1986; LEHURAY et al., 1988). The Sr isotopic composition of Guaymas Basin vent fluids is slightly more radiogenic than local basalts, reflecting a mixed basalt-sediment signal (VON DAMM et al., 1985b). At Escanaba Trough, the Pb isotopic composition of vent fluids reflects dominance of the sedimentary Pb composition over that of underlying basalts (LEHURAY et al., 1988; ZIERENBERG et al., 1993; GERMAN et al., 1995), while the Sr isotopic ratios are consistent with interaction of the vent fluids with basalt, overlying sediments and seawater (CAMPBELL et al., 1994; GERMAN et al., 1995).

The observed differences in the relative importance of sedimentary input on the Pb and Sr isotopes in fluids from sediment-covered spreading centers (i.e., Middle Valley < Guaymas Basin < Escanaba Trough) may reflect differences in the hydrologic regimes within the sediments at each vent fields. At Middle Valley, fluid flow is focused along relatively narrow zones, associated with fractures and faulting (GOODFELLOW and FRANKLIN, 1993; DAVIS and FISHER, 1994). This would have served to limit the amount of interaction between fluids and sediments during upflow, and preserved the signature of basalt-fluid interaction at depth. Guaymas Basin and Escanaba Trough, in contrast, are characterized by areas of more diffuse fluid flow through the sediments in addition to a component of fracture-focused discharge (HOLMES and ZIERENBERG, 1990; FISHER and BECKER, 1991; GIESKES et al., 1991; MAGENHEIM and GEISKES, 1994). Where fluid flow approaches that through an ideal porous medium, fluid-sediment interaction will be more pervasive, and can lead to a complete overprinting of any earlier basalt interaction that may have occurred.

Direct comparisons of metal concentrations in vent fluids with results of the experiments are difficult since significant uncertainties are associated with measured transition metal abundances in vent fluids (PHILPOTTS et al., 1987; VON DAMM, 1983, 1990; VON DAMM et al., 1985a,b; TREFRY et al., 1994). As is the case for fluid samples from the experiments, precipitation of metals from vent fluid samples upon cooling is a common phenomenon that results in the formation of black metal precipitates in the titanium fluid samplers (VON DAMM et al., 1985b; CAMPBELL et al., 1988a; BUTTERFIELD et al., 1994a). However, metal precipitation during sampling does not affect all metals uniformly. Laboratory experiments have demonstrated that Mn precipitation is kinetically inhibited and fluid samples may accurately record high temperature concentrations despite subsequent cooling, while precipitation of the chalcophile elements, Zn, Fe, Cu and Pb, as sulfide minerals due to temperature change occurs more rapidly (SEEWALD and SEYFRIED, 1990). This result is consistent with field data that in many instances show little scatter in the data used to extrapolate endmember Mn concentrations and a substantially larger degree of scatter in the data used to extrapolate endmember Zn, Fe, Cu, and Pb concentrations (VON DAMM et al, 1985a,b; BUTTERFIELD et al., 1994a,b; VON DAMM, 1983). Accordingly, aqueous Mn concentrations may represent a good candidate for the comparison of metal mobility in laboratory experiments and natural systems.

Endmember Mn concentrations in Middle Valley hydrothermal fluids vary from 78 μmol/kg at the Bent Hill vent site to 63 μmol/kg at the Dead Dog vent field where maximum vent fluid temperatures range from 265 to 276°C, respectively (BUTTERFIELD et al., 1994a). These Mn concentrations are slightly higher than aqueous concentrations observed during experiment MV at a similar temperature of 275°C, but are in excellent agreement with the aqueous concentrations observed at 325°C (Fig. 2-7). Considering the strong temperature dependence of Mn mobility during both sediment and basalt alteration, this comparison suggests that subsurface temperatures in the zone of last chemical equilibration may be a few tens of degrees hotter than the exit temperatures, but that extensive subsurface cooling of more than 50°C in response to conductive heat loss

or subsurface mixing with cold seawater has likely not occurred. This conclusion is consistent with temperature estimates for these fluids based on quartz geothermometry (BUTTERFIELD et al., 1994a). It must be borne in mind, however, that these temperature estimates do not preclude the possibility of higher temperatures during prior stages of hydrothermal circulation. Indeed, as noted by Butterfield et al. (1994a) the most likely explanation for Cl concentrations below seawater values in the fluids venting at ODP Mound near Bent is phase separation which requires temperatures ≥375°C at subsurface pressures (≥240 bars). Thus, the consistency between measured temperatures, temperatures estimated from Mn concentrations, and quartz geothermometry provide strong evidence that phase separated fluids at Middle Valley have cooled and chemically reequilibrated with sediment and/or basalt at or near 325°C before venting at the seafloor.

Maximum concentrations of Fe, Zn, and Pb in Middle Valley vent fluids are considerably lower than concentrations observed during the Middle Valley experiments conducted at the measured vent temperatures (Fig. 2-7; Tables 2-1 to 2-3). The high degree of scatter associated with the field data (BUTTERFIELD et al., 1994a) suggests that this discrepancy may be due to the loss of these elements by precipitation, either in the titanium samplers after collection or within the vent structures themselves prior to sampling. The discrepancy between aqueous concentrations observed during the experiments and those measured in natural fluid samples is larger for Pb than the other metals and may suggest that Pb is affected to a greater extent by sampling artifacts. However, low levels of Pb in massive sulfide deposits at Middle Valley (GOODFELLOW and FRANKLIN, 1993; KRASNOV et al., 1994) suggest that it may never have been present in solution at levels attained during the experiments. Such a model is consistent with extensive reaction of hydrothermal fluids in deep-seated reaction zones with basalt, which contains 30 to 180 times less Pb than unaltered pelagic and terrigenous sediments (STUART et al., 1999). Additional evidence for a basaltic source of Pb in the Bent Hill massive sulfides is provided by Pb isotopic analysis that indicates 21 to 100 % of the Pb is derived from basaltic crust (STUART et al., 1999). Because basaltic rocks are relatively Pb-poor, the ore-forming fluids must have reacted with 40 to 900 times more basalt than

sediment (STUART et al., 1999). In contrast, the Pb isotopic composition of sulfides from Escanaba Trough is dominated by sedimentary Pb (LEHURAY et al., 1988). Thus, it can be postulated that prior to sampling, hydrothermal fluids at Escanaba Trough may contain Pb concentrations that approach values observed during the experiments, which may account for the occurrence of galena in hydrothermal polymetallic sulfides from that site (KOSKI et al., 1988; ZIERENBERG et al., 1993).

Values for measured Cu concentrations in vent fluids from Middle Valley are comparable to values obtained during the experiments (Fig. 2-7). However, the vent fluid Cu data from Middle Valley has a high degree of scatter and may underestimate actual vent fluid concentrations.

Maximum measured concentrations of Mn, Fe, and Zn at Guaymas Basin in comparison with the sediment alteration experiments are also shown in Figure 2-7. Taken as a whole, there is greater uncertainty associated with Fe and Zn data relative to Mn in the vent samples, suggesting some of the fluids may have been affected by metal precipitation during sampling (VON DAMM, 1983; VON DAMM et al., 1985b). However, we have plotted the data for vent areas 3 and 4, which had the highest measured metal concentrations and least amount of scatter, suggesting that the measured values may represent actual fluid concentrations. For a given temperature, the concentrations of *all* metals in fluids from Guaymas Basin are substantially lower than those observed during the Guaymas Basin sediment alteration experiment, but in reasonable agreement with values observed during Middle Valley sediment and basalt alteration experiments (Figs. 2-4 and 2-7). The disparity between the natural fluids and experiment GB cannot be attributed to variations in sulfide mineral solubility in response to different H_2S activities because the experimental fluids contain up to twice as much H_2S as has been measured in vent fluids (Tables 2-2 to 2-4). The similarity between metal concentrations in Guaymas Basin fluids and the fluids derived from basalt alteration experiments could be used as evidence to suggest that fluid composition is regulated by reaction with basalt. However, basalt is not likely to be the only source of metals since the high abundance of sediment-derived aqueous species such as CO_2, CH_4, NH_3, alkali and alkali earth elements, and

petroleum, indicate that hydrothermal fluids are reacting with the sediments. In addition, the isotopic composition of Pb and Sr in fluids and minerals provides compelling evidence for extensive interaction with organic-rich sediment (CHEN et al., 1986; LEHURAY et al., 1988). We believe the higher metal concentrations in fluids from experiment GB are the result of lower fluid:sediment mass ratios relative to the natural system. Lower fluid:sediment mass ratios during the experiment (1.6 to 0.7 versus 9.2 to 13.4 for the natural system) would result in higher CO_2 and Ca concentrations in response to organic matter degradation and plagioclase albitization. This would in turn result in greater calcite precipitation, the generation of higher amounts of acidity according to reaction (1), and subsequently greater metal mobility.

The lack of Pb concentration data for experiment GB precludes comparison with Pb concentrations in Guaymas Basin vent fluids. Comparison of results from Guaymas Basin vents with the results from the Middle Valley sediment alteration experiments, however, reveals substantially lower Pb concentrations in the vent fluids. The vent fluid data contain a high level of scatter (VON DAMM et al., 1985b) suggesting that reported concentrations may represent minimums due to precipitation during sampling. The presence of galena in concentrations up to 5 vol. % in sulfide samples from Guaymas Basin (PETER and SCOTT, 1988), suggests that some fluids may contain relatively high Pb concentrations.

Except for vent areas 4 and 5 which contained 1.1 and 0.1 μmol/kg Cu, respectively, Cu abundances were below detection in fluids from Guaymas Basin (VON DAMM, 1983; VON DAMM et al., 1985b). Low Cu values may reflect precipitation in the samplers upon cooling. Alternatively, the low concentrations may be the result of extremely reducing conditions during fluid-sediment interaction as indicated by H_2 concentrations as high as 2.3 mmol/kg (SEEWALD et al., 1998).

Within the context of early models for hot spring systems at sediment-covered spreading centers, whereby fluids first react with basalt before entering the sediment pile, differences in the composition of fluids from sedimented and unsedimented systems are attributed to reactions with sediments. In particular, it is hypothesized that the

concentrations of ore-forming metals, which are approximately an order of magnitude lower in vent fluids from sediment-covered spreading centers relative to fluids from bare-rock systems, resulted from titration of acidity during fluid-sediment interaction. This model raised the intriguing possibility that an ore deposit could be forming in the subsurface at the interface between basaltic crust and sediment. The results of our experiments, however, do not support the critical assumption that reaction with sediment produces a hydrothermal fluid characterized by higher pH and therefore lower metal content relative to reaction with basalt. Indeed, the laboratory experiments indicate exactly the opposite: for a given temperature and pressure, fluid-sediment chemical interaction results in equal to or higher metal mobility relative to fluid-basalt interaction. This is because pH is not buffered solely by carbonate equilibria but is controlled by competing carbonate and aluminosilicate reactions. In the case of Guaymas Basin, increased CO_2 concentrations that result from organic matter alteration lead to calcite precipitation rather than dissolution and a subsequent decrease in fluid pH. Accordingly, it does not appear that the differences in reaction mechanisms controlling vent fluid chemistry during sediment and basalt alteration are responsible for low metal concentrations in hydrothermal fluids at sediment-covered spreading centers relative to bare-rock systems (Table 2-1).

Lower aqueous metal concentrations in vent fluids from sediment-covered spreading centers can be accounted for by the role of temperature in regulating metal mobility during fluid-sediment interaction. Measured vent temperatures show a high degree of variability with maximum temperatures at Middle Valley, Escanaba Trough, and Guaymas Basin of 276, 217, and 317°C, respectively (VON DAMM et al., 1985b; CAMPBELL et al., 1988a; BUTTERFIELD et al., 1994a; CAMPBELL et al., 1994; SEEWALD et al., 1998). These values are significantly lower than at unsedimented hydrothermal systems where temperatures in the range of 300 to 400°C are routinely observed (VON DAMM et al., 1985a; CAMPBELL et al., 1988a,b; TIVEY et al., 1990; VON DAMM, 1995). Considering the strong temperature dependence of metal mobility during the experiments, especially at conditions approaching the critical point of seawater, the low concentrations

of ore-forming metals in vent fluids from sedimented systems likely reflect the lower vent temperatures that characterize these systems. In many cases, however, measured vent temperatures are not indicative of maximum temperatures encountered by a fluid during reaction with a basaltic heat source. At Middle Valley and Escanaba Trough, the presence of Cl-depleted vent fluids with temperatures <276°C (BUTTERFIELD et al., 1994a; JAMES et al., 1999) provide compelling evidence that these fluids were sufficiently hot (>375°C) to undergo phase separation. The presence of sediments apparently creates subsurface hydrologic conditions that in many cases prevent vent fluids from reaching the seafloor without undergoing extensive cooling due to conductive heat loss or subsurface mixing with cool seawater. This cooling is occurring at sufficient depths to allow almost complete re-equilibration of fluid composition prior to venting. Thus, although temperatures in the deepest and hottest regions of subsurface reaction zones may be similar to those in bare-rock systems, the only evidence for such interaction may be limited to species such as Cl that are not affected by continued reaction at lower temperatures during ascent to the seafloor.

Extensive cooling and re-equilibration of metal-rich fluids during upflow suggests subsurface metal deposition at sediment-covered spreading centers may widespread. Although sample coverage is extremely limited, large-scale subsurface sulfide deposits within the sediment pile have not yet been identified, but may be forming. Deposition of sulfides within the feeder zones underlying the Bent Hill massive sulfide deposit at Middle Valley, however, provides evidence for subsurface metal precipitation (SHIPBOARD SCIENTIFIC PARTY, 1997; JAMES et al., 1998; ZIERENBERG et al., 1998). That the bulk of Bent Hill massive sulfide deposit is located on the seafloor suggests that extensive subsurface cooling did not affect the fluids responsible for its formation and is consistent with fluid inclusion and mineralogical data that suggest formation from fluids with temperatures of 350 to 400°C (GOODFELLOW and FRANKLIN, 1993; PETER et al., 1994). These temperatures are substantially higher than present day vent temperatures in the vicinity of Bent Hill and suggest that the composition of these actively venting fluids is not representative of those responsible for the formation of the sulfide deposit.

Accordingly, the absence of substantial subsurface cooling likely played a key role in the formation of this large sulfide deposit at the seafloor.

2.5. CONCLUSIONS

Reaction of organic-rich and organic-poor sediments from Guaymas Basin and Middle Valley with seawater and Na-Ca-K-Cl fluids of seawater chlorinity at 275-400°C, 350-500 bars resulted in the mobilization of high concentrations of Fe, Mn, and Zn from the sediments. While temperature is a key variable regulating the amount of metals that could be released from the sediments, differences in sediment composition, specifically the amount of organic matter present, also influence metal concentrations. Alteration of organic matter generates substantial amounts of CO_2 that, combined with the release of Ca from albitization, trigger calcite precipitation and the generation of acidity. In organic-poor sediments, fluid pH is dominated by equilibrium between aluminosilicate minerals, which generates lower amounts of acidity relative to calcite precipitation. Comparison of these results with earlier basalt alteration experiments conducted at similar temperatures and pressures indicates that sediment alteration leads to equal or greater concentrations of Fe, Mn, and Zn in hydrothermal fluids. Aqueous Cu concentrations during sediment alteration are lower than during basalt alteration, however, due to more reducing conditions created by the presence of sedimentary organic matter.

Differences between the endmember Fe, Mn, Zn and Pb concentrations in 276°C Middle Valley vent fluid and the concentrations generated during our alteration experiment are consistent with the cooling of fluids that had equilibrated with sediment and/or basalt at temperatures of approximately 325°C before venting at the seafloor. In Guaymas Basin, however, the lower concentrations of all metals in vent fluids relative to our experimental fluids reflect the use of a lower fluid:sediment ratio in the experiment relative to the natural system.

Our results indicate that for a given temperature and pressure, sediment alteration

does not necessarily lead to lower aqueous metal concentrations relative to basalt alteration. Thus, differences in reactions regulating pH are not responsible for low metal concentrations in hydrothermal fluids from sediment-covered systems relative to bare-rock ridge-crest environments. This difference can be accounted for by the critical role of temperature in regulating metal mobility during fluid-sediment interaction. In general the maximum temperature observed at sediment-covered vent fields are significantly lower than those observed at bare-rock vents. The presence of sediments appears to facilitate subsurface cooling and re-equilibration of high temperature fluids prior to venting at the seafloor.

ACKNOWLEDGEMENTS

We thank Tom McCollom, Peter Saccocia and Meg Tivey for thoughtful comments that clarified an earlier version of this manuscript. Joris Gieskes and two anonymous reviewers also provided insightful comments that greatly improved this manuscript. We thank Lary Ball and the WHOI ICP Facility for their assistance in the use of their Finnigan MAT sector field inductively coupled plasma mass spectrometer in making the trace metal measurements. The Petroleum Research Fund (32310-AC2), administered by the American Chemical Society and the National Science Foundation (OCE-9618179) supported this research. This is WHOI contribution number 10453.

Table 2-1. Endmember transition metal concentrations from selected hydrothermal vents.

Vent	Fe	Mn	Zn	Cu	Pb	Cl	H_2S	Temp
	μm	μm	μm	μm	μm	mm	mm	°C
21°N (EPR)[a,b]	646-2429	640-1024	40-106	<0.02-44	0.183-0.359	489-579	6.6-8.4	270-355
TAG (MAR)[c,d]	1640-5590	680-1000	46-400	3-150	-	636-659	0.5-3.5	273-366
MARK (MAR)[c,d,e]	1832-2560	443-493	47-52	10-18	-	563-559	2.7-6.1	335-356
Guaymas Basin (EPR)[c,f]	8-180	128-236	0.1-40	0.02-1.1	<0.020-0.652	581-637	3.8-6.0	270-315
Middle Valley (JdFR)[g]	10-20	63-78	0.7-1.7	0.3-1.3	0.050-0.125	578-412	3	265-276
Escanaba Trough (GR)[h]	0-10	10-21	-	-	-	668	1.1-1.5	108-217

-: not analyzed; mm: mmolal; μm: μmolal; EPR: East Pacific Rise; MAR: Mid-Atlantic Ridge; JdFR: Juan de Fuca Ridge; GR: Gorda Ridge.

References:

[a]Campbell et al. (1988a)
[b]Von Damm et al. (1985a)
[c]Campbell et al. (1988b)
[d]Edmond et al. (1995)
[e]Jean-Baptiste et al. (1991)
[f]Von Damm et al. (1985b)
[g]Butterfield et al. (1994a)
[h]Campbell et al. (1994)

Table 2-2. Dissolved concentrations of selected aqueous species during hydrothermal alteration of Middle Valley sediment with Na-Ca-K-Cl fluid (experiment MV), at 275-350°C, 350 bars, and a water:sediment ratio of 9.8-3.7.

Time	Temp	W:S	Na	Ca	K	Cl	H_2	H_2S	CO_2	CH_4	Fe	Mn	Zn	Cu	Pb
hrs	°C		mm	mm	mm	mm	mm	mm	mm	mm	μm	μm	μm	μm	μm
0	25		500	15.3	15.0	538	<0.01	<3.0	-	<0.001	<1.5	<0.01	<0.1	<0.1	<0.01
170	275	9.8	483	30.4	27.7	564	0.02	<3.0	41.8	0.3	243	39.5	8.7	1.4	1.4
341	275	8.9	441	29.5	27.6	515	0.03	<3.0	41.3	0.4	150	38.2	9.7	1.2	1.0
477		----------Temperature increased to 325°C----------													
628	325	7.8	424	32.5	44.5	516	0.35	<3.0	54.0	0.8	505	107	55.3	4.7	7.3
845	325	6.9	428	31.9	48.2	542	0.32	<3.0	57.3	1.1	308	97.2	37.6	1.4	5.8
1017		----------Temperature increased to 350°C----------													
1177	350	5.7	419	30.8	60.6	547	0.38	<3.0	57.8	1.6	827	258	88.1	1.6	12.7
1634	350	4.4	413	29.0	65.2	535	0.36	6.7	59.7	2.4	476	224	104	1.9	10.5
1686		----------Temperature decreased to 325°C----------													
1849	325	3.7	414	29.2	63.6	537	0.23	-	59.1	2.4	445	98.7	44.9	1.5	10.0

-: not analyzed; mm: mmolal; μm: μmolal.

Table 2-3. Dissolved concentrations of selected aqueous species during hydrothermal alteration of Middle Valley sediment plus added calcite with Na-Ca-K-Cl fluid (experiment MVCAL), at 275-350°C, 350 bars, and a water:sediment ratio of 8.0-3.7.

Time	Temp	W:S	Na	Ca	K	Cl	H_2	H_2S	CO_2	CH_4	Fe	Mn	Zn	Cu	Pb
hrs	°C		mm	mm	mm	mm	mm	mm	mm	mm	µm	µm	µm	µm	µm
0	25		501	14.9	20.1	551	<0.01	<1.6	-	<0.001	<3.4	<0.1	<0.4	<0.1	<0.01
239	275	8.0	461	29.1	28.5	545	0.02	2.1	42.1	0.3	429	29.6	41.0	3.6	2.0
384	275	7.2	461	30.0	29.1	534	0.02	3.5	43.4	0.4	121	28.0	15.2	1.1	1.3
404		----------Temperature increased to 325°C----------													
549	325	6.4	428	35.1	47.1	532	0.25	<1.6	68.1	0.8	105	47.5	47.6	1.1	4.4
743	325	5.6	400	32.0	46.9	506	0.37	1.7	74.6	1.1	86.2	46.7	37.3	1.0	2.3
812		----------Temperature increased to 350°C----------													
1151	350	4.5	390	35.4	64.1	522	0.72	5.5	112	1.7	247	56.1	77.5	1.0	7.8
1582	350	3.7	405	34.3	68.8	525	0.79	6.5	82.2	1.6	844	57.8	93.8	1.4	7.0

-: not analyzed; mm: mmolal; µm: µmolal

Table 2-4. Dissolved concentrations of selected aqueous species during hydrothermal alteration of Guaymas Basin sediment with original porewaters (experiment GB), at 325°C, 500 bars and 400°C, 400 bars, and a water:sediment ratio of 1.6-0.7.

Time	Temp	W:S	§Na	§Mg	§Ca	§K	§Cl	$^{\S}H_2$	$^{\S}SO_4$	$^{\S}H_2S$	$^{\S}NH_3$	$^{\S}CO_2$	$^{\S}CH_4$	Fe	Mn	Zn	Cu	Pb
hrs	°C		mm	mm	mm	mm	mm	mm	mm	mm	mm	mm	mm	µm	µm	µm	µm	µm
0	25	1.6	475	58.2	10.9	16.4	542	<0.01	37.3	<0.05	<2	-	-	39.0	89.6	<0.01	<10	-
98	325	1.3	409	0.14	33.6	19.5	516	1.5	0.19	14.9	50.4	388	30	-	-	-	-	-
241	325	1.2	348	0.36	47.5	35.1	508	1.6	0.14	8.92	52.7	449	40	-	-	-	-	-
410	325	1.1	346	0.37	46.9	36.6	511	1.7	0.15	8.65	55.3	476	46	748	750	62.9	<10	-
414		----------Temperature increased to 400°C, Pressure decreased to 400 bars----------																
533	400	0.9	193	0.38	59.3	68.3	478	5.1	0.06	13.8	-	570	105	3563	6116	411	<10	-
1161	400	0.7	269	0.13	38.3	94.1	508	6.9	0.07	14.1	88.5	65	33	3420	3094	1062	<10	-

-: not analyzed; §data from Seewald et al. (1994); mm: mmolal; µm: µmolal

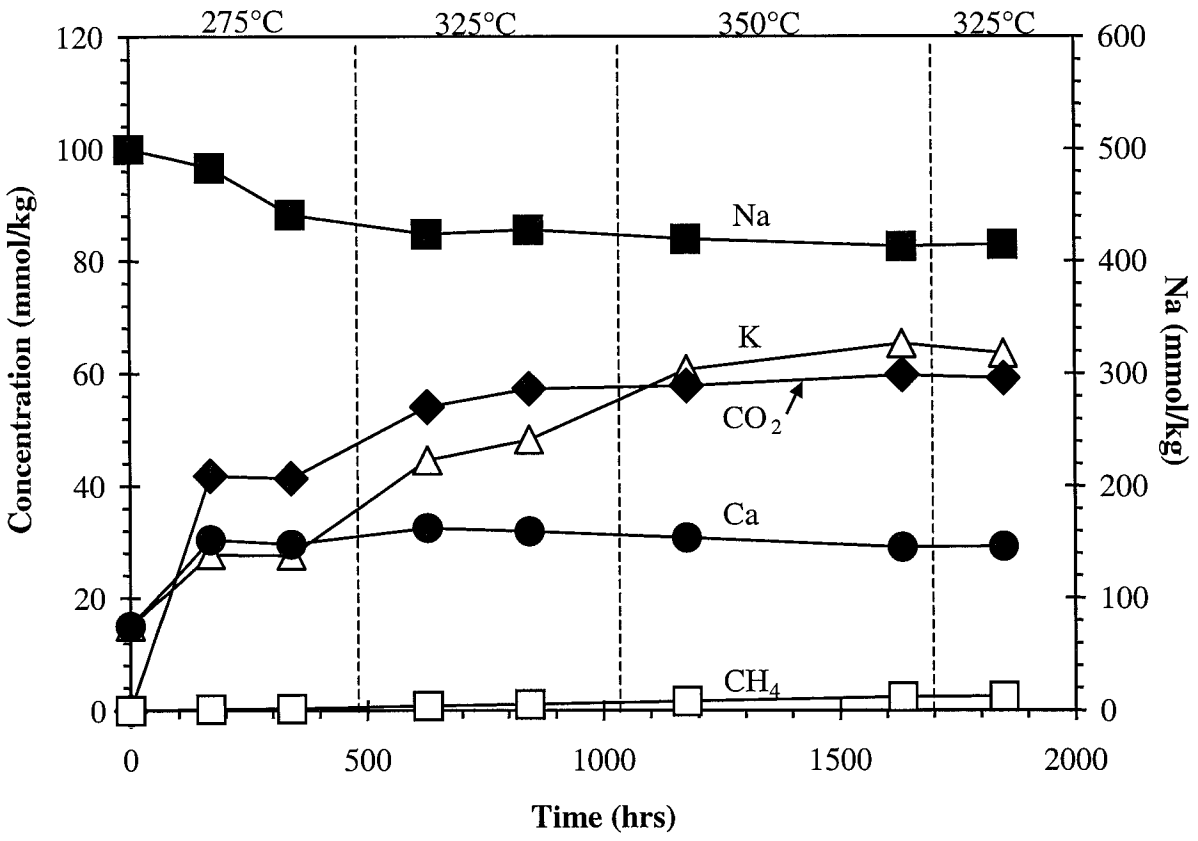

Figure 2-1. Concentrations of selected dissolved species versus time during alteration of organic-lean sediment by Na-Ca-K-Cl fluid (experiment MV) at 275-350°C, 500 bars.

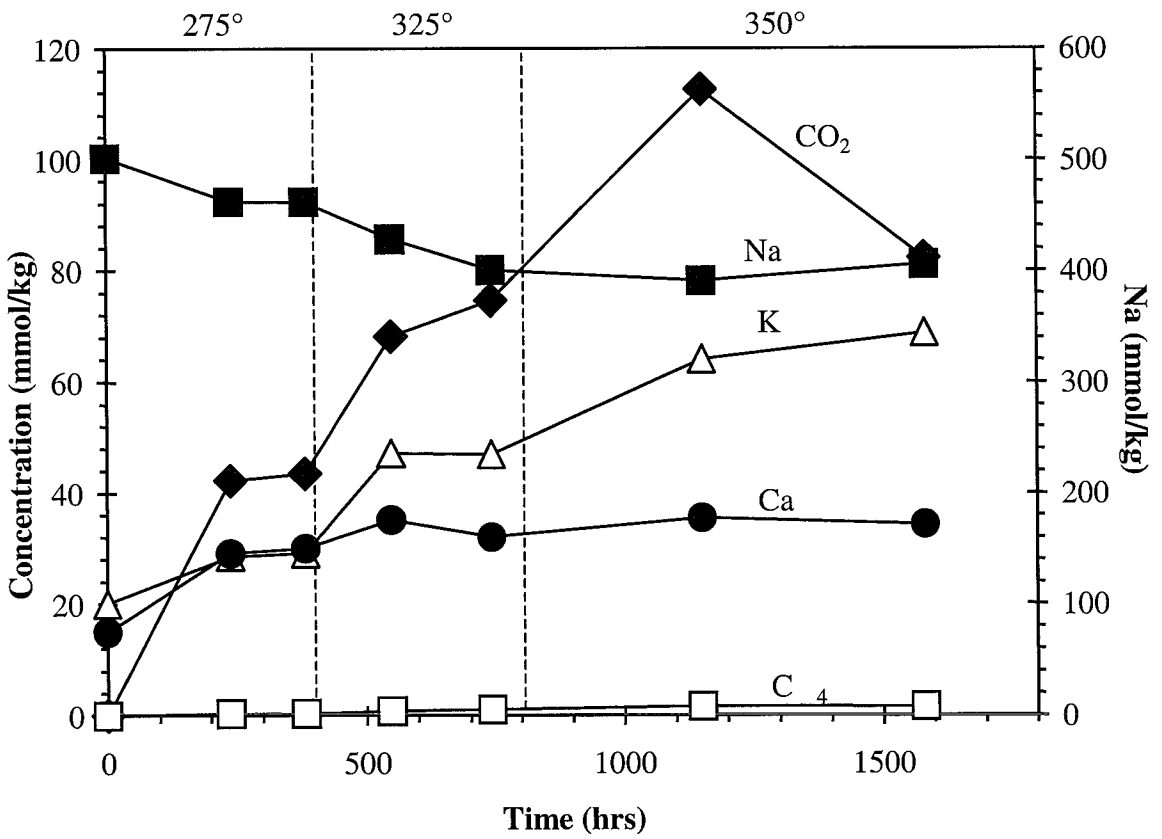

Figure 2-2. Concentrations of selected dissolved species versus time during alteration of organic-lean sediment plus calcite by Na-Ca-K-Cl fluid (experiment MVCAL) at 275-350°C, 500 bars.

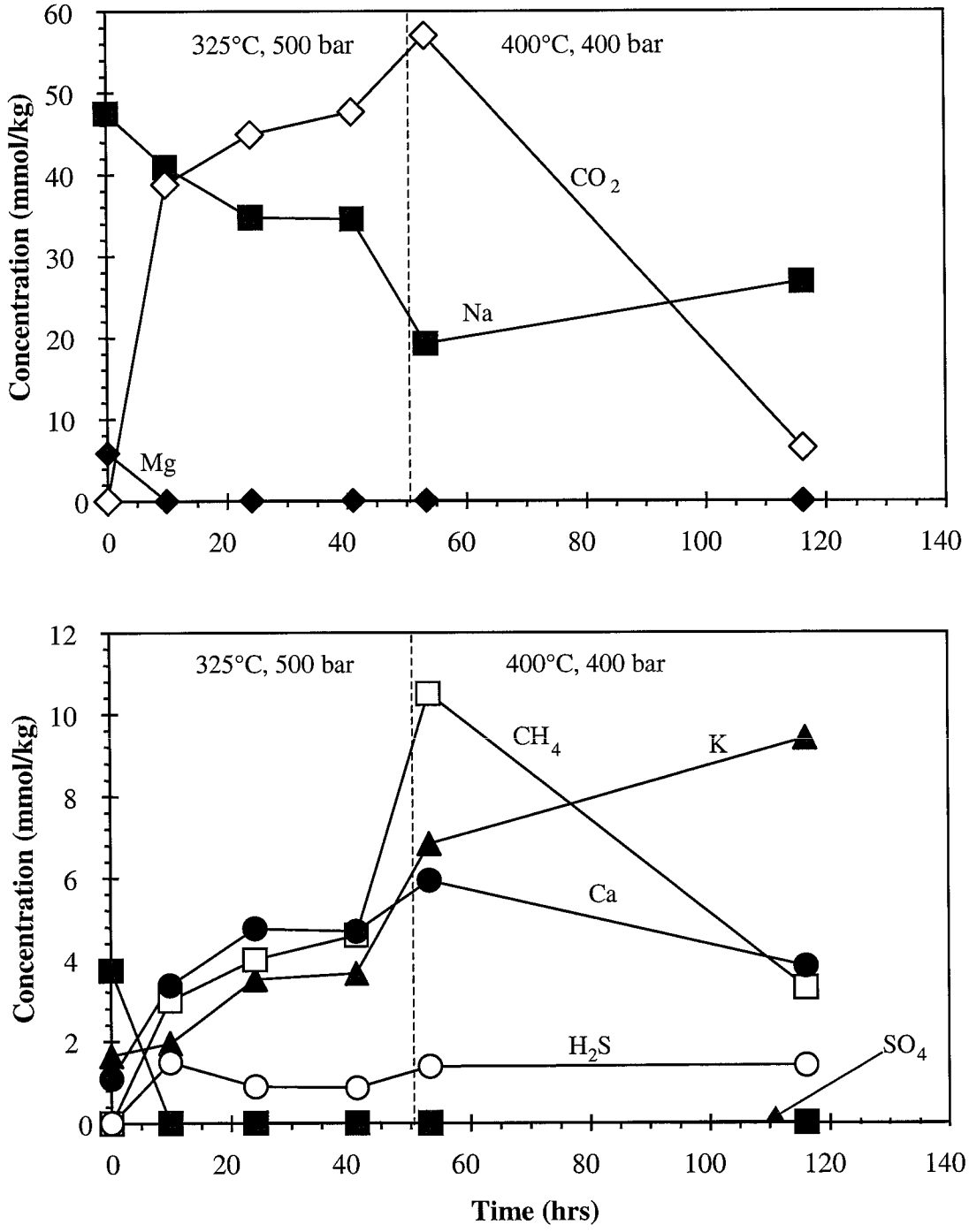

Figure 2-3. Concentrations of selected dissolved species versus time during alteration of organic-rich sediment by pore waters (experiment GB) at 325°C, 500 bars and 400°C, 400 bars. Redrawn from Seewald et al. (1994).

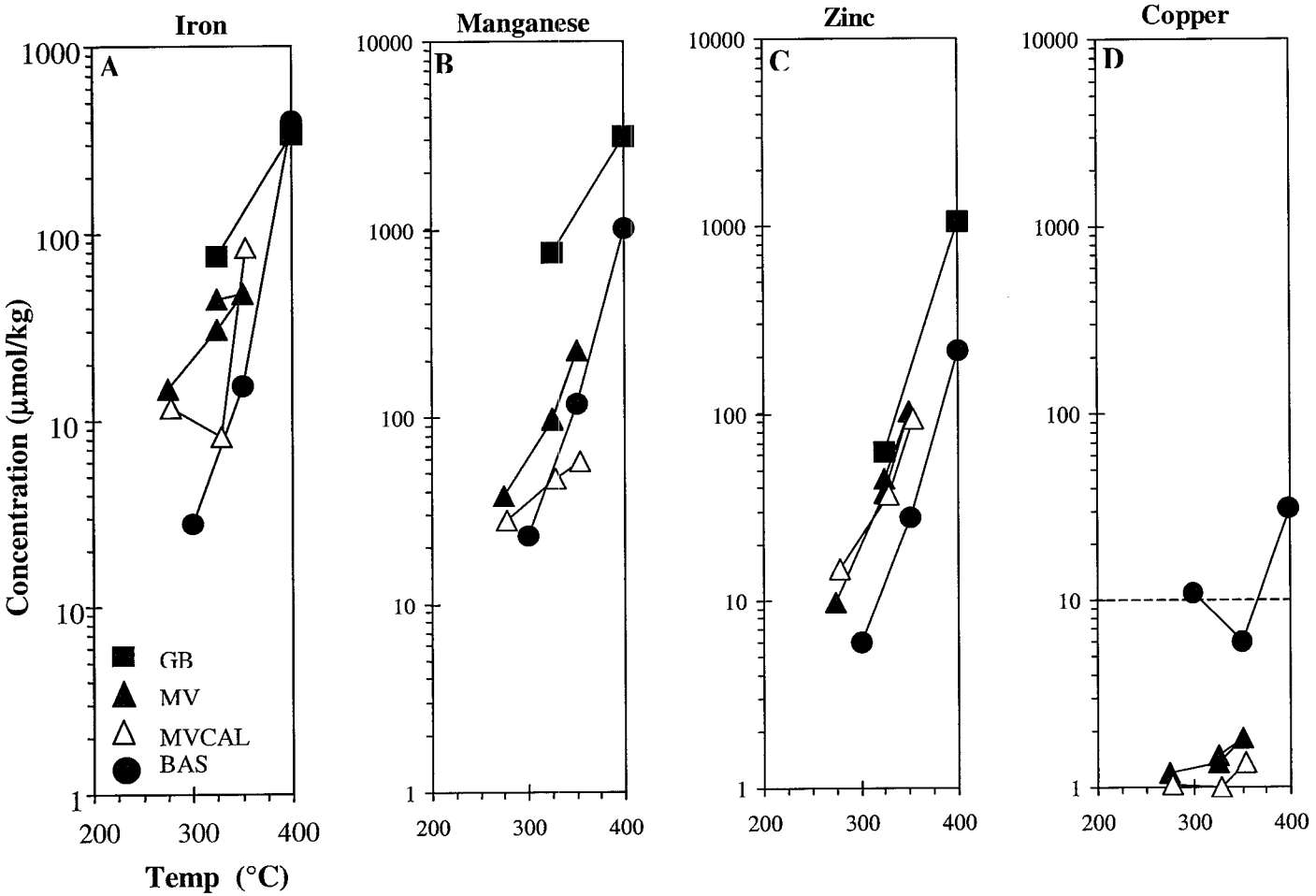

Figure 2-4. Concentrations of dissolved metals versus temperature during sediment alteration experiments MV, MVCAL and GB and basalt alteration experiment BAS. **A.)** Iron; **B.)** Manganese; **C.)** Zinc; **D.)** Copper. Data points correspond to the concentration in the final time point at a given temperature. The dashed line on the Cu graph indicates detection limits during experiment GB. Basalt data from Seewald and Seyfried (1990).

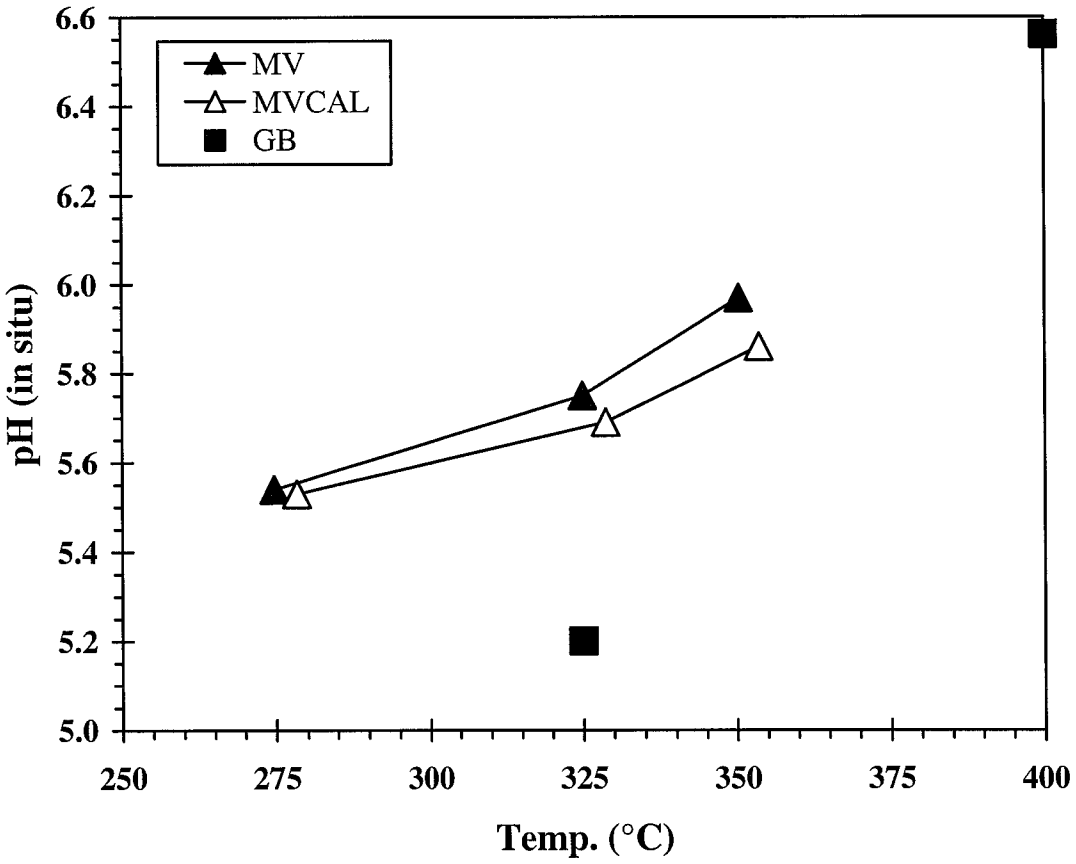

Figure 2-5. Calculated *in-situ* pH values for sediment alteration experiments involving Guaymas Basin and Middle Valley sediments using calcite saturation as a constraint on the activity of total ionizable H^+. Calculations were made using EQ3NR (WOLERY, 1992) with data from the SUPCRT92 database (JOHNSON et al., 1992). The MV results are upper limits on in situ pH during this experiment due to calcite undersaturation during the 325 and 350°C phases of the experiment (see text for discussion).

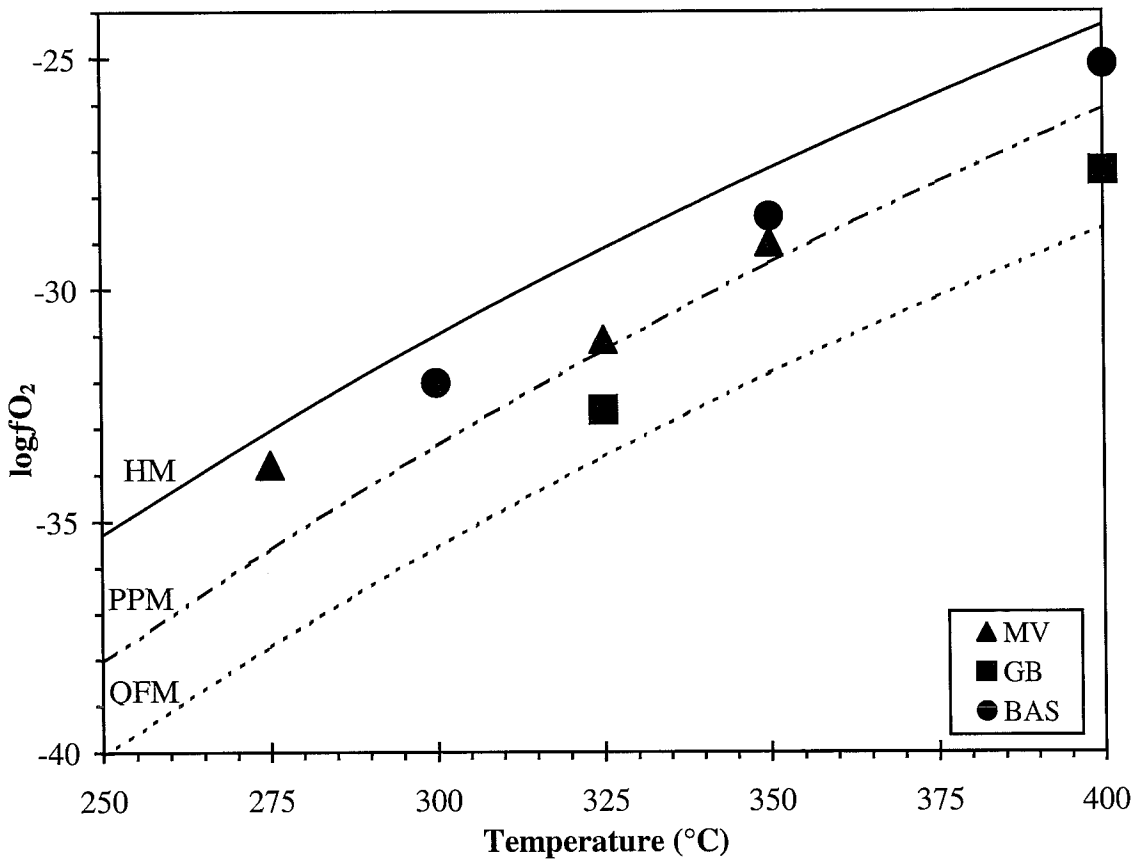

Figure 2-6. Calculated O_2 fugacities based on the H_2-H_2O redox couple as a function of temperature during hydrothermal alteration experiments involving organic-rich sediments (GB), organic-lean sediments (MV) and basalt (BAS). GB data are from Seewald et al. (1994), BAS data are from Seewald and Seyfried (1990) and MV data are from this study. HM, PPM and QFM refer to the commonly utilized mineral assemblage redox buffers hematite-magnetite, pyrite-pyrrhotite-magnetite and quartz-fayalite-magnetite, respectively. Thermodynamic data requisite for the construction of this diagram are from the SUPRCRT92 database (JOHNSON et al., 1992).

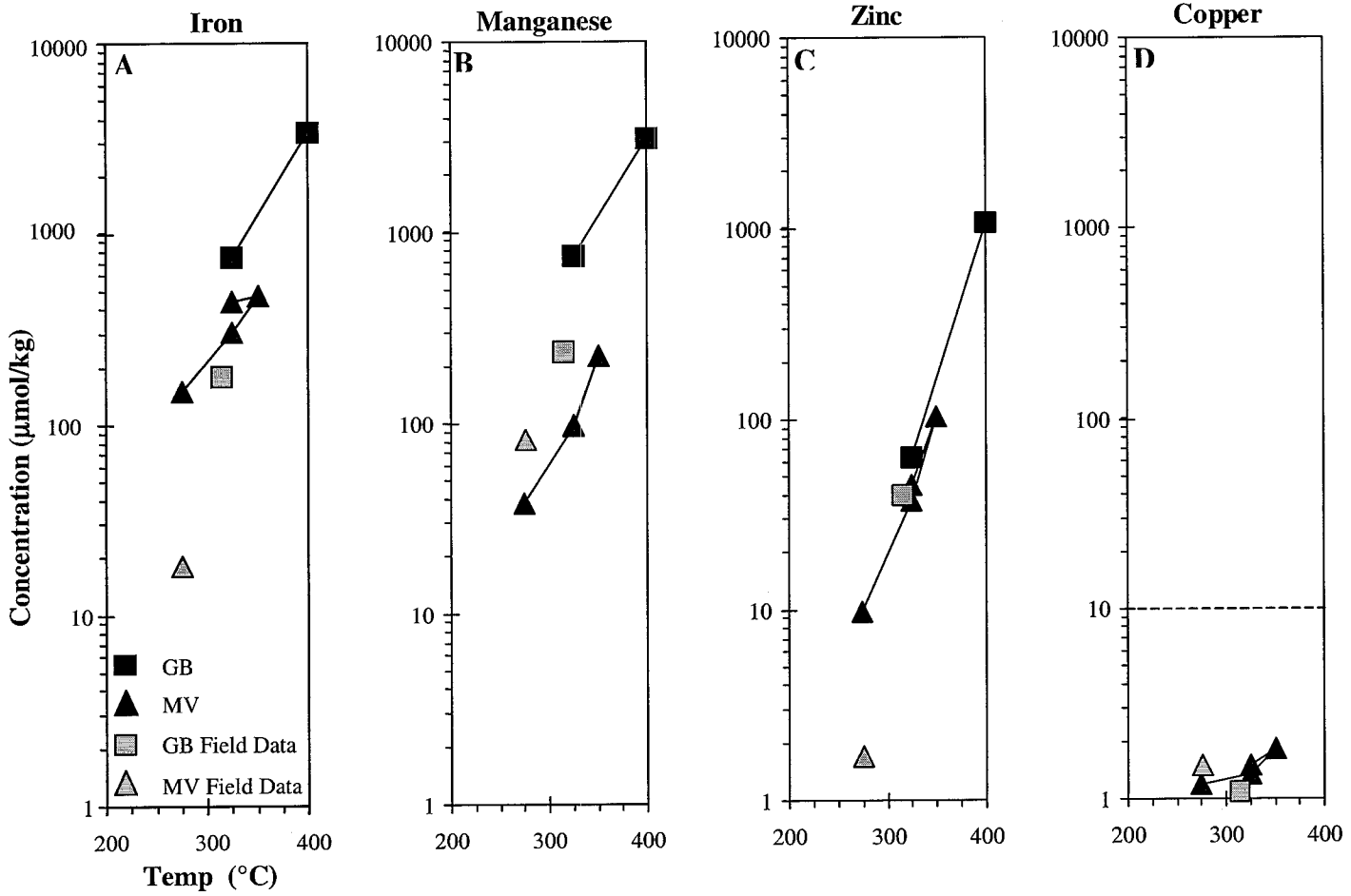

Figure 2-7. Concentrations of dissolved metals versus temperature in sediment alteration experiments MV and GC compared to calculated end-member concentrations from active vents at Middle Valley, northern Juan de Fuca Ridge and Guaymas Basin, Gulf of California. **A.)** Iron; **B.)** Manganese; **C.)** Zinc; **D.)** Copper. Data points correspond to the concentration in the final time point at a given temperature. The dashed line on the Cu graph indicates detection limits for experiment GB. Calculated endmember concentrations in Middle Valley vent fluid from Butterfield et al. (1994a). Calculated endmember concentrations in Guaymas Basin vent fluid from Campbell et al. (1988a) and Von Damm et al. (1985b).

2.6. REFERENCES

ALT J. C., ANDERSON T. F., and BONNELL L. (1989) The geochemistry of sulfur in a 1.3 km section of hydrothermally altered oceanic crust, DSDP hole 504B. *Geochim. Cosmochim. Acta* **53**, 1011-1023.

BERNDT M. E., SEYFRIED, W. E., JR., and JANECKY, D. R. (1989) Plagioclase and epidote buffering of cation ratios in mid-ocean ridge hydrothermal fluids. *Geochim. Cosmochim. Acta* **53**, 2283-2300.

BISCHOFF J. L. and DICKSON F. W. (1975) Seawater-basalt interaction at 200°C and 500 bars: Implications for the origin of sea-floor heavy-metal deposits and the regulation of seawater chemistry. *Earth Planet. Sci. Lett.* **25**, 385-397.

BISCHOFF J. L., RADTKE A. S., and ROSENBAUER R. J. (1981) Hydrothermal alteration of graywacke by brine and seawater: Roles of alteration and chloride complexing on metal solubilization at 200° and 350°C. *Econ. Geol.* **76**, 659-676.

BJERKGÅRD T., COUSENS B. L., and FRANKLIN J. M. (2000) The Middle Valley sulfide deposits, northern Juan de Fuca Ridge: Radiogenic isotope systematics. *Econ. Geol.* **95**, 1473-1488.

BOWERS T. S., VON DAMM K. L., and EDMOND J. M. (1985) Chemical evolution of mid-ocean ridge hot springs. *Geochim. Cosmochim. Acta* **49**, 2239-2252.

BUTTERFIELD D. A., MCDUFF R. E., FRANKLIN J., and WHEAT C. G. (1994a) Geochemistry of hydrothermal vent fluids from Middle Valley, Juan de Fuca Ridge. In *Proceedings of the Ocean Drilling Program, Scientific Results* (ed. M. J. Mottl, E. E. Davis, A. T. Fisher, and J. F. Slack), **139**, pp. 395-410.

BUTTERFIELD D. A., MCDUFF R. E., MOTTL M. J., LILLEY M. D., LUPTON J. E., and MASSOTH G. J. (1994b) Gradients in the composition of hydrothermal fluids from the Endeavour segment vent field: Phase separation and brine loss. *J. Geophys. Res.* **99**, 9561-9583.

CAMPBELL A. C., BOWERS T. S., and EDMOND J. M. (1988a) A time-series of vent fluid compositions from 21°N, EPR (1979, 1981, and 1985) and the Guaymas Basin, Gulf of California (1982, 1985). *J. Geophys. Res.* **93**, 4537-4549.

CAMPBELL A. C., PALMER M. R., KLINKHAMMER G. P., BOWERS T. S., EDMOND J. M., LAWRENCE J. R., CASEY J. F., THOMPSON G., HUMPHRIS S., RONA P. A., and KARSON J. A. (1988b) Chemistry of hot springs on the Mid-Atlantic Ridge.

Nature **335**, 514-519.

CAMPBELL A. C., GERMAN C. R., PALMER M. R., GAMO T., and EDMOND, J. M. (1994) Chemistry of hydrothermal fluids for the Escanaba Trough, Gorda Ridge. In *Geologic, Hydrothermal, and Biologic Studies at Escanaba Trough, Gorda Ridge, Offshore Northern California* (ed. J. L. Morton, R. A. Zierenberg, and C. A. Reiss), *USGS Bull.* **2022**, pp. 201-221.

CAPOBIANCO C. and NAVROTSKY A. (1987) Solid-solution thermodynamics in $CaCO_3$-$MnCO_3$. *American Mineral.* **72**, 312-318.

CHEN J. H., WASSERBURG G. J., VON DAMM K. L., and EDMOND J. M. (1986) The U-Th-Pb systematics in hot springs on the East Pacific Rise at 21°N and Guaymas Basin. *Geochim. Cosmochim. Acta* **50**, 2467-2479.

DAVIS E. E. and FISHER A. T. (1994) On the nature and consequences of hydrothermal circulation in the Middle Valley sedimented rift: Inferences from geophysical and geochemical observations, Leg 139. In *Proceedings of the Ocean Drilling Program, Scientific Results* (ed. M. J. Mottl, E. E. Davis, A. T. Fisher, and J. F. Slack), **139**, pp. 695-717.

DAVIS E. E., MOTTL M. J., FISHER A. T., et al. (1992) *Proc. ODP, Init. Rept.* **139**. Ocean Drilling Program.

DEER W. A., HOWIE R. A., and ZUSSMAN J. (1962) *Rock-Forming Minerals.* Wiley.

DISNAR J. R. and SUREAU J. F. (1990) Organic matter in ore genesis: Progress and perspectives. *Org. Geochem.* **16**, 577-599.

EDMOND J. M., CAMPBELL A. C., PALMER M. R., KLINKHAMMER G. P., GEMAN C. R., EDMONDS H. N., ELDERFIELD H., THOMPSON G., and RONA P. (1995) Time series studies of vent fluids from the TAG and MARK sites (1986, 1990) Mid-Atlantic Ridge: a new solution chemistry model and mechanism for Cu/Zn zonation in massive sulphide orebodies. In Hydrothermal Vents and Processes (ed. L. M. Parson, C. L. Walker and D. R. Dixon) *Geological Society Special Publication* **87**, pp. 77-86.

FISHER A. T. and BECKER K. (1991) Heat flow, hydrothermal circulation and basalt intrusions in the Guaymas Basin, Gulf of California. *Earth Planet. Sci. Lett.* **103**, 84-99.

FRANKLIN J. M. (1993) Volcanic-associated massive sulphide deposits. In Mineral Deposit Modeling (ed. R. V. Kirkham, W. D. Sinclair, R. I. Thorpe, J. M. Duke)

Geological Association of Canada Special Paper **40**, pp. 315-334.

FRANKLIN J. M., LYDON J. W., and SANGSTER D. F. (1981) Volcanic-associated massive sulfide deposits: *Econ. Geol., 75th Anniv. Vol.*, 485-627.

GIESKES J. M., SHAW T., BROWN T. STURZ A., and CAMPBELL A. C. (1991) Interstitial water and hydrothermal water chemistry, Guaymas Bain, Gulf of California. In *The Gulf and Peninsular Province of the Californias* (ed. J. P. Dauphin and B. R. T. Simoneit) *AAPG Memoir* **47**, pp753-779.

GERMAN C. R., BARREIRO B. A., HIGGS N. C., NELSEN T. A., LUDFORD E. M., and PALMER M. R. (1995) Seawater-metasomatism in hydrothermal sediments (Escanaba Trough, northeast Pacific). *Chem. Geol.* **119**, 175-190.

GOODFELLOW W. D. and BLAISE B. (1988) Sulphide formation and hydrothermal alteration of hemipelagic sediment in Middle Valley, Northern Juan de Fuca Ridge. *Canadian Mineral.* **26**, 675-696.

GOODFELLOW W. D. and FRANKLIN J. M. (1993) Geology, mineralogy, and chemistry of sediment-hosted massive sulfides in shallow cores, Middle Valley, Northern Juan de Fuca Ridge. *Econ. Geol.* 88, 2037-2068.

GOODFELLOW W. D. and PETER J M. (1994) Geochemistry of hydrothermally altered sediment, Middle Valley, northern Juan de Fuca Ridge. In *Proceedings of the Ocean Drilling Program, Scientific Results* (ed. M. J. Mottl, E. E. Davis, A. T. Fisher, and J. F. Slack), **139**, pp. 207-289.

HANNINGTON M. D., JONASSON I.R., HERZIG P. M., and PETERSEN S. (1995) Physical and chemicalprocesses of seafloor mineralization at mid-ocean ridges. In *Seafloor Hydrothermal Systems: Physical, Chemical, Biological, and Geological Interactions* (ed. S. E. Humphis, R. A. Zierenberg, L. S. Mullineaux, and R. E. Thomson), *Geophysical Monograph* **91**, pp. 115-157.

HOLMES M. L. and ZIERENBERG, R. A. (1990) Submersible observations in Escanaba Trough, southern Gorda Ridge. In *Gorda Ridge: A Seafloor Spreading Center in the United States' Exclusive Economic Zone* (ed. G. R. Murray), pp. 93-115.

JAMES R. H., DUCKWORTH R. C., PALMER M. R., and THE ODP LEG 169 SHIPBOARD SCIENTIFIC PARTY (1998) Drilling of sediment-hosted massive sulphide deposits at the Middle Valley and Escanaba Trough spreading centers: ODP Leg 169. In *Modern Ocean Floor Processes and the Geological Record* (ed. R. A. Mills and K. Harrison), *Geological Society Special Publication* **148**, pp. 177-199.

JAMES R. H., RUDNICKI M. D., and PALMER M. R. (1999) The alkali element and boron geochemistry of the Escanaba Trough sediment-hosted hydrothermal system. *Earth Planet. Sci. Lett.* **171**, 157-169.

JEAN-BAPTISTE P., CHARLOU J. L., STIEVENARD M., DONVAL J. P., BOUGAULT, H., and MEVEL C. (1991) Helium and methane measurements in hydrothermal fluids from the Mid-Atlantic Ridge; the Snake Pit site at 23 degrees N. *Earth Planet. Sci. Lett.* **106**, 17-28.

JOHNSON J. W., OELKERS E. H., and HELGESON H. C. (1992) SUPCRT92: A software package for calculating the standard molal thermodynamic properties of minerals, gases, aqueous species, and reactions from 1 to 5000 bar and 0 to 1000°C. *Comput. Geosci.* **18**, 899-947.

KOSKI R. A., LONSDALE P. F., SHANKS W. C., III, BERNDT M. E., and HOWES S. S. (1985) Mineralogy and geochemistry of a sediment-hosted hydrothermal sulfide deposit from the southern trough of Guaymas Basin, Gulf of California. *J. Geophys. Res.* **90**, 6695-6707.

KOSKI R. A., SHANKS W. C., III, BOHRSON W. A., and OSCARSON R. L. (1988) The composition of sediment-hosted massive sulfide deposits from Escanaba Trough, Gorda Ridge: Implications for fluid-sediment interaction and depositional processes. *Canadian Mineral.* **26**, 655-673.;

KRASNOV S., STEPANOVA T., AND Stepanova M. (1994) Chemical composition and formation of a massive sulfide deposit, Middle Valley, northern Juan de Fuca Ridge (Site 856). In *Proceedings of the Ocean Drilling Program, Scientific Results* (ed. M. J. Mottl, E. E. Davis, A. T. Fisher, and J. F. Slack), **139**, pp. 353-367.

LEYBOURNE M. I. and GOODFELLOW W. D. (1994) Mineralogy and mineral chemistry of hydrothermally altered sediment, Middle Valley, Juan de Fuca Ridge. In *Proceedings of the Ocean Drilling Program, Scientific Results* (ed. M. J. Mottl, E. E. Davis, A. T. Fisher, and J. F. Slack), **139**, pp. 155-206.

LEHURAY A. P., CHURCH S. E., KOSKI R. A., and BOUSE R. M. (1988) Pb isotopes in sulfides from mid-ocean ridge hydrothermal sites. *Geology* **16**, 362-365.

LONDSDALE P. F., BISCHOFF J. L., BURNS V. M., KASTNER M., and SWEENEY, R. E. (1980) A high-temperature hydrothermal deposit on the seabed at a Gulf of California spreading center. *Earth Planet. Sci. Lett.* **49**, 8-20.

MAGENHEIM A. J. and GIESKES J. (1994) Evidence for hydrothermal fluid flow through

surficial sediments, Escanaba Trough. In *Geologic, Hydrothermal, and Biologic Studies at Escanaba Trough, Gorda Ridge, Offshore Northern California* (ed. J. L. Morton, R. A. Zierenberg, and C. A. Reiss), *USGS Bull.* **2022**, pp. 241-255.

MOTTL M. J. and HOLLAND H. D. (1978) Chemical exchange during hydrothermal alteration of basalt by seawater—I. Experimental results for major and minor components of seawater. *Geochim. Cosmochim. Acta* **42**, 1103-1115.

MOTTL M., HOLLAND H. D., and CORR R. F. (1979) Chemical exchange during hydrothermal alteration of basalt by seawater- II. Experimental results for Fe, Mn and sulfur species. *Geochim. Cosmochim. Acta* **43**, 869-884.

PETER J. M., GOODFELLOW W. D., and LEYBOURNE M. I. (1994) Fluid inclusion petrography and microthermometry of the Middle Valley hydrothermal system, northern Juan de Fuca Ridge. In *Proceedings of the Ocean Drilling Program, Scientific Results* (ed. M. J. Mottl, E. E. Davis, A. T. Fisher, and J. F. Slack), **139**, pp. 411-428.

PETER J. M. and SCOTT S. D. (1988) Mineralogy, composition, and fluid-inclusion microthermometry of seafloor hydrothermal deposits in the southern trough of Guaymas Basin, Gulf of California. *Canadian Mineral.* **26**, 567-587.

PHILPOTTS J. A., ARUSCAVAGE P. J., and VON DAMM, K. L. (1987) Uniformity and diversity in the composition of mineralizing fluids from hydrothermal vents on the southern Juan de Fuca Ridge. *J. Geophys. Res.* **92**, 11,327-11,333.

SCOTT S. D. (1985) Seafloor polymetallic sulfide deposits: Modern and ancient. *Marine Mining* **5**, 191-212.

SEEWALD J. S. and SEYFRIED W. E., JR. (1990) The effect of temperature on metal mobility in subseafloor hydrothermal systems: Constraints from basalt alteration experiments. *Earth Planet. Sci. Letters* **101**, 388-403.

SEEWALD J. S., CRUSE A. M., LILLEY M. D., and OLSON E. J. (1998) Hot-Spring Fluid Chemistry at Guaymas Basin, Gulf of California: Temporal Variations and Volatile Content: *Eos*, v. 79, p. F47.

SEEWALD J. S., EGLINTON L. B., and ONG Y.-L. (2000) An experimental study of organic-inorganic interactions during vitrinite maturation. *Geochim. Cosmochim. Acta* **64**, 1577-1591.

SEEWALD J. S., SEYFRIED W. E., JR., and THORNTON E. C. (1990) Organic-rich sediment alteration: An experimental and theoretical study at elevated temperatures and

pressures. *Appl. Geochem.* **5**, 193-209.l

SEEWALD J. S., SEYFRIED W. E., JR., and SHANKS, W. C., III (1994) Variations in the chemical and stable isotope composition of carbon and sulfur species during organic-rich sediment alteration: An experimental and theoretical study of hydrothermal activity at Guaymas Basin, Gulf of California. *Geochim. Cosmochim. Acta* **58**, 5065-5082.

SEYFRIED W. E., JR. (1987) Experimental and theoretical constraints on hydrothermal alteration processes at mid-ocean ridges. *Ann. Rev. Earth Planet. Sci.* **15**, 317-335.

SEYFRIED W. E., Jr. and BISCHOFF J. L. (1981) Experimental seawater-basalt interaction at 300°C, 500 bars: Chemical exchange, secondary mineral formation and implications for the transport of heavy metals. *Geochim. Cosmochim. Acta* **45**, 135-149.

SEYFRIED W. E., JR. and DING K. (1993) The effect of redox on the relative solubilities of copper and iron in Cl-bearing aqueous fluids at elevated temperatures and pressures: An experimental study with application to subseafloor hydrothermal systems. *Geochim. Cosmochim. Acta*, **57**, 1905-1917.

SEYFRIED W. E., JR. and JANECKY D. R. (1985) Heavy metal and sulfur transport during subcritical and supercritical hydrothermal alteration of basalt: Influence of fluid pressure and basalt composition and crystallinity. *Geochim. Cosmochim. Acta* **49**, 2545-2560.

SEYFRIED W. E., JR. and MOTTL M. J. (1982) Hydrothermal alteration of basalt under seawater-dominated conditions. *Geochim. Cosmochim. Acta* **46**, 985-1002.

SEYFRIED W. E., JR., JANECKY D. R., and BERNDT M. E. (1987) Rocking autoclaves for hydrothermal experiments II. The flexible reaction-cell system. In *Experimental Hydrothermal Techniques* (ed. G. C. Ulmet and H. L. Barnes), pp. 216-240. John Wiley and Sons.

SEYFRIED W. E., JR., DING K., and BERNDT M. E. (1991) Phase-equilibria constraints on the chemistry of hot-spring fluids at midocean ridges. *Geochim. Cosmochim. Acta* **55**, 3559-3580.

SHIPBOARD SCIENTIFIC PARTY (1997) Middle Valley: Bent Hill Area (Site 1035). In *Proceedings of the Ocean Drilling Program, Initial Results* (ed. Y. Fouquet, R. A. Zierenberg, D. J. Miller et al.), **169**, pp. 35-152.

STUART F. M., ELLAM R. M., and DUCKWORTH R. C. (1999) Metal sources in the Middle Valley massive sulphide deposit, northern Juan de Fuca Ridge: Pb isotope constraints. *Chem. Geol.*, **153**, 213-225.

STUART F. M., TURNER G., DUCKWORTH R. C., and Fallick A. E. (1994) Helium-isotopes as tracers of trapped hydrothermal fluids in ocean-floor sulfides. *Geology* **22**, 823-826.

STUMM W. J. and MORGAN J. J. (1996) *Aquatic Chemistry, Third Edition.* Wiley.

THORTON E. C. and SEYFRIED W. E., JR. (1987) Reactivity of organic-rich sediment in seawater at 350°C, 500 bars: Experimental and theoretical constraints for the Guaymas Basin hydrothermal system. *Geochim. Cosmochim. Acta* **51**, 1997-2010.

TIVEY M. K., OLSON L. O., MILLER V. W., and LIGHT, R. D. (1990) Temperature measurements during initiation and growth of a black smoker chimney. *Nature* **346**, 51-54.

TREFRY J. H., BUTTERFIELD D. B., METZ S., MASSOTH G. J., TROCINE R. P., and FEELY, R. A. (1994) Trace metals in hydrothermal solutions from Cleft segment on the southern Juan de Fuca Ridge. *J. Geophys. Res.* **99**, 4925-4935.

VON DAMM K. L. (1983) Chemistry of Submarine Hydrothermal Solutions at 21°N, East Pacific Rise and Guaymas Basin, Gulf of California. PhD Thesis, MIT/WHOI, WHOI-84-3, 240p.

VON DAMM K. L. (1990) Seafloor hydrothermal activity: Black smoker chemistry and chimneys. *Ann. Rev. Earth Planet. Sci.* **18**, 173-205.

VON DAMM K. L. (1991) A comparison of Guaymas Basin hydrothermal solutions with other sedimented systems and experimental results. In *The Peninsular Province of the Californias* (ed. J. P. Dauphin and B. R. T. Simoneit), *AAPG Memoir* **47**, pp. 742-751.

VON DAMM K. L. (1995) Controls on the chemistry and temporal variability of seafloor hydrothermal fluids. In *Seafloor Hydrothermal Systems: Physical, Chemical, Biological, and Geological Interactions* (ed. S. E. Humphis, R. A. Zierenberg, L. S. Mullineaux, and R. E. Thomson), *Geophysical Monograph* **91**, pp. 222-247.

VON DAMM K. L., EDMOND J. M., GRANT B., and MEASURES C. I. (1985a) Chemistry of submarine hydrothermal solutions at 21°N, East Pacific Rise. *Geochim. Cosmochim. Acta* **49**, 2197-2220.

VON DAMM K. L., EDMOND J. M., MEASURES C. I., and GRANT B. (1985b) Chemistry of submarine hydrothermal solutions at Guaymas Basin, Gulf of California. *Geochim. Cosmochim. Acta* **49**, 2221-2237.

WOLERY T. J. (1992) *EQ3NR, A Computer Program for Geochemical Aqueous Speciation-Solubility Calculations: Theoretical Manual, User's Guide, and Related Documentation (Version 7.0).* Lawrence Livermore National Lab.

ZIERENBERG R. A. and 27 others (1998) The deep structure of a seafloor hydrothermal deposit. *Nature* **392**, 485-487.

ZIERENBERG R. A., KOSKI R. A., MORTON J. L., BOUSE R. M., and SHANKS W. C. (1993) Genesis of massive sulfide deposits on a sediment-covered spreading center, Escanaba Trough, Southern Gorda Ridge. *Econ. Geol.* **88**, 2069-2098.

CHAPTER 3. GEOCHEMISTRY OF LOW-MOLECULAR WEIGHT HYDROCARBONS IN HYDROTHERMAL VENT FLUIDS FROM MIDDLE VALLEY, NORTHERN JUAN DE FUCA RIDGE

ABSTRACT

The presence of organic matter in aqueous fluids has the potential to influence a range of chemical processes in hydrothermal vent environments. In order to rigorously constrain the role of organic compounds in crustal alteration processes, fundamental knowledge of the abundances of these compounds and the mechanisms that control their distributions are required. To address this issue, hydrothermal vent fluids from Middle Valley, a sediment-covered mid-ocean ridge on the northern Juan de Fuca Ridge, were sampled in July, 2000, utilizing a newly developed gas-tight sampler which allows the measurement of a range of volatile, semi-volatile and aqueous compounds on a single fluid sample. Eight different vents with exit temperatures of 186 to 281°C were sampled from two areas of hydrothermal venting: Dead Dog and ODP Mound fields. The fluids from the Dead Dog field are characterized by higher concentrations of NH_3 and organic compounds (C_1-C_4 alkanes, ethene, propene, benzene and toluene) compared to the fluids from the ODP Mound field. The ODP Mound fluids are characterized by higher $C_1/(C_2+C_3)$ and benzene/toluene ratios than fluids from the Dead Dog field. Taken together, these compositional trends indicate that the aqueous organic compounds in the ODP Mound field have experienced a greater degree of secondary thermal alteration than those in the Dead Dog field, due to higher temperatures or longer residence times in the subsurface. Subsurface reaction zone temperatures, calculated by assuming that thermodynamic equilibrium is attained between alkene, alkane and hydrogen, are consistent with the dissolved Cl concentrations and suggest that thermodynamic equilibrium may control fluid compositions in natural environments. Higher benzene/toluene ratios in the Dead Dog fluids as compared to the ODP Mound fluids are consistent with a greater degree of alteration of organic compounds at the ODP Mound field. The persistence of toluene in these fluids, despite a strong drive for its conversion to benzene at estimated subsurface reaction zone conditions, reflects kinetic barriers to the attainment of equilibrium. The isotopic composition of methane increases with increasing maturity of the sediments due to the kinetics of C-bond cleavage. C_2-C_4 alkanes, benzene and toluene show no variation in isotopic composition with inferred extent of organic alteration. The net concentration and isotopic composition of these compounds are unaffected by the balance between consumption and generation reactions during alteration. Abiotic methane oxidation appears to have occurred in the subsurface, leading to chemical and isotopic equilibration between CO_2 and CH_4. Fluids from Shiner Bock and 1035H vents contain H_2 concentrations that are among the highest yet measured due to its formation via methane oxidation. This observation demonstrates that

organic compounds may play a key role in regulating the chemistry of subsurface fluids even in regions where the sediments are relatively lean in organic carbon.

3.1. INTRODUCTION

At Middle Valley, located on the northern Juan de Fuca Ridge (Figure 1-1) at approximately 2400 meters depth, the ridge axis is covered by up to 1.5 kilometers of hemipelagic and turbiditic sediments that contain approximately 0.5 wt. % organic matter (GOODFELLOW and BLAISE, 1988). Here, hot circulating seawater interacts with rocks of basaltic composition as well as the sediments that blanket the ridge axis. High heat flow from the underlying basement results in hydrothermal venting in two main regions located approximately 4 km apart: the Dead Dog and ODP Mound vent fields (DAVIS and VILLINGER, 1992; Fig. 1). The sediments that blanket the ridge serve to insulate the hot basement, trapping heat and maintaining hydrothermal circulation in the region for prolonged periods. For example, based on models of the physical properties of the sediments in the Dead Dog field, Davis and Wang (1994) estimate that temperatures throughout the sediment section have been maintained near 280°C for the past 125,000 years. Maintenance of hydrothermal circulation in an area can have important consequences for extent and style of crustal alteration reactions. Sediments are compositionally and mineralogically more variable than fresh oceanic basalt. One key difference is that organic matter is essentially absent in basalt, but present in sediments in varying amounts. Thermal alteration of the sedimentary organic matter results in the release of myriad organic alteration products to solution (CRUSE and SEEWALD, 2001; MARTENS, 1990; SIMONEIT et al., 1994). These compounds can play a key role in many processes occurring at mid-ocean ridges, such as the formation of massive sulfide deposits (CRUSE and SEEWALD, 2001; DISNAR and SUREAU, 1990, and references therein) and represent energy sources for the large and diverse biological communities that inhabit hydrothermal vent environments (HESSLER and KAHARL, 1995).

Organic compounds can also potentially serve as geochemical indicators for the conditions under which fluid-rock interactions occur deep within the subsurface, where direct measurements cannot be made. In traditional models of organic matter alteration

in sedimentary basins, the amounts and isotopic compositions of alteration products are controlled entirely by kinetic factors (HUNT, 1996; TISSOT and WELTE, 1984). Recent theoretical and laboratory work, however, suggests that metastable thermodynamic equilibrium among organic compounds, inorganic minerals and water may regulate the abundances of compounds such as carbon dioxide, hydrocarbons and organic acids (HELGESON, 1991; HELGESON et al., 1993; MCCOLLOM et al., 2001; SEEWALD, 1994, 1997; SEEWALD, 2001a; SEEWALD, 2001b). The concentrations and isotopic compositions of the organic compounds in hydrothermal vent fluids can be analyzed within the framework of such models to constrain subsurface conditions. Reactions involving organic compounds will likely be characterized by different kinetics and will respond to changes in pressure, temperature and redox differently than inorganic species such as Si that are also used as proxies for subsurface reaction conditions. Different chemical species will record conditions in different regimes during hydrothermal fluid flow, allowing the development of more detailed models of crustal alteration processes. In this study, vent fluids were collected from Middle Valley in July, 2000, in order to determine the key reactions that control the distributions of organic compounds in these fluids and the role that interaction of organic and inorganic compounds play in crustal alteration processes.

3.2. EXPERIMENTAL

3.2.1. Geologic Setting

Middle Valley is an axial rift valley located at 48°27'N latitude on the northern edge of the Juan de Fuca Ridge, an intermediate-spreading ridge with a half-spreading rate of 30 mm/yr (GOODFELLOW and BLAISE, 1988; Fig. 1-1). Active spreading jumped westward from Middle Valley to West Valley during the last 200,000 years, and perhaps as early as 10,000 years ago (KARSTEN et al., 1986). Middle Valley was completely filled with terrestrial and hemipelagic sediments derived from the continental shelf during Pleistocene sea-level lowstands. The sediment cover ranges in thickness from a few hundred meters in the south up to 1.5 kilometers in the north (GOODFELLOW and BLAISE,

1988). Sedimentation was contemporaneous with active extension and volcanism, so that the uppermost basement consists of a basaltic-sill/sediment complex (DAVIS and VILLINGER, 1992). Past hydrothermal activity resulted in the creation of two massive sulfide deposits that formed from the direct precipitation of sulfide minerals on the seafloor: the Bent Hill massive sulfide deposit, which is estimated to contain over 8 million tons of ore, and the slightly younger Ore Drilling Program (ODP) Mound massive sulfide deposit (ZIERENBERG et al., 1998). Current hydrothermal activity is localized in two areas: the Dead Dog vent field and the ODP Mound vent field (Fig. 1-3A,B). We sampled fluids from five regions of focused venting within the Dead Dog field: Heineken Hollow, Dead Dog mound, Inspired Mounds, Chowder Hill and Puppy Dog (Table 3-1; Fig. 1-3A). The vent sites consist of mounds, ranging from 5 to 15 meters high and 10 to 30 meters in diameter. Many mounds are topped by a single large chimney 1-5 meters high, and have smaller (<2 meters) spires located on the sides. In many instances, diffuse flow (shimmering water) can be seen emanating from the sulfide rubble and sediments that make up the mounds, or from the base of the chimney itself. The chimneys are dominantly composed of anhydrite and contain minor disseminated pyrrhotite, sphalerite, isocubanite, chalcopyrite and galena (AMES et al., 1993). Maximum vent fluid exit temperatures measured in 2000 were 187, 274, 281, 261, and 202°C for fluids sampled from Heineken Hollow, Dead Dog mound, Chowder Hill, Inspired Mounds and Puppy Dog vents, respectively (Table 3-1).

Prior to drilling during ODP Leg 169 in 1996, known venting at the ODP Mound area was confined to a single spire located on the northern flank of the ODP Mound massive sulfide (BUTTERFIELD et al., 1994a), referred to as Lone Star vent (ZIERENBERG and MILLER, 2000). During a camera survey to spud Hole 1035H during Leg 169, a second area of hydrothermal venting was tentatively identified approximately 30 m to the north of Hole 1035H (ZIERENBERG and MILLER, 2000). A small area of hydrothermal venting was confirmed on *Alvin* Dive 3239 in 1998 and hydrothermal fluids were sampled from a 1.5 m high anhydrite chimney named Shiner Bock vent (ZIERENBERG and MILLER, 2000). In July 2000, hydrothermal fluids were observed to discharge from ODP

Leg 169 drillholes 1035F, 1035H and 1035G. ODP drillhole 1035H is unique in that a large anhydrite structure approximately 10 meters tall has formed over the drillhole within two years (Zierenberg, pers. comm.). Hydrothermal fluid was also observed to vent from several 0.5 to 5 meter high chimneys and spires that cover the ODP Mound. The chimneys and spires were not observed in 1998 (Zierenberg, pers. comm.) and thus represent a new area of venting in the ODP Mound field that was at most only two years old when sampled in 2000. It is hypothesized that the silicified layer at the top of the sediments acted as a hydrologic seal. When this layer was punctured during Leg 169 drilling operations, upflow of previously confined fluids began. As part of this study in July, 2000, fluids were sampled from Shiner Bock vent, ODP Leg 169 drillhole 1035H, and from Spire vent in the area of new venting (Table 3-1; Fig. 1-3B). All of these vents are located on the ODP Mound. Fluids from ODP Leg 169 drillhole 1035F, located near the Bent Hill massive sulfide deposit were also sampled. Measured exit temperatures were only 40°C for the fluids venting from 1035F, but were 272°C, 263°C and 267°C for Shiner Bock, Spire and 1035H, respectively (Table 3-1). The temperature of the fluid venting from ODP Hole 1035G was measured at 10°C, but a sample was not collected.

Hydrothermal circulation at Middle Valley is thought to consist of two decoupled circulation systems, a shallow, low-temperature one hosted within the sediments, and a deeper, high-temperature system that penetrates into the basement (STEIN and FISHER, 2001; STEIN et al., 1998). The systems are separated by an indurated, silicified sediment layer located at 30 meters below the seafloor (mbsf) at the Dead Dog field and at approximately 150 mbsf at the ODP Mound field (SHIPBOARD SCIENTIFIC PARTY, 1992b, 1998a). It is hypothesized that vent fluids are resupplied to the deeper, primary system via flow along the normal faults and linear unsedimented basement ridges that border Middle Valley (STEIN and FISHER, 2001), rather than by diffusive flow through the sediments themselves (RABINOWICZ et al., 1998). The Dead Dog vent field is situated over a buried basement edifice located at 258 mbsf (SHIPBOARD SCIENTIFIC PARTY, 1992b) that acts to focus the upflow of fluid from the deeper, hotter circulation system to the field (DAVIS and FISHER, 1994). Individual vents within the Dead Dog field are likely

located over localized pathways of higher permeability through the hydrologic seal represented by the indurated sediment layer. A similar region of overpressured, high permeability basement was intersected by drilling during ODP Leg 169, with drillholes 1035F, 1035H and 1035G providing anthropogenic conduits through the indurated sediment cap at 150 mbsf (SHIPBOARD SCIENTIFIC PARTY, 1992b, 1998a). Similar to the Dead Dog field, the location of active vents and spires that cover the ODP Mound likely reflect localized channels of high permeability through the ODP Mound.

At Dead Dog, a second convection system is thought to exist only within the sediments that overlie the indurated layer as high temperatures and low pressures within the vent conduits draw pore fluids through the sediments toward the vents (STEIN and FISHER, 2001; STEIN et al., 1998). This upper system is maintained by slow recharge of bottom seawater through the sediments as well as by more focused flow through regions of higher permeability, such as sandy turbidite layers (STEIN and FISHER, 2001). Additionally, a relict hydrothermal circulation system was active during the formation of the Bent Hill and ODP Mound massive sulfide deposits. Mineralogical and fluid inclusion data from sulfides in the Bent Hill deposit indicate precipitation from hydrothermal fluids that reached temperatures of 350 to 400°C (GOODFELLOW and FRANKLIN, 1993; PETER et al., 1994). Such fluids were apparently derived from a deep, hot reaction zone located in the basaltic basement with upflow focused along faults and fissures that were subsequently sealed by mineral precipitation (ZIERENBERG et al., 1998).

3.2.2. Sample Collection

Vent fluid samples were collected using isobaric gas-tight fluid samplers that maintain the fluid at seafloor pressures while subsamples are withdrawn through a micrometering valve (SEEWALD et al., 2002). At least two different gas-tight samples were collected at each vent. Additional samples were also taken from some vents using the 755 mL titanium syringe bottles commonly referred to as the "major" samplers, which are not gas tight (EDMOND et al., 1992; VON DAMM et al., 1985a). Fluids from these samplers were utilized only for analysis of the non-volatile species NH_4 and Cl, and semi-volatile H_2S. Consequently, since no gas-tight samplers were available to collect

fluid from Dead Dog mound, no data from that fluid is reported in this chapter. Temperatures were measured using the *Alvin* high temperature probe and zero-point corrected by 2°C, taking into account the cold-junction temperature.

Utilizing a comprehensive analytical strategy, we determined the concentrations of a range of volatile, semi-volatile and non-volatile organic and inorganic aqueous species for each vent fluid sample. Samples for H_2, CH_4, H_2S and pH (25°C) were withdrawn into glass gas-tight syringes and analyzed on board ship. Fluid aliquots for the determination of CO_2 were stored in evacuated 30 mL culture tubes that had been previously combusted at 400°C and sealed with butyl rubber stoppers. A subset of the culture tubes were pre-spiked with $HgCl_2$ in order to act as a poison if any microbial organisms were in the fluids. No difference in measured CO_2 concentrations was detected between Hg-treated and untreated samples, indicating that microbial processes did not affect the sampled fluids during storage. Samples for determination of the aqueous concentrations of low-molecular weight volatile organic compounds (C_2-C_6 hydrocarbons, benzene and toluene) and isotopic composition of CO_2, C_1-C_6 alkanes, benzene and toluene were withdrawn into evacuated 6 mm or 9 mm ID Pyrex® glass tubes fitted with gas-tight valves. After filling, the tubes were stored in water at 5°C until anlyzed at WHOI. Samples for the determination of Cl, Mg, and NH_4 were stored in acid-cleaned (ACS-grade 2 N HCl) Nalgene® bottles at 5°C. Samples for Si analysis were diluted 100-fold with Milli-Q water prior to storage in acid-cleaned Nalgene® bottles.

3.2.3. Sample Analysis

Aqueous H_2 and CH_4 concentrations were measured on board *Atlantis* using an HP 5890 Series II gas chromatograph (GC) equipped with a thermal conductivity detector (TCD) and 5 Å molecular sieve column following headspace extraction of the sample in the syringe using N_2. The analytical uncertainty for these analyses (1σ) was <4% of the mean. Because the concentrations of these species were measured in a known volume of fluid, they are reported in units of mmol/L fluid, while data for other species measured on shore are reported in units of mmol/kg fluid in Table 3-1. For fluids of seawater salinity

and less, conversion between these two units influences the reported concentrations by less than 2%.

The major ions (Cl, Ca, Na, K and Mg) were measured using ion chromatography, and ΣNH_3 ($NH_{3(aq)} + NH_4^+$) concentrations were measured spectrophotometrically by flow injection analysis using the Berthelot reaction (KOROLEFF, 1976). Analytical uncertainties for the major ions and ΣNH_3 are estimated to be $\pm$2% and $\pm$5% respectively. Dissolved Si concentrations were analyzed using inductively-coupled plasma optical emission spectroscopy, with estimated analytical uncertainties of $\pm$5%.

Carbon dioxide concentrations were determined by adding 5 mL of 25% phosphoric acid to the fluid in the culture tube and then sparging the headspace gas into a purge and trap device interfaced to a HP 5890 Series II gas chromatograph (GC) that utilized a Porapak-Q packed column and TCD. Helium was utilized as carrier gas, and the oven was programmed at 50°C for 3 minutes, ramped at 10°C/min to 100°C, at 12 °C/min to 160°C, 16°C/min to 240°C, and held there for 2 minutes. The relative analytical uncertainties are estimated to be $\leq$ 10%.

The C_2-C_4 alkanes, benzene and toluene were quantified using a purge-and-trap method with the same GC conditions as for the CO_2 analyses, except that the final hold time was extended to 12 minutes. Samples were also analyzed on an HP 6890 GC using an AT-Q capillary column interfaced directly to the purge and trap device in order to achieve lower detection limits to quantify the aqueous ethene, propene, and toluene concentrations. The initial setpoint for the GC oven was 10°C, and was held there for 4 minutes to allow all of the gas from the purge and trap device to be swept onto the column. Thereafter, the oven temperature was raised at 10°C/min to 240°C, and held there for 8 minutes. The column flow rate was controlled by a constant flow regulator, which was adjusted to deliver the carrier gas at 26 psi when the oven was at 10°C. Analytical accuracy for the hydrocarbon gases ranged from $\pm$5% for ethane, and propane; $\pm$10% for ethene, propene, butane, benzene and toluene; and $\pm$15% for iso-butane and butene. The ethene concentrations for samples from the Dead Dog vent fluids had to be

measured using the packed column method because the tailing of the ethane peak precluded quantitation of the ethene peak on the capillary gas chromatgrams, their analytical uncertainty is estimated to be ±20%.

The stable carbon isotopic composition of CO_2, the C_1-C_4 alkanes, benzene and toluene were quantified using GC-isotope ratio monitoring mass spectrometry (GC-IRMS). The GC-IRMS system consisted of a HP 6890 GC with a Gerstel PTV injector and a capillary AT-Q column, interfaced to a Finnigan MAT Delta Plus mass spectrometer via an oxidation furnace consisting of Ni, Pt and Cu wires held at 940°C. Because of the several orders of magnitude differences in concentrations between CO_2, CH_4 and the other species of interest, two different injection techniques and GC conditions were used. Fluid and headspace gas from the glass tubes were first withdrawn into a 100 mL glass gas-tight syringe that was preloaded with 5 mL 25% phosphoric acid. The syringe was fitted with a septum adaptor, allowing smaller subsamples (100 µL to 1 mL) of headspace gas to be withdrawn into a second glass gas-tight syringe for direct injection onto the GC column for the CO_2 and CH_4 analyses. The oven was initially held at 40°C for five minutes, and then ramped at 75°C/min to 240°C, and held for 5.84 minutes. After analyses of CO_2 and CH_4 (typically 2 to 3 replicates), 10 mL of approximately 25% NaOH was added to the fluid in the 100 mL syringe to remove the CO_2 from the headspace. The remaining headspace gas was then transferred to a 10 mL glass gas-tight syringe. Aliquots of this gas, ranging from 25 µL to 5 mL, depending on the hydrocarbon and aromatic concentrations in the sample, were initially trapped on deactivated Si beads in a 1/8" OD, 0.085" ID stainless steel tube placed in liquid N_2 and then refocused on the head of the column at -30°C. The oven temperature was then ramped at 50°C/min to 40°C, held for 3 minutes, ramped to 240°C at 10°C/min and held there for 2 minutes. The stable carbon isotopic composition of the gases is reported using standard delta notation, where $\delta^{13}C$ is expressed in permil (‰) units, and is calculated as the relative difference in the $^{13}C/^{12}C$ ratio of the sample, R_s, and the Vienna PDB (VPDB) standard (R_{VPDB}; $^{13}C/^{12}C = 0.011180$; ZHANG and WEN-JUN, 1990):

$$\delta^{13}C\,(‰) = \left[\frac{R_S - R_{VPDB}}{R_{VPDB}}\right] * 1000. \qquad (1)$$

The GC-IRMS precision (1σ) was 0.8‰ CO_2 and CH_4 and 0.5‰ for the C_2-C_6 alkanes. Because the concentrations of the C_1-C_4 hydrocarbons are nearly zero in ambient seawater, the measured isotopic composition was taken as that of the species in the endmember hydrothermal fluid. CO_2, however, has a concentration in ambient seawater of 2.3 mmol/kg fluid, so that this assumption is not valid. The $\delta^{13}C$ of the CO_2 in the endmember hydrothermal fluid was calculated via an isotopic mass balance:

$$\delta^{13}CO_{2,HT} = [\delta^{13}CO_{2,M}C_M - (\delta^{13}CO_{2,SW}C_{SW}(1-f))]/\,[C_{HT}(f)], \qquad (2)$$

where C is the measured concentration of CO_2, f refers to the fraction of hydrothermal fluid in the sample, calculated from the Mg concentration data, and the subscripts HT, M and SW refer to the hydrothermal, measured and seawater components, respectively. For each vent, at least two aliquots of fluid were analyzed, one from each of the two gas-tight samplers when possible. All analyses were averaged to give a single carbon isotopic composition for the different compounds for each vent, which is reported in Table 3-2.

3.3. RESULTS

Because fluid samplers have a finite dead volume that is filled with bottom seawater prior to deployment, and seawater entrainment occurs to varying degrees during sampling, the fluid that is collected represents a mixture between seawater and hydrothermal vent fluid. Laboratory experiments have demonstrated near quantitative removal of Mg from seawater during hydrothermal seawater-basalt interaction at temperatures, pressures and water/rock ratios that exist in ridge-crest hydrothermal systems (BISCHOFF and DICKSON, 1975; MOTTL and HOLLAND, 1978; SEYFRIED and BISCHOFF, 1981). Therefore, the composition of endmember hydrothermal vent fluids is calculated by extrapolating the concentrations of individual species to zero Mg using linear least squares regression of vent fluid and seawater compositions (VON DAMM et al., 1985a; 1985b). Calculated endmember concentrations are reported in Table 3-1 for each

vent, along with the chemical data for each fluid sample. Plots of individual species versus Mg for each vent are given in Figure 3-1. For most of the vents, at least one of the sampled fluids had a measured Mg concentration of <20% of the seawater value (Table 3-1). Only one gas-tight sample was acquired for ODP Hole 1035F, which consisted of 82% entrained seawater. Therefore, the extrapolated endmember concentrations of the volatile species for this vent are subject to a large degree of uncertainty, and should be interpreted with caution.

3.3.1. Inorganic Species

Chloride concentrations are quite distinct for the two vent fields. Concentrations in fluids from the Dead Dog field range between 546-586 mmol/kg fluid, while at the ODP Mound vent field concentrations are depleted relative to seawater, ranging from 432-449 mmol/kg. Aqueous H_2 concentrations for the Dead Dog fluids range between 1.9-2.6 mmol/L fluid, while at the ODP Mound field the concentrations spanned a wider range from 2.1-8.2 mmol/L fluid. Endmember CO_2 concentrations range between 7.2 and 13.1 mmol/kg fluid, with no distinct geographic trend. Endmember Si concentrations range between 8.05-11.9 mmol/kg fluid, with the exception of ODP Hole 1035F, which had a concentration of only 5.79 mmol/kg fluid.

Endmember concentrations of NH_3, a sedimentary-derived inorganic compound, are elevated in fluids from the Dead Dog field, relative to fluids from the ODP Mound field. NH_3 concentrations in the Dead Dog fluids range from 2865-3108 μmol/kg fluid. Fluids from Spire, Shiner Bock and 1035H all have endmember concentrations that range from 2096-2340 μmol/kg fluid. Fluids from 1035F have the lowest endmember concentration of only 1263 μmol/kg fluid.

3.3.2. Organic Species

Similar to the trends observed for NH_3, endmember concentrations for the organic species (C_1-C_4 alkanes, benzene and toluene) are all elevated in the Dead Dog fluids relative to the ODP Mound fluids (Table 3-1; Fig. 3-2). For example, methane concentrations from the Dead Dog and ODP Mound fields range from 18.5 to 22.6 and 2.99 to 7.07 and mmol/L fluid, respectively. In general, the endmember concentrations

of the alkanes decrease approximately exponentially with increasing chain length. For example, the C_1 to n-C_4 concentrations in Inspired Mounds vent are 21.6 mmol/L and 230, 60 and 6.1 μmol/kg fluid, respectively. Iso- and n-butane concentrations are approximately equal in the Dead Dog field fluids, while in the ODP Mound field fluids, n-C_4 concentrations are approximately three times higher than i-C_4 concentrations (Table 3-1; Fig. 3-2A). Calculated endmember ethene and propene concentrations were quite low, ranging between 3.1-30 nmol/kg fluid and 3.7-40 nmol/kg fluid, respectively (Table 3-1; Fig. 3-2B).

Benzene is enriched by an order of magnitude in Dead Dog fluids as compared to ODP Mound fluids, with maximum concentrations of approximately 22 and 2.4 μmol/kg fluid, respectively. Toluene concentrations are 25 times greater in Dead Dog fluids than in ODP Mound fluids, with maximum concentrations of 5 and 0.2 μmol/kg fluid, respectively(Table 3-1; Fig. 3-2C) .

3.3.3. $\delta^{13}C$

The stable carbon isotopic composition was measured for CO_2, C_1-C_4 alkanes, benzene and toluene and is reported with the standard deviation (1σ) of all analyses used to calculate an average value for each vent in Table 3-2. The $\delta^{13}C$ of CO_2 was relatively light (i.e., depleted in ^{13}C) as compared to seawater CO_2 (-0.6‰ for bottom seawater collected on the flank of the Juan de Fuca Ridge:SANSONE et al., 1998) for vent fluids from both areas, ranging from -20.7 to –27.8‰ in the Dead Dog field fluids, and, with the exception of fluids from 1035F, -33.4 to –34.6‰ in the ODP Mound fluids. The $\delta^{13}C$ of CO_2 from the 1035F drillhole was -24.8‰. Methane $\delta^{13}C$ values ranged between -53.3 and –55.5‰ in Dead Dog field fluids, and was slightly lighter in the ODP Mound fluids, ranging between –50.8 and –51.6‰, with the exception of fluids from the 1035F drillhole (-53.3‰). The isotopic composition of ethane and propane in the Dead Dog and ODP Mound fluids were very similar, ranging between –20.3 and -22.7‰. n-Butane in the Dead Dog fluids was enriched in ^{13}C compared to both the shorter-chained alkanes and iso-butane, ranging between –18.3 to –19.0, while iso-butane values fell between -21.8 to –23.6‰. The isotopic composition of both butane isomers in the ODP Mound

fluids overlapped with each other and the shorter-chained alkane composition. Within the accuracy of our measurements, the benzene and toluene $\delta^{13}C$ in the ODP Mound fluids was also identical to that for the C_2-C_4 alkanes, ranging between –22.5 to –21.5‰ and –24.4 to –22.2‰, respectively. In the Dead Dog fluids, however, the benzene was slightly depleted relative to the ODP Mound fluids, ranging between –23.2 and –22.5‰. Toluene in the Dead Dog fluids was slightly enriched relative to the benzene, ranging between –22.3 and –20.2‰.

3.4. Discussion

3.4.1. Subsurface Conditions

As seawater circulates through the crust and undergoes progressive heating and reaction with basement rocks or sediments, the point of maximum heating is referred to as the "reaction zone" (Alt, 1995; Fig. 1-2). Traditionally this is thought of as occurring at the point of deepest circulation prior to buoyant forces causing the fluid to rise back toward the seafloor. While pressures in this region can be constrained if there is geophysical evidence for an axial magma chamber, temperature is much more difficult to estimate. Exit temperatures measured in hydrothermal fluid at chimney orifices typically do not reflect the maximum temperatures to which fluids are exposed in the reaction zone. This can be due to adiabatic and conductive cooling of fluids during ascent as well as to the mixing of cold seawater with hydrothermal fluid within the chimney or vent structure. For example, at Puppy Dog vent, a low (~0.5 m high) mound covered with tube worm beds, shimmering water that appears to be diffuse flow exits the mound from around the clumps of worms. Fluid temperatures of only 17°C were measured in the flow just above the worms. However, when a clump of worms was removed so that the temperature probe could be inserted into an orifice at the base of the mound, a temperature of 202°C was recorded.

Chemical proxies must therefore be utilized to constrain conditions in subsurface reaction zones. Inorganic compounds such as Cl and Si have often been relied upon in the past as geothermometers. However, since the Si proxy is based on the assumption

that Si concentrations are controlled by quartz solubility, if cooling and re-equilibration occurs during upflow or if a silicate phase other than quartz is precipitated, calculated temperatures will not accurately reflect the hottest, deepest reaction zone conditions. In regions such as Middle Valley where hydrothermal fluids also interact with organic-carbon containing sediments, organic compounds may also serve as geothermometers, providing further insight into subsurface temperature regimes.

3.4.4.1. Cl concentrations. Chloride is mostly conservative in water-rock reactions, so that large deviations in Cl concentrations with respect to seawater values can be attributed to phase separation processes in the subsurface (BUTTERFIELD et al., 1994b; LILLEY et al., 1993; SEYFRIED et al., 1991). Non-conservative behavior of Cl caused by the precipitation of a mineral such as halite is thought to occur only under transient conditions shortly after an eruption (VON DAMM, 2000). These conditions do not characterize Middle Valley, where venting temperatures have remained stable between 184-280°C over the ten-year period from 1990 to 2000 (BUTTERFIELD et al., 1994a; ZIERENBERG and MILLER, 2000; Table 3). These temperatures are similar to subsurface temperatures measured in ODP Hole 858G, drilled into the Bent Hill massive sulfide deposit, which were isothermal at 272°C between 90 mbsf and the bottom of the hole at 209 mbsf (SHIPBOARD SCIENTIFIC PARTY, 1998b). Fluid inclusion homogenization temperatures and the assemblages of alteration minerals in the basaltic sills of ODP Site 858 are also consistent with maximum subsurface temperatures of 260-270°C (STAKES and SCHIFFMAN, 1999).

Chloride concentrations in Dead Dog fluids are enriched relative to seawater by a maximum of only 8%, which can be attributed to hydration reactions during sediment and basalt alteration, and is consistent with these fluids not having undergone phase separation (Fig. 3-3). In contrast, the ODP Mound fluids are all depleted in Cl relative to seawater by 17 to 20%, indicating that these fluids must have undergone phase separation during their history. At seafloor pressures of 240 bars, fluid temperatures of at least 385° are required to phase separate fluids of seawater chlorinity (Fig. 3-3). The fluids venting

at the ODP Mound field have thus experienced approximately 120-145° of cooling during upflow from the subsurface reaction zone to the seafloor.

3.4.1.2. Alkene and alkane abundances. Elevated concentrations of NH_3, and organic compounds with depleted $\delta^{13}C$ signatures below –20‰ in Middle Valley fluids provide compelling evidence for extensive interaction of the fluids with the sediments as well as with basalt. Interaction with the sediments can potentially occur during recharge, when fluids are circulating downward through the sediment section, as well as during upwelling. High concentrations of B and NH_3 measured in pore fluids from ODP Hole 858G in the Dead Dog vent field, which was cased through the sediment section and terminated in basaltic basement (SHIPBOARD SCIENTIFIC PARTY, 1998b), indicate that hydrothermal fluids must be interacting with sediments during recharge. Given that fluid flow appears to be focused along channels of high permeability during upflow (STEIN and FISHER, 2001), the extent of interaction with fresh, unaltered sediment during upflow is likely minor compared to the interaction that occurs during recharge. Organic compounds leached from the sediments by recharging fluids are carried into the reaction zone, which is considered to be the deepest, hottest portion of the basement through which the fluids pass. Increasing temperatures during circulation allow secondary post-generation degradation reactions to occur among the aqueous organic compounds.

Laboratory hydrous and anhydrous pyrolysis experiments demonstrate that low-molecular weight alkenes are generated as unstable reaction intermediates during the thermal maturation of sedimentary organic matter (MANGO et al., 1994; MONTHIOUX et al., 1985; TANNENBAUM and KAPLAN, 1985a, b). The presence of these compounds in natural gases are used as evidence for their recent generation under conditions of hydrothermal activity (WHITICAR et al., 1994). Using laboratory experiments designed to investigate the interaction of organic compounds with water and minerals found in natural environments under geologically reasonable temperatures and pressures, Seewald (1994; 1997; 2001a) demonstrated that the relative aqueous abundances of alkenes may be regulated by metastable thermodynamic equilibrium with the corresponding alkane and H_2, as in:

$$C_2H_{4(aq)} + H_{2(aq)} = C_2H_{6(aq)} \qquad (3)$$

ethene ethane

$$C_3H_{6(aq)} + H_{2(aq)} = C_2H_{8(aq)} \qquad (4).$$

propene propane

Reactions proceed in the direction that favors a decrease in the Gibbs free energy which is calculated as:

$$\Delta G_{rxn} = \Delta G^\circ + RT\ln Q, \qquad (4)$$

where R is the gas constant, T is temperature in Kelvin, and Q is the reaction quotient, calculated as the ratio of the concentrations of products to the concentrations of the reactants. At equilibrium:

$$\Delta G^\circ = -RT\ln K \qquad (5),$$

where K is the thermodynamic equilibrium constant for the reaction at the temperatures and pressure of interest. By substituting this expression into Equation 4, the Gibbs free energy for a given reaction can be calculated as:

$$\Delta G_{rxn} = RT\ln(Q/K) \qquad (6).$$

By assuming that alkanes and alkenes attain equilibrium in natural systems, measured fluid concentrations can be used to determine the temperatures in subsurface reaction zones. The values of Q were calculated from the calculated endmember concentrations for each vent. Values for K were taken from the SUPCRT92 database (JOHNSON et al., 1992). Since the equilibrium state of a reaction depends on both temperature and pressure, it was assumed that the subsurface reaction zone pressure was at 260 bars for the Dead Dog field which corresponds to the top of the basement beneath the vent field (SHIPBOARD SCIENTIFIC PARTY, 1992b, 1998b). For the ODP Mound field, a pressure of 280 bars was assumed to approximate the top of the regional basement at this location (SHIPBOARD SCIENTIFIC PARTY, 1998a). At these conditions, K values, and therefore temperature estimates are insensitive to pressure effects. However, at conditions in the near-critical region, pressure effects become more significant.

Temperatures estimated from Reactions 3 and 4 are 20 to 50°C lower for the Dead Dog field fluids relative to the ODP Mound field, and lower than those required for phase

separation (Table 3-3; Fig. 3-4). This relationship is consistent with the Cl concentrations, which indicate that the Dead Dog fluids have not phase separated. Temperatures calculated for ethene-ethane equilibrium in the ODP Mound fluids at 280 bars are within 2-5°C of the phase boundary for seawater (BISCHOFF and ROSENBAUER, 1985), and are consistent with the evidence from Cl concentrations that temperature in the subsurface reaction zone is hot enough to cause phase separation. Temperatures estimated assuming propene-propane equilibrium are slightly lower than for ethene-ethane equilibrium, and exhibit more scatter (Table 3-3; Fig. 3-4), which may reflect the greater uncertainty associated with the analytical data. Analytical difficulties notwithstanding, the lower calculated temperatures for the Dead Dog fluids as compared to the ODP Mound fluids, and the agreement of calculated temperatures for the ODP Mound fluids with the two-phase boundary for seawater, suggest that metastable alkene-alkane equilibria is attained in high temperature reaction zones. The estimated temperatures in Dead Dog fluids are only slightly hotter than the ~280-300°C estimated for the basement at the Dead Dog field based on models of the sediment physical properties, heat flow measurements and the geochemistry and mineralogy of altered basaltic sills at ODP Site 857 (DAVIS and VILLINGER, 1992; DAVIS and WANG, 1994; STAKES and SCHIFFMAN, 1999). Downhole temperatures were also measured in several holes (1035A, D and E) drilled near and on the Bent Hill massive sulfide deposit during Leg 169 (SHIPBOARD SCIENTIFIC PARTY, 1998a). Subsurface temperatures estimated from these measurements at the top of the regional basement from these measurements range between 150-329°C. This indicates that cooling of the ODP Mound fluids from maximum temperatures near 400°C occurred in the subsurface prior to venting, but that alkane and alkene concentrations were quenched at concentrations reflecting maximum reaction zone conditions. The rate of attainment for alkane-alkene equilibration is dependant upon the redox state of the system, with reactions proceeding at slower rates under more reducing conditions because sulfur species of intermediate oxidation states, the concentrations of which are highest under oxidizing conditions, catalyze Reactions such as 3 and 4 (SEEWALD, 2001a). In the relatively reducing environment at Middle

Valley, indicated by aqueous H_2 concentrations between 2 to 8 mmol/L, the kinetics of alkane-alkene equilibration may be slowed enough relative to the cooling and subsequent venting of fluids at the seafloor to preserve a record of maximum reaction zone conditions.

The H_2 concentration of Spire vent is quite low compared to that for 1035H and Shiner Bock vents. This difference likely reflects the consumption of H_2 generated in subsurface reaction zones through reaction with sulfide minerals in the ODP Mound during upflow (see Chapter 4). Therefore, temperatures calculated using the H_2 concentrations in Spire vent fluids should be lower than those calculated for 1035H and Shiner Bock vents, and will reflect temperature conditions in the upflow zone (Table 3-3).

3.4.1.3. Silica. If it is assumed that aqueous silica concentrations are controlled by quartz solubility, then it can also be utilized as a proxy for reaction zone conditions. However, if conductive cooling of the fluids during upflow leads to precipitation of silica, then calculated temperatures will not reflect reaction zone conditions. Using the quartz solubility model of Von Damm et al. (1991) with density data for seawater at elevated temperatures and pressures (BISCHOFF and ROSENBAUER, 1985), the temperatures at which the measured SiO_2 concentrations would be in equilibrium with quartz at 260 bars for the Dead Dog field and at 280 bars for the ODP Mound field can be calculated (Table 3-3). The values range from 250-290°C for the Dead Dog vents and ~400-425°C for the ODP Mound field vents. The calculated temperature range is in good agreement with the temperatures calculated from the other organic and inorganic temperature indicators in these systems, and further demonstrate the utility of aqueous organic compounds as geochemical indicators of subsurface conditions.

3.4.2. Alkane Abundances

Two trends are apparent in the n-alkane distributions at Middle Valley: (1) the fluids from the Dead Dog field are enriched in C_1-C_4 n-alkanes relative to fluids from the ODP Mound field; and (2) the concentrations of the hydrocarbons decrease with increasing chain length (Table 3-1; Fig. 3-2A). These trends are both evidence of a

greater extent of secondary thermal alteration of the aqueous organic compounds after generation from sediments in the ODP Mound field fluids. The more mature nature of the alkane distribution in the ODP Mound fluids as compared to the Dead Dog fluids also results in higher concentrations of methane relative to the longer-chained alkanes, which results in higher values of calculated $C_1/(C_2+C_3)$ ratios (Table 3-1). As the alkane-bearing fluids travel through the subsurface and undergo progressive heating, secondary post-generation degradation reactions serve to shift the alkane abundances toward relative enrichments in methane. The hotter subsurface reaction zone conditions at the ODP Mound field would lead to a greater enrichment in methane relative to fluids from the Dead Dog field. Time and temperature are interchangeable variables for kinetically-controlled reactions (BRAUN and ROTHMAN, 1975; BURNHAM et al., 1995; HUNT, 1996; TISSOT and WELTE, 1984; WAPLES, 1984). Therefore, the alkane distributions could also reflect a longer residence time of the fluids in a hot subsurface reaction zone prior to venting at the ODP Mound field relative to the residence time of fluids in the subsurface at the Dead Dog field.

The i-C_4/n-C_4 ratio decreases from approximately 1 in the Dead Dog fluids to 0.3 in the ODP Mound field fluids, which is also consistent with higher subsurface temperatures at the ODP Mound field. At temperatures greater than approximately 90°C, free radical reactions favor the fomation of straight-chained alkanes, which leads to a predominance of straight-chained alkanes over their branched counterparts (HUNT, 1985; HUNT et al., 1980; WHELAN et al., 1988).

The aromatic compounds benzene and toluene are also enriched in Dead Dog fluids relative to ODP Mound fluids (Table 3-1; Figure 3-2C). While benzene concentrations are greater than toluene concentrations in all fluids, the ODP Mound fluids exhibit higher benzene/toluene ratios than the Dead Dog fluids. Benzene persists in high temperature geologic environments owing to stability of the aromatic ring structure. Toluene, however, may be oxidized to benzene via a decarboxylation pathway:

$$\underset{\text{toluene}}{C_6H_5CH_{3(aq)}} + 2\ H_2O \rightarrow \underset{\text{benzene}}{C_6H_{6(aq)}} + CO_{2(aq)} + 3\ H_{2(aq)} \qquad (7)$$

under hydrothermal conditions (McCollom et al., 2001). Kinetic barriers precluded the attainment of equilibrium according to Reaction 7 in laboratory experiments conducted at 300-330°C, 350 bars (McCollom et al., 2001). The higher benzene/toluene ratios observed in the ODP Mound fluids relative to the Dead Dog fluids are consistent with hotter subsurface temperatures at ODP Mound. Calculated ΔG_{rxn} values at seafloor conditions for Reaction 7 indicate that this reaction is favored to proceed in the forward direction only for Chowder Hill vent, with Inspired Mounds and Shiner Bock in equilibrium (Fig. 3-6A). At subsurface reaction zone temperatures estimated from the ethane-ethene geothermometer, ΔG_{rxn} values are negative, indicating a drive for the conversion of toluene to benzene via the decarboxylation pathway (Fig. 3-6B). The apparent lack of a thermodynamic drive at the seafloor could then be attributed to conductive cooling of fluids during upflow. The low concentrations of Mg in collected fluids rules out the entrainment of cold seawater during upflow as a cooling mechanism.

The aqueous organic compounds in these fluids could be derived from the alteration of several different sources. For example, dissolved organic carbon in sedimentary porewaters could be transported in downwelling fluids into the hot subsurface reaction zones and then undergo maturation due to the high temperatures. Alternatively, aqueous organic compounds could be derived from the thermal maturation of sedimentary kerogen due to the high heat fluxes in both vent fields. However, the generation of compounds from the heating of sedimentary organic matter will occur along the entire flowpath during recharge, and won't be confined simply to the hottest portion of the subsurface reaction zone. It is not possible to distinguish between these two sources with the data presented in this thesis. Making this distinction has little bearing on the use of these compounds as geochemical indicators of subsurface conditions, since the reactions that are recording subsurface conditions occur after generation from the source. However, understanding the relative amount of these two sources may be important in quantifying the role of hydrothermal vents in the global carbon cycle, and in understanding whether the reduced carbon compounds released in vent fluids are "new" (i.e., produced from sedimentary organic matter) or "recycled"

(produced from oceanic dissolved organic matter that has been carried into the subsurface by recharging fluids).

3.4.3. Isotopic Systematics

3.4.3.1. Hydrocarbons. The kinetic processes that control the distributions of n-alkanes derived from organic matter alteration also affect the stable carbon isotopic composition of those compounds. Biogenic formation of methane by microbial degradation of organic matter leads to methane with a large range of $\delta^{13}C$ values (–42 to –105‰) that varies with community structure, metabolic pathway and environmental variables, such as temperature (SCHOELL, 1988; and references therein). Methane formed from the alteration of sedimentary organic matter at elevated temperatures (termed "thermogenic") typically falls in the range –25 to –50‰, while methane synthesized abiotically from mantle-derived CO_2 and H_2 is typically heavier, ranging between –20 to –10‰ (DES MARAIS et al., 1981; KELLEY and FRÜH-GREEN, 1999; SHERWOOD LOLLAR et al., 1993; WELHAN, 1988). The $\delta^{13}C$ values of ethane and propane generated in both natural environments and laboratory pyrolysis experiments are enriched relative to the co-existing methane, and typically range between –18 and –34‰, with propane 5 to 8‰ heavier than ethane (BERNER et al., 1995; DES MARAIS et al., 1988; LORANT et al., 1998; ROONEY et al., 1995). The isotopic ratios of thermogenic methane, ethane and propane typically increase with increasing maturity (BERNER et al., 1995; LORANT et al., 1998, and references therein; ROONEY et al., 1995).

The relationship between maturity and the stable carbon isotopic composition of generated hydrocarbons can be assessed by plotting the $\delta^{13}C$ values versus the $C_1/(C_2+C_3)$ ratio (Fig. 3-7). Free gases recovered from sediments at Site 858 (Bent Hill) and Site 856 (Dead Dog) during ODP Leg 139 were characterized by similar isotopic compositions and $C_1/(C_2+C_3)$ ratios as the aqueous alkanes from the Dead Dog field (WHITICAR et al., 1994; Fig. 3-7). Whiticar et al. (1994) used a two-component mixing model to calculate that 80-85% of the methane in the free gases recovered from Leg 139 sediments was derived from a bacterial source. Such a predominance of bacterially-derived CH_4 is further evidence for extensive interaction of the fluids with sediments

during recharge. During upflow and in the reaction zone, fluid temperatures were sufficiently hot to exceed the estimated upper temperature limit for microbial life (~115°C; BLOCHL et al., 1997; PLEDGER and BAROSS, 1991; STETTER et al., 1990).

Taken together, the fluids from both vent sites define a trend of increasing $\delta^{13}C$ with increasing $C_1/(C_2+C_3)$, which reflects an increasing extent of reaction among the organic compounds in these fluids. Methane, ethane and propane are derived from the sediments during fluid recharge. Based on previous modeling results (WHITICAR et al., 1994), a large fraction of the methane is apparently derived from bacterial processes in those sediments that are not hot enough to inhibit microbial life and have porewater sulfate concentrations of zero due to bacterial sulfate reduction processes. Heating of the fluids as they circulate through the subsurface causes secondary (i.e. after generation from the sedimentary organic matter) alteration reactions among the organic compounds. During these reactions, ^{12}C-^{12}C bonds are preferentially broken relative to ^{12}C-^{13}C bonds, which will lead to the formation of methane that is lighter than the precursor compounds but heavier than the bulk of the methane in the fluid that had been derived from bacterial processes. The residual organic compounds will become enriched in ^{13}C relative to the initial composition. Accordingly, methane derived from ^{13}C-enriched residual material will become heavier with continued reaction. The degradation reactions, whereby longer-chained hydrocarbons become smaller, will also lead to an increase in $C_1/(C_2+C_3)$ ratios as is observed (Fig. 3-7A). The heavier $\delta^{13}C$ of methane and higher $C_1/(C_2+C_3)$ ratios in the ODP Mound fluids relative to the Dead Dog fluids is consistent with the other evidence for hotter subsurface reaction zone temperatures beneath the ODP Mound (Cl concentrations; fluid inclusions in the Bent Hill massive sulfide deposit; calculated alkene:alkane equilibration temperatures).

The carbon isotopic composition of the C_2-C_4 alkanes, benzene and toluene generally lie in a narrow range between –20 and –23‰, with no difference relative to subsurface temperature or inferred extent of alteration of the aqueous organic compounds in the two fields (Table 3-2, Fig. 3-7,B-D). The isotopic similarity of ethane, propane and butane in fluids from the two fields, despite the higher temperatures at the ODP

Mound field, indicates that the isotopic composition of these compounds are not affected by the degradation reactions that contribute to the shift in heavier methane values in the ODP Mound fluids as compared to the Dead Dog fluids. Degradation reactions do not produce only methane; C_2-C_4 compounds will also be produced from longer-chained hydrocarbons (HUNT, 1996; SEEWALD, 2001a; TISSOT and WELTE, 1984). In this scenario, production and loss of the C_2-C_4 alkanes in both vent fluids are such that the carbon isotopic compositions are not shifted relative to each other. If the degradation reactions are occurring via homolytic cracking processes, which involves cleavage of C-C bonds, maximum reaction zone temperatures at both vent fields may not be hot enough to initiate cleavage of C_2-C_4 compounds. The slight enrichment in the $\delta^{13}C$ of n-C_4 as compared to the i-C_4 in the Dead Dog fluids (Table 3-2; Fig. 3-7C) may reflect a slightly slower generation rate from the original sedimentary source material, causing the n-C_4 to be initially enriched in ^{13}C. The isotopic composition of benzene and toluene show no difference between the two fields because of the stability of the aromatic ring. Decarboxylation of toluene to form benzene will affect the methyl group, not the carbon atoms contained within the ring itself.

3.4.3.2. Carbon Dioxide. Carbon dioxide is unique among the carbon-containing species in that its abundance can also be controlled by the precipitation and dissolution of carbonate minerals, in addition to being produced and consumed during organic matter alteration. Carbon dioxide derived from magma degassing ranges from –2 to –10‰ (SHANKS, 2001). Because the CO_2 in sedimentary carbonates can be derived from bacterial as well as inorganic sources, the $\delta^{13}C$ of this material can be quite variable, ranging from seawater values of ~0‰ to as low as -50‰ in low-temperature sedimentary environments where microbial methane oxidation occurs (COLEMAN et al., 1981). CO_2 generated from the high-temperature alteration of sedimentary organic matter will be depleted in ^{13}C relative to CO_2 derived from sedimentary inorganic carbonate sources alone (KROUSE et al., 1988).

The $\delta^{13}C$ values of ΣCO_2 in fluids from the two vent fields are depleted in ^{13}C relative to magmatic values, ranging between –20.7 to –26.4‰ for the Dead Dog field

and ODP Drillhole 1035F, and –33.4 to –34.6‰ for the ODP Mound field (Table 3-2). Sedimentary carbonates in drillcores recovered during Leg 139 have $\delta^{13}C$ values ranging between –5 and –22‰ at Bent Hill and –6.8 and -21.1‰ from Dead Dog, with three recovered samples having a $\delta^{13}C$ of –32‰ (FRÜH-GREEN et al., 1994). The light carbonate in the three samples was attributed to bacterial methane oxidation processes, with the values between –6.8 and –21.2‰ reflecting the mixing of light CO_2 derived from the thermal alteration of sedimentary organic matter with seawater CO_2 (FRÜH-GREEN et al., 1994). A larger range for $\delta^{13}C$ of CO_2 (-10.6 to -38.9‰) previously reported for Middle Valley vent fluids was attributed to pyrolysis of sedimentary organic carbon as well as a contribution from dissolution of sedimentary carbonate (TAYLOR, 1992).

In addition to more negative $\delta^{13}C$ values of aqueous CO_2, the ODP Mound fluids also contain 3-4 times greater concentrations of aqueous H_2 than the Dead Dog fluids (Table 3-1). Aqueous H_2 concentrations of 6 and 8 mmol/L in 1035H and Shiner Bock vents respectively are among the highest yet reported from hydrothermal vent fluids. Methane oxidation:

$$CH_{4(aq)} + 2\ H_2O = CO_{2(aq)} + 4\ H_{2(aq)} \qquad (8)$$

could be the source of the high H_2 concentrations in the ODP Mound fluids, as well as a source of the isotopically lighter CO_2, as compared to the Dead Dog fluids and the sedimentary carbonates. Abiotic methane oxidation with minerals such as hematite (Fe_2O_3), and cupric and manganese oxides has been demonstrated in laboratory experiments, and proposed to be an important mechanism for fractionating carbon isotopes in the subsurface (KIYOSU and KROUSE, 1989). Hematite and magnetite are present as alteration minerals within the massive sulfide facies at ODP Mound (SHIPBOARD SCIENTIFIC PARTY, 1998a). Calculation of the ΔG_{rxn} for Reaction 8, utilizing our measured vent fluid compositions and the SUPCRT92 thermodynamic database, indicates that this reaction is not favored to proceed from left to right at seafloor conditions for any of the vents (Fig. 3-8A). Methane, CO2 and H2 will equilibrate according to Reaction 8 at temperatures of 292-307° at 260 bars in the Dead Dog fluids

and of 316-350°C and higher at 280 bars in the ODP Mound fluids (Fig. 3-3). Production of such high levels of H_2 from the oxidation of methane, as well as other organic compounds, indicates the potential that organics have to influence the inorganic chemistry of vent fluids. That such an effect is observed in fluids that interact with sediments containing relatively low levels of organic carbon (0.2 to 1.2 wt.%;SHIPBOARD SCIENTIFIC PARTY, 1992a) points to the potential importance of organic compounds in crustal alteration processes in a range of environments.

Previous work with other natural and experimental systems demonstrate that chemical equilibrium between CH_4 and CO_2 is not typically attained (ARNÓRSSON and GUNNLAUGSSON, 1985; JANECKY et al., 1986; WELHAN, 1988), except in systems characterized by the production of CH_4 at concentrations greater than equilibrium (SEEWALD et al., 1994). This discrepancy may reflect a difference in the reaction kinetics and the direction of approach to equilibrium. While the reaction rates in the forward and backward direction is the same at equilibrium, they need not be identical when the system is removed from equilibrium. In organic-poor systems, an approach to equilibrium from excess CO_2 may be inhibited by sluggish reaction kinetics (BARNES, 1981, 1987). In contrast, in sedimented systems with high concentrations of CH_4, rapid reaction kinetics for its oxidation may facilitate the attainment of chemical equilibrium (SEEWALD et al., 1994). Interaction of recharging fluids with the sediment cover at Middle Valley led to relatively high (> 5 mmol/kg fluid) aqueous CH_4 concentrations. As these fluids entered the basaltic basement and encountered higher temperatures, chemical equilibrium among CH_4 and CO_2 might have been obtained.

In addition to chemical equilibrium, CO_2 and CH_4 can also achieve isotopic equilibrium. It is widely accepted that CO_2 and CH_4 do not typically achieve equilibrium in the subsurface due to kinetic barriers precluding reaction at temperatures under 200°C (SACKETT and CHUNG, 1979). However, those experiments were conducted under anhydrous conditions that do not characterize the hydrothermal vent system. Recent work by Horita (2001) demonstrated that in the presence of transition metal catalysts, isotopic equilibrium was achieved between CO_2 and CH_4 at temperatures ranging

between 200-600°C. The isotopic composition of the coexisting CO_2 and CH_4 define apparent equilibrium temperatures that are higher (425-450°C) for the ODP Mound fluids than for the Dead Dog fluids (200-290°C; Figure 3-8B; Table 3-3), but are in good agreement with other organic and inorganic geochemical indicators of subsurface temperatures, considering the uncertainties inherent in these calculations. The temperature of isotopic equilibrium for Inspired Mound vent fluids is lower than for the other Dead Dog fluids, and has the poorest agreement with temperatures calculated with other proxies. This reflects the greater error associated with calculated $\delta^{13}C$ of hydrothermal CO_2 for the Inspired Mound fluid due to the greater amount of seawater entrainment when sampling fluids from this vent. The preservation of temperatures of subsurface reaction zone conditions in the $\delta^{13}C$ of coexisting CH_4 and CO_2 in these fluids is a consequence of the CO_2 being derived largely from the pool of CH_4 rather than an external source, such as magma degassing. This allows the attainment of both chemical and isotopic equilibrium because sufficient reaction time is available. Thus, in certain environments characterized by abundant organic compounds to serve as the dominant source of CO_2, the $\delta^{13}C$ of coexisting CH_4 and CO_2, may be a sensitive indicator of subsurface conditions.

3.5. CONCLUSIONS

The differences in the organic geochemistry of fluids from two areas of hydrothermal activity, the Dead Dog field and ODP Mound field, at Middle Valley are related to the differences in subsurface reaction zone conditions. While measured exit temperatures in the two fields are grossly similar, Cl concentrations indicate that the ODP Mound fluids have undergone phase separation in the subsurface and that the hottest portion of the reaction zone is hotter than at Dead Dog. Fluids predominantly interact with sediments during recharge, so that organic compounds leached from the sediments are circulated through high-temperature reaction zones and can undergo further secondary interactions. Laboratory experiments have demonstrated the rapid attainment of alkane:alkene equilibrium at hydrothermal conditions. If this is assumed to also occur

in these systems, calculated temperatures for equilibration among ethene-ethane and propene-propane are consistent with the differences in subsurface temperatures indicated by the Cl concentrations. Silica concentrations are also consistent with subsurface reaction zone temperatures indicated by both Cl and the organic compounds.

The concentrations and isotopic compositions of C_1-C_4 alkanes also indicate that the subsurface reaction zone temperature is hotter at ODP Mound. Specifically, fluids from the ODP Mound field have heavier $\delta^{13}C$ of methane and higher $C_1/(C_2+C_3)$ ratios. As fluids containing organic compounds derived from the alteration of sedimentary organic matter travel through the subsurface and encounter progressively hotter temperature conditions, secondary alteration reactions among the aqueous organic compounds occur. These reactions lead to the generation of increasing amounts of methane that gets progressively heavier with either increasing temperature or increasing residence time above a critical temperature threshold that favors reaction progress.

Abiotic oxidation of methane after its generation from organic matter appears to be a key reaction in the ODP Mound fluids, leading to more negative $\delta^{13}C$ values of CO_2 as compared to the Dead Dog fluids. Despite the prevailing hypothesis that CH_4 and CO_2 do not equilibrate chemically or isotopically in natural environments, the equilibration temperature for CO_2 and CH_4 isotopic compositions in ODP Mound fluids are consistent with evidence for reaction zone temperatures from other chemical and geological evidence. Methane oxidation generates H_2 as a product and could be the source for the extremely high H_2 concentrations observed in fluids from ODP Mound vents. Organic compounds in hydrothermal vent fluids can thus play a key role in regulating overall fluid compositions and subsequent interaction of these fluids with crustal rocks. That the sediments from Middle Valley contain relatively low levels of organic carbon compared to the sediments that overlie other mid-ocean ridges such as Guaymas Basin, yet can still affect the vent fluid compositions to such a degree, indicates the importance of further investigation of organic compounds in other hydrothermal systems and their inclusion in models of crustal alteration.

Table 3-1: Concentrations of aqueous species in vent fluids from Middle Valley, Northern Juan de Fuca Ridge.

Vent	Sample	exit T °C	Mg mmol/kg	Cl mmol/kg	H_2 mmol/L	CO_2 mmol/kg	NH_4 μmol/kg	Si μmol/kg
DEAD DOG								
Heineken Hollow	BGT-3597-1		51.0	544	0.03	2.71	64	0.32
	BGT-3597-2		11.3	589	1.5	6.92	2792	8.72
	M-3596-12C		3.13	581			2855	
	M-3596-1C		2.25	576			2996	
	M-3597-12		45.9	557			282	
	M3597-15		27.9	554			1350	
	Endmember	67-187	0	583	1.9	8.15	3180	9.12
Chowder Hill	BGT-3596-3		1.90	572	2.5	7.54	3045	
	BGT-3596-4		1.12	576	2.6	8.96	3103	11.6
	Endmember	281		575	2.6	8.43	3164	11.9
Inspired Mounds	BGT-3597-3		34.4	551	0.81	5.65	993	3.25
	BGT-3597-4		41.0	542	0.53	4.23	524	2.49
	M-3597-6C		30.3	541			1251	
	M-3597-11C		43.0	557			551	
	Endmember	255-261	0	546	2.3	11.6	2866	9.17
Puppy Dog	BGT-3599-3		6.16	582	1.8	7.65	2646	7.15
	BGT-3599-4		44.6	544	0.3	3.42	351	1.18
	Endmember	202	0	586	2.0	8.35	2986	8.05
ODP MOUND								
1035F	BGT-3598-3		43.2	527	0.39	3.44	232	1.23
	M-3598-6C		46.7	542			160	
	M-3598-11C		46.7	528			121	
	Endmember	40	0	448	2.1	8.24	1263	5.79
Shiner Bock	BGT-3595-1		1.61	435	8.0	11.7	2262	10.3
	BGT-3595-2		3.40	439	7.6	11.4	2099	9.85
	M-3595-11C		5.99	444			2130	
	M-3595-6C		12.7	467			1800	
	M-3595-1C		28.7	495			1070	
	M-3595-12		3.10	443			2240	
	Endmember	272	0	434	8.2	12.0	2340	10.5
Spire	BGT-3595-3		1.64	434	2.1	12.7	2107	10.5
	BGT-3595-4		22.5	479	1.2	8.50	1264	5.68
	M-3595-15		4.12	442			2215	
	Endmember	263	0	432	2.2	13.1	2270	10.6
1035H	BGT-3599-1		17.0	479	4.2	7.86	1446	6.58
	BGT-3599-2		20.9	481	3.7	7.62	1262	5.82
	M-3599-12		29.3	508			938	
	M-3599-15		30.3	506			855	
	Endmember	267	0	449	6.1	10.7	2096	9.55
BSW*	M-3598-6C	2.1	53.0	543	0	2.33	0.8	0.18

*bottom seawater. Samples that begin with "M" were taken in non-gas tight majors samplers, and were not used in the analysis of the volatile species.

Table 3-1 (continued): Endmember concentrations of aqueous species in vent fluids from Middle Valley, Northern Juan de Fuca Ridge.

Vent	Sample	CH_4	C_2H_4	C_2H_6	C_3H_6	C_3H_8	i-C_4H_{10}	n-C_4H_{10}	Benzene	Toluene	$C_1/(C_2+C_3)$
		mmol/L	nmol/kg	µmol/kg	nmol/kg	µmol/kg	µmol/kg	µmol/kg	µmol/kg	µmol/kg	
Dead Dog											
Heineken Hollow	BGT-3597-1	0.45	—	4.74	1.58	1.21	0.12	0.13	0.49	0.08	
	BGT-3597-2	17.7	3.85	186	—	47.7	4.85	5.34	21.8	4.70	
	M-3596-12C										
	M-3596-1C										
	M-3597-12										
	M3597-15										
	Endmember	22.6	4.03	236	40.7	60.7	6.18	6.79	27.83	5.99	76.1
Chowder Hill	BGT-3596-3	19.2	6.01	219	4.72	53.2	5.83	5.95	23.6	4.59	
	BGT-3596-4	20.3	2.92	231	2.43	56.8	6.12	6.19	21.8	4.95	
	Endmember	20.3	4.58	232	3.67	56.6	6.15	6.24	23.4	4.92	70.5
Inspired Mounds	BGT-3597-3	7.58	4.80	219	4.72	53.2	58.3	59.5	23.6	4.59	
	BGT-3597-4	4.88	4.28	231	2.43	56.8	61.2	61.9	21.8	4.95	
	M-3597-6C										
	M-3597-11C										
	Endmember	21.6	14.6	232	16.4	57.5	5.87	6.07	23.8	4.52	74.4
Puppy Dog	BGT-3599-3	16.4	3.37	175	—	44.3	4.42	5.22	19.2	3.78	
	BGT-3599-4	2.88	—	31.6	—	7.77	0.75	0.83	3.08	0.56	
	Endmember	18.5	3.82	198	—	50.1	5.00	5.90	21.7	4.27	74.6
ODP Mound											
1035F	BGT-3598-3	0.56	5.59	2.07	2.23	0.48	—	—	0.19	0.09	
	M-3598-6C										
	M-3598-11C										
	Endmember	2.99	29.9	11.1	11.9	2.58	—	—	0.99	0.09	219
Shiner Bock	BGT-3595-1	6.92	8.37	23.2	3.97	4.47	0.35	0.98	2.55	0.19	
	BGT-3595-2	6.56	7.53	23.1	2.98	4.36	0.33	0.98	2.46	0.20	
	M-3595-11C										
	M-3595-6C										
	M-3595-1C										
	M-3595-12										
	Endmember	7.07	8.35	24.3	3.66	4.63	0.36	1.03	2.63	0.20	245
Spire	BGT-3595-3	6.52	19.1	23.4	5.71	4.26	0.31	0.80	2.15	0.15	
	BGT-3595-4	3.84	13.0	14.3	3.94	2.74	0.23	0.59	1.52	0.12	
	M-3595-15										
	Endmember	6.71	20.4	24.3	6.11	4.48	0.34	0.87	2.31	0.17	233
1035H	BGT-3599-1	3.98	9.43	15.6	3.54	3.09	23.8	0.71	1.46	0.12	
	BGT-3599-2	3.54	—	14.3	—	2.72	19.7	0.65	1.26	—	
	M-3599-12										
	M-3599-15										
	Endmember	5.85	13.9	23.2	5.21	4.52	0.34	1.06	2.12	0.18	211
BSW*		0	0	0	0	0	0	0	0	0	

*bottom seawater

Table 3-2: Average stable carbon isotopic compositions for aqueous low-molecular weight organic compounds in vent fluids from Main Endeavour Field, northern Juan de Fuca Ridge.

Vent	CO_2[§]		CH_4		C_2H_6		C_3H_8		i-C_4H_{10}		n-C_4H_{10}		Benzene		Toluene	
	$\delta^{13}C$ (‰)	1σ (n)	$\delta^{13}C$ (‰)	1σ (n)	$\delta^{13}C$ (‰)	1σ (n)	$\delta^{13}C$ (‰)	1σ (n)	$\delta^{13}C$ (‰)	1σ (n)	$\delta^{13}C$ (‰)	1σ (n)	$\delta^{13}C$ (‰)	1σ (n)	$\delta^{13}C$ (‰)	1σ (n)
Dead Dog																
Heineken Hollow	-27.8	0.2 (2)	-53.3	0.0 (2)	-20.9	0.7 (2)	-20.5	0.4 (2)	-23.6	1.8 (2)	-18.7	0.8 (2)	-23.2	0.3 (2)	-21.2	0.6 (2)
Chowder Hill	-23.8	0.5 (5)	-54.3	0.3 (5)	-21.0	0.4 (3)	-20.3	0.2 (4)	-22.8	1.1 (5)	-19.0	0.1 (5)	-23.2	0.0 (4)	-21.3	0.8 (5)
Inspired Mounds	-20.7	0.9 (9)	-55.5	1.3 (11)	-21.2	0.3 (3)	-20.3	0.3 (3)	-21.3	0.5 (4)	-18.3	0.4 (4)	-23.0	0.4 (3)	-20.2	0.1 (3)
Puppy Dog	-26.4	0.6 (6)	-54.0	0.0 (2)	-20.8	0.2 (3)	-21.0	1.3 (3)	-21.8	0.3 (2)	-19.0	0.3 (2)	-22.5	1.1 (3)	-22.3	2.4 (3)
ODP Mound																
1035F	-24.8	0.3 (5)	-53.0	0.5 (6)	-22.0	0.4 (3)	-22.3	1.0 (3)	—		-22.2	— (1)	-22.5	0.8 (3)	-24.4	— (1)
Shiner Bock	-34.6	0.7 (6)	-50.8	0.8 (8)	-20.6	0.4 (4)	-20.1	0.3 (4)	-22.2	0.6 (4)	-21.7	0.4 (4)	-21.5	0.3 (4)	-22.2	0.6 (4)
Spire	-33.9	0.4 (3)	-51.6	0.6 (7)	-21.8	0.3 (3)	-21.5	0.6 (3)	-25.3	— (1)	-22.1	0.5 (3)	-22.1	0.5 (3)	-23.3	— (1)
1035H	-33.4	0.6 (12)	-51.2	0.9 (9)	-22.7	1.4 (6)	-21.2	1.2 (6)	-23.5	1.2 (3)	-21.9	1.0 (6)	-21.9	0.4 (6)	-22.5	1.4 (2)
BSW	0.6[1]															

[§]The reported $\delta^{13}C$ is the value calculated for the endmember hydrothermal vent fluid, assuming two-component mixing between a seawater endmember containing 2.33 mmol/kg CO_2, with a $\delta^{13}C$ of –0.6‰ and the endmember vent fluid with the calculated CO_2 concentration reported in Table 2. See text for discussion.

—: not analyzed. (n): total number of replicate analyses, for all tubes analyzed for a particular vent. 1σ is the standard deviation for all of the analysis averaged together to give a value for a particular vent

[1]Sansone et al. (1998)

Table 3-3: Middle Valley reaction zone temperatures (°C) estimated from several chemical proxies.

Vent	Cl	Ethene-Ethane[†]	Propene-Propane[†]	Si[‡]	CO_2-CH_4[†]	$\delta^{13}C$, CO_2-CH_4[§]
DEAD DOG AREA			reaction zone depth: 260 mbsf			
Heineken Hollow	<365[*]	337	338	260	292	290
Chowder Hill	<365[*]	348	304	290	308	230
Inspired Mounds	<365[*]	361	330	261	307	190
Puppy Dog	<365[*]	326	—	250	301	250
ODP MOUND AREA			reaction zone depth: 280 mbsf			
1035F	397[**]	395	380	425	319	250
Shiner Bock	397*[*]	393	373	405	358	450
Spire	397[**]	392	359	405	316	425
1035H	397[**]	395	374	410	350	425

[*]temperature of two-phase boundary for seawater at 260 bars.
[**]minimum temperature for phase separation to have occurred at estimated reaction zone depths.
[†]based on assumed chemical equilibrium according to reactions in text
[‡]based on assumed equilibrium with quartz at estimated reaction zone depths
[§]based on assumed isotopic equilibrium

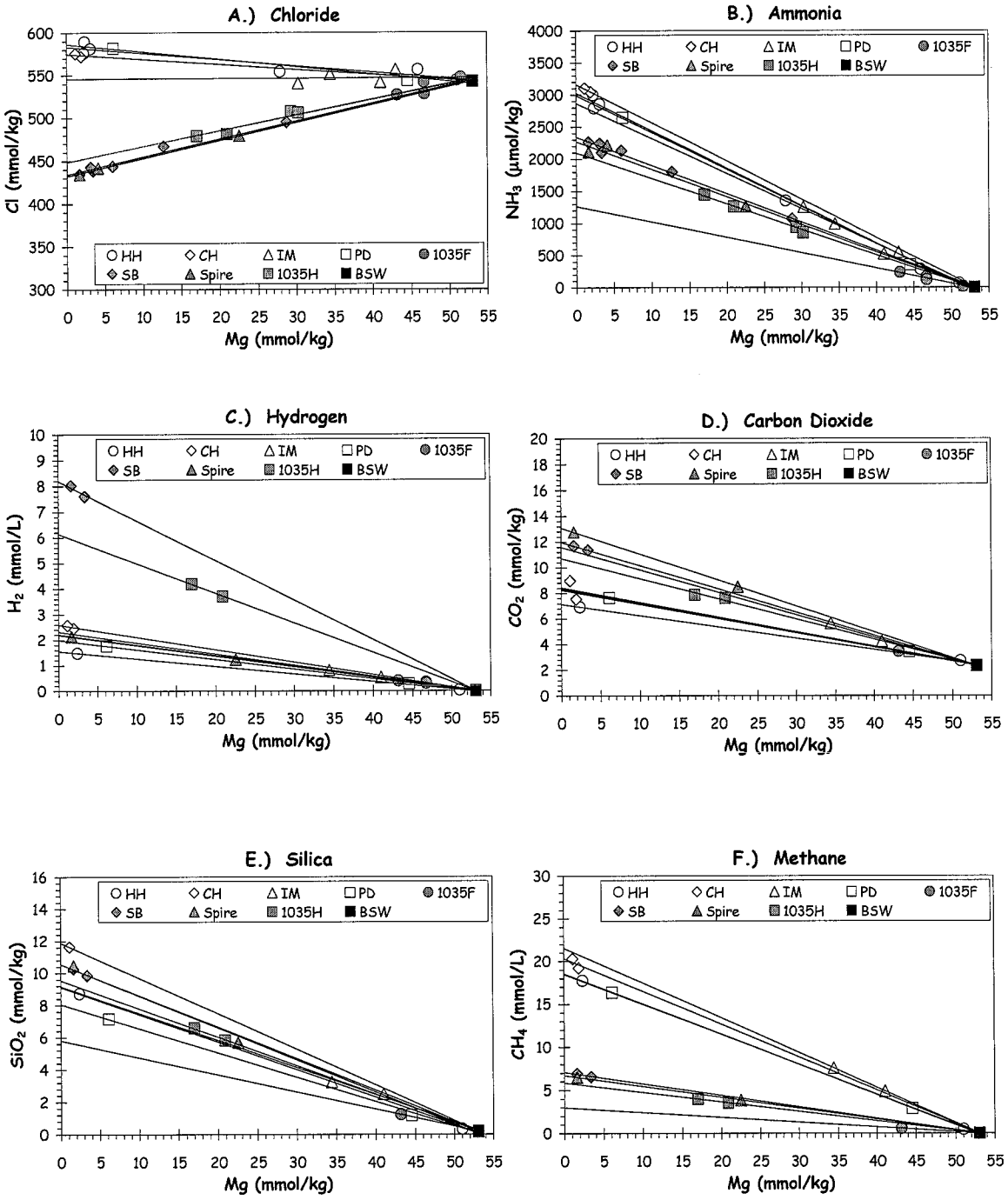

Figure 3-1. Graphs of individual chemical species versus Mg for sampled vent fluids: **(A)** Chloride; **(B)** Ammonia; **(C)** Hydrogen; **(D)** Carbon Dioxide; **(E)** Silica; **(F)** Methane. Key to vents: HH: Heineken Hollow; CH: Chowder Hill; IM: Inspired Mounds; PD: Puppy Dog; SB: Shiner Bock

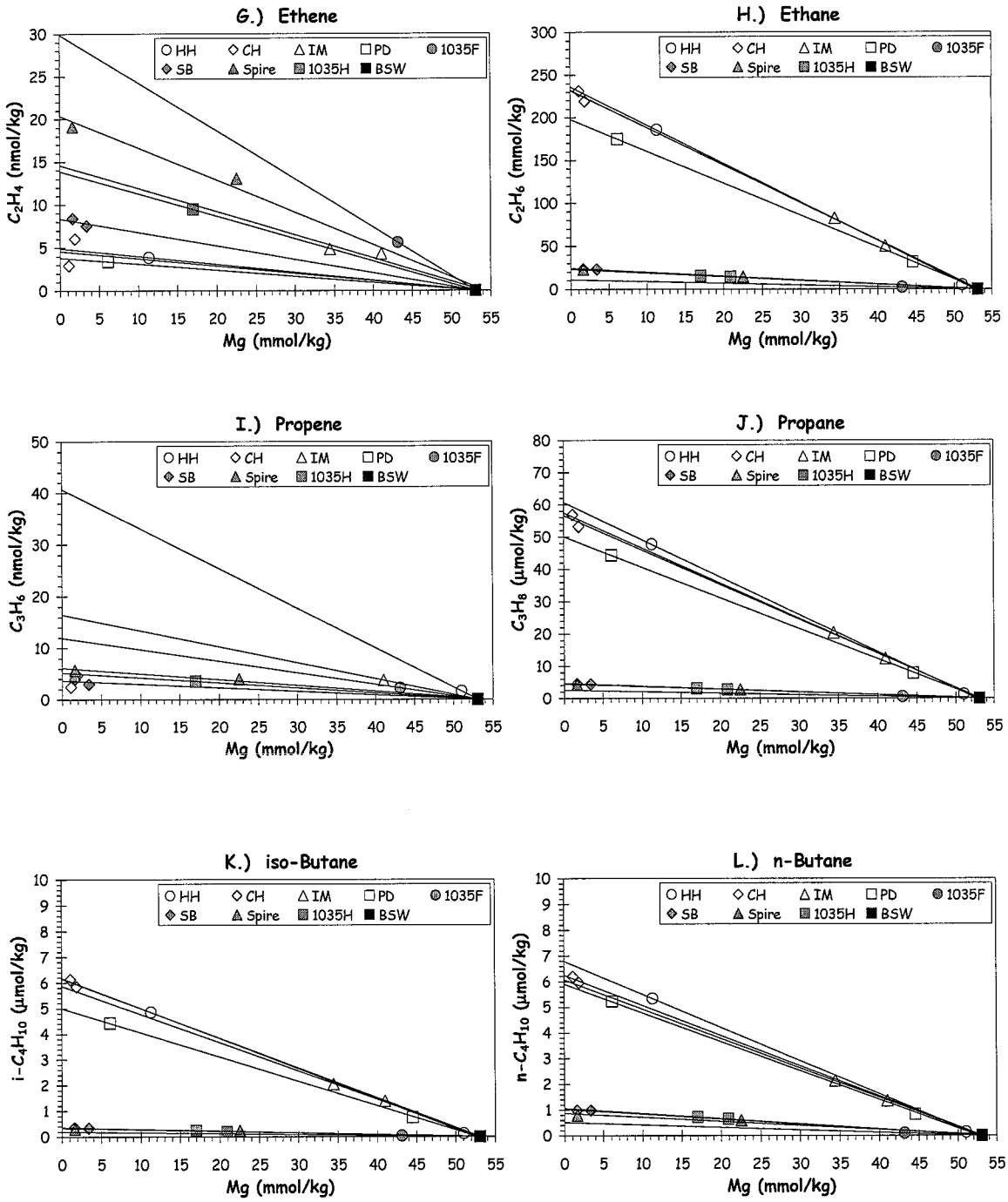

Figure 3-1, continued. **(G)** Ethene; **(H)** Ethane; **(I)** Propene; **(J)** Propane; **(K)** iso-Butane; **(L)** n-Butane. Key to vents: HH: Heineken Hollow; CH: Chowder Hill; IM: Inspired Mounds; PD: Puppy Dog; SB: Shiner Bock

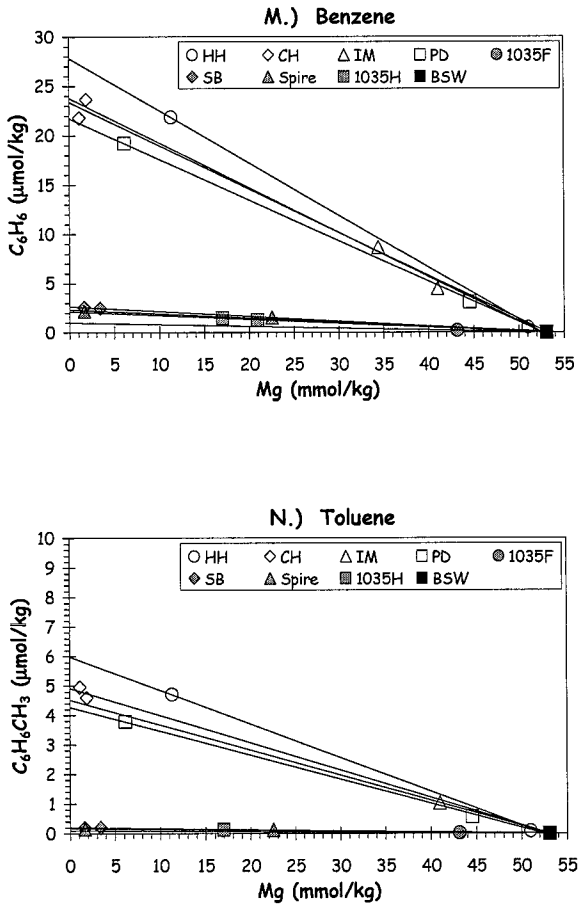

Figure 3- 1, continued. **(M)** Benzene; **(N)** Toluene. Key to vents: HH: Heineken Hollow; CH: Chowder Hill; IM: Inspired Mounds; PD: Puppy Dog; SB: Shiner Bock

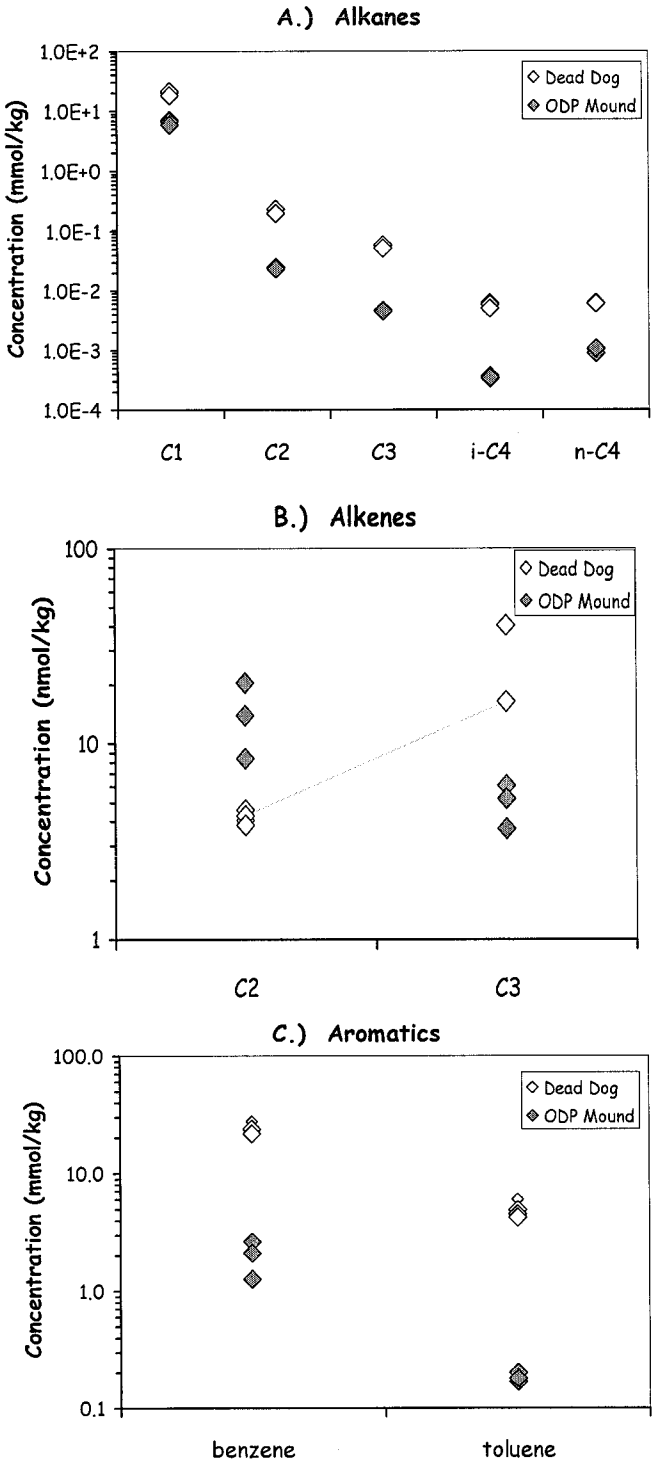

Figure 3-2. Endmember concentrations of **(A)** alkanes; **(B)** alkenes and **(C)** aromatics in Middle Valley hydrothermal vents. Note the log concentration scales.

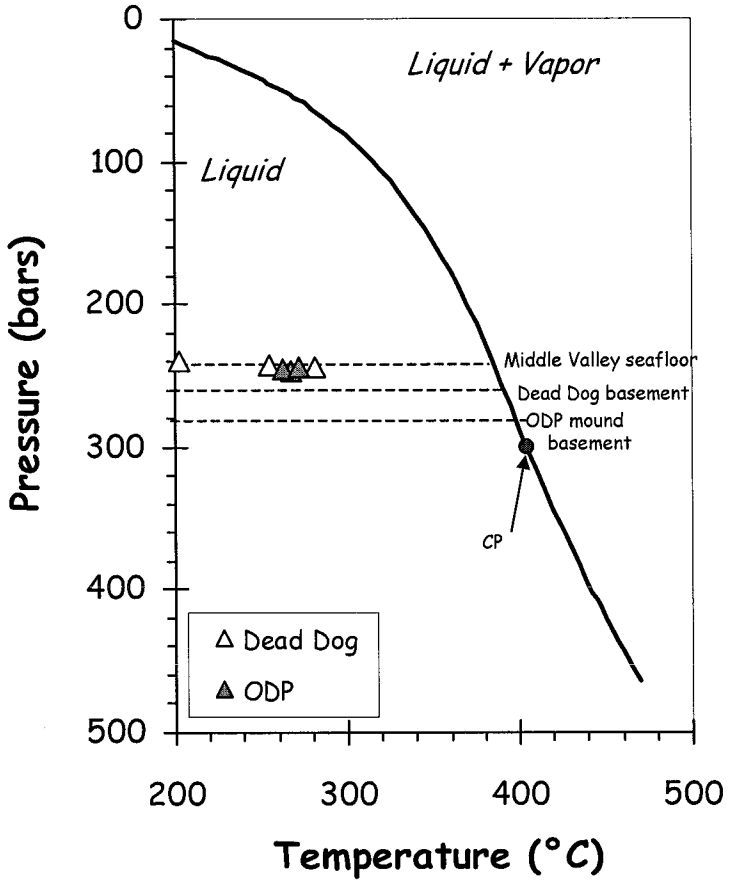

Figure 3-3. Two-phase diagram for seawater (3.2 eq. Wt. % NaCl) redrawn from Bischoff and Rosenbauer (1985). The measured exit temperatures and pressures for the sampled vents are indicated with triangles. At seafloor conditions of 240 bars and measured fluid temperatures, all of the vents are within the single phase region, indicating that significant cooling must occur in the ODP Mound fluids during ascent to account for Cl concentrations depleted relative to seawater. CP: critical point of seawater. Lines drawn at 260 and 280 bars represent minimum dpeths in assumed subsurface reaction zones at Dead Dog and ODP Mound fields, respectively.

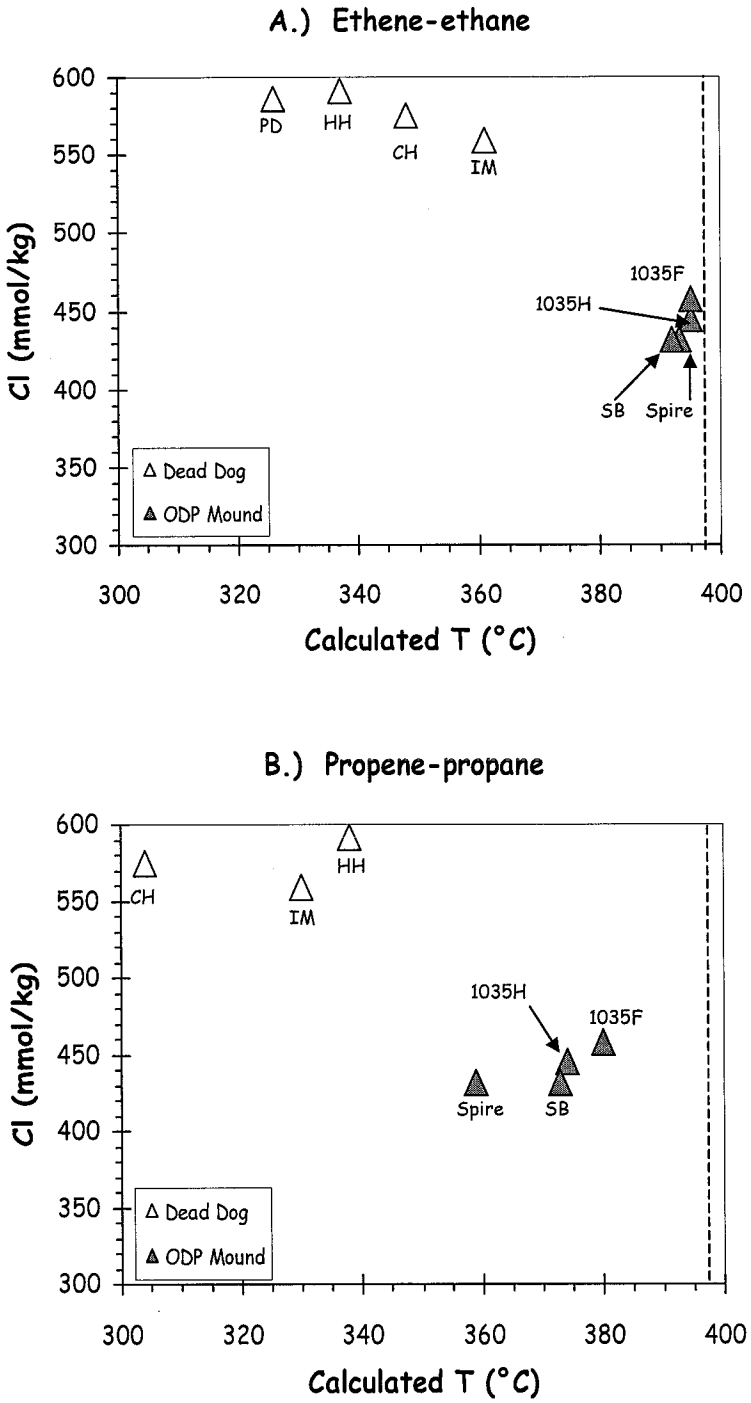

Figure 3-4. Equilibration temperatures calculated for (A) ethene:ethane and (B) propene:propane versus endmember Cl concentrations. For reference, the two-phase boundary at 280 bars, 397°C is indicated with a dotted line. Key to vents: PD: Puppy Dog; HH: Heineken Hollow; CH: Chowder Hill; IM: Inspired Mounds; SB: Shiner Bock

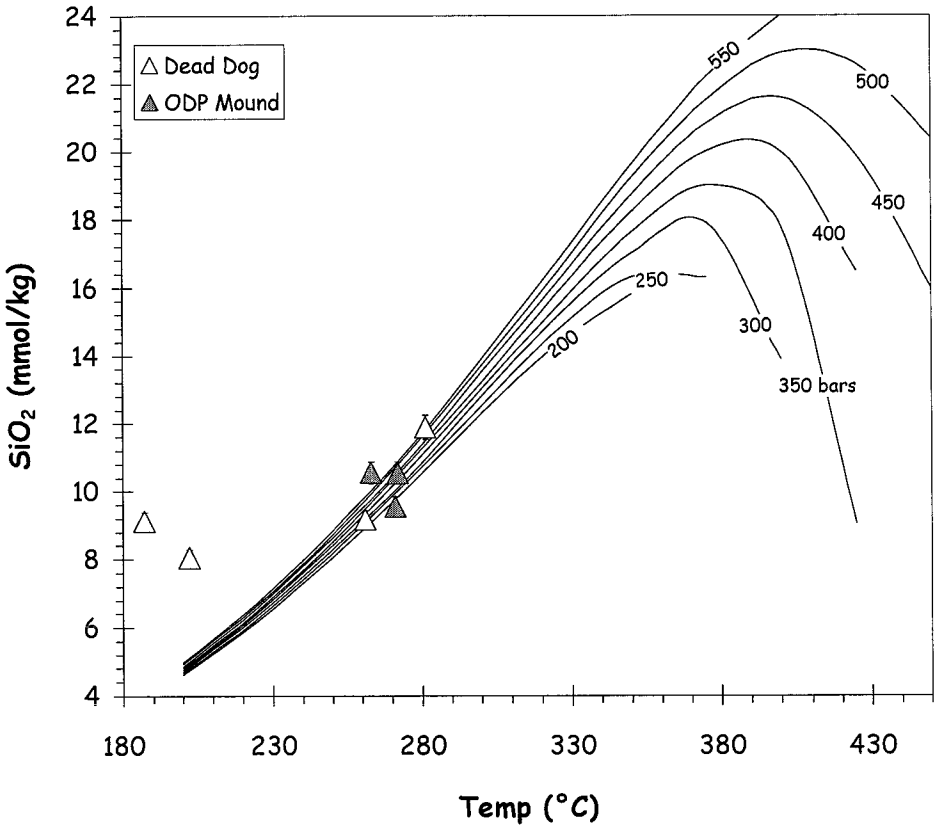

Figure 3-5. Isobars of expected silica concentrations in seawater in equilibrium with quartz as a function of temperature. The hydrothermal vent fluids from the Dead Dog and ODP Mound fields are also plotted at their measured exit temperatures. At estimated basement temperatures of 240 bars (Dead Dog field) and 260 bars (ODP Mound field), the measured silica concentrations are consistent with fluid equilibration with quartz at 250-290°C at the Dead Dog field and ~400-425°C at the ODP Mound field. Isobars of silica concentrations based on data presented in Von Damm et al. (1991).

$$C_6H_5CH_{3(aq)} + 2\ H_2O \rightarrow C_6H_{6(aq)} + CO_{2(aq)} + 3\ H_{2(aq)}$$

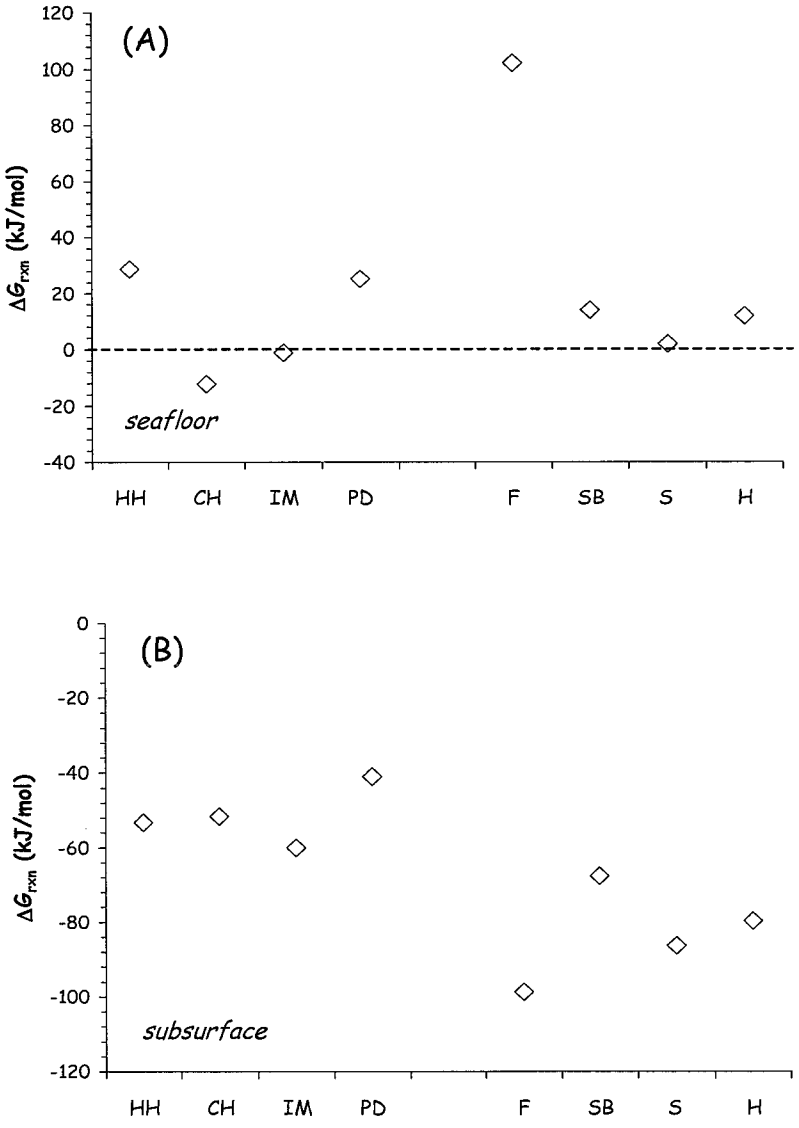

Figure 3-6. ΔG_{rxn} in kJ/mol for the degradation of toluene to benzene via Reaction 7 at **(A)** seafloor conditions and **(B)** estimated subsurface conditions using the ethane-ethene geothermometer (Table 3-3). A lack of thermodynamic drive at seafloor conditions for most of the vents reflects cooling during upflow. Thermodynamic data requiste to the construction of this figure is from the SUPCRT92 database (Johnson et al., 1992). Key to vent names: HH: Heineken Hollow; CH: Chowder Hill; IM: Inspired Mounds; F: 1035F; SB: Shiner Bock; S: Spire; H: 1035H.

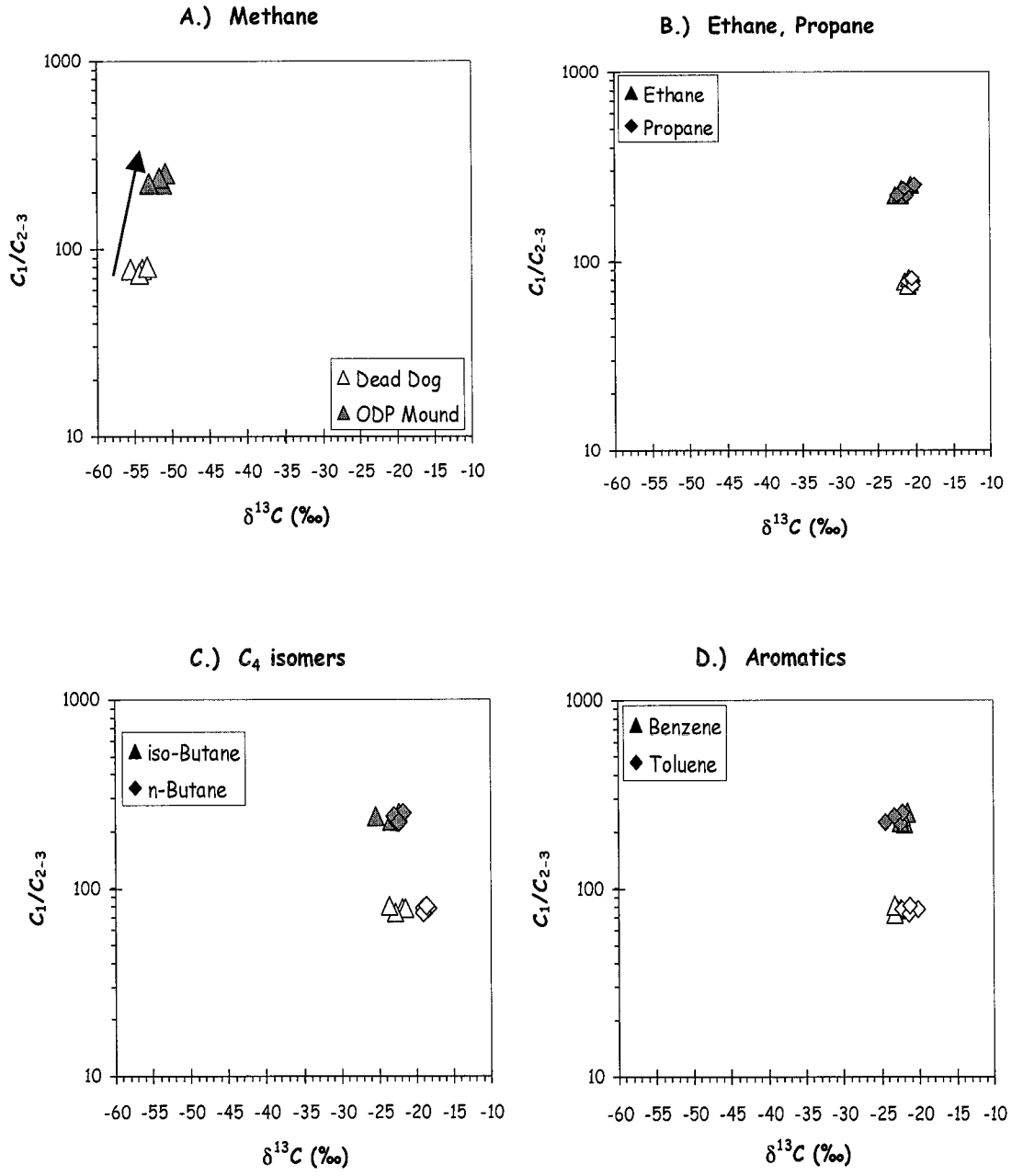

Figure 3-7. $C_1/(C_2+C_3)$ versus $\delta^{13}C$ for **(A)** methane; **(B)** ethane and propane; **(C)** C_4 isomers and **(D)** aromatic compounds. The arrow on Figure 7A indicates the proposed trend for increasing sediment maturity in high heat flow environments.

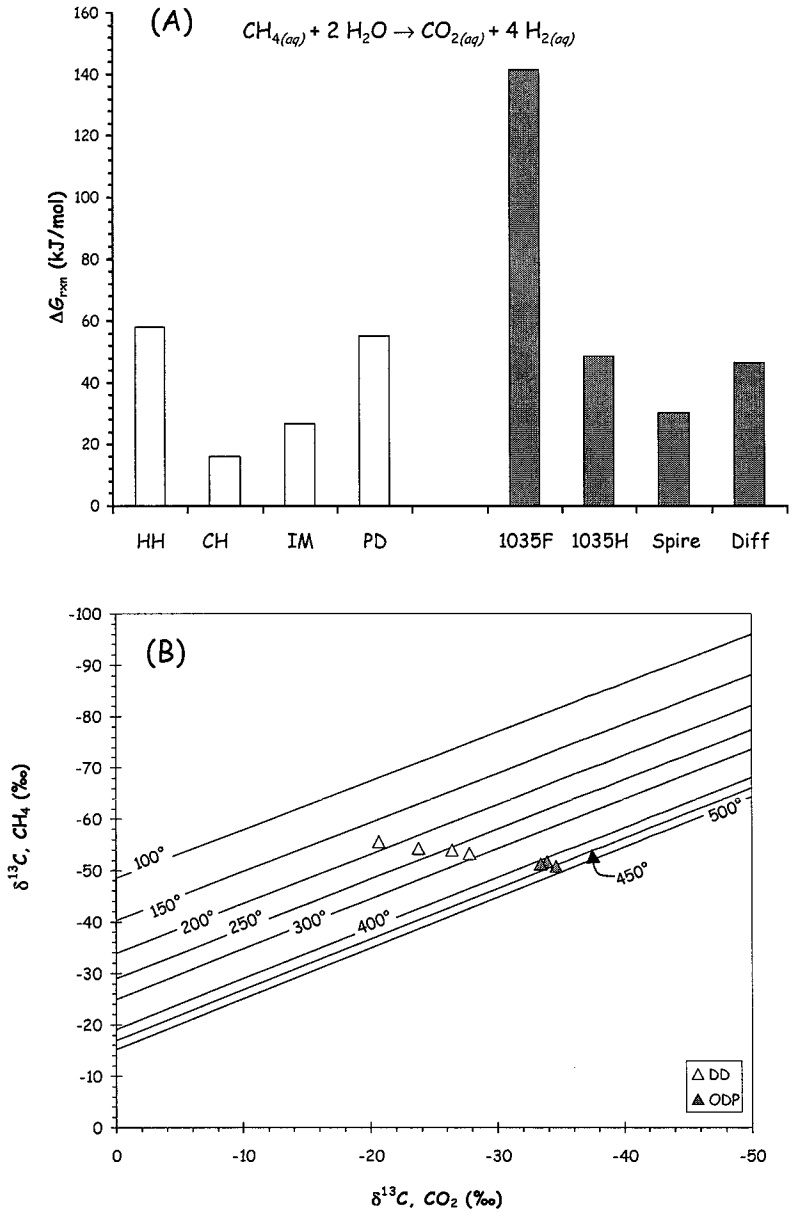

Figure 3-8. **(A)** Calculated ΔG_{rxn} for methane oxidation at seafloor conditions. **(B)** Isotopic composition of CO_2 and CH_4 in Dead Dog (white triangles) and ODP Mound (gray triangles) vent fluids shown with calculated equilbrium isotopic compositions at 100 to 500°C (from Horita, 2001). Key to vents: HH: Heineken Hollow; CH: Chowder Hill; IM: Inspired Mounds; PD: Puppy Dog.

3.6. REFERENCES

ALT J. C. (1995) Subseafloor processes in mid-ocean ridge hydrothermal systems. In *Seafloor Hydrothermal Systems: Physical, Chemical, Biological, and Geological Interactions*, Geophysical Monograph **91** (ed. S. E. Humphris, R. A. Zierenberg, L. S. Mullineaux, and R. E. Thomson), pp. 85-114.

AMES D. E., FRANKLIN J. M., and HANNINGTON M. H. (1993) Mineralogy and geochemistry of active and inactive chimneys and massive sulfide, Middle Valley, northern Juan de Fuca Ridge: An evolving hydrothermal system. *Can. Mineral.* **31**, 997-1024.

ARNÓRSSON S. and GUNNLAUGSSON E. (1985) New gas geothermometers for geothermal exploration-Calibration and application. *Geochim. Cosmochim. Acta* **49**, 1307-1325.

BARNES H. L. (1981) Measuring thermodynamically interpretable solubilities at high tempertures and pressures. In *Chemistry and Geochemistry of Solutions at High Temperatures and Pressures*, Nobel Symp. Phys. Chem. Earth **13/14** (ed. D. T. Rickard and F. E. Wickman), pp. 321-338.

BARNES H. L. (1987) Buffers for pH and redox control of hydrothermal systems. In *Hydrothermal Experimental Techniques* (ed. G. C. Ulmer and H. L. Barnes), pp. 507-514. Wiley.

BERNER U., FABER E., SCHEEDER G., and PANTEN D. (1995) Primary cracking of algal and landplant kerogens: kinetic models of isotope variations in methane, ethane and propane. *Chem. Geol.* **126**, 233-245.

BISCHOFF J. L. and DICKSON F. W. (1975) Seawater-basalt interaction at 200°C and 500 bars: Implications for the origin of sea-floor heavy-metal deposits and the regulation of seawater chemistry. *Earth Planet. Sci. Lett.* **25**, 385-397.

BISCHOFF J. L. and ROSENBAUER R. J. (1985) An empirical equation of state for hydrothermal seawater (3.2 percent NaCl). *Am. J. Sci.* **285**, 725-763.

BLOCHL E., RACHEL R., BURGGRAF S., HAFENBRADL D., JANNASCH H. W., and STETTER K. O. (1997) *Pyrolobus fumarii*, gen. and sp. nov., represents a novel group of archaea extending the upper temperature limit of life to 113°C. *Extremophiles* **1**, 14-21.

BRAUN R. L. and ROTHMAN A. J. (1975) Oil-shale pyrolysis: Kinetics and mechanism of oil production. *Fuel* **54**, 129-131.

BURNHAM A. K., SCHMIDT B. J., and BRAUN R. L. (1995) A test of the parallel reaction model using kinetic measurements on hydrous pyrolysis residues. *Org. Geochem.* **23**, 931-939.

BUTTERFIELD D. A., MCDUFF R. E., FRANKLIN J., and WHEAT C. G. (1994a) Geochemistry of hydrothermal vent fluids from Middle Valley, Juan de Fuca Ridge. In *Proc. ODP, Sci. Results* **139** (ed. M. J. Mottl, E. E. Davis, A. T. Fisher, and J. F. Slack), pp. 395-410.

BUTTERFIELD D. A., MCDUFF R. E., MOTTL M. J., LILLEY M. D., LUPTON J. E., and MASSOTH G. J. (1994b) Gradients in the composition of hydrothermal fluids from the Endeavour segment vent field: Phase separation and brine loss. *J. Geophys. Res.* **99**, 9561-9583.

COLEMAN M. L., RISATTI J. B., and SCHOELL M. (1981) Fractionation of carbon and hydrogen isotopes by methane-oxidizing bacteria. *Geochim. Cosmochim. Acta* **45**, 1033-1037.

CRUSE A. M. and SEEWALD J. S. (2001) Metal mobility in sediment-covered ridge-crest hydrothermal systems: Experimental and theoretical constraints. *Geochim. Cosmochim. Acta* **65**, 3233-3247.

DAVIS E. E. and FISHER A. T. (1994) On the nature and consequences of hydrothermal circulation in the Middle Valley sedimented rift: Inferences from geophysical and geochemical observations, Leg 139. In *Proc. ODP, Sci. Results* **139** (ed. M. J. Mottl, E. E. Davis, A. T. Fisher, and J. F. Slack), pp. 695-717.

DAVIS E. E. and VILLINGER H. (1992) Tectonic and thermal structure of the Middle Valley sedimented rift, northern Juan de Fuca Ridge. In *Proc. ODP, Init. Rept.* **139** (ed. E. E. Davis, M. J. Mottl, A. T. Fisher, and et al.), pp. 9-41.

DAVIS E. E. and WANG K. (1994) Present and past temperatures of sediments at Site 857, Middle Valley, northern Juan de Fuca Ridge. In *Proc. ODP, Sci. Results* **139** (ed. M. J. Mottl, E. E. Davis, A. T. Fisher, and J. F. Slack), pp. 565-570.

DES MARAIS D. J., DONCHIN J. H., NEHRING N. L., and TRUESDELL A. H. (1981) Molecular carbon isotopic evidence for the origin of geothermal hydrocarbons. *Nature* **292**, 826-828.

DES MARAIS D. J., STALLARD M. L., NEHRING N. L., and TRUESDELL A. H. (1988) Carbon isotope geochemistry of hydrocarbons in the Cerro Prieto geothermal field, Baja California Norte, Mexico. *Chem. Geol.* **71**, 159-167.

DISNAR J. R. and SUREAU J. F. (1990) Organic matter in ore genesis: Progress and perspectives. *Org. Geochem.* **16**, 577-599.

EDMOND J. M., MASSOTH G., and LILLEY M. D. (1992) Submersible-deployed samplers for axial vent waters. *RIDGE Events* **3**, 23-24.

FRÜH-GREEN G. L., MCKENZIE J. A., BONI M., KARPOFF A. M., and BUATIER M. (1994) Stable isotope and geochemical record of convective hydrothermal circulation in the sedimentary sequence of Middle Valley, Juan de Fuca Ridge, Leg 139. In *Proc. ODP, Sci. Results* **139** (ed. M. J. Mottl, E. E. Davis, A. T. Fisher, and J. F. Slack)

GOODFELLOW W. D. and BLAISE B. (1988) Sulfide formation and hydrothermal alteration of hemipelagic sediment in Middle Valley, northern Juan de Fuca Ridge. *Can. Mineral.* **26**, 675-696.

GOODFELLOW W. D. and FRANKLIN J. M. (1993) Geology, mineralogy, and chemistry of sediment-hosted clastic massive sulfides in shallow cores, Middle Valley, Northern Juan de Fuca R idge. *Econ. Geol.* **88**, 2037-2068.

HELGESON H. C. (1991) Organic/inorganic reactions in metamorphic processes. *Can. Mineral.* **29**, 707-739.

HELGESON H. C., KNOX A. M., OWENS C. E., and SHOCK E. L. (1993) Petroleum, oil field waters, and authigenic mineral assemblages: Are they in metastable equilibrium in hydrocarbon reservoirs? *Geochim. Cosmochim. Acta* **57**, 3295-3339.

HESSLER R. R. and KAHARL V. A. (1995) The deep-sea hydrothermal vent community: An overview. In *Seafloor Hydrothermal Systems: Physical, Chemical, Biological, and Geological Interactions*, Geophysical Monograph **91** (ed. S. E. Humphris, R. A. Zierenberg, L. S. Mullineaux, and R. E. Thomson), pp. 72-84.

HORITA J. (2001) Carbon isotope exchange in the system CO2-CH4 at elevated temperatures. *Geochim. Cosmochim. Acta* **65**, 1907-1919.

HUNT J. M. (1985) Generation and migration of light hydrocarbons. *Science* **226**, 1265-1270.

HUNT J. M. (1996) *Petroleum Geochemistry and Geochemistry*. W. H. Freeman.

HUNT J. M., WHELAN J. K., and HUC A.-Y. (1980) Genesis of petroleum hydrcarbons in marine sediments. *Science* **209**, 403-404.

JANECKY D. R., SEYFRIED W. E., JR., and BERNDT M. E. (1986) Fe-O-S redox reactions and kinetics in hydrothermal systems. *5th Intl. Symp. Water-Rock Interaction Extended Abstr.*, 282-285.

JOHNSON J. W., OELKERS E. H., and HELGESON H. C. (1992) SUPCRT92: A software package for calculating the standard molal thermodynamic properties of minerals, gases, aqueous species, and reactions from 1 to 5000 bar and 0 to 1000°C. *Comput. Geosci.* **18**, 899-947.

KARSTEN J. L., HAMMOND S. R., DAVIS E. E., and CURRIE R. (1986) Detailed morphology and neotectonics of the Endeavour segment, Northern Juan de Fuca Ridge: New results from Seabeam swath mapping. *Geol. Soc. Am. Bull.* **97**, 213-221.

KELLEY D. S. and FRÜH-GREEN G. L. (1999) Abiogenic methane in deep-seated mid-ocean ridge environments: Insights from stable isotope analysis. *J. Geophys. Res.* **104**, 10,439-14,460.

KIYOSU Y. and KROUSE H. R. (1989) Carbon isotope effect during abiogenic oxidation of methane. *Earth Planet. Sci. Lett.* **95**, 302-306.

KOROLEFF F. (1976) Determination of nutrients. In *Methods of Seawater Analysis* (ed. K. Grasshoff), pp. 125-157. Verlag-Chemie.

KROUSE H. R., VIAU C. A., ELIUK L. S., UEDA A., and HALAS S. (1988) Chemical and isotopic evidence of thermochemical sulphate reduction by light hydrocarbon gases in deep carbonate reservoirs. *Nature* **333**, 415-419.

LILLEY M. D., BUTTERFIELD D. A., OLSON E. J., LUPTON J. E., MACKO S. A., and MCDUFF R. E. (1993) Anomalous CH_4 and NH_4^+ concentrations at an unsedimented mid-ocean-ridge hydrothermal system. *Nature* **364**, 45-47.

LORANT F., PRINZHOFER A., BEHAR F., and HUC A.-Y. (1998) Carbon isotopic and molecular constraints on the formation and the expulsion of thermogenic hydrocarbon gases. *Chem. Geol.* **147**, 249-264.

MANGO F. D., HIGHTOWER J. W., and JAMES A. T. (1994) *Nature* **368**, 536-538.

MARTENS C. S. (1990) Generation of short-chain organic acid anions in hydrothermally altered sediments of the Guaymas Basin, Gulf of California. *Appl. Geochem.* **5**, 71-76.

MCCOLLOM T. M., SEEWALD J. S., and SIMONEIT B. R. T. (2001) Reactivity of monocyclic aromatic compounds under hydrothermal conditions. *Geochim. Cosmochim. Acta* **65**, 455-468.

MONTHIOUX M., LANDAIS P., and MONIN J. C. (1985) *Org. Geochem.* **8**, 275-292.

MOTTL M. J. and HOLLAND H. D. (1978) Chemical exchange during hydrothermal alteration of basalt by seawater-I. Experimental results for major and minor components of seawater. *Geochim. Cosmochim. Acta* **42**, 1103-1115.

PETER J. M., GOODFELLOW W. D., and LEYBOURNE M. I. (1994) Fluid inclusion petrography and microthermometry of the Middle Valley hydrothermal system, northern Juan de Fuca Ridge. In *Proc. ODP, Sci. Results* **139** (ed. M. J. Mottl, E. E. Davis, A. T. Fisher, and J. F. Slack), pp. 411-428.

PLEDGER R. J. and BAROSS J. A. (1991) Preliminary description and nutritional characterization of a heterotrophic archaeobacterium growing at temperatures of up to 110°C isolated from a submarine hydrothermal vent environement. *J. Gen. Microbiol.* **137**.

RABINOWICZ M., BOULÈGUE J., and GENTHON P. (1998) Two- and three-dimensional modeling of hydrothermal convection in the sedimented Middle Valley segment, Juan de Fuca Ridge. *J. Geophys. Res.* **103**, 24,045-24,065.

ROONEY M. A., CLAYPOOL G. E., and CHUNG H. M. (1995) Modeling thermogenic gas generation using carbon isotope ratios of natural gas hydrocarbons. *Chem. Geol.* **126**, 219-232.

SACKETT W. M. and CHUNG H. M. (1979) Experimental confirmation of the lack of carbon isotope exchange between methane and carbon oxides at high temperature. *Geochim. Cosmochim. Acta* **43**, 273-276.

SANSONE F. J., MOTTL M. J., OLSON E. J., WHEAT C. G., and LILLEY M. D. (1998) CO2-depleted fluids from mid-ocean ridge-flank hydrothermal springs. *Geochim. Cosmochim. Acta* **62**, 2247-2252.

SCHOELL M. (1988) Multiple origins of methane in the Earth. *Chem. Geol.* **71**, 1-10.

SEEWALD J. S. (1994) Evidence for metastable equilibrium between hydrocarbons under hydrothermal conditions. *Nature* **370**, 285-287.

SEEWALD J. S. (1997) Mineral redox buffers and the stability of organic compounds under hydrothermal conditions. In *Aqueous Chemistry and Geochemistry of Oxides, Oxyhydroxides, and Related Materials*, Materials Research Society Symposium Proceedings **432** (ed. J. A. Voight, T. E. Wood, B. E. Bunker, W. H. Casey, and L. J. Crossey), pp. 317-331.

SEEWALD J. S. (2001a) Aqueous geochemistry of low molecular weight hydrocarbons at elevated temperatures and pressures: Constraints from mineral buffered laboratory experiments. *Geochim. Cosmochim. Acta* **65**, 1641-1664.

SEEWALD J. S. (2001b) Model for the origin of carboxylic acids in basinal brines. *Geochim. Cosmochim. Acta* **65**, 3779-3789.

SEEWALD J. S., DOHERTY K. W., HAMMAR T. R., and LIBERATORE S. P. (2002) A new gas-tight isobaric sampler for hydrothermal fluids. *Deep-Sea Res. I* **49**.

SEEWALD J. S., SEYFRIED W. E., JR., and SHANKS W. C., III. (1994) Variations in the chemical and stable isotope composition of carbon and sulfur species during organic-rich alteration: An experimental and theoretical study at Guaymas Basin, Gulf of California. *Geochim. Cosmochim. Acta* **58**, 5065-5082.

SEYFRIED W. E., JR. and BISCHOFF J. L. (1981) Experimental seawater-basalt interaction at 300°C, 500 bars: Chemical exchange, secondary mineral formation and implications for the transport of heavy metals. *Geochimica et Cosmochimica Acta* **45**, 135-149.

SEYFRIED W. E., JR., DING K., and BERNDT M. E. (1991) Phase-equilibria constraints on the chemistry of hot-spring fluids at midocean ridges. *Geochim. Cosmochim. Acta* **55**, 3559-3580.

SHANKS W. C., III. (2001) Stable isotope systematics in seafloor hydrothermal systems: Vent fluids, hydrothermal deposits, hydrothermal alteration, and microbial processes. In *Stable Isotope Geochemistry* (ed. J. W. Valley and D. R. Cole), pp. 469-525.

SHERWOOD LOLLAR B., FRAPE S. K., WEISE S. M., FRITZ P., MACKO S. A., and WELHAN J. A. (1993) Abiogenic methanogenesis in crystalline rocks. *Geochim. Cosmochim. Acta* **57**, 5087-5097.

SHIPBOARD SCIENTIFIC PARTY. (1992a) Site 855. In *Proceedings of the Ocean Drilling Program, Initial Results* **139** (ed. E. E. Davis, M. J. Mottl, A. T. Fisher, and et al.), pp. 101-160.

SHIPBOARD SCIENTIFIC PARTY. (1992b) Site 858. In *Proc. ODP, Init. Rept.* **139** (ed. E. E. Davis, M. J. Mottl, A. T. Fisher, and et al.), pp. 431-569.

SHIPBOARD SCIENTIFIC PARTY. (1998a) Middle Valley: Bent Hill Area (Site 1035). In *Proc. ODP, Init. Rept.* **169** (ed. Y. Fouquet, R. A. Zierenberg, D. J. Miller, and et al.), pp. 35-152.

SHIPBOARD SCIENTIFIC PARTY. (1998b) Middle Valley: Dead Dog Area (Site 1036). In *Proc. ODP, Init. Rept.* **169** (ed. Y. Fouquet, R. A. Zierenberg, D. J. Miller, and et al), pp. 153-203.

SIMONEIT B. R. T., PRAHL F. G., LEIF R. N., and MAO S.-Z. (1994) Alkenones in sediments of Middle Valley, Leg 139. In *Proc. ODP, Sci. Results* **139** (ed. M. J. Mottl, E. E. Davis, A. T. Fisher, and J. F. Slack), pp. 479-484.

STAKES D. S. and SCHIFFMAN P. (1999) Hydrothermal alteration within the basement of the sedimented ridge environment of Middle Valley, northern Juan de Fuca Ridge. *GSA Bull.* **111**, 1294-1314.

STEIN J. S. and FISHER A. T. (2001) Multiple scales of hydrothermal circulation in Middle Valley, northern Juan de Fuca Ridge: Physcial constraints and geological models. *J. Geophys. Res.* **106**, 8563-8580.

STEIN J. S., FISHER A. T., LANGSETH M., JIN W., ITURRINO G., and DAVIS E. (1998) Fine-scale heat flow, shallow heat sources, and decoupled circulation systems at two hydrothermal sites, Middle Valley, northern Juan de Fuca Ridge. *Geology* **26**, 1115-1118.

STETTER K. O., FIALA G., HUBER G., and SEGERER A. (1990) Hyperthermophilic microorganisms. *FEMS Microbiol. Rev.* **75**, 117-124.

TANNENBAUM E. and KAPLAN I. R. (1985a) *Nature* **317**, 708-710.

TANNENBAUM E. and KAPLAN I. R. (1985b) *Geochim. Cosmochim. Acta* **49**, 2589-2604.

TAYLOR B. E. (1992) Degassing of CO2 from Kilauea: Carbon isotopic evidence and implications for magmatic contributions to sediment-hosted submarine hydrothermal systems. *Rept. Geol. Surv. Japan* **279**, 205-206.

TISSOT B. and WELTE D. H. (1984) *Petroleum Formation and Occurrence*. Verlag.

VON DAMM K. L. (2000) Chemistry of hydrothermal vent fluids from 9°-10°N, East Pacific Rise: "Time zero," the immediate posteruptive period. *J. Geophys. Res.* **105**, 11,203-11,222.

VON DAMM K. L., BISCHOFF J. L., and ROSENBAUER R. J. (1991) Quartz solubility in hydrothermal seawater: An experimental study and equation describing quartz solubility for up to 0.5 M NaCl solutions. *Am. J. Sci.* **291**, 977-1007.

VON DAMM K. L., EDMOND J. M., GRANT B., MEASURES C. I., WALDEN B., and WEISS R. F. (1985a) Chemistry of submarine hydrothermal solutions at 21°N, East Pacific Rise. *Geochim. Cosmochim. Acta* **49**, 2197-2220.

VON DAMM K. L., EDMOND J. M., MEASURES C. I., and GRANT B. (1985b) Chemistry of submarine hydrothermal solutions at Guaymas Basin, Gulf of California. *Geochim. Cosmochim. Acta* **49**, 2221-2237.

WAPLES D. W. (1984) Thermal models for oil generation. In *Advances in Petroleum Geochemistry* **1** (ed. J. Brooks and D. Welte), pp. 7-67.

WELHAN J. A. (1988) Origins of methane in hydrothermal systems. *Chem. Geol.* **71**, 183-198.

WHELAN J. K., SIMONEIT B. R. T., and TARAFA M. E. (1988) C_1-C_8 hydrocarbons in sediments from Guaymas Basin, Gulf of California--Comparison to Peru Margin, Japan Trench and California Borderlands. *Org. Geochem.* **12**, 171-194.

WHITICAR M. J., FABER E., WHELAN J. K., and SIMONEIT B. R. T. (1994) Thermogenic and bacterial hydrocarbon gases (free and sorbed) in Middle Valley, Juan de Fuca Ridge, Leg 139. In *Proc. ODP, Sci. Results* **139** (ed. M. J. Mottl, E. E. Davis, A. T. Fisher, and J. F. Slack), pp. 467-477.

ZHANG Q.-L. and WEN-JUN L. (1990) A calibrated measurement of the atomic weight of carbon. *Chinese Sci. Bull.* **35**, 290-296.

ZIERENBERG R. A., FOUQUET Y., MILLER D. J., BAHR J. M., BAKER P. A., BJERKGÅRD T., BRUNNER C. A., GOODFELLOW W. D., GRÖSCHEL-BECKER H. M., GUÈRIN G., ISHIBASHI J., ITURRINO G., JAMES R. H., LACKSCHEWITZ K. S., MARQUEZ L. L., NEHLING P., PETER J. M., RIGSBY C. A., SCHULTHEISS P., III W. C. S., SIMONEIT B. R. T., SUMMIT M., TEAGLE D. A. H., URBAT M., and ZUFFA G. G. (1998) The deep structure of a sea-floor hydrothermal deposit. *Nature* **392**, 485-488.

ZIERENBERG R. A. and MILLER D. J. (2000) Overview of Ocean Drilling Program Leg 169: Sedimented Ridges II. In *Proc. ODP, Sci. Results* **169** (ed. R. A. Zierenberg, Y. Fouquet, D. J. Miller, and W. R. Normark), pp. 1-39.

CHAPTER 4. TEMPORAL VARIABILITY AND ORGANIC-INORGANIC INTERACTIONS IN HYDROTHERMAL VENT FLUIDS, MIDDLE VALLEY, NORTHERN JUAN DE FUCA RIDGE

ABSTRACT

Hydrothermal vents located on sedimented mid-ocean ridges, such as Middle Valley, northern Juan de Fuca Ridge, could represent key sources of reduced C to the deep ocean basins. In order to constrain the potential importance of this source to the overall global carbon cycle, the temporal variability of vent fluid chemistry must be understood. The data generated in this study can be compared to compositions of fluids sampled in 1990 and 1991 to assess the chemical variability over a ten-year scale. The inorganic ions are characterized by stable concentration over the last decade. Invariant concentrations of sediment-derived NH_3 over that time period indicate a continual supply of fresh sediment for reaction with fluids that may reflect continuous adjustment of fluid flowpaths within subsurface aquifers, or, alternatively, indicate that the sediment reservoir with which fluids react has not yet been exhausted. The concentrations of H_2 and H_2S and the $\delta^{34}S$ of H_2S are quite different in Shiner Bock, 1035H and Spire vents sampled at the ODP Mound field in 2000, despite their close spatial proximity. Spire vent, which was less than two years old at the time of sampling, has H_2 concentrations of 2.2 mmol/L fluid, as compared to the 6.1 and 8.2 mmol/L fluid measured in 1035H and Shiner Bock vent fluids, respectively. The H_2S concentration of Spire vent fluid is 7.9 mmol/kg, while it is only 4.0 and 4.3 mmol/kg fluid in 1035H and Shiner Bock vent fluids, respectively. These variations reflect equilibration of fluids containing high H_2 concentrations with sulfide minerals during upflow through the ODP Mound (i.e, reduction of pyrite to pyrrhotite). The presence of aqueous organic compounds can affect not only the inorganic chemical speciation in vent fluids (e.g., generation of the high H_2 concentrations in 1035H and Shiner Bock vent fluids from methane oxidation), but also the mineralogy of associated sulfide deposits . Also, large changes in the H_2S and H_2 concentrations during upflow can lead to variations in the concentrations of other inorganic species such as the transition metals Fe, Mn, Zn and Cu. Therefore, care must be taken in assuming that the relative abundances of such species necessarily reflect conditions in the deepest subsurface reaction zones.

4.1. INTRODUCTION

Convective circulation of seawater through the oceanic crust at mid-ocean ridges is a major mechanism by which heat and material is transferred from the interior of the Earth to the oceans. The flux of material to and from the oceanic crust in hydrothermal

vent systems has been invoked as a driving mechanism for controlling aspects of seawater and atmospheric compositions on geologic time scales (BERNER et al., 1983; RICHTER et al., 1992). Middle Valley, northern Juan de Fuca Ridge is a sedimented mid-ocean ridge spreading axis with two regions of hydrothermal venting: the Dead Dog and ODP Mound fields (Fig. 1-3). Hydrothermal fluids interact with sediments containing up to 1.2 wt. % organic carbon (SHIPBOARD SCIENTIFIC PARTY, 1992), leading to concentrations of organic species as high as 20 mmol/kg fluid in endmember fluids (Chapter 3, this thesis). Such vents may therefore be important local sources of reduced carbon-containing compounds to the deep ocean. A key aspect in the assessment of hydrothermal fluxes and their impact on global biogeochemical cycles is the characterization of vent fluid compositions and their temporal variability. Studies of vent fluids from Guaymas Basin, Gulf of California, 21°N on the East Pacific Rise (EPR) and the Main Endeavour field (MEF), northern Juan de Fuca Ridge, during the 1980's revealed that vent fluid compositions were remarkably stable over time scales of several years (BUTTERFIELD et al., 1994b; CAMPBELL et al., 1988). However, in the early 1990's, studies at 9-10°N, EPR, and North Cleft, southern Juan de Fuca Ridge, indicated that vent fluid temperatures and chemical compositions fluctuated on time scales of weeks in response to recent volcanic activity (BUTTERFIELD and MASSOTH, 1994; VON DAMM et al., 1995). Recent investigations have also demonstrated large changes in fluid compositions from the Main Endeavour field following seismic activity in 1999 (DING et al., 2001a; SEEWALD et al., 2002a; SEYFRIED et al., 2002).

The temporal variability of Middle Valley vent fluid compositions can be assessed over two time scales. Vent fluid samples were collected at Middle Valley in 1990 and 1991 (BUTTERFIELD et al., 1994a). Four of the vents sampled, Heineken Hollow, Dead Dog Mound, Inspired Mounds, and Chowder Hill, were sampled again in 2000 (this thesis), providing a decade-long record of the major and minor inorganic ion compositions. A similar analysis can also be made of ODP Mound fluids since Butterfield et al. (1994a) sampled fluids from a vent in the ODP Mound field that was later named Lone Star vent (ZIERENBERG and MILLER, 2000). Although Lone Star vent

was not sampled in this study, precluding a direct vent-to-vent comparison, temporal changes in the inorganic fluid chemistry over a decade can be assessed at the scale of the entire ODP Mound field.

Spatial variability in vent fluid compositions is also investigated here, using fluids from a recently created vent site at the ODP Mound field. The new area of venting developed on the ODP Mound due to the puncturing of a hydrologic seal located at approximately 150 meters below the seafloor (mbsf) during ODP Leg 169 drilling. Venting of hydrothermal fluid was immediately observed in Holes 1035F and 1035H following drilling in 1996. Hydrothermal venting through the ODP Mound also resulted in the development of a new field containing several small spires and chimneys on the eastern side of ODP Mound (Chapter 3, this thesis). This field was not observed during *Alvin* operations in 1998 (Zierenberg, pers. comm.), and therefore was less than two years old when it was sampled as part of this thesis. A comparison of the fluids from one of these new vents, referred to here as Spire vent, with fluids sampled from Shiner Bock and ODP Leg 169 drillhole 1035H, can provide insight into the fluid-rock reactions that control vent fluid chemistry on very short (< 2 years) time scales.

4.2. EXPERIMENTAL

4.2.1. Geologic Setting

Middle Valley is an axial rift valley located at 48°27'N latitude on the northern edge of the Juan de Fuca Ridge, an intermediate-spreading ridge with a half-spreading rate of 30 mm/yr (GOODFELLOW and BLAISE, 1988; Fig. 1-1). Active spreading jumped westward from Middle Valley to West Valley during the last 200,000 years, and perhaps as early as 10,000 years ago (KARSTEN et al., 1986). Middle Valley was completely filled with terrestrial and hemipelagic sediments derived from the continental shelf during Pleistocene sea-level lowstands. The sediment cover ranges in thickness from a few hundred meters in the south up to 1.5 kilometers in the north (GOODFELLOW and BLAISE, 1988). Sedimentation was contemporaneous with active extension and volcanism, so that the uppermost basement consists of a basaltic-sill/sediment complex (DAVIS and

VILLINGER, 1992). Hydrothermal activity in the past resulted in the creation of two massive sulfide deposits that formed from the direct precipitation of sulfide minerals on the seafloor: the Bent Hill massive sulfide deposit, which is estimated to contain over 8 million tons of ore, and the slightly younger Ore Drilling Program (ODP) Mound massive sulfide deposit which was sampled by ODP Hole 1035H (SHIPBOARD SCIENTIFIC PARTY, 1998a; ZIERENBERG et al., 1998). Mineralogical and fluid inclusion data from sulfides in the Bent Hill deposit indicate precipitation of the sulfide minerals from hydrothermal fluids that reached temperatures of 350 to 400°C (GOODFELLOW and FRANKLIN, 1993; PETER et al., 1994). Such fluids were apparently derived from a hot reaction zone located in the basaltic basement with upflow focused along faults and fissures that were subsequently sealed by mineral precipitation (ZIERENBERG et al., 1998).

Multiple episodes of hydrothermal venting are apparent at ODP Mound, which consists of three stacked sequences of massive sulfide, each of which are underlain by sediment-hosted feeder zone mineralization (SHIPBOARD SCIENTIFIC PARTY, 1998a; ZIERENBERG et al., 1998). Within the lowermost feeder zone is a narrow band rich in Cu-Fe sulfides that trends northward to the Bent Hill massive sulfide deposits, and is referred to as the Deep Copper Zone (DCZ; SHIPBOARD SCIENTIFIC PARTY, 1998a; ZIERENBERG et al., 1998). The top of the DCZ is marked by an area of intensely silicified sediments that forms an impermeable caprock preventing hydrothermal fluids from reaching the seafloor, except when it is penetrated by fracturing or drilling (see below; ZIERENBERG et al., 1998). Within the feeder zones, sulfide mineralization largely consists of veins and bands of pyrrhotite, chalcopyrite/isocubanite, pyrite and minor sphalerite contained within hydrothermally altered mudstone and sandstones (SHIPBOARD SCIENTIFIC PARTY, 1998a). Late anhydrite veins that crosscut the sulfide minerals are present within some sections of the feeder zones. Overlying the feeder zones are massive to semi-massive sulfide assemblages that consist predominantly of sphalerite-pyrrhotite-pyrite-magnetite that is highly variable in terms of the relative abundances of the different sulfide minerals (SHIPBOARD SCIENTIFIC PARTY, 1998a). The topmost interval of Hole 1035H consists of sulfide breccias of pyrite, marcasite, Fe-rich sphalerite and minor Cu-sulfides and

pyrrhotite that formed largely in situ with little or no sedimentary transport of the sulfides (SHIPBOARD SCIENTIFIC PARTY, 1998a). Both pyrite and marcasite have been observed to replace primary hexagonal pyrrhotite in this facies (SHIPBOARD SCIENTIFIC PARTY, 1998a) and could be related to post-depositional weathering of the basalt by seawater-like fluids.

Current hydrothermal activity is localized in two areas: the ODP Mound vent field and the Dead Dog vent field (Fig. 1-3). In July, 2000, fluids were sampled from Shiner Bock vent, ODP Leg 169 drillhole 1035H and Spire vent, all of which are located on the ODP Mound massive sulfide deposit (Table 4-1; Fig. 1-3B). Fluids venting from ODP Leg 169 drillhole 1035F, located near the Bent Hill massive sulfide deposit were also sampled. Measured exit temperatures were 272°C, 263°C and 267°C for Shiner Bock, Spire and 1035H, respectively, and only 40°C for the fluids venting from 1035F (Table 4-1). Fluids were also sampled from five regions of focused venting within the Dead Dog field: Heineken Hollow, Dead Dog Mound, Inspired Mounds, Chowder Hill and Puppy Dog (Table 4-1; Fig. 1-3A). Maximum vent fluid exit temperatures were 187, 274, 281, 261, and 202°C for fluids sampled from Heineken Hollow, Dead Dog Mound, Chowder Hill, Inspired Mounds and Puppy Dog vents, respectively (Table 4-1).

4.2.2. Sample Collection and Analysis

Vent fluid samples were collected using isobaric gas-tight fluid samplers that maintain the fluid at seafloor pressures onboard ship while subsamples are withdrawn through a micrometering valve (SEEWALD et al., 2002b). At least two different gas-tight samples were collected at each vent. Additional samples were also taken from some vents using the 755 mL titanium syringe bottles commonly referred to as the "major" samplers, which are not gas tight (EDMOND et al., 1992; VON DAMM et al., 1985). Temperatures were measured using the *Alvin* high temperature probe and zero-point corrected by 2°C, taking into account the cold-junction temperature.

Utilizing a comprehensive analytical strategy, we determined the concentrations of a range of volatile, semi-volatile and non-volatile organic and inorganic aqueous

species for each vent fluid sample. Full details of the sample collection procedure are reported in Chapter 3 of this thesis.

Fluids were analyzed for dissolved Na, Ca, K, Cl, Br and SO_4^{2-} using ion chromatography with conductivity detection. No precautions were taken to prevent oxidation of reduced sulfur species during storage, so that measured SO_4^{2-} concentrations may not accurately represent fluid compositions at the time of sampling. ΣNH_3 ($NH_{3(aq)}$ + NH_4^+) concentrations were measured spectrophotometrically by flow injection analysis using the Berthelot reaction (KOROLEFF, 1976). Analytical uncertainties for the major ions and NH_3 are estimated to be $\pm$2% and $\pm$5%, respectively. Dissolved Si and Sr concentrations were analyzed using inductively-coupled plasma optical emission spectroscopy, with estimated analytical uncertainties of $\pm$5%. Aqueous CO_2, H_2 and CH_4 concentrations were measured using gas chromatography, with estimated analytical uncertainties of <10% for CO_2 and < 4% for H_2 and CH_4. Full analytical details for the volatile species are reported in Chapter 3.

Aqueous ΣH_2S ($H_2S_{(aq)} + HS^- + S^{2-}$) concentrations were determined gravimetrically following precipitation as Ag_2S in a 5 wt. % $AgNO_3$ solution. The analytical uncertainty is estimated to be $\leq$ 10%. The stable sulfur isotopic composition of aqueous H_2S was measured in the laboratory of R. Zierenberg at the University of California at Davis using and Isoprime® continuous flow gas ratio mass spectrometer interfaced with an automated Carlo Erba® elemental analyzer (EA). Ag_2S precipitates were combusted to SO_2 in a stream of high purity oxygen in the EA. The SO_2 was carried by a He stream through a chromatography column to spearate it from the other gases and introduced into the Canyon Diablo Troilite (CDT) standard (R_{CDT}; $^{34}S/^{32}S$ = 0.0450045; OHMOTO and RYE, 1979) using IAEA reference maerials S-1, S-2 and S-3 with accepted values of –0.3‰, 22.6‰, and –32.55‰, respectively (DING et al., 2001b). Isotope ratios are reported using standard delta notation, where $\delta^{34}S$ is expressed in per mil (‰) units, and is calculated as the relative difference in the $^{34}S/^{32}S$ ratio of the sample, R_S, and the Canyon Diablo Troilite (CDT) standard:

$$\delta^{34}S\,(‰) = \left[\frac{R_S - R_{CDT}}{R_{CDT}}\right] * 1000. \qquad (1)$$

The precision of the $\delta^{34}S$ analyses was 0.6‰ (1σ). One to two different samples of Ag_2S were analyzed for each fluid collected. For a given vent, all measured Ag_2S values were averaged together to give a single sulfur isotopic composition of aqueous H_2S. These are reported in Table 4-1 with the standard deviation and number of sample measurements used to calculate the average value.

4.3. RESULTS

Because fluid samplers have a finite dead volume that is filled with bottom seawater prior to deployment, and seawater entrainment occurs to varying degrees during sampling, the fluid that is collected represents a mixture between seawater and hydrothermal vent fluid. Laboratory experiments have demonstrated near-quantitative removal of Mg from seawater during hydrothermal seawater-basalt interaction at temperatures, pressures and water/rock ratios that exist in ridge-crest hydrothermal systems (BISCHOFF and DICKSON, 1975; MOTTL and HOLLAND, 1978; SEYFRIED and BISCHOFF, 1981b). Therefore, the composition of endmember hydrothermal vent fluids is calculated by extrapolating the concentrations of individual species to zero Mg using linear least squares regression of vent fluid and seawater compositions (VON DAMM et al., 1985). Calculated endmember concentrations are reported in Table 4-1 for each vent, along with the chemical data for each fluid sample. Plots of individual species versus Mg for each vent are given in Figure 4-1. For most of the vents, at least one of the sampled fluids had a measured Mg concentration < 20% of the seawater concentration (Table 4-1). Only one gas-tight sample was acquired for ODP Hole 1035F, which consisted of 82% entrained seawater. Therefore, the extrapolated endmember concentrations of the volatile species for this vent are subject to a large degree of uncertainty, and should be interpreted with caution.

4.3.1. Aqueous Concentrations

Chloride concentrations are quite distinct for the two vent fields. Concentrations in fluids from the ODP Mound vent field are depleted relative to seawater, ranging from 432-449 mmol/kg fluid, while at the Dead Dog field concentrations are slightly enriched relative to seawater, ranging between 546-586 mmol/kg fluid (Table 4-1). Bromide concentrations are likewise depleted relative to seawater in the ODP Mound fluids, ranging from 742-769 μmol/kg fluid, and enriched in the Dead Dog fluids, ranging from 995-1037 μmol/kg fluid. The major cations (Na, Ca, K) are also depleted in ODP Mound fluids relative to Dead Dog fluids. For example, Na concentrations range between 357-395 mmol/kg fluid in ODP Mound fluids and between 402-416 mmol/kg fluid in Dead Dog fluids. Sodium concentrations are depleted relative to seawater in all the vent fluids, while Ca and K concentrations are enriched. Silica concentrations range between 5.8-12 mmol/kg fluid, with no clear differences in concentrations between the two fields. Strontium concentrations are depleted in the ODP Mound fluids relative to the Dead Dog fluids, ranging between 121-139 and 197-235 μmol/kg fluid in the two fields, respectively.

Endmember concentrations of aqueous H_2 and H_2S are very similar for all vents in the Dead Dog field, ranging between 1.9-2.6 mmol/L fluid and 2.4-3.8 mmol/kg fluid, respectively. In contrast, at the ODP Mound field, a wide range in concentrations is observed between the three vents located on the ODP Mound massive sulfide, despite being separated by distances of <~40 meters. Aqueous H_2 concentrations are 8.2, 6.1 and 2.2 mmol/L fluid for Shiner Bock, Hole 1035H and the newly formed Spire vent, respectively. Endmember H_2S concentrations are highest in Spire vent at 7.9 mmol/kg fluid, which had the lowest H_2 concentration, and 4.3 and 4.0 mmol/kg fluid in Shiner Bock and Hole 1035H vents, respectively (Table 4-1).

4.3.2. $\delta^{34}S$

The sulfur isotopic composition of aqueous H_2S in all sampled fluids is enriched in ^{34}S relative to basaltic sulfide (0.1 ‰; SAKAI et al., 1984; Fig. 4-3) in all samples. At the Dead Dog field, $\delta^{34}S$ ranged between +5.7 and +7.2‰. There is a striking difference

between the stable sulfur isotopic compositions between the three vents located on the ODP Mound. At Spire vent, where aqueous H_2S was the most abundant, the $\delta^{34}S$ value of +3.2 ‰ is the most depleted in ^{34}S. H_2S from Shiner Bock and Hole 1035H fluids are the most enriched of all sampled fluids relative to basaltic sulfide, having values of +10.4 and +9.7 ‰, respectively (Table 4-1; Fig. 4-3).

4.4. DISCUSSION

4.4.1. Decade Scale Variability

Previous work has shown that vent fluid compositions from both sediment-covered and bare-rock hydrothermal vent sites can remain stable over periods of years in the absence of tectonic or volcanic activity (BUTTERFIELD et al., 1994b; CAMPBELL et al., 1988). Butterfield et al. (1994a) used their reported vent fluid data to calculate an average endmember concentrations for the entire Dead Dog vent field in 1990. To allow for a comparison on the scale of individual vents, the data in Butterfield et al. (1994a) were used to recalculate endmember compositions for Heineken Hollow, Dead Dog mound, Inspired Mounds and Chowder Hill vents from the Dead Dog field, and Lone Star vent from the ODP Mound field. These data are presented in Table 4-2 along with data for the endmember composition of fluids collected from these vents in 2000 as part of this thesis. Chowder Hill vent was sampled in both 1990 and 1991, but the samples from 1991 contained between 87-95% entrained bottom seawater, so that a large uncertainty would be associated with the calculated endmember composition. Therefore these data were regressed as one set with the 1990 data. Lone Star vent was not sampled in 2000 as part of this study, so Shiner Bock vent data was used for comparison. Between 1990 and 2000, the temperature and chemistry were stable at the individual vents within the uncertainty for the various analytical techniques (Table 4-2).

Elemental ratios (Na/Cl, Ca/Cl, Ca/Na) exhibit very little variation over time for a given vent (Table 4-2). However, a comparison of the elemental ratios for the Dead Dog field fluids with the ODP Mound fluids exhibit some striking differences. Na/Cl ratios are lower and Ca/Cl ratios are higher in Dead Dog fluids relative to ODP Mound fluids.

As noted by Butterfield et al. (1994a), this may indicate that the low chlorinity ODP Mound fluids did not form from the phase separation of a source fluid common to both fields. The ODP Mound fluids are also characterized by a lower Ca/Na ratio as compared to the Dead Dog fluids (Table 4-2). Butterfield et al. (1994a) suggested that higher Na/Cl ratios and lower Ca concentrations in the ODP Mound fluids relative to the Dead Dog fluids were caused by less fixation of a Na in mineral phases (i.e., albitization of plagioclase) at higher reaction zone temperatures.

The average concentration of H_2S is identical between 1990 and 2000 for the Dead Dog fluids. An average H_2S concentration of 3 mmol/kg fluid was also reported in 1990 for Lone Star (BUTTERFIELD et al., 1994a). This is very similar to the concentrations of 4.0 and 4.3 mmol/kg fluid observed in 2000 at 1035H and Shiner Bock vents (Table 4-2). Due to uncertainties associated with the 1990 data, the 1 mmol/kg fluid difference in H_2S concentrations between 1990 and 2000 for Lone Star, Shiner Bock and 1035H must be interpreted with caution. Spire vent, however, which was less than 2 years old at the time of sampling, had H_2S concentrations twice as high as those measured in the other ODP Mound vents, a difference that is well outside the analytical uncertainty (Table 4-2).

Carbon dioxide concentrations are approximately twice as high in 2000 as compared to 1999 for the Dead Dog field, but are identical in the ODP Mound fluids. However, since non-gas-tight samplers may have been utilized in 1999 to collect the CO_2 samples, it is unclear if this difference reflects changes in geochemical conditions or the limitation of sampler technology.

Variations in concentrations of NH_3, which is almost quantitatively removed from sediment during alteration, cannot be assessed at the scale of individual vents, since only an average value for the entire Dead Dog field was reported by Butterfield et al. (1994a). The average concentration was 2.9 mmol/kg fluid in 1990, which is nearly identical to the average value of 3.1 mmol/kg fluid calculated from the 2000 results. This indicates that over the ten-year period from 1990-2000, there has been no change in the amount of fresh sediment with which the fluids venting at the Dead Dog field interact. This may be

caused by the continuous exposure of reacting fluids with fresh sediment surfaces due to the progressive subsidence of less-altered sediment or changes in the flowpath of fluids within subsurface aquifers. A seemingly continuous source of fresh sediment could also result from reaction of hydrothermal fluids with a spatially large reservoir of sediments. This would mean that, in effect, the source of sediment-derived fluids has not yet been exhausted. In a conceptual model of hydrothermal convection, a spatially large sediment source would be the equivalent of altering fluids having only made one pass through this source, so that the effects of alteration on endmember concentrations of NH_3 cannot yet be observed.

The relative stability of major and minor ion concentrations over a ten-year period from 1990-2000 are consistent with the regulation of fluid compositions by interaction with a rock or sediment composition that has remained unchanged over the last 10 years. Whether this rock is fresh basalt, which would then require a constantly expanding reaction zone as in the cracking front model of Lister (1983), or reaction of the fluid with progressively altered rock cannot be determined from this data set. One clear indicator of continued reaction with fresh rock would be constant concentrations of the mobile trace elements Li, Rb and Cs. However, given the evidence for pervasive interaction of these fluids with overlying sediments (Chapter 3, this thesis), which are also sources of these elements, use of their concentrations to characterize water/basalt ratios in the subsurface reaction zone may not be possible in this area.

4.4.2. Reactivation of Hydrothermal Circulation at the ODP Mound Field

In contrast to the similarity of the inorganic ion concentrations in fluids sampled from the three vents at the ODP Mound field, aqueous H_2 and H_2S concentrations are strikingly different, despite their very close (< ~40 m) spatial proximity. Shiner Bock vent was discovered in 1996 prior to drilling Hole 1035H during ODP Leg 169. Vigorous hydrothermal venting was immediately initiated in ODP Hole 1035H when the subsurface hydrologic seal at 150 mbsf was punctured during drilling. Hydrothermal fluids had been flowing through this conduit for at least four years prior to sampling of the fluids as part of this study. Reactivation of fluid flow through the ODP Mound also

caused the development of a new field of small spires on the eastern side of ODP Mound that were not observed in 1998 (Zierenberg, pers. comm.). Fluids sampled from Shiner Bock vent and ODP Hole 1035H contain endmember aqueous H_2 concentrations of 8.2 and 6.1 mmol/L fluid, respectively, while the concentration in Spire vent, from the newly formed field is only 2.2 mmol/L fluid. H_2S concentrations are twice as high in the Spire vent fluids as compared to 1035H and Shiner Bock (Table 4-1).

Thermodynamic calculations suggest that the high H_2 concentrations observed in 1035H and Shiner Bock vent fluids can be generated by oxidation of methane and organic matter by reactions of the type:

$$CH_{4(aq)} + 2\ H_2O \rightarrow CO_{2(aq)} + 4\ H_{2(aq)} \qquad (1)$$

in the subsurface reaction zone (Chapter 3, this thesis). Given the close spatial proximity of Spire vent to 1035H and Shiner Bock vents (within ~40 m), similar exit temperatures, and geochemical indicators that the three vents derive fluids from the same sediment source region (i.e., NH_3 concentrations; Chapter 5, this thesis), methane oxidation should also be occurring in fluids that vent from Spire. Therefore, Spire vent fluids would also be expected to contain similarly high H_2 concentrations as Shiner Bock and 1035H vent fluids. The anomalously low H_2 concentrations in Spire vent are also associated with H_2S concentrations that are twice as high as in the fluids from 1035H and Shiner Bock vents (Table 4-1). This suggests that other reactions during upflow are consuming H_2 derived from Reaction 1, generating the additional H_2S.

One potential reaction that would consume H_2 and produce H_2S is thermochemical sulfate reduction:

$$SO_4^{2-} + 6\ H_{2(aq)} \rightarrow H_2S_{(aq)} + 4\ H_2O + 2\ H^+ \qquad (2)$$

within the upflow zones. If sulfate reduction during upflow was affecting vent fluid chemistry at Spire vent, the H_2S produced from this reaction would be expected to be enriched relative to that in Hole 1035H and Shiner Bock vent fluids, since seawater sulfate has a $\delta^{34}S$ of +21‰ (REES et al., 1978). However, the $\delta^{34}S$ of aqueous H_2S from Spire is actually depleted by ~ 7‰ relative to Shiner Bock and Hole 1035H fluids and by ~17‰ relative to the anhydrite present in the 1035H chimney structure (Fig. 4-2),

indicating that Reaction 2 is not responsible for the observed differences in vent fluid composition.

Another possible reaction for the consumption of H_2 and concomitant production of H_2S is the reduction of pyrite to pyrrhotite during upflow through the ODP Mound massive sulfide:

$$\underset{\text{pyrite}}{FeS_2} + H_{2(aq)} \rightarrow \underset{\text{pyrrhotite}}{FeS} + H_2S_{(aq)}. \qquad (3)$$

This reaction consumes H_2 and produces H_2S in equimolar amounts, which is approximately the differences observed in aqueous H_2 and H_2S concentrations (Table 4-1). Consideration of mineral stability relationships in the system Fe-O-S at seafloor conditions of 270°C, 240 bars indicates that all of the fluids venting at Middle Valley are within the pyrrhotite stability field. However, the Spire fluid is displaced toward the pyrite-pyrrhotite join relative to the compositions of Shiner Bock and 1035H vents (Fig. 4-3).

Taken together, these data suggest a model in which high concentrations of H_2 derived from subsurface methane oxidation processes are consumed as fluids at Spire vent equilibrate with mineral phases during upflow. A schematic diagram of this process is shown in Figure 4-4. Fluids venting from ODP Hole 1035H were released when the drillhole punctured the silicified layer that acted as a hydrologic seal in the subsurface. Fluids that vent from this hole represent pristine fluids from the underlying reaction zone, and their composition is unchanged during upflow because rapid flow through a pipe will preclude extensive interaction with pyrite in the mound. Fluids were first observed to be venting from Shiner Bock vent prior to drilling Hole 1035H (SHIPBOARD SCIENTIFIC PARTY, 1998a). Fluid compositions at this vent are no longer modified by reduction of pyrite because of the longer period of time (> 4 years at the time of sampling) that fluids have been venting through this structure. When fluid flow occurs along a given path over an extended period of time, an increasingly greater proportion of any pyrite available for reaction with H_2-rich fluids will be converted to a pyrrhotite. Mass balance considerations indicate that conversion of the increasingly smaller amounts of remaining pyrite to pyrrhotite will no longer regulate fluid compositions. Fluids will then vent from

the chimney structure with a composition that is unchanged with respect to the original composition attained in the subsurface reaction zone.

This hypothesis was tested using the computer program EQ6 (WOLERY and DAVELER, 1992) to model the reaction of 1035H and Shiner Bock fluids with pyrite during upflow. Fluid calculations were performed at 270°C, which corresponds to the exit temperatures measured in the three chimneys (Table 4-1). This temperature is also similar to the temperature measured between 98 and 206 mbsf in ODP Hole 858G drilled at the Dead Dog field (SHIPBOARD SCIENTIFIC PARTY, 1998b). Downhole temperatures were also measured in several holes (1035A, D and E) drilled near and on the Bent Hill massive sulfide deposit during Leg 169 (SHIPBOARD SCIENTIFIC PARTY, 1998a). Subsurface temperatures estimated at a depth of 150 mbsf from these measurements range between 150-329°C.

Fluid speciation calculations were first performed using the measured endmember fluid composition and the computer program EQ3NR (WOLERY, 1992), using thermodynamic data from SUPCRT92 (JOHNSON et al., 1992), with data for $MgSO_4$ and $NaSO_4^-$ species added (MCCOLLOM and SHOCK, 1997). Measured pH (25°C) was used as a constraint on total ionizable H to calculate fluid pH at *in situ* conditions. Redox at the temperature of interest was calculated using the H_2-H_2O couple and measured $H_{2(aq)}$ concentrations. Measured endmember SO_4^{2-} concentrations were not input as a species since no precautions were taken to prevent oxidation of H_2S in the samples during storage. Instead, endmember SO_4^{2-} concentrations were assumed to be zero due to the formation of anhydrite from heated seawater at temperatures above 150°C during recharge (SEYFRIED and BISCHOFF, 1979, 1981a). Fe concentrations have not been measured in the ODP Mound fluids collected in 2000. Endmember Fe concentrations of 10-20 μmol/kg fluid were calculated for fluids collected at Middle Valley in 1990 by Butterfield et al (1994a). However, those data used were characterized by a large degree of scatter due to possible precipitation of sulfides within the sample bottles or entrainment of sulfide mineral particles during fluid collection. Hydrothermal alteration experiments conducted using unaltered Middle Valley sediment and a Na-Ca-K-Cl fluid

of seawater chlorinity indicate that Fe concentrations in fluids originating from hot subsurface reaction zones may be at least an order of magnitude greater than those calculated by Butterfield et al. (1994a). However, the choice of an input Fe concentration for the EQ3NR calculation makes no difference when using the reaction path program EQ6 (WOLERY and DAVELER, 1992), because the final calculated fluid composition was regulated by mineral solubilities.

The fluid speciation calculated with EQ3NR was then utilized as the input file by the reaction path program EQ6 (WOLERY and DAVELER, 1992). EQ6 was used to calculate the final fluid composition for a titration of 1 kg of either 1035H or Shiner Bock vent fluids with 1 mole of pyrite. During the course of the reaction, H_2S concentrations increased, while H_2 concentrations decreased. Pyrite was consumed to produce pyrrhotite as the stable mineral phase. The final fluid composition at the end of this calculation for 1035H vent fluid was nearly identical to the fluid composition measured at Spire vent (Fig. 4-3). The reaction calculations ended when the fluid composition attained equilibrium with pyrite and pyrrhotite, so the calculated final fluid composition (circles on Fig. 4-3) should be coincident with the phase boundary between pyrite and pyrrhotite. The discrepancy between the phase boundaries and the final calculated fluid composition arises from the fact that the EQ6 database does not account for the non-ideal activity of pyrrhotite (TOULMIN and BARTON, 1964). If the activity of pyrrhotite was accounted for by EQ6, the final calculated fluid composition would be coincident with the phase boundary. What is important to note, is that the direction in which the fluid composition evolved when 1035H fluid is reacted with pyrite (dotted line on Fig. 4-3), which passes through the composition of Spire vent fluids. While the fluids from Spire vent have not yet fully equilibrated with pyrite during upflow, their composition is consistent with the approach to equilibrium with pyrite and pyrrhotite.

That pyrite reduction is likely occurring in fluids from the Spire vent and not in fluids from 1035H or Shiner Bock vents can be explained as functions of both the relative ages of the various vents and fluid flow paths through the mound. During the initial stages of fluid flow along a path through the mound, reaction is characterized by low

water/pyrite mass ratios, so that fluid composition is regulated by equilibrium with the mineral phases (Fig. 4-5). With continued flow of fluids along the same path for increasing amounts of time, a greater proportion of pyrite originally present along that path will have been converted to pyrrhotite. With less pyrite present, water/pyrite mass ratios increase with time. As seen in Figure 4-5, at sufficiently high water/pyrite ratios, the absolute amount of pyrite that is reduced to form pyrrhotite becomes vanishingly small compared to the mass of fluid. As the amount of pyrite in contact with fluids decreases at Shiner Bock, the ability to influence fluid composition is reduced and fluids will discharge at the seafloor with an unaltered composition (Fig. 4-4). A similar result occurs for differences in the tortuosity of a flow path. For flow through a pipe, as through ODP Hole 1035H (Fig. 4-4), there is little exposed mineral surface area with which fluids can interact. This will preclude regulation of fluid chemistry by reactions with pyrite. This is also equivalent to having reactions occur at high water/pyrite mass ratios. If fluids flow along a highly tortuous flow path, as may be occurring underneath Spire vent (Fig. 4-4), many more mineral surfaces are available for reaction, allowing fluid-mineral reactions to regulate fluid chemistry.

The differences in the measured $\delta^{34}S$ of aqueous H_2S between the ODP Mound vents is also consistent with pyrite reduction in the mound at Spire vent. The $\delta^{34}S$ of the total system at a given point can be calculated with an isotopic mass balance:

$$R_T S_T = R_A S_A + R_M S_M \qquad (4)$$

where R is the $^{34}S/^{32}S$ and S is the molar amount of the component of interest. The subscripts T, A and M stand for the total system, aqueous H_2S and mineral phases under consideration, respectively. The overall reaction represented by Reaction 3 can be conceptualized as occurring in two discrete steps: 1.) dissolution of pyrite to form aqueous H_2S; and 2.) precipitation of pyrrhotite from the total aqueous H_2S pool (Fig. 4-6). It was assumed that the pyrrhotite that forms from reduction of pyrite precipitated in isotopic equilibrium with the co-existing aqueous H_2S to calculate the isotopic composition of the pyrite with which fluids of 1035H composition reacted to achieve the isotopic composition measured in the Spire fluids.

The details of the isotopic mass balance calculations are given in Table 4-3. The final system is considered to consist of aqueous H_2S and precipitated pyrrhotite. The isotopic composition and amount of S in the H_2S component is taken to be the measured composition of the Spire vent fluid (Table 4-1). The amount of S in the pyrrhotite component was calculated from the amount of pyrrhotite formed at the end of the EQ6 calculations. The isotopic composition of the pyrrhotite was calculated by assuming isotopic equilibrium with the aqueous H_2S at 270°C, using the fractionation factor of 1.000339 calculated from the data reported in (OHMOTO and RYE, 1979). The composition of this total mixture was then utilized to calculate the isotopic composition of the initial pyrite that reacted with the 1035H fluids to produce the $\delta^{34}S$ of the Spire vent fluids. The required isotopic composition of pyrite in this initial system is thus calculated to be –0.05‰ (Table 4-4). This composition is depleted relative to the isotopic composition of pyrite in the Bent Hill massive sulfide deposit, which ranges between +1.9 to +12.4‰ (ZIERENBERG, 1994). Thus, the initial source of pyrite to the ODP Mound massive sulfide could have a more depleted isotopic composition than the Bent Hill massive sulfide source due to a greater proportion of basalt-derived sulfide in the original source fluid. A second possible source of the more depleted pyrite could be reaction of hydrothermal fluids with both isotopically depleted bacteriogenic pyrite and hydrothermal pyrite within the mound structure. Unlike the Bent Hill massive sulfide deposit, which contains no sediment within the mound, the ODP Mound massive sulfide consists of three discrete lenses of massive sulfides interlayered with sediments (SHIPBOARD SCIENTIFIC PARTY, 1998a; ZIERENBERG et al., 1998). Maximum fractionations of sulfate to sulfide during bacterially-mediated sulfur reduction in sediments is on the order of 45-50‰ (CANFIELD, 2001), which, under open system conditions, will lead to the formation of diagenetic pyrite with an isotopic composition of ~ –24 to –29‰. An initial pyrite source with an isotopic composition of –0.05‰ will result from a mixture of 79% hydrothermal pyrite with an isotopic composition of +6‰ and 21% diagenetic pyrite with an isotopic composition of –24‰.

Replacement of pyrrhotite by pyrite in response to the high H_2 concentrations generated by methane oxidation in the subsurface indicates the pervasive influence of organic compounds not only on fluid chemistry but the mineral chemistry of associated massive sulfide deposits as well. This process may also have secondary influences on other inorganic aqueous species. The large change in both H_2S concentrations and H_2 concentrations due to reaction during upflow will also have important implications for the applicability of some proxies for subsurface reaction zone conditions. For example, the use of dissolved Fe and H_2S concentrations have been suggested as indicators of pH and temperature, respectively, in subsurface reaction zones (DING and SEYFRIED, 1992) due to the insensitivity of their concentrations to cooling of fluids during upflow (DING and SEYFRIED, 1994). However, this work demonstrates that in very young vents, chemical reactions can alter H_2S concentrations during upflow so that the measured concentration will no longer reflect subsurface reaction zone conditions. Changes in aqueous H_2S and H_2 may also affect other aspects of fluid chemistry, such as the solubility of ore-forming metals such as Fe, Mn, Zn and Cu. For example, Seyfried and Ding (1993) have demonstrated that the abundances of Fe and Cu in vent fluids are a function of fluid pH and redox, and have suggested that the Fe/Cu ratios in such fluids may be a proxy for redox conditions in the deepest subsurface reaction zone. However, if aqueous H_2 is consumed during upflow, the Fe/Cu ratio in the fluids will reflect conditions during upflow—not those from the hottest part of the subsurface reaction zone. Thus, in certain situations, fluid compositions should not automatically be assumed to represent conditions in the deep subsurface and care must be taken when applying chemical proxies to model subsurface conditions.

4.5. CONCLUSIONS

Temporal variability can be assessed on two different scales at Middle Valley. Over a decade, the concentrations of major and minor inorganic ions in each of the two areas of venting—the Dead Dog and ODP Mound fields—exhibit very little variation. The differences in Na/Cl, Ca/Cl and Na/Ca ratios as well as the absolute concentrations

of these species may reflect the hotter subsurface conditions and phase separation processes occurring in the ODP Mound field. The invariant NH_3 concentrations with time indicate that fluids must be continuously reacting with fresh sediment. This may result from the continued subsidence of sediments over time, thereby providing fluids with a constant source of fresh reactant. Alternatively, the stable NH_3 concentrations may be a result of the reaction of fluids with a spatially large source of sediments, so that the total pool of sediment-derived fluids has not been completely tapped over the previous decade. The stable concentrations of the major and minor inorganic ions indicate that the fluids have reacted with a rock composition that has remained unchanged over the time scale of this study. It is not possible to assess if the composition of the rock composition consists of a fresh or altered basalt with the current dataset.

In contrast to the stability of the aqueous ions, concentrations of the volatile species H_2 and H_2S and the sulfur isotopic composition of H_2S exhibit a large variation in fluids from Shiner Bock, 1035H and Spire vents sampled at the ODP Mound field, despite their close spatial proximity. Reaction path modeling indicates that the lower H_2 and higher H_2S concentrations in Spire vent relative to Hole 1035H or Shiner Bock reflect re-equilibration of the vent fluid chemistry with the minerals in the mound. High H_2 concentrations derived from methane oxidation reactions in the subsurface induce the replacement of pyrite by pyrrhotite. These results indicate that not only does the presence of organic compounds affect the chemistry of vent fluids, but can also lead to unexpected changes in the chemistry of associated sulfide deposits. The large changes in H_2S and H_2 concentrations may also lead to large associated changes in the transition metal concentrations. This indicates that care must be taken in assuming that the concentrations of such species such as Fe and Cu necessarily record conditions in the deepest subsurface reaction zones in some environments.

Table 4-1: Concentrations of aqueous species in vent fluids from Middle Valley, northern Juan de Fuca Ridge.

Vent	Sample	exit T	Mg	Na	Na, cb[†]	Ca	K	Si	Sr	Cl	Br	SO_4^{2-}
		°C	mmol/kg	mmol/kg		mmol/kg	mmol/kg	µmol/kg	µmol/kg	mmol/kg	µmol/kg	mmol/kg
DEAD DOG												
Heineken Hollow	BGT-3597-1		51.0	463	458	12.9	10.6	0.32		544	815	25.6
	BGT-3597-2		11.3	415	415	78.4	19.1	8.72	220	589	1018	2.53
	M-3596-12C		3.13	411	416	72.5	19.4			581	1042	2.04
	M-3596-1C		2.25	408	407	74.2	19.8			576	1020	1.26
	M-3597-12		45.9	471	455	23.2	11.9			557	841	23.8
	M3597-15		27.9	443	422	45.7	15.0			554	914	14.6
	Endmember	67-187	0	408	408	78.7	19.9	9.12	226	583	1037	0.67
Dead Dog mound	M-3597-1C		1.51	410	416	73.9	19.7			584	1016	0.83
	M-3597-12C		2.03	410	418	73.2	19.6			585	1037	1.11
	Endmember	274	0	408	416	75.7	20.0			586	1034	0.07
Chowder Hill	BGT-3596-3		1.90	416	425	63.8	19.7			572	1003	1.41
	BGT-3596-4		1.12	416	430	63.2	19.7	11.6	232	576	1026	0.68
	Endmember	281	0	414	426	65.1	20.0	11.9	235	575	1020	0.28
Inspired Mounds	BGT-3597-3		34.4	459	437	34.3	13.6	3.25	126	551		18.4
	BGT-3597-4		41.0	472	437	26.7	12.4	2.49	111	542	871	21.2
	M-3597-6C		30.3	444	418	40.8	14.3			541	912	16.4
	M-3597-11C		43.0	466	454	25.9	12.3			557		23.4
	Endmember	255-261	0	402	373	78.6	19.4	9.17	197	546	995	1.98
Puppy Dog	BGT-3599-3		6.16	424	423	67.4	18.5	7.15	203	582	975	3.29
	BGT-3599-4		44.6	469	445	24.2	11.8	1.18	97	544	867	25.1
	Endmember	202	0	416	418	75.0	19.5	8.05	218	586	995	0.28
ODP MOUND												
1035F	BGT-3598-3		43.2	468	449	14.1	10.7	1.23	80	527	806	23.2
	M-3598-6C		46.7	464	454	15.4	10.9			542	811	23.4
	M-3598-11C		46.7	464	441	15.7	10.6			528	821	23.9
	Endmember	40	0	395	391	28.4	12.2	5.79	49.5	448	742	5.76
Shiner Bock	BGT-3595-1		1.61	362	354	34.0	13.7	10.3	132	435	730	1.74
	BGT-3595-2		3.40	371	357	33.8	13.4	9.85	130	439	745	2.89
	M-3595-11C		5.99	370	356	36.0	13.3			444	785	4.34
	M-3595-6C		12.7	386	379	32.7	13.1			467	778	7.35
	M-3595-1C		28.7	418	406	27.8	11.8			495	785	17.7
	M-3595-12		3.10	360	360	36.2	14.2			443	752	2.11
	Endmember	272	0	357	348	37.2	13.9	10.5	133	434	749	1.16
Spire	BGT-3595-3		1.64	364	355	39.3	13.3	10.5	145	434	754	7.81
	BGT-3595-4		22.5	407	395	27.0	12.2	5.68		479	774	13.2
	M-3595-15		4.12	368	354	36.0	13.6			442	798	2.64
	Endmember	263	0	358	349	39.1	13.6	10.6	139	432	769	3.93
1035H	BGT-3599-1		17.0	404	394	28.8	12.2	6.58	113	479	786	8.84
	BGT-3599-2		20.9	413	396	27.1	12.1	5.82	104	481	773	11.1
	M-3599-12		29.3	426	421	24.4	11.7			508	792	15.8
	M-3599-15		30.3	426	419	23.7	11.5			506	796	15.6
	Endmember	267	0	365	362	37.8	13.1	9.55	121	449	759	0.50
BSW[*]	M-3598-6C	2.1	53.0	482	459	11.3	10.4	0.18	87	543	820	27.2

[*]bottom seawater; [†]charge balance

Table 4-1 (continued): Endmember concentrations of aqueous species in vent fluids from Middle Valley, Northern Juan de Fuca Ridge.

Vent	Sample	pH 25°C	H_2 mmol/L	H_2S mmol/kg	$\delta^{34}S$ (‰)	$\delta^{34}S$ 1σ (n)‡	CO_2 mmol/kg	NH_4 µmol/kg	CH_4 mmol/L
Dead Dog									
Heineken Hollow	BGT-3597-1	7.2	0.03	0.2			2.71	64	0.45
	BGT-3597-2	5.8	1.5	3.2			6.92	2792	17.7
	M-3596-12C							2855	
	M-3596-1C							2996	
	M-3597-12	5.7						282	
	M3597-15	6.0						1350	
	Endmember		1.9	3.4	+7.2	0.7 (3)	8.15	3180	22.6
Dead Dog mound	M-3597-1C	5.8		3.0				3076	
	M-3597-12C	6.4		3.0				2933	
	Endmember	6.0		3.0	+6.4	0.5 (3)		3108	
Chowder Hill	BGT-3596-3	5.9	2.5	3.6			7.54	3045	19.2
	BGT-3596-4	5.8	2.6	3.7			8.96	3103	20.3
	Endmember		2.6	3.7	+5.7	— (1)	8.43	3164	20.3
Inspired Mounds	BGT-3597-3	6.1	0.81	0.8			5.65	993	7.58
	BGT-3597-4	6.2	0.53	—			4.23	524	4.88
	M-3597-6C	6.6						1251	
	M-3597-11C	5.8						551	
	Endmember		2.3	2.4	+6.8	— (1)	11.6	2866	21.6
Puppy Dog	BGT-3599-3	5.7	1.8	3.4			7.65	2646	16.4
	BGT-3599-4	6.5	0.3	0.7			3.42	351	2.88
	Endmember		2.0	3.8	—		8.35	2986	18.5
ODP Mound									
1035F	BGT-3598-3	6.4	0.39	0.3			3.44	232	0.56
	M-3598-6C	6.3		0.3				160	
	M-3598-11C	5.5		0.3				121	
	Endmember		2.1	1.7	+10.7	0.2 (2)	8.24	1263	2.99
Shiner Bock	BGT-3595-1	5.3	8.0	4.3			11.7	2262	6.92
	BGT-3595-2	5.4	7.6	3.9			11.4	2099	6.56
	M-3595-11C	2.6						2130	
	M-3595-6C							1800	
	M-3595-1C							1070	
	M-3595-12	5.6						2240	
	Endmember		8.2	4.3	+9.7	0.6 (6)	12.0	2340	7.07
Spire	BGT-3595-3	6.0	2.1	7.8			12.7	2107	6.52
	BGT-3595-4	5.7	1.2	4.5			8.50	1264	3.84
	M-3595-15							2215	
	Endmember		2.2	7.9	+3.2	0.4 (2)	13.1	2270	6.71
1035H	BGT-3599-1	5.5	4.2	2.7			7.86	1446	3.98
	BGT-3599-2	5.6	3.7	2.4			7.62	1262	3.54
	M-3599-12	6.3						938	
	M-3599-15	6.7						855	
	Endmember		6.1	4.0	+10.4	0.4 (3)	10.7	2096	5.85
BSW*			0	0	+20		2.33	0.8	0

*bottom seawater; ‡(n): number of replicate analyses for a particular vent; 1σ is the standard devation of the analyses used to calculate the average value.

Table 4-2: Time series (1990-2000) of calculated endmember vent fluid compositions from Middle Valley.

Vent	Year	exit T	Na, cb[†]	Ca	K	Si	Sr	Cl	Br	H_2S	Na/Cl	Ca/Cl	K/Cl	Ca/Na
		°C	mmol/kg	mmol/kg	mmol/kg	mmol/kg	µmol/kg	mmol/kg	µmol/kg	mmol/kg				
Dead Dog														
Heineken Hollow	1990	184	411	74.4	19.3	7.68	260	563	1087	—	0.730	0.132	0.034	0.18
	2000	67-187	408	78.7	19.9	9.12	226	583	1037	3.4	0.699	0.134	0.034	0.19
Dead Dog mound	1990	265-268	401	80.0	18.6	9.31	259	577	1058	1.2	0.695	0.139	0.032	0.20
	2000	274	416	75.7	20.0	—	—	586	1034	3.0	0.710	0.129	0.034	0.18
Chowder Hill	1990	257-276	399	82.1	18.1	10.2	256	578	1087	2.0	0.690	0.142	0.031	0.21
	2000	281	426	65.1	20.0	11.9	235	575	1020	3.7	0.741	0.113	0.035	0.15
Inspired Mounds	1990	254	402	79.7	18.8	10.1	257	575	1056	4.3	0.699	0.139	0.033	0.20
	2000	255-261	373	78.6	19.4	9.17	197	546	995	2.4	0.683	0.144	0.036	0.21
ODP Mound														
Lone Star	1990	265	319	40.4	13.5	10.3	160	412	768	2.4	0.774	0.098	0.033	0.13
Shiner Bock	2000	272	348	37.2	13.9	10.5	133	434	749	4.3	0.802	0.086	0.032	0.11
BSW[*]	2000	2	459	11.3	10.4	0.18	87	543	820	0	0.845	0.021	0.019	0.02

[*]bottom seawater

[†]charge balance

Endmember compositions in 1990 calculated from data in (BUTTERFIELD et al., 1994a).

Table 4-3: Details of isotopic mass balance calculations used to determine the isotopic composition of the initial pyrite reactant required to convert $\delta^{34}S$ of 1035H vent fluid to the $\delta^{34}S$ measured in Spire vent fluid.

	Component	S mmoles	Source	R	$\delta^{34}S$ ‰	Source
Final System	pyrrhotite	4.211	Po produced in EQ6 model	0.04516 38	+3.4	isotopic equilibrium with Spire $H_2S_{(aq)}$
	H_2S	8.553	measured in Spire fluid	0.04514 85	+3.2	measured in Spire fluid
	total	12.764	(Po produced in EQ6 model) + (H_2S measured in Spire fluid)	0.04515 35	+3.31	calculated from isotopic mass balance
Initial System	H_2S	4.108	measured in 1035H fluid	0.04547 25	+10.4	measured in 1035H fluid
	total	12.766	(Po produced in EQ6 model) + (H_2S measured in Spire fluid)	0.04515 35	+3.31	'Total' value calculated for "Final System"
	pyrite	8.658	(Po produced in EQ6 model) + (H_2S measured in Spire fluid) – (H_2S measured in 1035H fluid)	0.04500 21	**-0.05**	calculated from isotopic mass balance

Isotopic mass balance equation:

$$R_T S_T = R_A S_A + R_M S_M \qquad (4)$$

R: $^{34}S/^{32}S$ of the component of interest
S: molar amount of the component of interest
T: total system
A: aqueous H_2S
M: mineral phase under consideration.

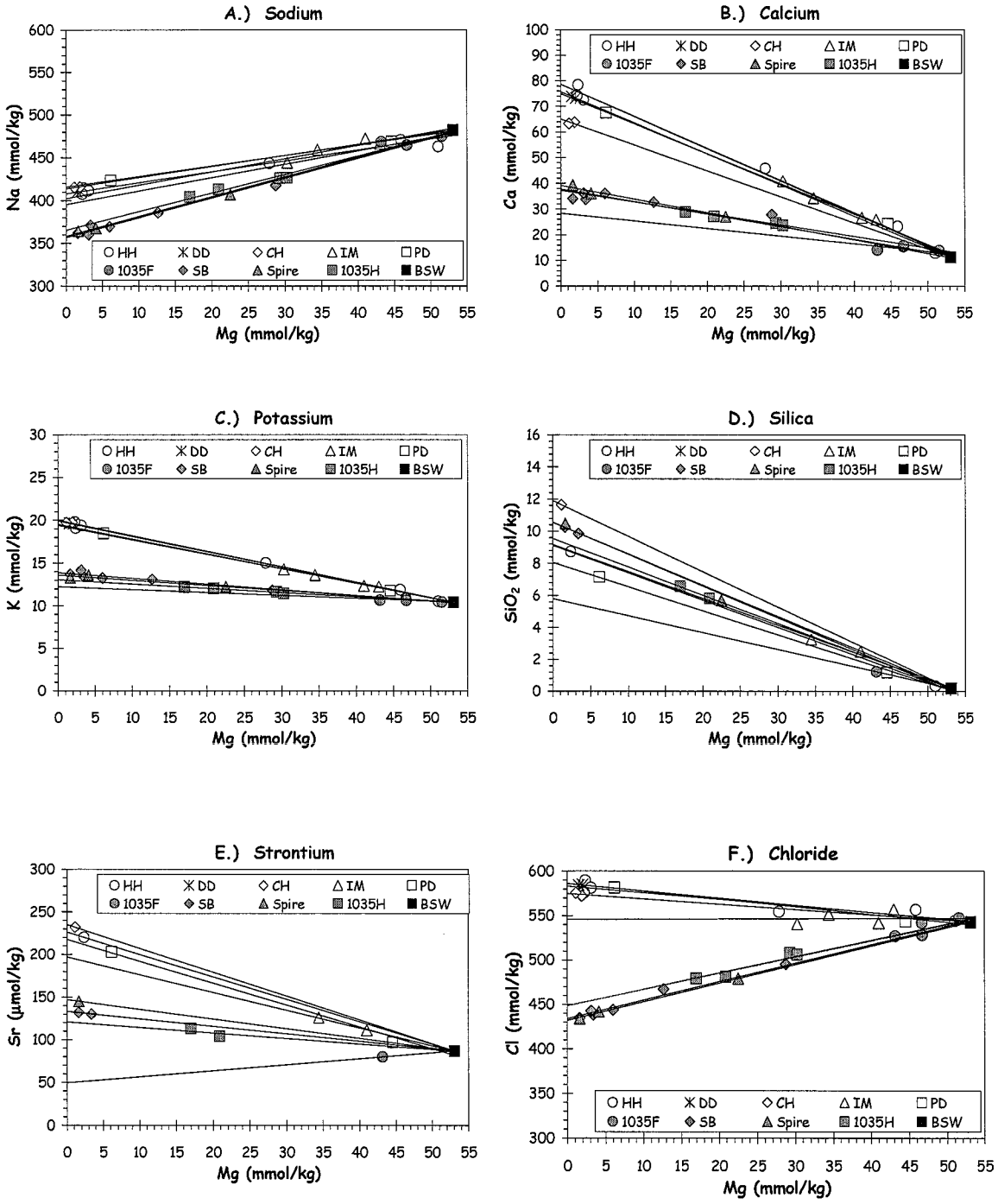

Figure 4-1. Graphs of individual chemical species versus Mg for sampled vent fluids. **(A)** Sodium; **(B)** Calcium; **(C)** Potassium; **(D)** Silica; **(E)** Strontium; **(F)** Chloride. Key to vents: HH: Heineken Hollow; DD: Dead Dog mound; CH: Chowder Hill; IM: Inspired Mounds; PD: Puppy Dog; SB: Shiner Bock.

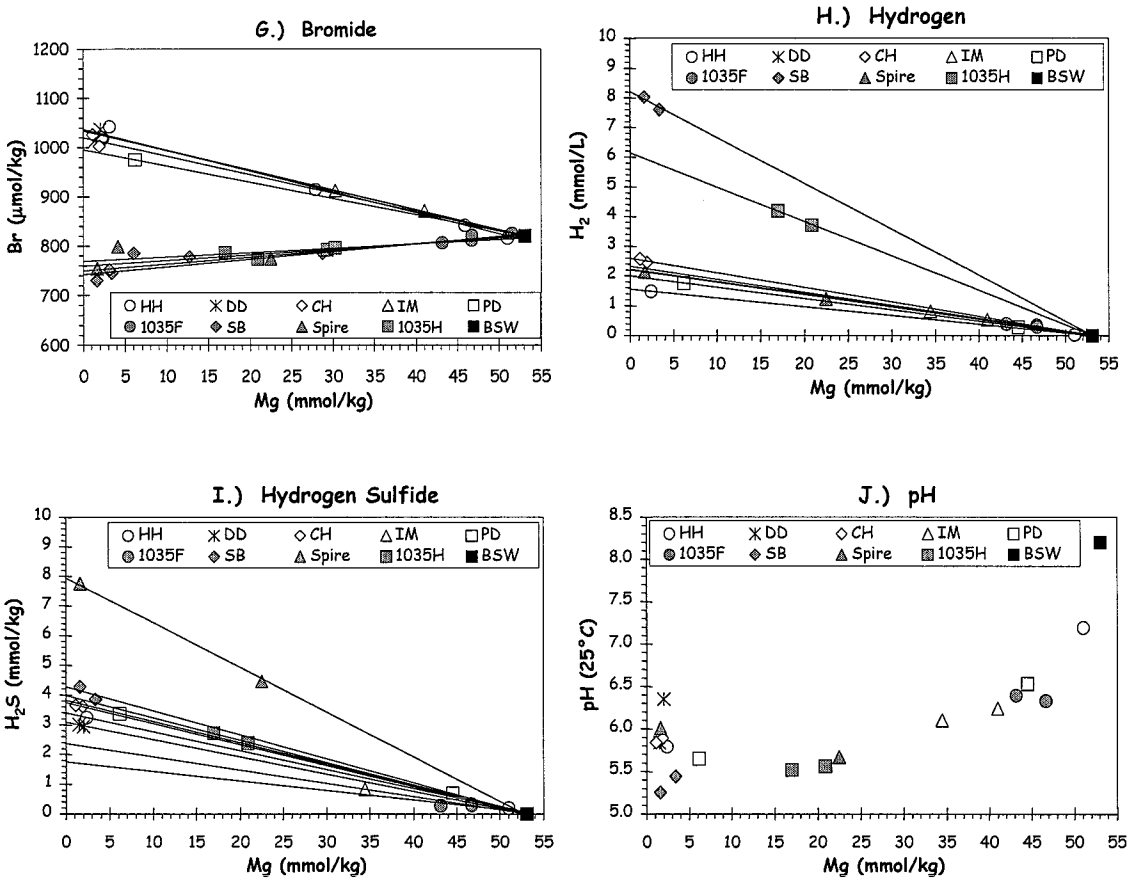

Figure 4-1, continued. (**G**) Bromide; (**H**) Hydrogen; (**I**) Hydrogen Sulfide (**J**) pH. Key to vents: HH: Heineken Hollow; DD: Dead Dog mound; CH: Chowder Hill; IM: Inspired Mounds; PD: Puppy Dog; SB: Shiner Bock.

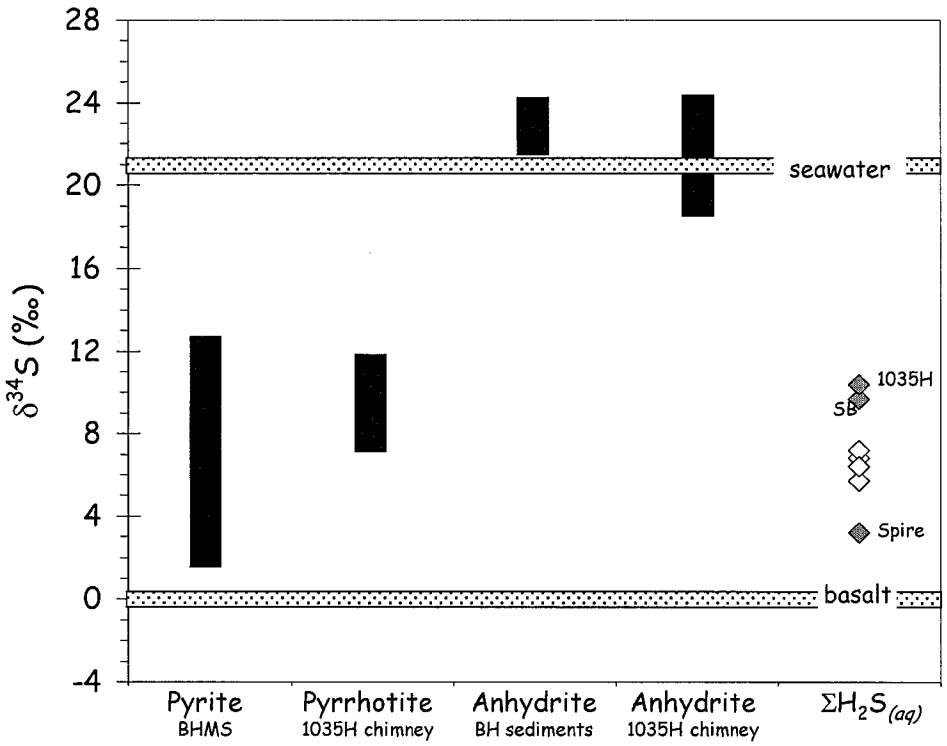

Figure 4-2. $\delta^{34}S$ of sulfate and sulfide minerals recovered from Bent Hill, the Bent Hill massive sulfide deposit, and the chimney at ODP Hole 1035H. Also shown in the stipled bars is the $\delta^{34}S$ of seawater sulfate Rees et al., 1978) and basaltic sulfide (Sakai et al., 1984). Data for minerals from Bent Hill from Zierenberg (1994). The $\delta^{34}S$ of the 1035H chimney minerals is unpublished data from Zierenberg (2002, pers. comm.).

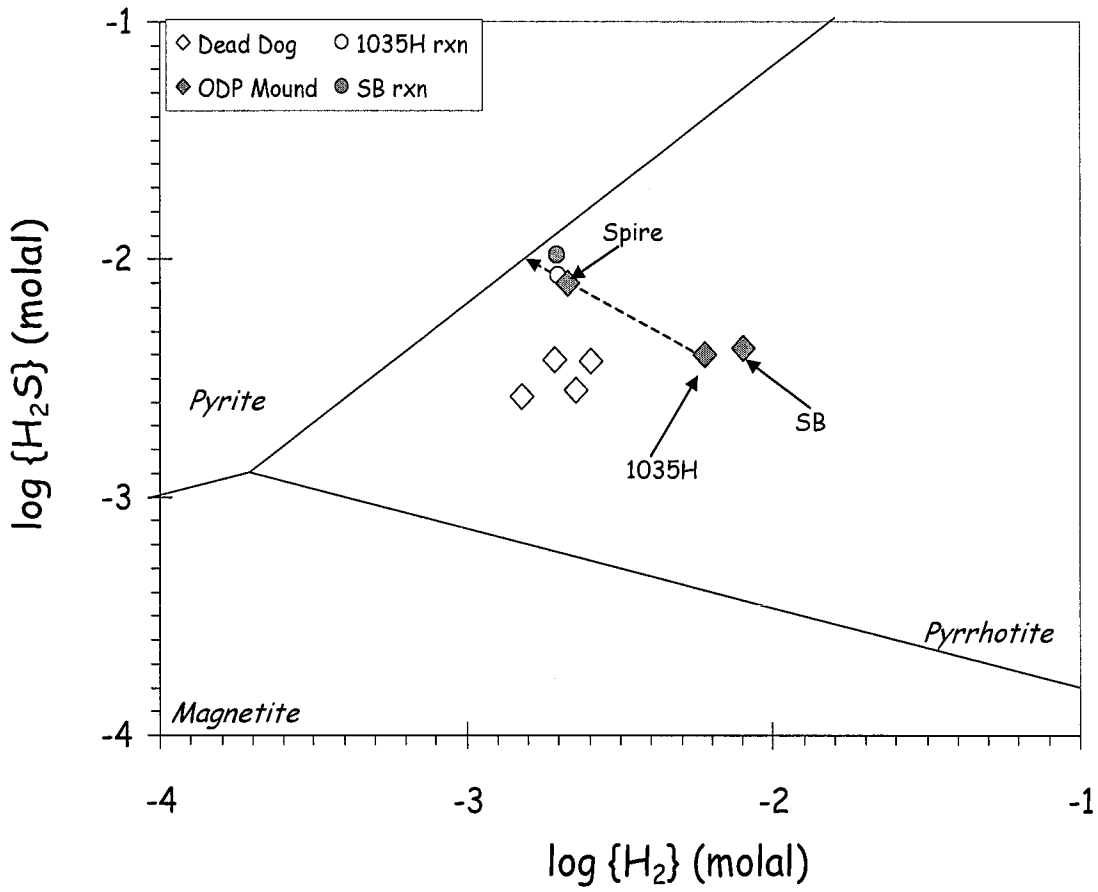

Figure 4-3. Phase diagram for Fe-O-S system at 270°C, 240 bars. Measured vent fluid compositions for Dead Dog are indicated with white diamonds. Vent fluid compositions for ODP Mound field fluids are indicated with gray diamonds. White and gray circles indicate the final fluid composition calculated using EQ6 (Wolery and Daveler, 1992) for reaction of pyrite with 1035H and Shiner Bock vent fluids, respectively. Thermodynamic data requisite for the construction of this figure are from Johnson et al. (1992) and Toulmin and Barton (1964). Key to vent labels: SB: Shiner Bock.

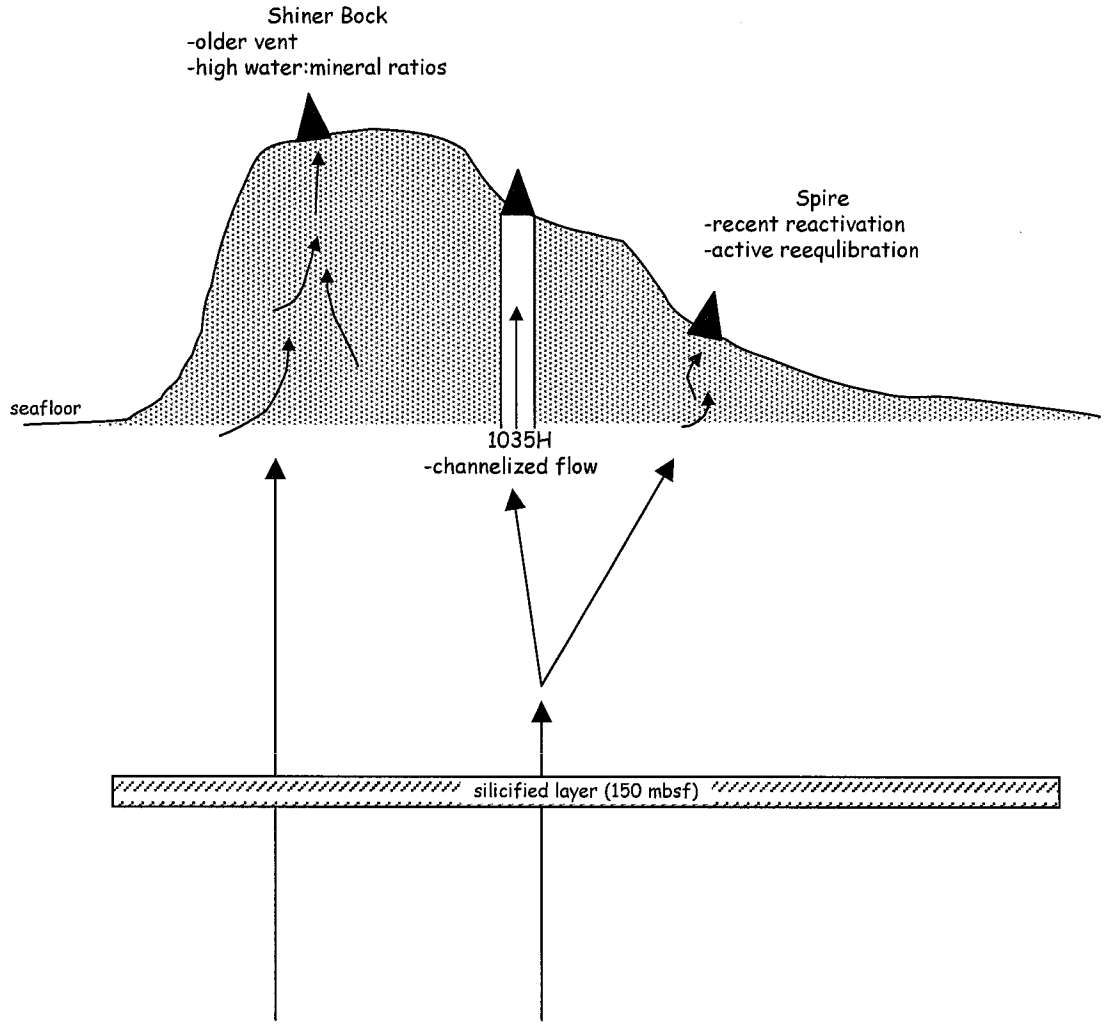

Figure 4-4. Schematic diagram showing differences in fluid flow reaction pathways in the ODP Mound field. Shiner Bock vent is several years old, leading to an exhaustion of the buffer capacity of the rock and reaction of fluid and pyrite at effectively high water/pyrite mass ratios. ODP Hole 1035H is a channelized flow path, precluding extensive interaction of venting fluid with minerals. Spire vent is from a new vent field that had formed within two years prior to sampling due to reactivation of flow through the mound caused by ODP Leg 169 drilling operations. Thus, the vent fluid composition is being actively buffered by the reduction of pyrite to pyrrhotite in response to the high H_2 concentrations generated by methane oxidation in the subsurface.

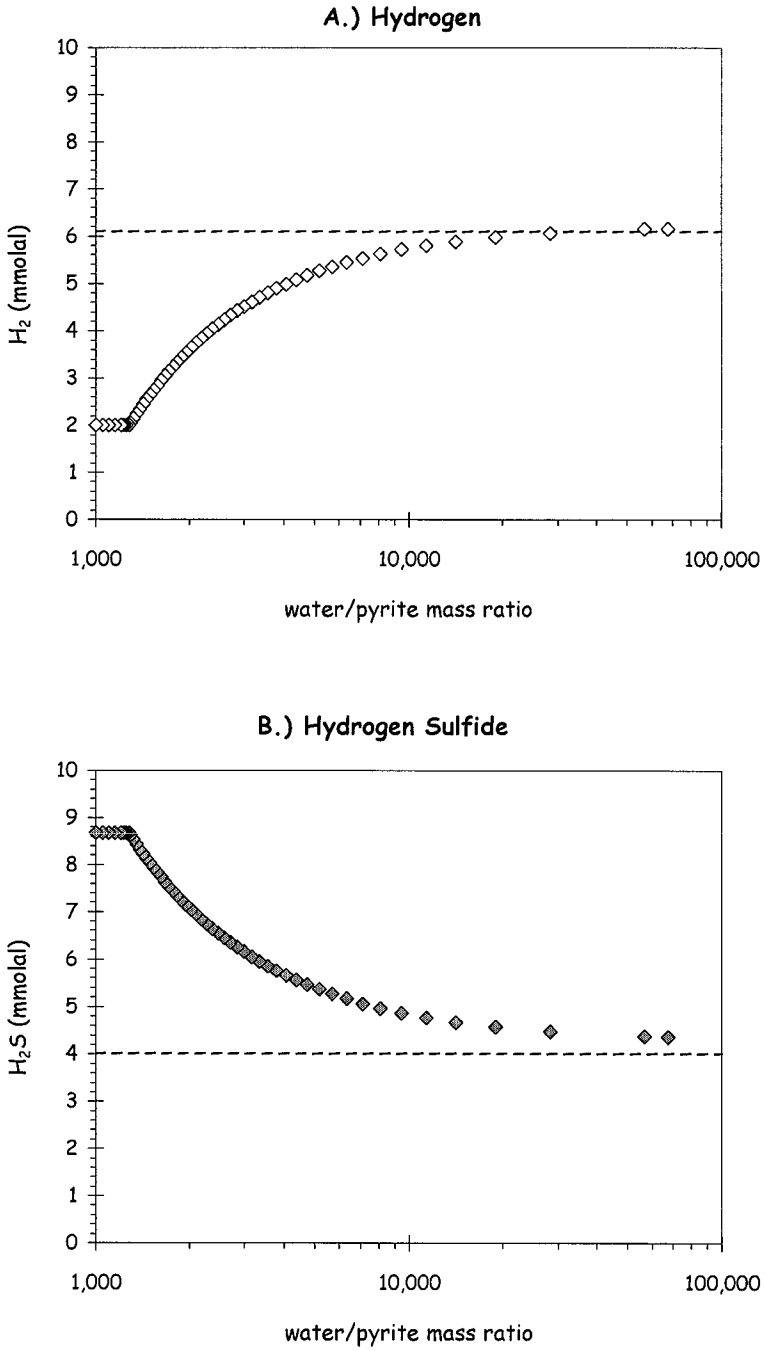

Figure 4-5. Evolution of aqueous **(A)** hydrogen and **(B)** hydrogen sulfide concentration in equilibrium with pyrite at increasing water/pyrite ratios. Dashed line represents initial H_2 and H_2S concentrations of 1035H fluids at 270°C, 240 bars, which was the initial fluid composition used in the EQ6 chemical modelling.

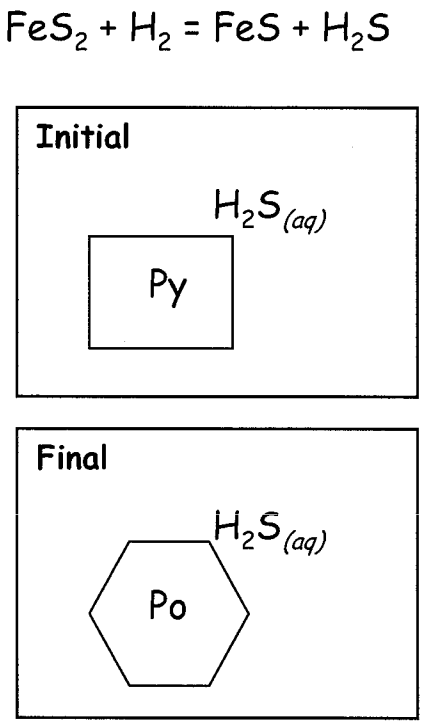

Figure 4-6. Conceptual model of the sulfur system during the conversion of pyrite to pyrrhotite used to calculate the stable sulfur isotopic composition of the intital pyrite. Py: pyrite. Po: pyrrhotite.

4.6. REFERENCES

BERNER R. A., LASAGA A. C., and GARRELS R. M. (1983) The carbonate-silicate geochemical cycle and its effect on atmospheric carbon dioxide over the past 100 million years. *Am. J. Sci.* **283**, 641-683.

BISCHOFF J. L. and DICKSON F. W. (1975) Seawater-basalt interaction at 200°C and 500 bars: Implications for the origin of sea-floor heavy-metal deposits and the regulation of seawater chemistry. *Earth Planet. Sci. Lett.* **25**, 385-397.

BUTTERFIELD D. A. and MASSOTH G. J. (1994) Geochemistry of North Cleft segment vent fluids: temporal changes in chlorinity and their possible relation to recent volcanism. *J. Geophys. Res.* **99**, 4951-4968.

BUTTERFIELD D. A., MCDUFF R. E., FRANKLIN J., and WHEAT C. G. (1994a) Geochemistry of hydrothermal vent fluids from Middle Valley, Juan de Fuca Ridge. In *Proc. ODP, Sci. Results* **139** (ed. M. J. Mottl, E. E. Davis, A. T. Fisher, and J. F. Slack), pp. 395-410.

BUTTERFIELD D. A., MCDUFF R. E., MOTTL M. J., LILLEY M. D., LUPTON J. E., and MASSOTH G. J. (1994b) Gradients in the composition of hydrothermal fluids from the Endeavour segment vent field: Phase separation and brine loss. *J. Geophys. Res.* **99**, 9561-9583.

CAMPBELL A. C., BOWERS T. S., and EDMOND J. M. (1988) A time-series of vent fluid compositions from 21°N, EPR (1979, 1981 and 1985) and the Guaymas Basin, Gulf of California (1982, 1985). *J. Geophys. Res.* **99**, 9561-9583.

CANFIELD D. E. (2001) Biogeochemistry of sulfur isotopes. In *Stable Isotope Geochemistry* (ed. J. W. Valley and D. R. Cole), pp. 607-636. Mineralogical Society of America.

DAVIS E. E. and VILLINGER H. (1992) Tectonic and thermal structure of the Middle Valley sedimented rift, northern Juan de Fuca Ridge. In *Proc. ODP, Init. Rept.* **139** (ed. E. E. Davis, M. J. Mottl, A. T. Fisher, and et al.), pp. 9-41.

DING K. and SEYFRIED W. E., JR. (1992) Determination of Fe-Cl complexing in the low pressure supercritical region (NaCl fluid) - Iron solubility constraints on pH of subseafloor hydrothermal fluids. *Geochim. Cosmochim. Acta* **56**, 3681-3692.

DING K. and SEYFRIED W. E., JR. (1994) Effect of conductive cooling on chemistry of mid-ocean ridge hydrothermal fluids: experimental and theoretical constraints. *Mineralogical Magazine* **58A**, 231-232.

DING K., SEYFRIED W. E., JR., TIVEY M. K., and BRADLEY A. M. (2001a) In situ measurement of dissolved H_2 and H_2S in high-temperature hydrothermal fluids at the Main Endeavour Field, Juan de Fuca Ridge. *Earth Planet. Sci. Lett.* **186**, 417-425.

DING T., VALKIERS S., KIPPHARDT H., DE BIÈVRE P., TAYLOR P. D. T., GONFIANTINI R., and KROUSE R. (2001b) Calibrated sulfur isotope abundance ratios of three IAEA sulfur isotope reference materials and V-CDT with a reassessment of the atomic weight of sulfur. *Geochim. Cosmochim. Acta* **65**, 2433-2437.

EDMOND J. M., MASSOTH G., and LILLEY M. D. (1992) Submersible-deployed samplers for axial vent waters. *RIDGE Events* **3**, 23-24.

GOODFELLOW W. D. and BLAISE B. (1988) Sulfide formation and hydrothermal alteration of hemipelagic sediment in Middle Valley, northern Juan de Fuca Ridge. *Can. Mineral.* **26**, 675-696.

GOODFELLOW W. D. and FRANKLIN J. M. (1993) Geology, mineralogy, and chemistry of sediment-hosted clastic massive sulfides in shallow cores, Middle Valley, Northern Juan de Fuca R idge. *Econ. Geol.* **88**, 2037-2068.

JOHNSON J. W., OELKERS E. H., and HELGESON H. C. (1992) SUPCRT92: A software package for calculating the standard molal thermodynamic properties of minerals, gases, aqueous species, and reactions from 1 to 5000 bar and 0 to 1000°C. *Comput. Geosci.* **18**, 899-947.

KARSTEN J. L., HAMMOND S. R., DAVIS E. E., and CURRIE R. (1986) Detailed morphology and neotectonics of the Endeavour segment, Northern Juan de Fuca Ridge: New results from Seabeam swath mapping. *Geol. Soc. Am. Bull.* **97**, 213-221.

KOROLEFF F. (1976) Determination of nutrients. In *Methods of Seawater Analysis* (ed. K. Grasshoff), pp. 125-157. Verlag-Chemie.

LISTER C. R. B. (1983) The basic physics of water penetration into hot rock. In *Hydrothermal Processes at Seafloor Spreading Centers* (ed. P. A. Rona, K. Boström, and K. L. Smith, Jr.), pp. 141-168. Plenum.

MCCOLLOM T. M. and SHOCK E. (1997) Geochemical constraints on chemolithoautotrophic metabolism by microorganisms in seafloor hydrothermal systems. *Geochim. Cosmochim. Acta* **61**, 4375-4391.

MOTTL M. J. and HOLLAND H. D. (1978) Chemical exchange during hydrothermal alteration of basalt by seawater-I. Experimental results for major and minor components of seawater. *Geochim. Cosmochim. Acta* **42**, 1103-1115.

OHMOTO H. and RYE R. O. (1979) Isotopes of carbon and sulfur. In *Geochemistry of Hydrothermal Ore Deposits* (ed. H. L. Barnes), pp. 798. John Wiley.

PETER J. M., GOODFELLOW W. D., and LEYBOURNE M. I. (1994) Fluid inclusion petrography and microthermometry of the Middle Valley hydrothermal system, northern Juan de Fuca Ridge. In *Proc. ODP, Sci. Results* **139** (ed. M. J. Mottl, E. E. Davis, A. T. Fisher, and J. F. Slack), pp. 411-428.

REES C. E., JENKINS W. J., and MONSTER J. (1978) The sulphur isotopic composition of ocean water sulphate. *Geochim. Cosmochim. Acta* **42**, 377-381.

RICHTER F. M., ROWLEY D. B., and DEPAOLO D. J. (1992) Sr isotope evolution of seawater: the role of tectonics. *Earth Planet. Sci. Lett.* **109**, 11-23.

SAKAI H., DES MARAIS D. J., UEDA A., and MOORE J. G. (1984) Concentrations and isotope ratios of carbon, nitrogen and sulfur in ocean-floor basalts. *Geochim. Cosmochim. Acta* **48**, 2433-2441.

SEEWALD J. S., CRUSE A. M., and SACCOCIA P. (2002a) Aqeous volatiles in hydrothermal fluids from the Main Endeavour Field, northern Juan de Fuca Ridge: Temporal variability following earthquake activity. *submitted to Earth and Planetary Science Letters.*

SEEWALD J. S., DOHERTY K. W., HAMMAR T. R., and LIBERATORE S. P. (2002b) A new gas-tight isobaric sampler for hydrothermal fluids. *Deep-Sea Res. I* **49**.

SEYFRIED W. E., JR. and BISCHOFF J. L. (1979) Low-temperature basalt alteration by seawater: an experimental study at 70°C and 150°C. *Geochim. Cosmochim. Acta* **43**, 1937-1947.

SEYFRIED W. E., JR. and BISCHOFF J. L. (1981a) Experimental seawater-basalt interaction at 300°C, 500 bars, chemical exchange, secondary mineral formation and implications for the transport of heavy meatals. *Geochim. Cosmochim. Acta* **45**, 135-147.

SEYFRIED W. E., JR. and BISCHOFF J. L. (1981b) Experimental seawater-basalt interaction at 300°C, 500 bars: Chemical exchange, secondary mineral formation and implications for the transport of heavy metals. *Geochimica et Cosmochimica Acta* **45**, 135-149.

SEYFRIED W. E., JR. and DING K. (1993) The effect of redox on the relative mobilities of Cu and Fe in Cl bearing aqueous fluids at elevated temperatures and pressures: An experimental study with application to subseafloor hydrothermal systems. *Geochim. Cosmochim. Acta* **57**, 1905-1917.

SEYFRIED W. E., JR., SEEWALD J. S., BERNDT M. E., DING K., and FOUSTOUKOS D. (2002) Chemistry of hydrothermal vent fluids from the Main Endeavour Field, Northern Juan de Fuca Ridge: Geochemical controls in the aftermath of June 1999 seismic events. *submitted to Journal of Geophysical Research.*

SHIPBOARD SCIENTIFIC PARTY. (1992) Site 855. In *Proceedings of the Ocean Drilling Program, Initial Results* **139** (ed. E. E. Davis, M. J. Mottl, A. T. Fisher, and et al.), pp. 101-160.

SHIPBOARD SCIENTIFIC PARTY. (1998a) Middle Valley: Bent Hill Area (Site 1035). In *Proc. ODP, Init. Rept.* **169** (ed. Y. Fouquet, R. A. Zierenberg, D. J. Miller, and et al.), pp. 35-152.

SHIPBOARD SCIENTIFIC PARTY. (1998b) Middle Valley: Dead Dog Area (Site 1036). In *Proc. ODP, Init. Rept.* **169** (ed. Y. Fouquet, R. A. Zierenberg, D. J. Miller, and et al), pp. 153-203.

TOULMIN P., III and BARTON P. B., JR. (1964) A thermodynamic study of pyrite and pyrrhotite. *Geochim. Cosmochim. Acta* **28**, 641-671.

VON DAMM K. L., EDMOND J. M., GRANT B., MEASURES C. I., WALDEN B., and WEISS R. F. (1985) Chemistry of submarine hydrothermal solutions at 21°N, East Pacific Rise. *Geochim. Cosmochim. Acta* **49**, 2197-2220.

VON DAMM K. L., OOSTING S. E., KOZLOWSKI R., BUTTERMORE L. G., COLODNER D. C., EDMONDS H. N., EDMOND J. M., and GREBMEIER J. M. (1995) Evolution of East Pacific Rise hydrothermal vent fluids following a volcanic erruption. *Nature* **375**, 47-50.

WOLERY T. J. (1992) *EQ3NR, A Computer Program for Geochemical Aqueous Speciation-Solubility Calculations: Theoretical Manual, User's Guide, and Related Documentation (Version 7.0).* Lawrence Livermore National Lab.

WOLERY T. J. and DAVELER S. A. (1992) *EQ6, A Computer Program for Reaction Path Modeling of Aqueous Geochemical Systems: Theoretical Manual, User's Guide, and Related Documents.* Lawrence Livermore National Lab.

ZIERENBERG R. A. (1994) Data Report: Sulfur content of sediment and sulfur isotope values of sulfide and sulfate minerals from Middle Valley. In *Proc. ODP, Sci. Results* **139** (ed. M. J. Mottl, E. E. Davis, A. T. Fisher, and J. F. Slack), pp. 739-748.

ZIERENBERG R. A., FOUQUET Y., MILLER D. J., BAHR J. M., BAKER P. A., BJERKGÅRD T., BRUNNER C. A., GOODFELLOW W. D., GRÖSCHEL-BECKER H. M., GUÈRIN G., ISHIBASHI J., ITURRINO G., JAMES R. H., LACKSCHEWITZ K. S., MARQUEZ L. L.,

NEHLING P., PETER J. M., RIGSBY C. A., SCHULTHEISS P., III W. C. S., SIMONEIT B. R. T., SUMMIT M., TEAGLE D. A. H., URBAT M., and ZUFFA G. G. (1998) The deep structure of a sea-floor hydrothermal deposit. *Nature* **392**, 485-488.

ZIERENBERG R. A. and MILLER D. J. (2000) Overview of Ocean Drilling Program Leg 169: Sedimented Ridges II. In *Proceedings of the Ocean Drilling Program, Scientific Results* **169** (ed. W. R. Normark), pp. 1-39.

CHAPTER 5. COMPARISON OF THE ORGANIC GEOCHEMISTRY OF VENT FLUIDS FROM THE MAIN ENDEAVOUR FIELD AND MIDDLE VALLEY, NORTHERN JUAN DE FUCA RIDGE

ABSTRACT

Although the Main Endeavour Field is hosted in a sediment-free ridge-crest environment, previously measured high concentrations of NH_3 and isotopically light CH_4 relative to other bare-rock sites suggest that the chemical composition of these fluids is affected by sub-seafloor alteration of sedimentary material (LILLEY et al., 1993). In contrast, at Middle Valley, located approximately 70 km to the north of the Main Endeavour field (MEF), vent fluids pass through up to 1.5 km of hemipelagic and turbiditic sediment prior to venting at the seafloor. The concentrations of organic compounds in the MEF fluids are less than those observed in fluids from Middle Valley, but are elevated compared to many other bare-rock vent sites. Compared to Middle Valley, the MEF fluids are enriched in methane over the longer-chained (C_2-C_3) alkanes, and the C_1-C_3 alkanes are characterized by isotopically heavier stable carbon compositions. These trends are consistent with a greater degree of post-generation alteration of the aqueous organic compounds at the MEF as compared to the Middle Valley sites. Ethane in the MEF fluids is more enriched, relative to the co-existing propane, suggesting that the degradation of the longer-chained alkanes proceeds via a stepwise oxidation reaction mechanism. Temperatures calculated from assumed equilibrium between aqueous alkene, alkane and hydrogen concentrations are similar to those estimated from inorganic chemical proxies of subsurface reaction zone conditions. Higher calculated oxygen fugacities in the Endeavour reaction zone allow this reaction mechanism to proceed faster at Endeavour than at Middle Valley. Endeavour fluids are characterized by higher benzene/toluene ratios than the Middle Valley fluids, consistent with a greater degree of alteration. Thermodynamic calculations indicate that there is no drive for the abiotic formation of the alkanes from carbon dioxide via Fisher-Tropsch type reactions, consistent with a hypothesized as-yet-unobserved sedimentary source for the organic compounds. NH_4 concentrations indicate that this source is on the scale of the whole field, rather than being localized to individual vent structures. Despite a large drive for methane oxidation to occur both at the seafloor and in the subsurface reaction zone, methane and carbon dioxide do not equilibrate chemically or isotopically at Endeavour. This is in contrast to Middle Valley where chemical and isotopic equilibrium do apparently occur between carbon dioxide and methane. This difference is likely due to the late-stage addition of magmatic CO_2 to fluids prior to upflow. Insufficient residence time following this addition likely precludes the attainment of chemical and isotopic equilibrium.

5.1. INTRODUCTION

Hydrothermal activity at mid-ocean ridges is a key mechanism by which heat and material is transferred from the crust to seawater. The fluxes of chemical species from high-temperature ridge-axis hydrothermal vents is proposed to be an important component in balancing the seawater budgets of such elements as P, S and Fe (ELDERFIELD and SCHULTZ, 1996). Since the discovery of the first hydrothermal vents at the Galapagos spreading center in 1977 (CORLISS et al., 1979), over 40 different vent sites have been identified at locations that span the globe (e.g., BUTTERFIELD, 2000; HANNINGTON et al., 2001; KELLEY et al., 2001b; VON DAMM, 1995). In the past 30 years, the key physical and chemical processes that regulate the major inorganic chemical species in hydrothermal vent fluids have been fairly well established (VON DAMM, 1995). However, there is little information regarding the composition and abundance of most aqueous organic species in vent fluids from mid-ocean ridge environments. Methane concentrations and stable carbon isotopic compositions have been measured in fluids collected from several venting sites, while the concentrations of higher hydrocarbons (C_2-C_4) have been measured at only four sites (Table 5-1 and references therein). A majority of the samples utilized in previous analyses were collected in non-gas-tight samplers, which can lead to large uncertainties in the reported concentrations of volatile and semi-volatile species. Organic compounds can play a key role in many processes occurring at mid-ocean ridges, such as the formation of massive sulfide deposits (CRUSE and SEEWALD, 2001; DISNAR and SUREAU, 1990, and references therein) and represent food and energy sources for the large and diverse biological communities that inhabit hydrothermal vent environments (HESSLER and KAHARL, 1995). Knowledge of the abundance of organic species and the processes that control their distributions in vent fluids is key before we can begin to evaluate their importance in crustal alteration and ore formation processes, in the origin and maintenance of life at hydrothermal vent communities, and the effects of hydrothermal venting on global biogeochemical cycles.

The Main Endeavour field (MEF), located on the northern Juan de Fuca Ridge (Fig. 1-4), has been the focus of extensive research over the last 20 years. Despite its

setting on basaltic crust, elevated CH_4, NH_4, Br and B concentrations and light (<-45‰) CH_4 carbon isotopic compositions have been suggested as evidence that the fluids are interacting with a buried organic carbon-bearing sedimentary source during convection (BUTTERFIELD et al., 1994; LILLEY et al., 1993; YOU et al., 1994). However, the location and composition of this sediment remains unconstrained. The MEF lies approximately 70 km to the south of Middle Valley, where the ridge-axis is overlain by up to 1.5 km of hemipelagic and turbiditic sediment. The organic compounds in Middle Valley fluids are derived from the alteration of this sedimentary organic matter, and the aqueous abundances are further altered by post-generative secondary degradation reactions (Chapter 3, this thesis). There is evidence that the presence of organic compounds in the Middle Valley vent fluids directly affects the inorganic chemical species in the fluids, specifically H_2. By comparing the distribution and abundances of organic compounds in MEF fluids with those from Middle Valley, we can constrain the relative importance of sediment alteration versus other processes (e.g., mantle degassing; abiotic synthesis; fluid-rock interaction) in regulating vent fluid chemistry. Here the abundances and isotopic compositions of low-molecular weight hydrocarbons from samples collected at MEF in 1999 and 2000 are reported. The results from this work can be compared with those from Middle Valley to further explore the reaction mechanisms that control the distributions of organic compounds at high temperatures and pressures.

5.2. EXPERIMENTAL

5.2.1. Geologic Setting

The MEF is located on the Endeavour Segment of the Juan de Fuca Ridge at 47°57'N and 129°05'W, approximately 70 km south of Middle Valley. The ridge in this location is spreading at an intermediate rate of 30 mm/year (half rate;KARSTEN et al., 1986), and is characterized by a well-developed axial rift valley 500-1000 meters wide with 100-150 m high walls. This segment of the ridge is characterized by a 500 m bathymetric bulge that may be related to the presence of a magma chamber, although seismic reflection and refraction surveys do not find any evidence for a magma chamber

larger than 1 km in width (CUDRAK and CLOWES, 1993; ROHR et al., 1988; WHITE and CLOWES, 1990). There is very little evidence for recent volcanic activity (DELANEY et al., 1992; TIVEY and DELANEY, 1985, 1986), and basalts dredged from the area are approximately twice as old as those from the East Pacific Rise or southern Juan de Fuca Ridge (VOLPE and GOLDSTEIN, 1990). A seismic event interpreted as being caused by amagmatic tectonic activity occurred in June, 1999 (JOHNSON et al., 2000), but subsurface dike intrusion or magma chamber replenishment cannot be ruled out (BOHNENSTIEHL et al., 2001). Sediments accumulate against a 400 m drop in basement located 20 km east of the ridge axis (ROHR, 1994), but no substantial surficial sediments have been observed within the rift valley itself.

The MEF, which covers an area of approximately 200 by 400 meters, is one of five high-temperature vent fields located along the Endeavour segment (KELLEY et al., 2001a). Hydrothermal venting at the MEF was first discovered in 1981 (KINGSTON and DELANEY, 1983), and vent fluid chemistry remained stable from 1984 to 1988 (BUTTERFIELD et al., 1994). Following the seismic activity in June, 1999, large and rapid depletions in Cl were observed in September, 1999, although they rapidly rebounded to pre-earthquake values in 2000 (BUTTERFIELD et al., 1994; SEEWALD et al., 2002a). Mineral precipitation has resulted in the development of at least 15 large (up to 30 m across at the base and up to 20 m high), steep-sided sulfate-sulfide-silica chimneys concentrated near the western axial valley wall (DELANEY et al., 1992; TIVEY and DELANEY, 1986; Fig. 4-1B). Venting at MEF is localized at the intersections of ridge-parallel normal faults and other fracture sets that trend oblique and perpendicular to the ridge axis (DELANEY et al., 1992). A unique feature of chimney formation at the MEF is the development of flanges or ledges that protrude from the edifice walls (DELANEY et al., 1992). These flanges are stabilized by amorphous silica that precipitates from conductively cooled hydrothermal fluids. The high ammonia concentrations in MEF vent fluids serve to buffer in situ pH during cooling thereby promoting silica deposition (TIVEY et al., 1999).

Vent fluid compositions at the MEF exhibit an along-field gradient, with chlorinities increasing from the southwest to the northeast and volatile concentrations decreasing along the same trend (BUTTERFIELD et al., 1994; SEEWALD et al., 2002a). Chlorinities less than seawater, maximum measured exit temperatures greater than 400°C, and two-fold enrichments in volatile concentrations in fluids with the lowest chlorinities have been used as evidence by Butterfield et al. (1994) for phase separation and brine segregation deep in the system and during upflow. Seewald et al. (2002a) examined time series data of aqueous volatiles and developed a model in which differences in vent fluid chemistry are due to mixing of various fractions of hydrothermal fluids of seawater chlorinity with a low-salinity vapor generated during phase separation at near-critical conditions. We sampled high temperature vent fluids from 7 or 8 different vent structures in the MEF: Hulk, Dante, Bastille, Cantilever and Sully in 1999; Hulk, Dante, LOBO, S&M and a vent located on or near Bastille in 2000 (Fig. 1-4). The vent located on or near Bastille may potentially be Bastille, Peanut or Needle; an unequivocal identification is not possible due to difficulties with the navigation during that dive, so this vent is referred to as PNB throughout this paper. Measured exit temperatures were typically between 340-382°C, which are in agreement with past observations (BUTTERFIELD et al., 1994; Table 4-2). A temperature of 120°C was measured in a flange pool at Hulk, but is not representative of the temperature of the black smoker chimney fluid that was venting from the top of the chimney structure.

5.2.2. Sample Collection

Vent fluid samples were collected using isobaric gas-tight fluid samplers that maintain the fluid at seafloor pressures while subsamples are withdrawn through a micrometering valve (SEEWALD et al., 2002b). In 1999, additional samples were also taken from some vents using the non-gas-tight 755 mL titanium syringe bottles commonly referred to as the "major" samplers (EDMOND et al., 1992; VON DAMM et al., 1985a). Only one gas-tight sampler was available for use in 1999. However, in 2000, each vent was sampled in triplicate with gas-tight samplers. For vents characterized by both chimney and flange style venting, fluids from both types of orifices were collected if

sufficient samplers were available. Temperatures were measured using the *Alvin* high temperature probe and zero-point corrected by 2°C, taking into account the cold-junction temperature.

Utilizing a comprehensive analytical strategy, we determined the concentrations of a range of volatile, semi-volatile and non-volatile organic and inorganic aqueous species for each vent fluid sample. Samples for H_2, CH_4, H_2S and pH (25°C) were withdrawn into glass gas-tight syringes and analyzed onboard ship. Fluid aliquots for the determination of CO_2 were stored in evacuated 30 mL culture tubes that had been previously combusted at 400°C and sealed with butyl rubber stoppers. In 2000, a subset of the culture tubes for CO_2 collection were pre-spiked with $HgCl_2$. No difference in measured CO_2 concentrations was detected between Hg-treated and untreated samples, indicating that microbial processes did not affect the sampled fluids during storage. In 1999, $HgCl_2$ poisoned culture tubes were also utilized for the low-molecular weight organic compounds (methane, ethene, ethane, benzene). In 2000, samples for determining the aqueous concentrations and isotopic composition of CO_2, C_1-C_3 alkanes, benzene and toluene were withdrawn into evacuated 6 mm or 9 mm ID Pyrex® glass tubes fitted with gas-tight valves. After filling, the tubes were stored in water at 5°C until analysis at WHOI. Samples for the determination of Cl, Mg, and NH_3 were stored in acid-cleaned polyethylene bottles at 5°C.

5.2.3 Sample Analysis

Concentrations of CO_2 in 1999 and 2000 and of methane, ethene, ethane and benzene in 1999 were determined by adding 5 mL of 25% phosphoric acid to the fluid in the culture tube and then sparging the headspace gas into a purge and trap device interfaced to a HP 5890 Series II gas chromatograph (GC) that utilized a Porapak-Q packed column and thermal conductivity (TCD) and flame ionization (FID) detectors connected in series. Helium was utilized as carrier gas, and the oven was programmed at 50°C for 3 minutes, ramped at 10°C/min to 100°C, at 12 °C/min to 160°C, 16°C/min to 240°C, and held there for 2 minutes. Estimated uncertainties for the 1999 analyses are $\leq$ 10% for CO_2 and ethene, $\leq$ 15% for benzene, and $\leq$ 5% for ethane.

In 2000, the C_2-C_4 alkanes, benzene and toluene were quantified using a purge-and-trap method with the same GC conditions as for the CO_2 analyses, except that the final hold time was extended to 12 minutes. Samples were also analyzed for aqueous ethene, propene and toluene concentrations on an HP 6890 GC using a purge-and-trap device interfaced to an AT-Q capillary column. The initial setpoint for the GC oven was 10°C, and was held there for 4 minutes to allow all of the gas from the purge and trap device to be swept onto the column. Thereafter, the oven temperature was raised at 10°C/min to 240°C, and held there for 8 minutes. The column flow rate was controlled by a constant flow regulator, which was adjusted to deliver the carrier gas at 26 psi when the oven was at 10°C. Analytical accuracy for the hydrocarbon gases ranged from $\pm$5% for ethane, and propane to $\pm$10% for ethene, propene, benzene and toluene.

The stable carbon isotopic composition of CO_2, the C_1-C_3 alkanes and benzene were quantified using GC-isotope ratio monitoring mass spectrometry (GC-IRMS). The GC-IRMS system consisted of a HP 6890 GC with a capillary AT-Q column, interfaced to a Finnigan MAT Delta Plus mass spectrometer via an oxidation furnace consisting of Ni, Pt and Cu wires held at 940°C. Because of the several orders of magnitude differences in concentrations between CO_2, CH_4 and the other species of interest, two different injection techniques and GC conditions were used. Fluid and headspace gas from the glass tubes were first withdrawn into a 100 mL glass gas-tight syringe that was preloaded with 5 mL 25% phosphoric acid. The syringe was fitted with a septum adaptor, allowing smaller subsamples (100 µL to 1 mL) of headspace gas to be withdrawn into a second glass gas-tight syringe for direct injection onto the GC column for the CO_2 and CH_4 analyses. The oven was initially held at 40°C for five minutes, and then ramped at 75°C/min to 240°C, and held for 5.84 minutes. After analyses of CO_2 and CH_4 (typically 2 to 3 replicates), 10 mL of approximately 25% NaOH was added to the fluid in the 100 mL syringe to remove the CO_2 from the headspace. The remaining headspace gas was then transferred to a 10 mL glass gas-tight syringe. Aliquots of this gas, ranging from 25 µL to 5 mL, depending on the hydrocarbon and aromatic concentrations in the sample, were initially cryogenically trapped on deactivated Si beads

in a 1/8" OD, 0.085" ID stainless steel tube and then refocused on the head of the column at -30°C. The oven temperature was then ramped at 50°C/min to 40°C, held for 3 minutes, ramped to 240°C at 10°C/min and held there for 2 minutes. The stable carbon isotopic composition of the gases is reported using standard delta notation, where $\delta^{13}C$ is expressed in permil (‰) units, and is calculated as the relative difference in the $^{13}C/^{12}C$ ratio of the sample, R_S, and the Vienna PDB (VPDB) standard (R_{VPDB}; $^{13}C/^{12}C$ = 0.011180; ZHANG and WEN-JUN, 1990):

$$\delta^{13}C\,(‰) = \left[\frac{R_S - R_{VPDB}}{R_{VPDB}}\right] * 1000. \qquad (1)$$

The GC-IRMS precision (1σ) was 0.8‰ for CO_2 and CH_4 and 0.5‰ for the C_2-C_6 alkanes. Because the concentrations of the hydrocarbons and benzene are effectively zero in ambient seawater, the measured isotopic values for each sample reflect the composition of the species in the endmember hydrothermal vent fluid. Entrained seawater, however, has a carbonate alkalinity concentration of 2.33 meq/kg fluid, that must be accounted for in measured carbon isotopic values. The $\delta^{13}C$ of the CO_2 in the endmember hydrothermal fluid was calculated via an isotopic mass balance:

$$\delta^{13}C_{HT} = [\delta^{13}C_M C_M - (\delta^{13}C_{SW} C_{SW}(1-f))]/[C_{HT}(f)], \qquad (2)$$

where C is the measured concentration of CO_2, f refers to the fraction of hydrothermal fluid in the sample as calculated from the Mg data, and the subscripts HT, M and SW refer to the hydrothermal, measured and seawater components, respectively. For each vent, at least two aliquots of fluid were analyzed, one from each of the two gas-tight samplers when possible. All analyses were averaged to give a single carbon isotopic composition for the different compounds for each vent, which is reported in Table 5-3. For most compounds, the standard deviation between the two different gas-tight samplers was less than 0.8‰ (Table 5-3).

5.3. RESULTS

Because fluid samplers have a finite dead volume that is filled with bottom seawater prior to deployment, and seawater entrainment occurs to varying degrees during sampling, the fluid that is collected represents a mixture between seawater and hydrothermal vent fluid. Laboratory experiments have demonstrated near quantitative removal of Mg from seawater during hydrothermal seawater-basalt interaction at temperatures, pressures and water/rock ratios that exist in ridge-crest hydrothermal systems (BISCHOFF and DICKSON, 1975; MOTTL and HOLLAND, 1978; SEYFRIED and BISCHOFF, 1981). Therefore, the composition of endmember hydrothermal vent fluids is calculated by extrapolating the concentrations of individual species to zero Mg using linear least squares regression of vent fluid and seawater compositions (VON DAMM et al., 1985a; 1985b). Calculated endmember concentrations are reported in Table 5-2 for each vent and plots of individual species versus Mg are shown in Figure 5-1. For most of the vents at least one fluid sample had a measure Mg concentration < 20 mmol/kg, indicating less than 40% seawater entrainment, which reduces the uncertainty associated with the extrapolation calculations. The exception is Sully vent, for which the gas-tight sample consisted almost entirely of entrained seawater leading to large uncertainties in the extrapolated endmember concentrations of the volatile species. The results from this vent should therefore be interpreted with caution.

5.3.1. Hydrocarbon Distributions

In 1999, only methane, ethane and benzene were quantified due to concerns of contamination of propane and the C_4 isomers (1-butene, n-butane and iso-butane) from the butyl rubber stopper used to seal the culture tubes. For both years, methane is elevated relative to concentrations observed in other bare-rock vent sites, and ethane concentrations are an order of magnitude higher than those measured in fluids from Kolbinsky and Grimsey vent fields on the Kolbeinsey Ridge, near Iceland, where fluids interact with sediments observed on the seafloor (BOTZ et al., 1999; Tables 5-1 and 5-2;). Within a single vent, alkane concentrations decrease with increasing chain length (Table 5-2; Fig. 5-2A). For example, concentrations of methane, ethane and propane in Hulk in

2000 were 1500, 2.75, and 0.132 μmol/kg fluid, respectively (Table 5-2). The enrichment in methane is quantified by the ratio $C_1/(C_2+C_3)$ [or C_1/C_2 for 1999], which ranges from 518-773 (Table 5-2). An exception is Sully vent in 1999, which had a C_1/C_2 ratio of only 106, although as discussed above, high uncertainty is associated with volatile endmember concentrations calculated for this vent. Ethene concentrations range from 14-62 nmol/kg fluid (1999) and 3-15 nmol/kg fluid (2000; Table 5-2; Fig. 5-2B). In 2000, the C_4 isomers were identified at trace levels that were too low to quantify.

Benzene concentrations are slightly elevated in the 2000 samples relative to the 1999 samples, ranging between 1.4 and 3.0 μmol/kg fluid and 1.3 to 3.7 μmol/kg fluid, respectively (Table 5-1; Fig. 5-3C). Toluene concentrations in the 2000 samples are approximately 0.02 mmol/kg fluid in all samples, one to two orders of magnitude less than the concentrations in Middle Valley fluids (Table 5-2; Fig. 5-2C).

5.3.2. $\delta^{13}C$

The $\delta^{13}C$ values for methane in MEF fluids collected in 2000 range between -49.3 to –50.5‰ (Tables 5-1 and 5-3), similar to the results reported by Lilley et al. (1993). Ethane and propane are enriched relative to methane, ranging between –14.4 to –16.3‰ and –17.0 to –19.4‰, respectively, while benzene has an isotopic composition of ~22.5‰ in all vent fluids (Table 5-3). Calculated isotopic compositions for the endmember CO_2 range between –4.9 to –6.7‰, similar to values reported for magmatic CO_2 (SHANKS et al., 1995).

5.4. DISCUSSION

5.4.1. Reaction Mechanism for Organic Matter Alteration

The concentrations of C_1-C_3 alkanes in the MEF fluids are among the highest measured at bare rock sites, although they are approximately an order of magnitude lower than those observed at Middle Valley (Table 5-1 and 5-2; Fig. 5-2A). The C_1-C_3 alkane concentrations decrease with increasing chain length, similar to the pattern observed at Middle Valley (Fig. 5-2A), although the relative enrichment of methane over the longer alkanes is much greater at MEF. Calculated $C_1/(C_2+C_3)$ [or C_1/C_2 for the 1999 fluid

samples] ratios at MEF range between 508 and 773, whereas the maximum values at Middle Valley were 76 and 244 for the Dead Dog and ODP Mound fields, respectively (Table 5-2; Chapter 3, this thesis). The $\delta^{13}C$ values of methane from MEF, which range from –49.3 to –51.5‰, are depleted in comparison to methane isotopic compositions measured in fluids from other bare rock sites (Table 5-1 and references therein). However, the $\delta^{13}C$ values of methane from MEF are enriched in ^{13}C as compared to fluids from Middle Valley which had $\delta^{13}C$ values ranging from –55.5 to –53.3‰ at the Dead Dog field and from -53.0 to –50.8‰ at the ODP Mound field (Chapter 3, this thesis; Table 5-3). The C_1/C_2+C_3 ratios and $\delta^{13}C$ of methane in the MEF vent fluids plot along the same trend of increasing $\delta^{13}C$ of methane with increasing C_1/C_2+C_3 ratios observed for fluids from the Dead Dog and ODP Mound fields from Middle Valley (Fig. 5-3A). This trend reflects increased alteration of sedimentary-derived aqueous organic compounds due to either higher redox conditions in the MEF subsurface reaction zone or higher reaction zone temperatures as compared to Middle Valley (Chapter 3, this thesis).

Aqueous organic compounds continue to undergo secondary reactions following their generation from a sedimentary source. When ethane and other longer chained alkanes undergo these degradation reactions, ^{12}C-^{12}C bonds will be preferentially broken relative to ^{12}C-^{13}C bonds. This can result in methane that is isotopically lighter than the precursor compounds, but heavier than methane already present in the fluid. Accordingly, increases in the $C_1/(C_2+C_3)$ ratio caused by increased organic alteration may be accompanied by heavier ^{13}C values for the aqueous methane (Fig. 5-3A). Because ^{12}C bonds are preferentially broken during alteration reactions, the $\delta^{13}C$ of the residual pool of C_{2+} alkanes also must increase with increasing extent of alteration. This trend is clearly observed in the ethane and propane data, with isotopic compositions in the MEF fluids enriched in ^{13}C by ~6‰ compared to the Middle Valley fluids (Fig. 5-3B). The isotopic composition of propane in the MEF fluids has more scatter associated with it, but also trends toward heavier isotopic compositions with increasing $C_1/(C_2+C_3)$ ratio relative to the Middle Valley fluids (Fig. 5-3B).

The enriched $\delta^{13}C$ of ethane in the MEF fluids relative to the co-existing propane may provide diagnostic evidence to identify the reaction mechanism of organic matter alteration in these fluids. In traditional models for the alteration of longer-chained hydrocarbons, degradation is hypothesized to occur via thermal cracking (HUNT, 1996; TISSOT and WELTE, 1984; WAPLES, 1984). Thermal cracking refers to the homolytic cleavage of C-C bonds caused by higher bond vibration frequencies in response to increasing temperature. In this case, the carbon isotopic composition of ethane found in sedimentary basins associated with gas generation, and at Middle Valley, is depleted to or equal to that of longer-chained alkanes (JAMES, 1983; MANGO, 1997; SHERWOOD LOLLAR et al., 1993; Fig. 5-3B). Alternatively, Seewald (2001) has proposed that the decomposition of aqueous low molecular weight hydrocarbons can proceed via a stepwise oxidation reaction mechanism in which alkanes undergo oxidation and hydration reactions with alkenes, alcohols, ketones and organic acids produced as reaction intermediaries. Degradation of C_{3+} alkanes results in the accumulation of ethane in the residual pool of remaining product. Because of this accumulation, the isotopic composition of the remaining ethane becomes heavier with increasing extent of reaction relative to longer-chained alkanes, as observed in the MEF fluids.

Within the stepwise oxidation reaction mechanism, the relative abundances of several compounds are regulated by metastable thermodynamic equilibrium (SEEWALD, 2001). The first step in the oxidative degradation of hydrocarbons is the formation of alkenes from alkanes, in amounts regulated by metastable thermodynamic equilibrium:

$$\underset{\text{ethene}}{C_2H_{4(aq)}} + H_{2(aq)} = \underset{\text{ethane}}{C_2H_{6(aq)}} \qquad (3)$$

$$\underset{\text{propene}}{C_3H_{6(aq)}} + H_{2(aq)} = \underset{\text{propane}}{C_2H_{8(aq)}} \qquad (4).$$

(SEEWALD, 1994, 1997; SEEWALD, 2001). If equilibrium is attained in natural settings, the concentrations of these compounds will be indicative of the pressure/temperature conditions at the point of last equilibration in the subsurface. Subsurface reaction zone depths are not well constrained at MEF given the lack of seismic evidence for an axial

magma chamber which would represent a maximum depth for fluid circulation (CUDRAK and CLOWES, 1993; ROHR, 1994; WHITE and CLOWES, 1990). Seismic reflection profiles taken across the Endeavour Segment indicate that the base of the sheeted dike complex lies at a depth of ~2 km below the seafloor (CUDRAK and CLOWES, 1993). If this marks the maximum depth of hydrothermal circulation, this corresponds to a pressure of 420 bars, assuming a hydrostatic pressure gradient. Dissolved Si and Cl concentrations, and aqueous volatile concentrations are consistent with subsurface reaction zone conditions of 300-350 bars and 380-420°C at MEF (SEEWALD et al., 2002a; SEYFRIED et al., 2002). Calculated equilibrium temperatures for these reactions at 350 bars ranges from 399-437°C for ethene-ethane equilibrium, and 404-408°C for propene-propane equilibrium (Fig. 5-4A, B). The temperatures estimated from Reactions 3 and 4 are the same as estimates derived from inorganic chemical species, and is consistent with the attainment of equilibrium among the alkenes, alkanes and H_2 in the subsurface reaction zone. The estimated temperatures are also very similar for both years, regardless of the differences in endmember Cl concentrations caused by near-critical phase separation (SEEWALD et al., 2002a).

The estimated subsurface reaction zone conditions at MEF are equal to or slightly higher than the temperatures of 395°C estimated for the ODP Mound field reaction zone at 280 bars (Chapter 3, this thesis). Given this similarity in temperature, it seems unlikely that this is the factor leading to a greater extent of organic alteration in the fluids at MEF. Therefore, the greater extent of alteration could reflect longer residence times of the organic-bearing fluids at elevated temperatures at MEF relative to the ODP Mound field. Another possibility is that the alteration reactions occur faster at MEF. The rate of redox-dependent degradation reactions, such as Reactions 3 and 4, was found to be faster in experiments where the redox conditions were buffered by the relatively oxidizing hematite-magnetite-pyrite (HMP) mineral buffer as compared to the more reducing pyrite-pyrrhotite-magnetite (PPM) buffer. This was hypothesized to be a consequence of the catalytic activity of aqueous sulfur species of intermediate oxidation states, the concentrations of which are strongly dependent on the redox state of the fluid (SEEWALD,

2001). Aqueous H_2 concentrations are an excellent indicator of redox conditions due to the rapid rate of equilibration for the reaction:

$$H_2O_{(l)} = H_{2(aq)} + ½\ O_{2(g)} \qquad (5)$$

Values of fO_2 for reaction zone conditions at MEF and the ODP Mound field calculated from the measured endmember aqueous H_2 concentrations and thermodynamic data included in the SUPCRT92 database (JOHNSON et al., 1992) reveal that the subsurface reaction zone at MEF is more oxidizing than at Middle Valley (Fig. 5-5). At MEF, mineral phases in the basaltic crust serve to buffer fluid redox at oxidizing values, leading to degradation of the organic compounds via stepwise oxidation. In contrast, the higher concentrations of reduced organic compounds in Middle Valley fluids regulate fluid redox conditions to lower values, so that stepwise oxidation proceeds at a much slower rate, if at all.

The concentrations of other organic compounds are also affected by oxidative degradation reactions. Aqueous benzene concentrations are comparable to those measured in the ODP Mound at Middle Valley, but toluene concentrations are approximately an order of magnitude lower than those at the ODP Mound field (Fig. 5-2C). Experiments by McCollom et al. (2001) indicate that under hydrothermal conditions toluene reacts rapidly to form benzene via oxidative decarboxylation:

$$\underset{\text{toluene}}{C_6H_5CH_{3(aq)}} + 2\ H_2O \rightarrow \underset{\text{benzene}}{C_6H_{6(aq)}} + CO_{2(aq)} + 3\ H_{2(aq)} \qquad (6)$$

The potential for Reaction 6 to proceed can be assessed by the calculation of the Gibbs free energy of the reaction:

$$\Delta G_{rxn} = \Delta G^\circ - RT\ln Q \qquad (7),$$

where ΔG° is the standard Gibbs free energy of the reaction, R is the universal gas constant, T is the temperature in kelvins and Q is the activity quotient of the compounds involved in the reaction. As shown in Chapter 3, Equation 7 can be recast as:

$$\Delta G_{rxn} = RT\ln(Q/K) \qquad (8),$$

where K is the thermodynamic equilibrium constant for the reaction at the temperature and pressure of interest. The calculated ethene:ethane equilibration temperatures at 350

bars were used to calculate ΔG_{rxn} for the four vents for which toluene was measured. A temperature of 400°C was assumed for S&M vent in the absence of a calculated ethene:ethane temperature. Values for K were obtained from the SUPCRT92 database (JOHNSON et al., 1992). Calculated ΔG_{rxn} values range between –101 and –118 kJ/mol (Fig. 5-6). The persistence of toluene despite such a large drive for the reaction to proceed suggests that equilibrium has not been attained, and may be indicative of relatively short residence times of fluids within subsurface reaction zones. Despite kinetic barriers that may preclude the attainment of equilibrium, the higher benzene:toluene ratios in the MEF fluids relative to Middle Valley fluids are consistent with thermodynamic drives and a greater extent of secondary alteration reactions among the aqueous organic compounds relative to the Middle Valley fluids. McCollom et al. (2001) also found that toluene reacted faster in experiments conducted in the presence of more oxidizing mineral buffers. Therefore, more oxidizing conditions in the Endeavour reaction zone as compared to Middle Valley also promote a greater extent of reaction among benzene and toluene.

5.4.2. Sources of Aqueous Organic Compounds

The hydrocarbon abundances and isotopic compositions reported in this work indicate that the MEF fluids are interacting with a sediment source in the subsurface that remains unconstrained in terms of location and composition. CH_4 and NH_4 abundances and isotopic composition and concentrations of the trace alkali elements (Li, Rb, Cs) and B reported by other workers (BUTTERFIELD et al., 1994; LILLEY et al., 1993; SEYFRIED et al., 2002) are also consistent with this hypothesis.

However, the abiogenic formation of alkanes from carbon dioxide and hydrogen via Fisher-Tropsch type reactions, such as:

$$CO2_{(aq)} + 4H2_{(aq)} = CH4_{(aq)} + 2H2O \quad (9)$$

$$2CO2_{(aq)} + 7H2_{(aq)} = C2H6_{(aq)} + 4H2O \quad (10)$$

$$3CO2_{(aq)} + 10H2_{(aq)} = C3H8_{(aq)} + 6H2O \quad (11)$$

has also been suggested as a possible mechanism for the formation of alkanes in hydrothermal vent fluids (SHOCK, 1990; SHOCK and SCHULTE, 1998). Abiotic synthesis

of methane and other vent fluids has been reported from sites such as Lost City, Rainbow and Menez Gwen, where serpentinization of ultramafic rocks is thought to catalyze the reduction of CO_2 to methane (CHARLOU et al., 2000; HOLM and CHARLOU, 2001; KELLEY et al., 2001b). However, this has not been demonstrated in laboratory experiments. Although Berndt et al. (BERNDT et al., 1996) reported the foramation of hydrocarbons during the serpentinization of olivine, subsequent experiments provided compelling evidence that these hydrocarbons were not synthesized de novo from aqueous CO_2, but were derived from organic compounds already present in the olivine (MCCOLLOM and SEEWALD, 2001).

The potential for abiotic synthesis of alkanes from CO_2 and H_2 in the MEF fluids can be assessed by calculating the Gibbs free energy for Reactions 9-11 above. Thermodynamic equilibrium constants (K) are functions of both temperature and pressure. The ΔG_{rxn} was calculated using thermodynamic data in the SUPCRT92 database (JOHNSON et al., 1992) for two different cases: (1) at the seafloor pressure of 220 bars and measured exit temperatures and (2) at a subsurface reaction zone pressure of 350 bars with temperatures using temperataures calculated from ethene-ethane equilibrium (Fig. 5-4A). A temperature of 400°C was assumed for S&M and Dante vents in the absence of measured ethene concentrations. In all cases, the calculated ΔG_{rxn} was positive (Fig. 5-7), indicating that there is no drive for the formation of C_1-C_3 alkanes from CO_2 in these fluids. Values of K decrease with increasing temperature and pressure, precluding the formation of C_1-C_3 alkanes from CO_2 within the subsurface. This result is consistent with the hypothesis that the organic compounds and NH_3 are derived from interaction with an organic carbon bearing sediment in the subsurface.

The relative amount of sediment-fluid interaction in the MEF fluids as compared to Middle Valley can be assessed with water:sediment ratios calculated from the NH_3 concentrations, assuming that nitrogen is quantitatively removed from the sediments during alteration. The water:sediment ratio is the mass of water which reacts with 1 kg of fresh sediment. The sedimentary source for MEF was assumed to contain 0.06 wt. % N, as is observed in unaltered Middle Valley sediments (GOODFELLOW and PETER, 1994).

For a given year, the calculated water/sediment ratios are relatively constant in all vents (Table 5-4), consistent with a source region on the scale of the whole field (SEEWALD et al., 2002a), rather than local to individual vents. The water:sediment ratios calculated for MEF fluids are ~65 in 1999 and ~85 in 2000, which is elevated compared to the values of ~14 for Dead Dog fluids and 18-20 for the ODP Mound field. The amount of fluid:sediment interaction is therefore only 4-6 times less at MEF than at the Middle Valley vent fields.

Benzene in vent fluids from both regions of venting at Middle Valley (the Dead Dog and ODP Mound fields) and MEF are characterized by the identical isotopic composition (Fig. 5-3C), suggesting that the sediments with which the MEF fluids interact have an organic carbon composition similar to that of the sediments located within Middle Valley. The location of the sediment source, however, remains unconstrained. A layer of sediments compositionally identical to those at Middle Valley could be buried under the vent field (LILLEY et al., 1993). Such a layer has not been imaged on seismic reflection or refraction studies of the region, but estimates made by Lilley et al. (1993) indicate that a sediment layer 1 km^2 in area would have to be only ~4 m thick to support the measured methane concentrations. The concentration and isotopic composition trends in the C_1-C_3 alkanes between fluids collected at Middle Valley and MEF suggest that Dead Dog-ODP Mound-MEF represent a continuum in terms of the extent of secondary degradation reactions, with fluids at the relatively cool Dead Dog field undergoing less alteration than fluids at MEF. The organic geochemical characteristics of ODP Mound fluids are intermediate between these two endmembers. The presence of up to 1.5 kilometers of sediment located at the ridge crest at Middle Valley, approximately 70 km to the northeast, and microearthquake data suggesting that hydrothermal fluid recharge is flowing from north to south for a distance of at least 2 km beneath Middle Valley, raises the intriguing possibility that the Middle Valley sediments themselves, or a buried pond of Middle Valley-like sediments somewhere between the two regions, are the organic carbon source for MEF fluids. A third possibility is that that the organic carbon is not derived from a sediment, but comes from local fauna, such as

tubeworms that inhabit the chimney mounds and flanges and whose tubes are found preserved within the chimney structures themselves (COOK and STAKES, 1995). However, this possibility was discounted by Lilley et al. (1993) based on elevated $\delta^{15}N$ values of aqueous NH_3 (+12.4‰) relative to the average $\delta^{15}N$ for organic nitrogen from vent fauna (-1.2‰). Further evidence against a nitrogen source local to each vent is in the constant water:sediment ratios calculated for MEF vents.

5.4.3. Methane and Carbon Dioxide Isotope Systematics

In contrast to Middle Valley, the $\delta^{13}C$ values of CO_2 measured in MEF fluids in 2000 are relatively enriched in ^{13}C as compared to the Middle Valley fluids, ranging between –4.9 and –6.7‰ (Table 5-3). The $\delta^{13}C$ values of CO_2 are consistent with derivation from both a magmatic as well as seawater source (KROOPNICK, 1985; SHANKS, 2001). However, the high concentrations of CO_2, between 24-100 mmol/kg fluid, cannot be derived from seawater which has a concentration of only 2.3 mmol/kg fluid. Therefore, the enriched $\delta^{13}C$ values indicate that CO_2 at MEF is derived from magmatic degassing processes, in contrast to Middle Valley, where light $\delta^{13}C$ values and thermodynamic calculations indicate that it is derived from oxidation of organic carbon compounds.

Recent work by Horita (2001) demonstrated that in the presence of transition metal catalysts, isotopic equilibrium was achieved between aqueous CO_2 and CH_4 at temperatures ranging between 200-600°C. If isotopic equilibrium between CO_2 and CH_4 in these fluids is assumed, apparent equilibrium temperatures range between 100-150°C, lower than temperatures measured at MEF or calculated using chemical proxies (Fig. 5-9). In the ODP Mound field at Middle Valley, apparent isotopic equilibrium temperatures were between 400-500°C, in good agreement with reaction zone temperatures calculated by other geochemical indicators (Chapter 3, this thesis).

The utility of the CO_2-CH_4 isotopic equilibrium temperature calculations for Middle Valley fluids but not for the MEF derives from the different sources of CO_2 in the two vent fields. At Middle Valley, CO_2 is derived from sediment alteration and from the aqueous methane itself. This presumably allows for sufficient reaction time to attain

chemical and isotopic equilibrium between these two species. At MEF, however, the majority of the CO_2 is derived from a magmatic rather than sedimentary source. Fluids containing aqueous methane from interaction with the sedimentary organic carbon source also contain CO_2 derived from the sedimentary source and or the methane itself. Given the thermodynamic drive for methane oxidation in the MEF fluids, which is hypothesized to promote the attainment of isotopic equilibrium in the Middle Valley fluids, isotopic disequilibrium between magmatic-derived CO_2 and the sedimentary CH_4 in MEF fluids may reflect short residence times of the fluids in the subsurface reaction zones after addition of CO_2, precluding the attainment of isotopic equilibrium. For example, a dike injected into the subsurface could provide a ready source of magmatic CO_2 to hydrothermal fluids shortly prior to venting at the seafloor.

5.4.4. Temporal Variability

The major element chemistry and temperature of the MEF vent fluids were relatively stable over a four-year period in the mid-1980's (BUTTERFIELD et al., 1994). Three months after seismic activity on the MEF segment in June, 1999, measured Cl concentrations decreased dramatically and temperatures and measured CO_2, H_2 and H_2S concentrations increased compared to pre-earthquake values (SEEWALD et al., 2002a). One year later, Cl concentrations had increased compared to 1999 values, while temperature and CO_2, H_2 and H_2S concentrations had decreased. In contrast, CH_4 and NH_4 concentrations have continually decreased since 1988 (SEEWALD et al., 2002a). The changes in the sedimentary-derived compounds reflect either an earthquake-induced change in the subsurface hydrology that reduced the contribution of recharge fluids that interact with sediments, or an exhaustion of the sediment supply with which the organic compounds interact. Temporal variability of other organic compounds can be assessed for Hulk vent for 1999 and 2000 (Fig. 5-9, A-I). In order to remove the effects of phase separation, the concentrations of CH_4, H_2, ethene, ethane, benzene and ammonia were normalized to seawater chloride concentrations. The normalized concentrations of methane and ethane increased by 5-7%, respectively between 1999 and 2000 (Fig. 5-9, C and E). Ammonia and benzene concentrations also increased, but the very dramatic

increases in benzene likely reflect the different analytical techniques used for its measurement in 1999 and 2000 (Fig. 10 G, H). The increases in all of the sediment-derived species suggests that the decrease in concentrations observed from 1988 to 1999 was due to a change in the subsurface hydrology that promoted a greater extent of fluid:basalt interaction as compared to fluid:sediment interaction. However, the increases are not large enough to unequivocally rule out the possibility that lower methane concentrations in 1999 as compared to pre-earthquake values resulted from the exhaustion of the sediment supply.

5.5. CONCLUSIONS

Hydrothermal fluids from the MEF contain some of the highest concentrations of C_1-C_3 alkanes measured in fluids from bare-rock systems. Comparison of the alkane and aromatic distributions and stable carbon isotopic compositions of C_1-C_3 alkanes at MEF and Middle Valley indicate that the organic compounds in MEF fluids have experienced a greater extent of post-generative secondary alteration than fluids from Middle Valley. The organic compounds are likely degraded via the stepwise oxidation reaction mechanism proposed by Seewald (2001). In this mechanism, the rates of redox-dependant oxidation reactions are faster in more oxidative environments. The stable carbon isotopic composition of ethane is enriched in ^{13}C relative to the coexisting propane in MEF fluids, in contrast to nearly identical values in the Middle Valley fluids, consistent with the oxidative degradation of organic compounds at MEF. At MEF, fluid redox is controlled by basaltic rocks, while at Middle Valley, the organic compounds in the fluids regulate redox to lower levels. Therefore, while oxidative degradation occurs in the MEF fluids, it is inhibited at Middle Valley. The first step of the oxidative degradation mechanism is the formation of alkenes in equilibrium with aqueous alkane and hydrogen concentrations. Subsurface reaction zone temperatures calculated for assumed ethene-ethane and propene-propane equilibrium are similar to conditions estimated from other inorganic species (SEEWALD, 2001; SEYFRIED et al., 2002). The

Main Endeavour field offers a clear example of the regulation of the distributions of organic compounds by inorganic minerals and aqueous compounds.

The isotopic systematics and concentrations of the C_1-C_3 alkanes in fluids from the Middle Valley vent fields and the Main Endeavour field represent a continuum of increasing alteration of aqueous organic compounds, with the Dead Dog field fluids having experienced less alteration than the ODP Mound fluids, which, in turn, are less altered than fluids from the MEF. Such a continuum is consistent with somewhat hotter subsurface reaction zone conditions estimated for the MEF as compared to Middle Valley, a greater amount of reaction time at elevated temperatures or more oxidizing conditions in the MEF reaction zone as compared to Middle Valley. Unlike the Middle Valley fluids, however, CH_4 and CO_2 are not in isotopic equilibrium in the MEF fluids. While CO_2 is likely generated from methane oxidation in those MEF fluids that have interacted with a sedimentary source, the vast majority of the CO_2 is derived from magma degassing, which swamps any signal of a sedimentary source in its isotopic composition. The isotopic disequilibrium between CH_4 and CO_2 indicates that the residence time of fluids in the reaction zone following mixing of fluids derived from sediment and basalt interaction is short relative to the kinetics of chemical and isotopic equilibration.

There is abundant chemical evidence for the interaction of the MEF fluids with a sedimentary source in the subsurface. Thermodynamic calculations support the hypothesis that the elevated levels of alkanes in MEF fluids are not derived from abiotic CO_2 reduction in Fisher Tropsch type reactions. Calculated water:sediment fluid ratios using NH_4 concentrations indicate that the organic matter is derived from a fluid source region that is on the same scale as the entire vent field, rather than on the scale of individual vents, as might be expected if vent biota was the source for organic compounds. The similarity of the organic geochemistry of fluids from Middle Valley and MEF suggests the intriguing possibility that sediments within Middle Valley are the source zone for MEF.

Table 5-1. Endmember aqueous hydrocarbon concentrations in mid-ocean ridge hydrothermal vent fluids.

Location*	Temp	Cl	CH_4		C_2H_6		C_3H_8		iso-C_4H_{10}	n-C_4H_{10}	$C_1/(C_2+C_3)$	Ref
	°C	mmol/kg	mmol/kg	‰, PDB	µmol/kg	‰, PDB	µmol/kg	‰, PDB	µmol/kg	µmol/kg		
MAR												
¤Rainbow	360	>750	2.2									1
Broken Spur	356-360	469	0.06									2
Lucky Strike	185-324	417-514	0.3-0.8									3
Menez Gwen	275-284	357-381	1.5-2.1									3
Snakepit	345	559	0.06									4
¤Lost City	40-75	546-549	0.13-0.28									5
EPR												
11°N		327-681	0.06-1.1									6
13°	317-381	712-763	0.03-0.18	-16.5 to –26.4								6-8
21°	273-355	489-579	0.05-0.09	-15.0 to –17.6								9-14
17-19°S	>210-340	190-871	0.008-0.13	-22.0 to –23.9	0.06-0.2		0.007					15
‡Guaymas	100-315	581-637	54									11, 12,14
JdFR												
Middle Valley												
‡Dead Dog	187-281	546-586	18.5-21.6	-53.3 to -55.5	194-232	-20.8 to -21.2	49.9-57.5	-20.3 to -21.0	5.00-6.15	5.58-6.24	70.5-76.1	16
‡ODP Mound	263-272	432-449	5.85-7.07	-50.8 to -53.0	23.2-24.3	-20.6 to -22.7	4.48-4.63	-20.1 to -22.3	0.34-0.36	0.87-1.06	211-245	16
Endeavour Segment												
MEF	120-370	31.8-505	1.7-3.4	-48.4 to -55.0	1.6-28	-14.3 to –16.3	0.06-0.1	-17.0 to –19.4				17-20
Cleft Segment												
Plume	224	1090	0.08	-20.8	0.2		0.05		0.004	0.006		21, 22
KR												
Kolbeinsey†	>100-131		0.06	-32.5 to -52.3	0.29		0.46				73.3	23
Grimsey†	200-250	274	0.02	-26.1 to -29.5	0.28	-15.5 to -16.2	0.02	-13.6 to –17.0		0.02	78.5	22, 24

*MAR: Mid-Atlantic Ridge; EPR: East Pacific Rise; JdFR: Juan de Fuca Ridge; KR: Kolbeinsey Ridge

References: [1]Donval et al. (1997); [2]James et al. (1995) [3]Charlou et al. (2000); [4]Jean-Baptiste et al. (1991); [5]Kelley et al. (2001b); [6]Kim et al. (1984); [7]Merlivat et al. (1987); [8]Michard et al. (1984); [9]Lilley et al. (1983); [10]Welhan and Craig (1983); [11]Seewald et al. (1998); [12]Von Damm (1983); [13]Von Damm et al. (1985a); [14]Von Damm et al. (1985b); [15]Charlou et al. (1996); [16]Chapter 3, this thesis; [17]Butterfield et al. (1994); [18]Lilley et al. (1993); [19]Seewald et al. (2002a); [20]This study; [21]Evans et al. (1988); [22]Von Damm and Bischoff (1987); [23]Botz et al. (1999); [24]Hannington et al. (2001).

†endmember hydrocarbon concentrations calculated for water samples and not gas bubble samples.

¤located on ultramafic rocks where the methane is believed to be derived from serpentinization processes

‡sedimented ridge axis

Table 5-2. Concentrations of aqueous species in vent fluids from the Main Endeavour field, Northern Juan de Fuca Ridge[§].

Vent	Sample	Structure	exit T	Mg	Cl	H_2S	H_2	NH_4	CO_2	CH_4
			°C	mmol/kg	mmol/kg	mmol/kg	mmol/L	μmol/kg	mmol/kg	mmol/L
SEPTEMBER,1999										
Hulk	M-3468-A	Flange	339	32.2	484	2.8	—	—	—	—
	M-3468-B	Flange	339	9.05	438	6.2	—	—	—	—
	M-3468-C	Chimney	341	1.49	422	6.5	—	—	—	—
	M-3468-D	Chimney	341	2.36	433	6.0	—	—	—	—
	BGT-3478	Flange	347	2.82	447	7.0	0.31	—	51	1.4
	Endmember			0	426	7.4	0.33	—	53	1.6
Dante	M-3470-A	Flange	350	13.3	446	7.8	—	472	—	—
	M-3470-B	Flange	350	14.9	457	11	—	437	—	—
	Endmember			0	419	13	—	612	—	—
Bastille	M-3470-C	Ex. Chim.[†]	368	5.84	438	2.2	—	546	—	—
	M-3470-D	Ex. Chim.	368	36.7	398	12	—	215	—	—
	BGT-3470	Ex. Chim.	368	29.0	239	20	0.55	308	55	1.5
	Endmember			0	207	22	0.62	620	61	1.7
Cantilever	M-3474-A	Flange	375	2.43	109	20	—	564	—	—
	BGT-3474	Flange	375	8.11	53.5	24	0.55	625	68	1.7
	Endmember			0	38.6	25	0.70	657	71	1.7
Sully	M-3474-B	Chimney	377	2.49	61.8	19	—	673	—	—
	BGT-3480	Chimney	379	52.9	534	3.6	0.036	19	6	0.061
	Endmember			0	31	20	0.96	705	100	1.7
JULY, 2000										
Hulk	BGT-3591-2	Chimney	n.a.	5.63	484	5.3	0.20	446	26.5	1.4
	BGT-3591-3	Flange	120	35.6	520	1.9	0.083	159	11.9	0.5
	BGT-3591-4	Flange	120	35.6	518	1.7	0.076	155	10.8	0.5
	Endmember			0	477	5.8	0.23	493	29	1.5
Dante	BGT-3590-2	Flange	341	2.58	474	7.3	0.29	495	26.0	1.3
	BGT-3590-3	Flange	341	2.76	463	8.9	0.27	499	23.9	1.3
	BGT-3590-4	Flange	341	2.79	459	7.3	0.28	486	23.9	1.3
	Endmember			0	461	8.3	0.29	520	26	1.4
LOBO	BGT-3592-2	Chimney	n.a.	7.41	468	7.3	0.14	417	20.5	1.2
	BGT-3592-3	Flange	342	14.9	468	5.7	0.25	343	18.0	1.0
	BGT-3592-4	Flange	342	9.77	472	6.8	0.31	413	20.4	1.2
	Endmember			0	452	8.6	0.29	488	24	1.4
S&M	BGT-3593-2	Diff. Flow	40	48.6	521	0.9	0.04	41	4.3	0.11
	BGT-3593-3	Chimney	367	5.12	391	13	0.48	444	31.7	1.5
	BGT-3593-4	Chimney	367	1.62	377	14	0.53	504	32.1	1.7
	Endmember			0	373	14	0.54	506	34	1.7
PNB	BGT-3594-2	Chimney	382	29.7	452	6.0	0.21	228	12.9	0.56
	BGT-3594-3	Chimney	382	5.34	367	13	0.43	432	25.2	1.2
	BGT-3594-4	Chimney	382	28.3	449	6.5	0.23	231	14.0	0.61
	Endmember			0	347	14	0.47	476	27	1.3
BSW[*]			2.1	54.0	543	0	0	1	2.3	0

[§]data previously reported in Seewald et al. (submitted). [*]Bottom seawater. [†]Excavated chimney.

Table 5-2 (continued). Concentrations of aqueous species in vent fluids from the Main Endeavour field, Northern Juan de Fuca Ridge.

Vent	Sample	C_2H_4 nmol/kg	C_2H_6 µmol/kg	C_3H_6 nmol/kg	C_3H_8 µmol/kg	Benzene µmol/kg	Toluene nmol/kg	$C_1/(C_2+C_3)^\dagger$
SEPTEMBER,1999								
Hulk	M-3468-A	—	—	—	—	—	—	
	M-3468-B	—	—	—	—	—	—	
	M-3468-C	—	—	—	—	—	—	
	M-3468-D	—	—	—	—	—	—	
	BGT-3478	58.5	2.74	—	—	1.28	—	
	Endmember	62	2.89	—	—	1.35	—	518
Dante	M-3470-A	—	—	—	—	—	—	
	M-3470-B	—	—	—	—	—	—	
	Endmember	—	—	—	—	—	—	—
Bastille	M-3470-C	—	—	—	—	—	—	
	M-3470-D	—	—	—	—	—	—	
	BGT-3470	38.3	2.17	—	—	1.71	—	
	Endmember	43	2.43	—	—	1.91	—	682
Cantilever	M-3474-A	—	—	—	—	—	—	
	BGT-3474	13.5	2.40	—	—	1.88	—	
	Endmember	14	2.51	—	—	1.97	—	692
Sully	M-3474-B	—	—	—	—	—	—	
	BGT-3480	58.3	1.07	—	—	0.14	—	
	Endmember	2891	53.1	—	—	3.71	—	106
JULY, 2000								
Hulk	BGT-3591-2	12.0	2.44	—	0.12	2.41	12	
	BGT-3591-3	—	1.02	2.38	0.055	0.97	7.4	
	BGT-3591-4	8.6	0.93	2.53	0.045	0.96	10	
	Endmember	13	2.75	7.2	0.13	2.72	14	520
Dante	BGT-3590-2	—	2.51	—	0.12	3.16	—	
	BGT-3590-3	—	2.28	—	0.13	2.52	—	
	BGT-3590-4	—	2.38	—	0.12	2.76	—	
	Endmember	—	2.52	—	0.12	2.97	—	508
LOBO	BGT-3592-2	—	—	—	—	—	—	
	BGT-3592-3	—	—	—	—	—	—	
	BGT-3592-4	21.5	1.94	12.5	0.089	2.29	18	
	Endmember	26	2.38	15	0.11	2.81	22	548
S&M	BGT-3593-2	—	0.18	—	0.007	0.17	2.0	
	BGT-3593-3	—	2.45	—	0.10	—	—	
	BGT-3593-4	—	2.38	3.16	0.092	1.76	—	
	Endmember	—	2.57	3.3	0.10	1.81	23	635
PNB	BGT-3594-2	8.30	0.69	3.0	0.027	0.61	8.4	
	BGT-3594-3		1.37	—	0.050	—	—	
	BGT-3594-4		0.86	—	0.032	—	—	
	Endmember	19	1.57	7	0.057	1.39	19	773
BSW*		0	0	0	0	0	0	—

*Bottom seawater; $^\dagger C_1/C_2$ calculated for 1999 samples.

Table 5-3. Average stable carbon isotopic compositions for aqueous low-molecular weight organic compounds in vent fluids from Main Endeavour Field, northern Juan de Fuca Ridge.

Vent	CO_2[§]		CH_4		C_2H_6		C_3H_8		Benzene		Toluene	
	$\delta^{13}C$ (‰)	1σ (n)[†]	$\delta^{13}C$ (‰)	1σ (n)	$\delta^{13}C$ (‰)	1σ (n)	$\delta^{13}C$ (‰)	1σ (n)	$\delta^{13}C$ (‰)	1σ (n)	$\delta^{13}C$ (‰)	1σ (n)
SEPTEMBER, 2000												
Hulk	-4.9	0.4 (5)	-50.1	0.9 (5)	-16.3	0.4 (3)	-17.0	— (1)	-22.5	0.0 (2)		
Dante	-5.3	0.4 (4)	-50.0	1.2 (13)	-15.5	0.7 (2)	—		-22.5	0.2 (2)		
LOBO	-6.7	0.2 (2)	-50.5	0.9 (10)	-15.2	0.2 (3)	-19.4	— (1)	-22.5	0.2 (3)		
S&M	-5.3	0.2 (5)	-49.3	0.7 (6)	-14.4	0.3 (3)	-17.2	— (1)	-22.3	0.3 (3)		
PNB	-5.2	0.4 (10)	-51.5	0.9 (9)	-14.3	0.8 (4)	-18.9	3.2 (2)	-22.5	0.2 (3)	-28.0	— (1)
BSW	0.6[1]											

[§]The reported $\delta^{13}C$ is the value calculated for the endmember hydrothermal vent fluid, assuming two-component mixing between a seawater endmember containing 2.33 mmol/kg CO_2, with a $\delta^{13}C$ of –0.6‰ and the endmember vent fluid with the calculated CO_2 concentration reported in Table 2.

—: not analyzed.

[†](n): total number of replicate analyses, for all tubes analyzed for a particular vent. 1σ is the standard deviation for all of the analysis averaged together to give a value for a particular vent

[1]Sansone et al. (1998)

Table 5-4. Calculated water/sediment mass ratios* for hydrothermal fluids from Endeavour and Middle Valley.

Vent	W:S
ENDEAVOUR, 1999	
Dante	70.0
Bastille	69.1
Cantilever	65.2
Sully	60.8
ENDEAVOUR, 2000	
Hulk	86.9
Dante	82.4
LOBO	87.8
S&M	84.7
PNB	90.0
DEAD DOG, MIDDLE VALLEY	
Heineken Hollow	14.1
Chowder Hill	13.4
Inspired Mounds	14.9
Puppy Dog	14.3
ODP MOUND, MIDDLE VALLEY	
Shiner Bock	18.2
Spire	18.8
1035H	20.3

*calculated assuming complete mobilization of 0.06 wt% N from sediments

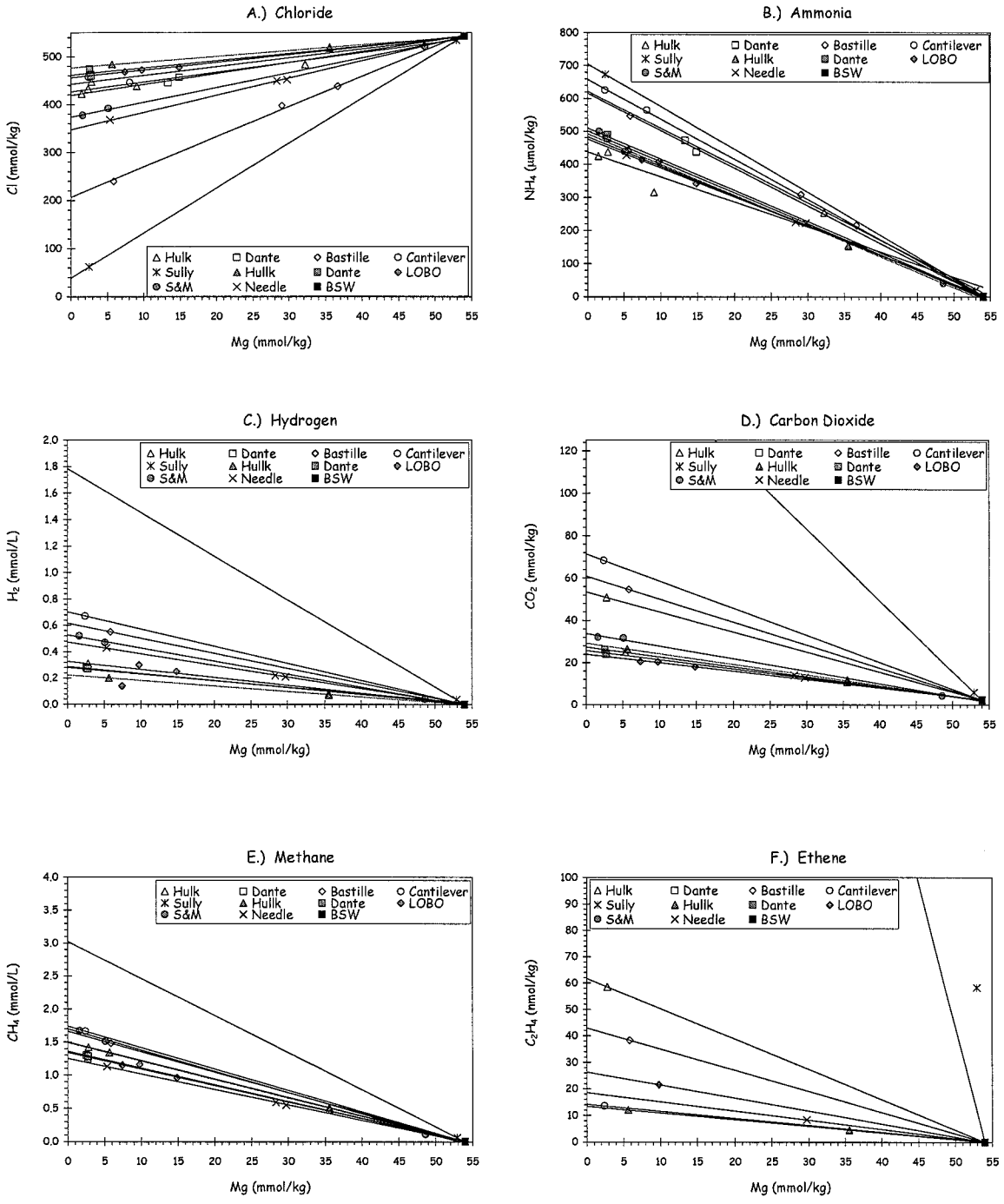

Figure 5-1. Graphs of individual chemical species versus Mg. **(A)** Chloride; **(B)** Ammonia; **(C)** Hydrogen; **(D)** Carbon Dioxide; **(E)** Methane; **(F)** Ethene. 1999 data: white symbols. 2000 data: gray symbols. 1999 data for Cl, NH_4, H_2, CO_2 and CH_4 from Seewald et al. (2002).

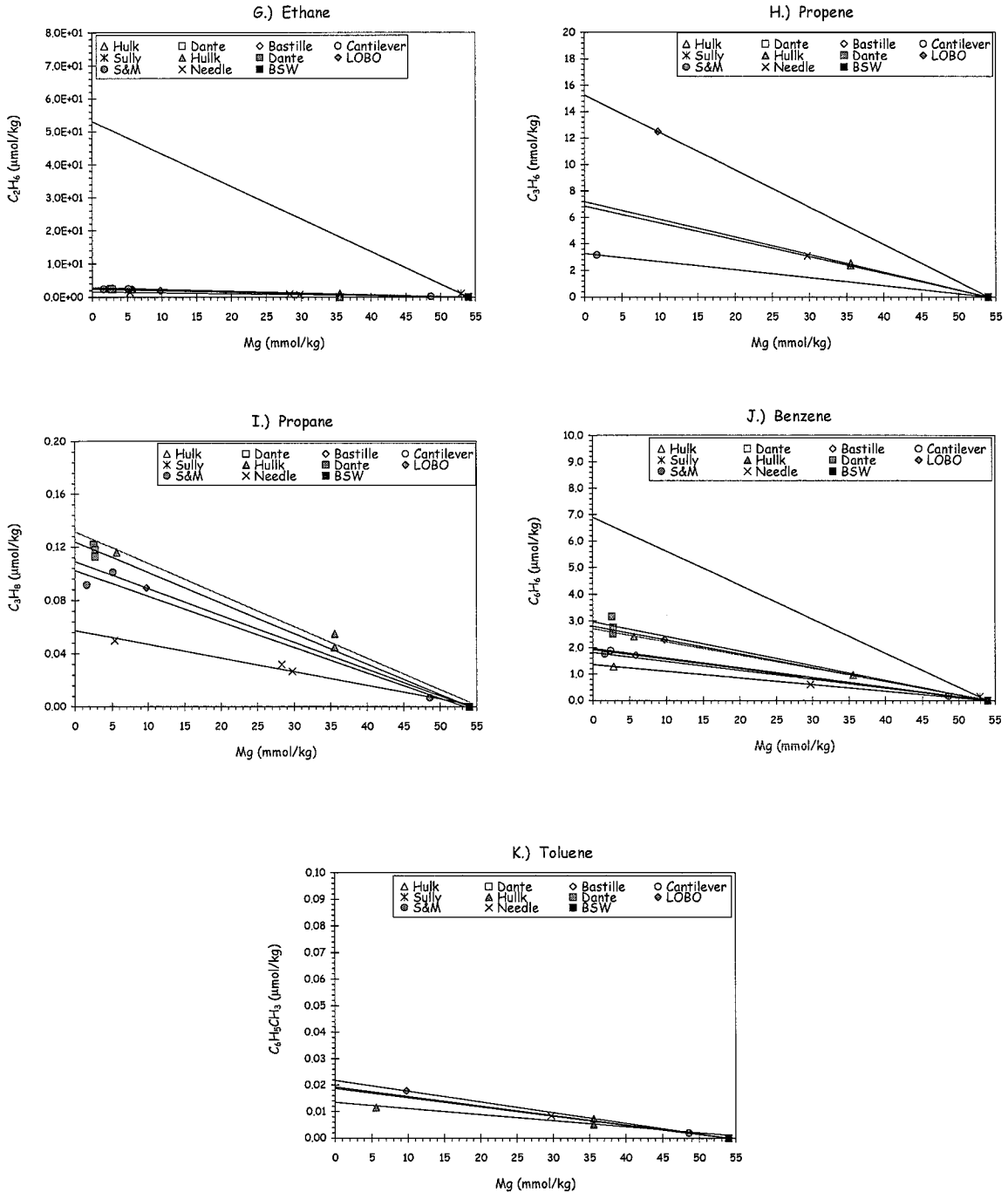

Figure 5-1, continued. **(G)** Ethane; **(H)** Propene; **(I)** Propane; **(J)** Benzene; **(K)** Toluene. 1999 data: white symbols. 2000 data: gray symbols. 1999 data for Cl, NH_4, H_2, CO_2 and CH_4 from Seewald et al. (2002).

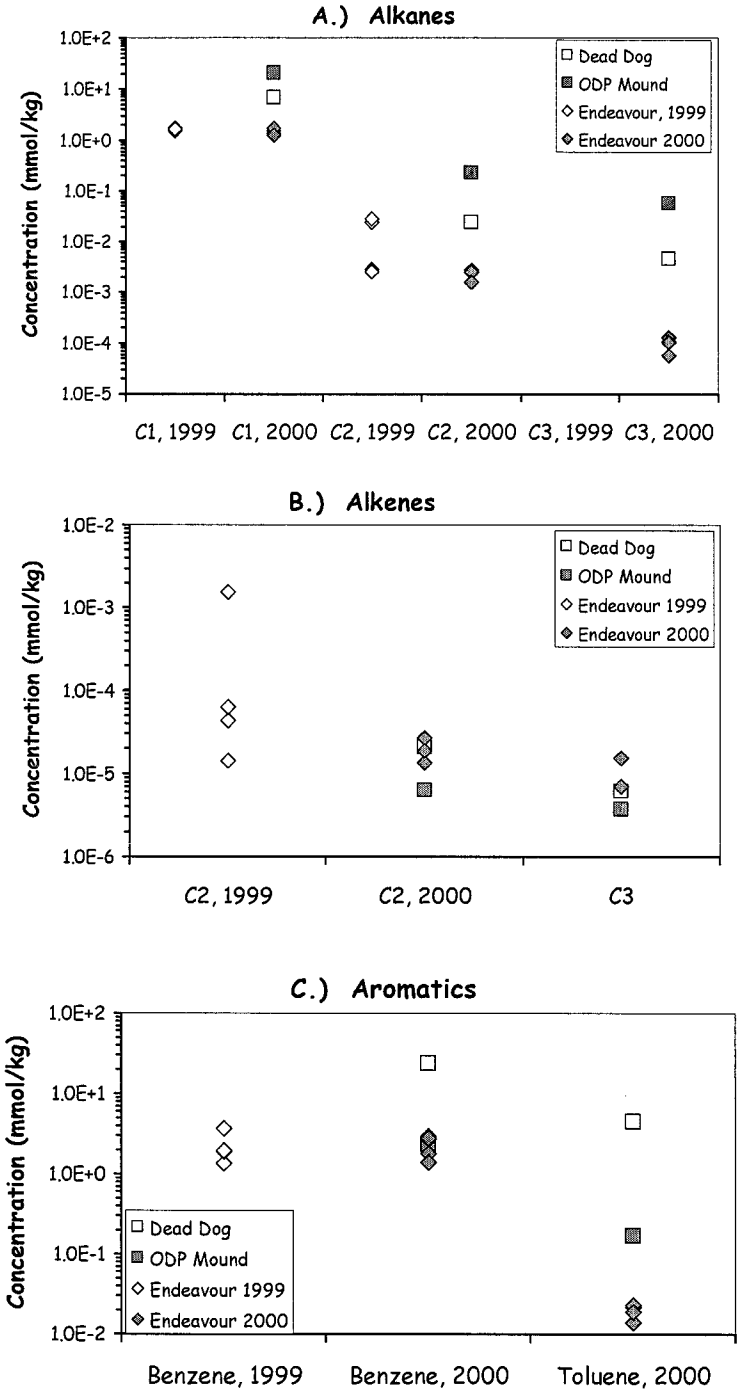

Figure 5-2. Endmember concentrations of **(A)** alkanes, **(B)** alkenes and **(C)** aromatics in Endeavour vent fluids. White diamonds are data from fluids collected in 1999; gray diamonds are data from fluids collected in 2000. For comparison, data from the Dead Dog (represented by Chowder Hill vent) and ODP Mound (represented by 1035H vent) fields, Middle Valley are shown in the white and gray squares, respectively. Middle Valley data from Chapter 3 of this thesis.

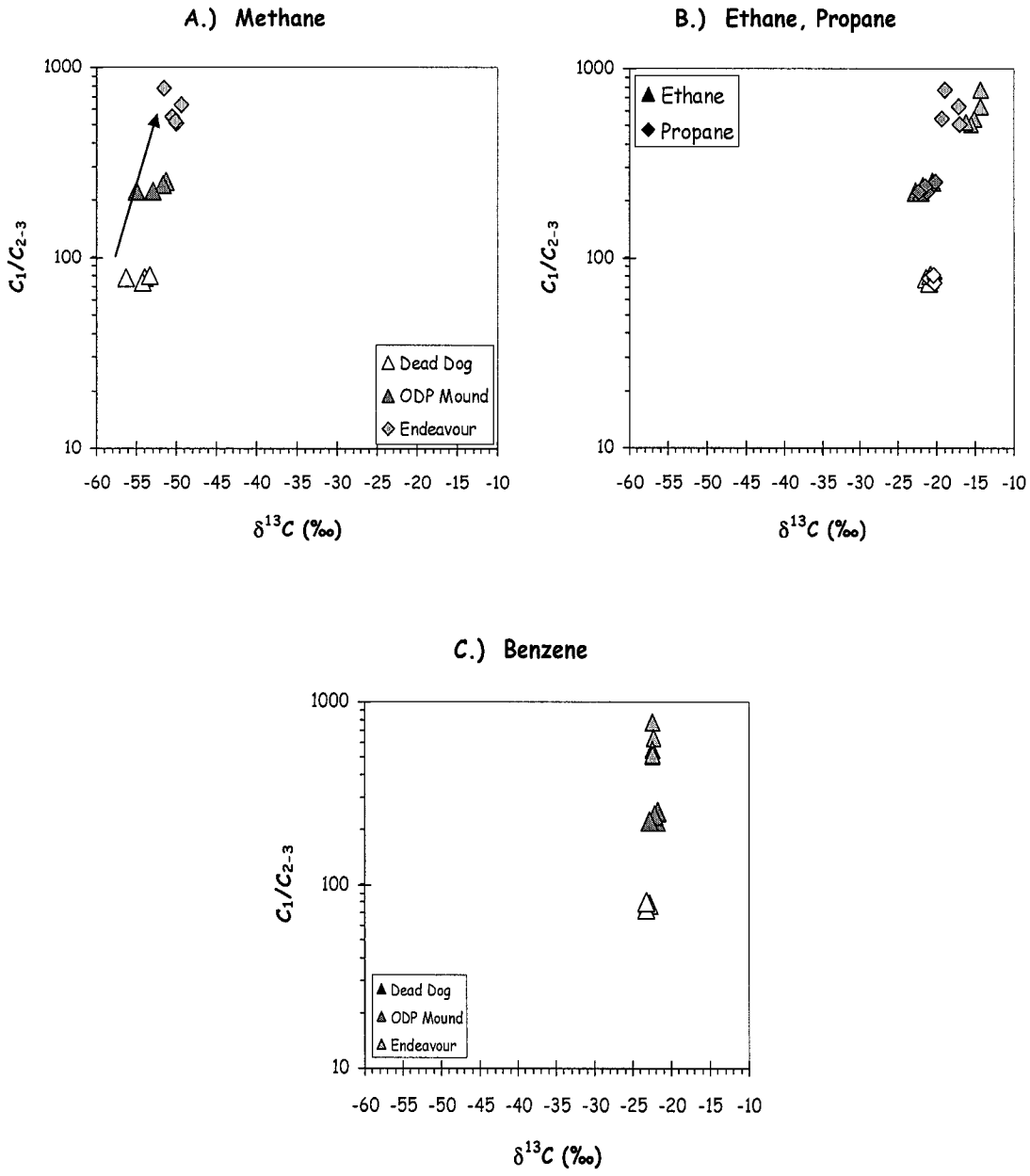

Figure 5-3. $C_1/(C_2+C_3)$ versus $\delta^{13}C$ for **(A)** methane; **(B)** ethane and propane; and **(C)** benzene. The arrow on Figure 5-3A indicates the proposed trend for increasing alteration of aqueous organic compounds in high heat flow environments.

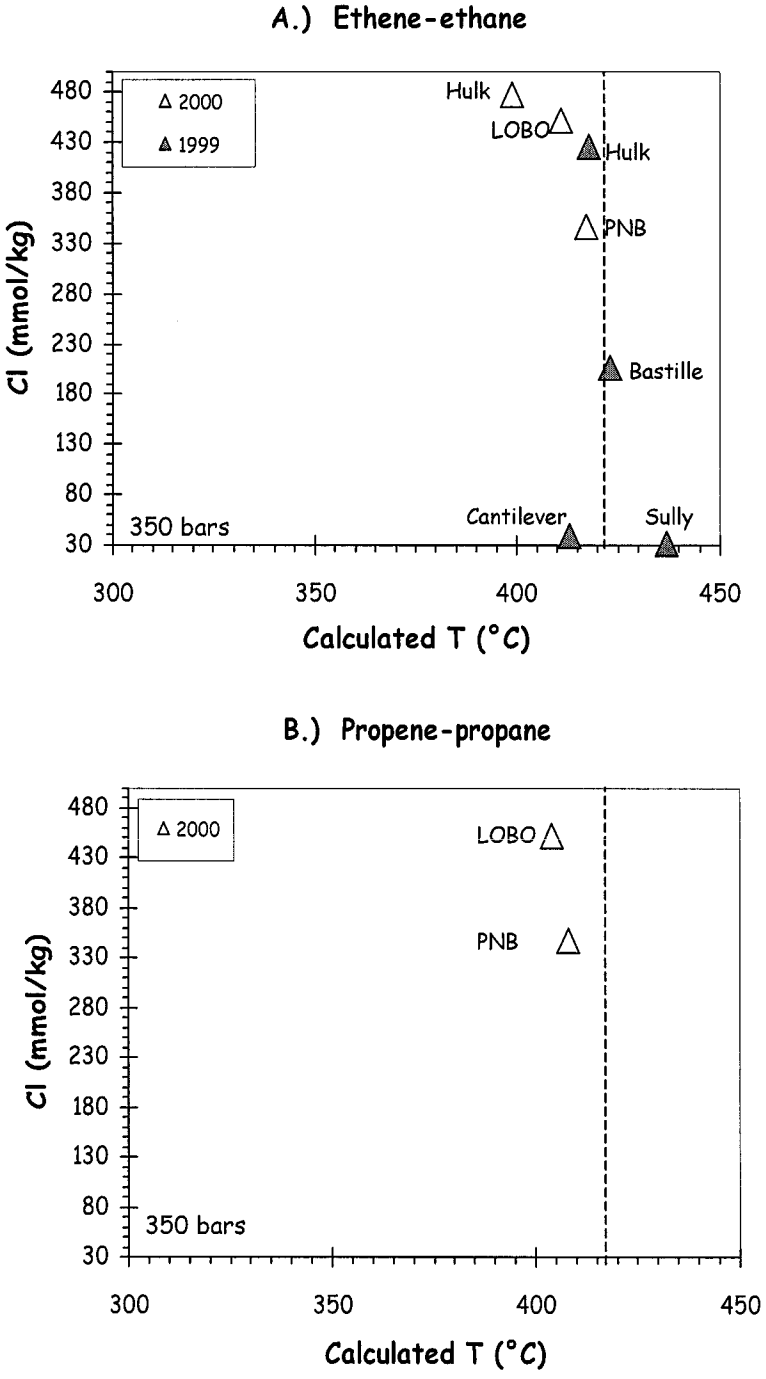

Figure 5-4. Temperatures calculated for Endeavour vents assuming equilbration of ethane-ethene (diamonds) and propane-propene (triangles) at assumed suburface reaction zone pressures of 350 bars using thermodynamic data from the SUPCRT92 database (Johnson et al., 1992). Two-phase boundary for seawater at 422°C, 350 bars is shown in the dotted line (Bischoff and Rosenbauer , 1985).

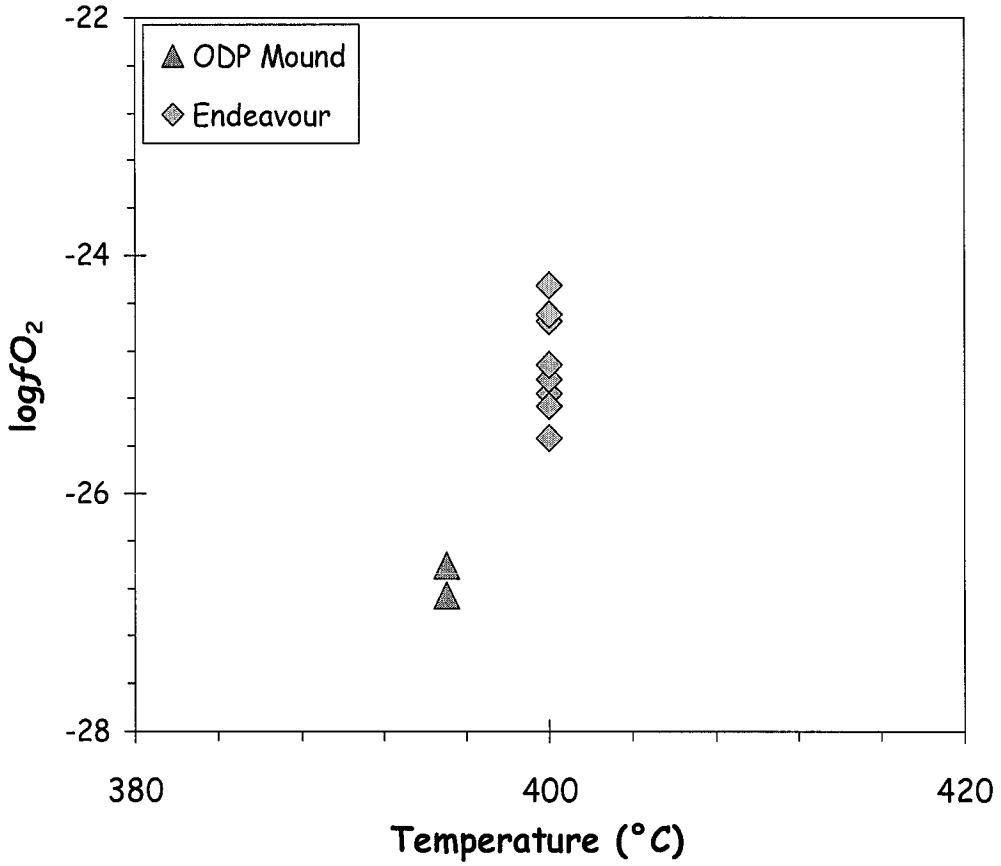

Figure 5-5. Calculated $\log fO_2$ based on the H_2O-H_2 redox couple for assumed subsurface reaction zone conditions of 395°C, 280 bars (ODP Mound field) and 350 bars, 400°C (Endeavour field). Thermodynamic data requisite for the construction of this diagram are from the SUPCRT92 database (Johnson et al., 1992)

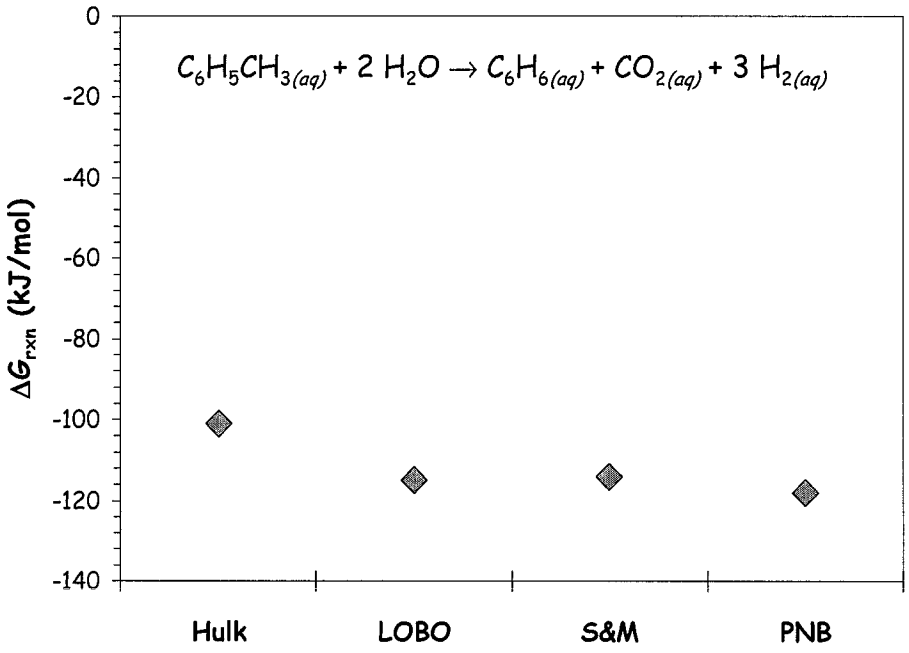

Figure 5-6. ΔG_{rxn} for conversion of toluene to benzene via a decarboxylation reaction at estimated reaction zone conditions. Thermodynamic data requisite to the construction of these diagrams from the SUPCRT92 database (Johnson et al., 1992).

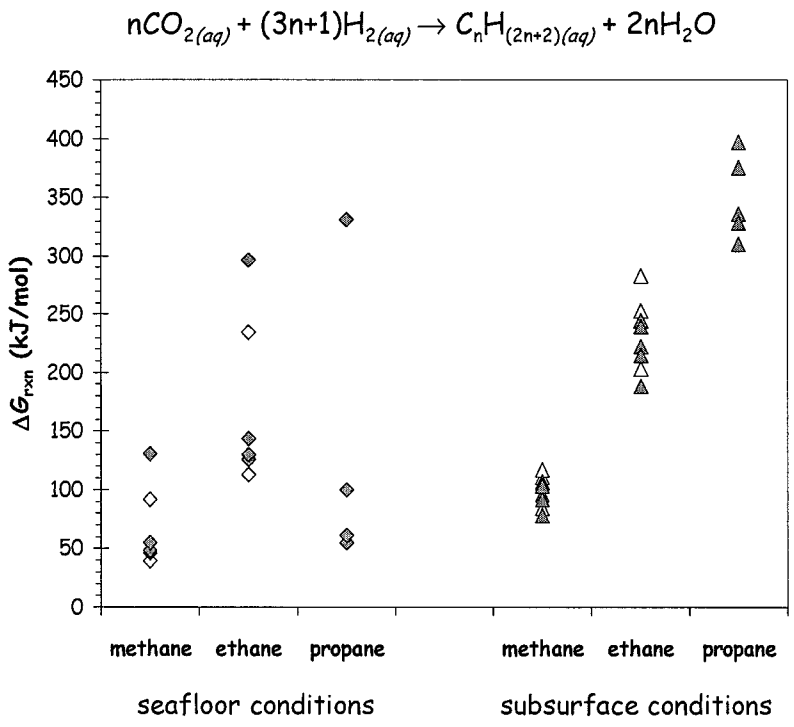

Figure 5-7. ΔG_{rxn} for the abiotic formation of C_1-C_3 alkanes from CO_2 in Endeavour vent fluids (Reactions 9-11, see text). In all cases, the ΔG_{rxn} is positive, indicating that there is no drive for the abiotic formation of alkanes from carbon dioxide, consistent with the hypothesis that organic compounds reflect the interaction of Endeavour fluids with an organic carbon-bearing sedimentary source. Thermodynamic data requisite to the construction of this figure is from the SUPCRT92 database (Johnson et al., 1992).

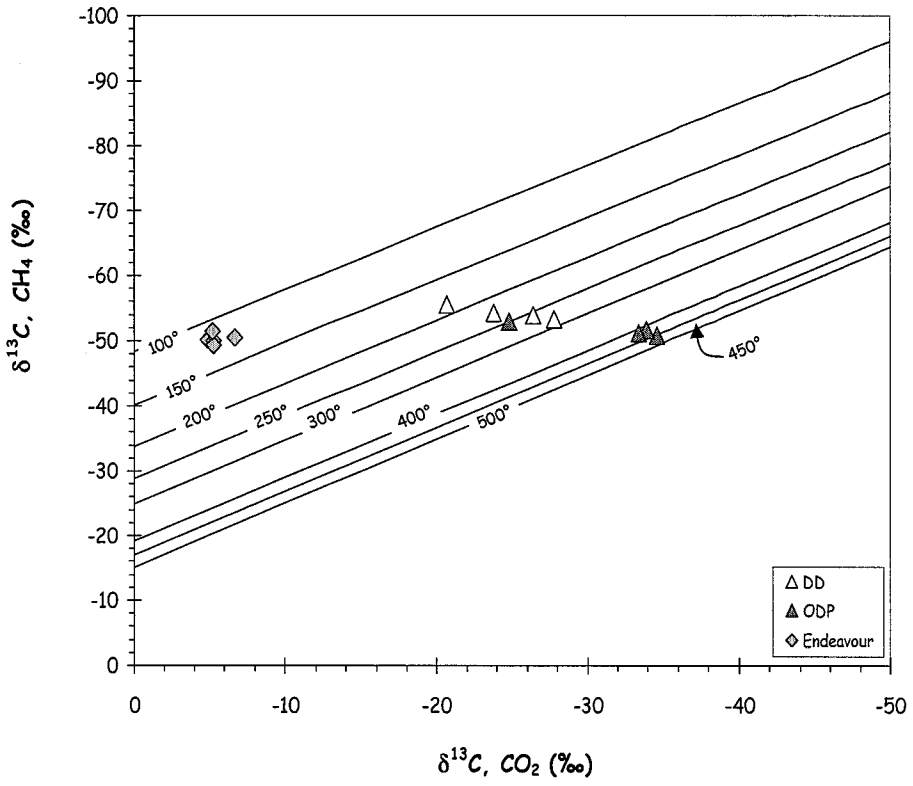

Figure 5-8. Isotopic composition of CO_2 and CH_4 in MEF (gray diamonds) and Middle Valley (Dead Dog field: white triangles; ODP Mound field: gray triangles) vent fluids shown with calculated equilibrium isotopic compositions at 100 to 500°C based on Horita (2001).

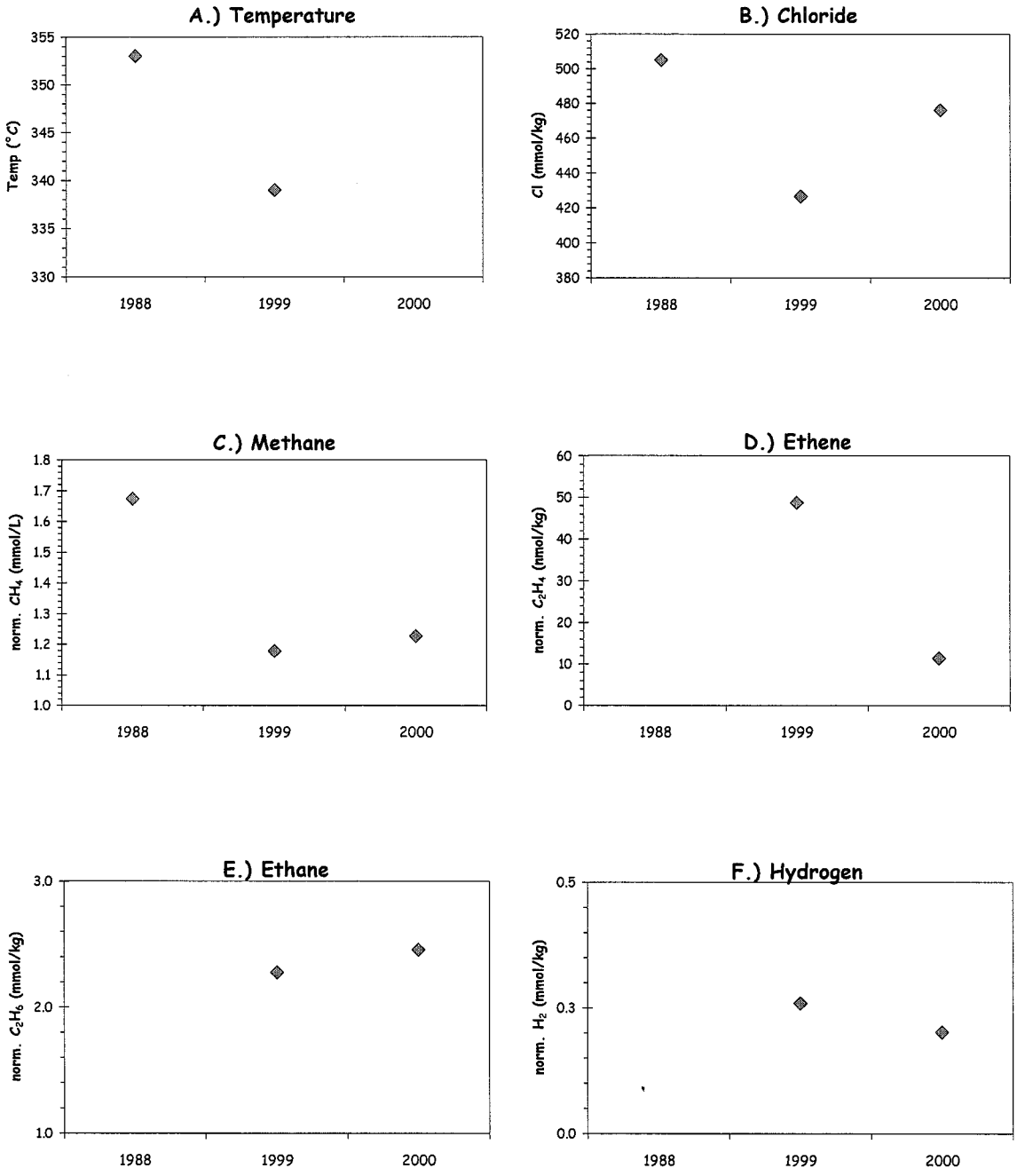

Figure 5-9. Temporal variability of **(A)** temperature, and endmember concentrations of **(B)** Cl, **(C)** methane, **(D)** ethene, **(E)** ethane **(F)** hydrogen, **(G)** benzene and **(H)** ammonia in Hulk vent. To remove the effects of phase separation, concentrations were normalized to seawater chlorinity (543 mmol/kg).

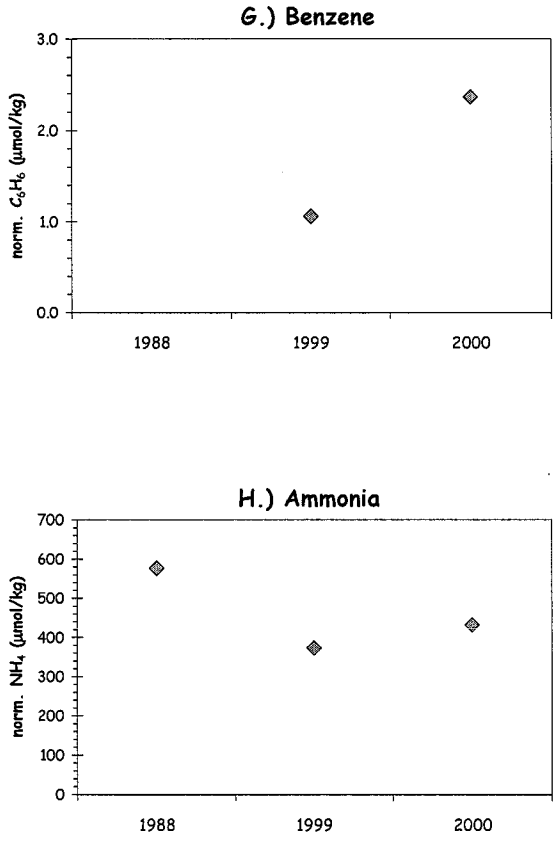

Figure 5-9, continued.

5.6. REFERENCES

BERNDT M. E., ALLEN D. E., and SEYFRIED W. E., JR. (1996) Reduction of CO_2 during serpentinization of olivine at 300°C and 500 bar. *Geology* **24**, 351-354.

BISCHOFF J. L. and DICKSON F. W. (1975) Seawater-basalt interaction at 200°C and 500 bars: Implications for the origin of sea-floor heavy-metal deposits and the regulation of seawater chemistry. *Earth Planet. Sci. Lett.* **25**, 385-397.

BOHNENSTIEHL D. W. R., DZIAK R. P., FOX C. G., and SMITH D. K. (2001) The June 1999 Endeavour earthquake sequence: evidence for a non-tectonic origin. *Eos* **82**, F856.

BOTZ R., WINCKLER G., BAYER R., SCHMITT M., SCHMIDT M., GARBE-SCHÖNBERG D., STOFFERS P., and KRISTJANSSON J. K. (1999) Origin of trace gases in submarine hydrothermal vents of the Kolbeinsey Ridge, north Iceland. *Earth Planet. Sci. Lett.* **171**, 83-93.

BUTTERFIELD D. A. (2000) Deep Ocean Hydrothermal Vents. In *Encyclopedia of Volcanoes* (ed. H. Sigurdsson, B. F. Houghton, S. R. McNutt, H. Rymer, and J. Stix), pp. 857-875. Academic Press.

BUTTERFIELD D. A., MCDUFF R. E., MOTTL M. J., LILLEY M. D., LUPTON J. E., and MASSOTH G. J. (1994) Gradients in the composition of hydrothermal fluids from the Endeavour segment vent field: Phase separation and brine loss. *J. Geophys. Res.* **99**, 9561-9583.

CHARLOU J. L., DONVAL J. P., DOUVILLE E., JEAN-BAPTISTE P., RADFORD-KNOERY J., FOUQUET Y., DAPOIGNY A., and STIEVENARD M. (2000) Compared geochemical signatures and the evolution of Menez Gwen (37°50'N) and Lucky Strike (37°17'N) hydrothermal fluids, south of the Azores triple junction on the Mid-Atlantic Ridge. *Chem. Geol.* **171**, 49-75.

CHARLOU J. L., FOUQUET Y., DONVAL J. P., and AUZENDE J. M. (1996) Mineral and gas chemistry of hydrothermal fluids on an ultrafast spreading ridge: East Pacific Rise, 17° to 19°S (Naudur cruise, 1993) phase separation processes controlled by volcanic and tectonic activity. *J. Geophys. Res.* **101**, 15889-15919.

COOK T. L. and STAKES D. S. (1995) Biogeological mineralization in deep-sea hydrothermal deposits. *Science* **267**, 1975-1979.

CORLISS J. B., DYMOND J., GORDON L. I., EDMOND J. M., VON HERZEN R. P., BALLARD R. D., GREEN K., WILLIAMS D., BAINBRIDGE A., CRANE K., and VAN ANDEL T. H. (1979) Submarine thermal springs on the Galapagos Rift. *Science* **203**, 1073-1083.

CRUSE A. M. and SEEWALD J. S. (2001) Metal mobility in sediment-covered ridge-crest hydrothermal systems: Experimental and theoretical constraints. *Geochim. Cosmochim. Acta* **65**, 3233-3247.

CUDRAK C. F. and CLOWES R. M. (1993) Crustal structure of Endevour Ridge Segment, Juan de Fuca Ridge, from a detailed seismic refraction survey. *J. Geophys. Res.* **98**, 6329-6349.

DELANEY J. R., ROBIGOU V., MCDUFF R. E., and TIVEY M. K. (1992) Geology of a vigorous hydrothermal system on the Endeavour Segment, Juan de Fuca Ridge. *J. Geophys. Res.* **97**, 19,663-19, 682.

DISNAR J. R. and SUREAU J. F. (1990) Organic matter in ore genesis: Progress and perspectives. *Org. Geochem.* **16**, 577-599.

DONVAL J. P. and AL. E. (1997) High H_2 and CH_4 content in hydrothermal fluids from Rainbow site newly sampled at 36°14' on the AMAR segment, Mid-Atlantic Rigde (diving FLORES cruise, July 1997). Comparison with other MAR sites. *Eos* **78**, 832.

EDMOND J. M., MASSOTH G., and LILLEY M. D. (1992) Submersible-deployed samplers for axial vent waters. *RIDGE Events* **3**, 23-24.

ELDERFIELD H. and SCHULTZ A. (1996) Mid-ocean ridge hydrothermal fluxes and the chemical composition of the ocean. *Ann. Rev. Earth Planet. Sci.* **24**, 191-224.

EVANS W. C., WHITE L. D., and RAPP J. B. (1988) Geochemistry of some gases in hydrothermal fluids from the southern Juan de Fuca Ridge. *J. Geophys. Res.* **93**, 15,305-15,313.

GOODFELLOW W. D. and PETER J. M. (1994) Geochemistry of hydrothermally altered sediment, Middle Valley, northern Juan de Fuca Ridge. In *Proc. ODP, Sci. Results* **139** (ed. M. J. Mottl, E. E. Davis, A. T. Fisher, and J. F. Slack), pp. 207-289.

HANNINGTON M., HERZIG P., SCHOLTEN J., BOTZ R., GARBE-SCHÖNBERG D., JONASSON I. R., ROEST W., and SHIPBOARD SCIENTIFIC PARTY. (2001) First observations of high-temperature submarine hydrothermal vents and massive anhydrite deposits off the north coast of Iceland. *Mar. Geol.* **177**, 199-220.

HESSLER R. R. and KAHARL V. A. (1995) The deep-sea hydrothermal vent community: An overview. In *Seafloor Hydrothermal Systems: Physical, Chemical, Biological, and Geological Interactions*, Geophysical Monograph **91** (ed. S. E. Humphris, R. A. Zierenberg, L. S. Mullineaux, and R. E. Thomson), pp. 72-84.

HOLM N. G. and CHARLOU J. L. (2001) Initial indications of abiotic formation of hydrocarbons in the Rainbow ultramafic hydrothermal system, Mid-Atlantic Ridge. *Earth Planet. Sci. Lett.* **191**, 1-8.

HORITA J. (2001) Carbon isotope exchange in the system CO2-CH4 at elevated temperatures. *Geochim. Cosmochim. Acta* **65**, 1907-1919.

HUNT J. M. (1996) *Petroleum Geochemistry and Geochemistry*. W. H. Freeman.

JAMES A. T. (1983) Correlation of natural gas by use of a carbon isotopic distribution between hydrocarbon components. *AAPG Bull.* **67**, 1176-1191.

JAMES R. H., ELDERFIELD H., and PALMER M. R. (1995) The chemistry of hydrothermal fluids from the Broken Spur site, 29°N Mid-Atlantic Ridge. *Geochim. Cosmochim. Acta* **59**, 651-659.

JEAN-BAPTISTE P., CHARLOU J. L., STIEVENARD M., DONVAL J. P., BOUGAULT H., and MEVEL C. (1991) Helium and methane measurements in hydrothermal fluids from the mid-Atlantic ridge: the Snake Pit site at 23°N. *Earth Planet. Sci. Lett.* **106**, 17-28.

JOHNSON H. P., HUTNAK M., DZIAK R., FOX C. G., URCUYO I., COWEN J. P., NABELEK J., and FISHER C. (2000) Earthquake-induced changes in a hydrothermal system on the Juan de Fuca mid-ocean ridge. *Nature* **407**, 174-177.

JOHNSON J. W., OELKERS E. H., and HELGESON H. C. (1992) SUPCRT92: A software package for calculating the standard molal thermodynamic properties of minerals, gases, aqueous species, and reactions from 1 to 5000 bar and 0 to 1000°C. *Comput. Geosci.* **18**, 899-947.

KARSTEN J. L., HAMMOND S. R., DAVIS E. E., and CURRIE R. (1986) Detailed morphology and neotectonics of the Endeavour segment, Northern Juan de Fuca Ridge: New results from Seabeam swath mapping. *Geol. Soc. Am. Bull.* **97**, 213-221.

KELLEY D. S., DELANEY J. R., LILLEY M. D., BUTTERFIELD D. A., and ROBIGOU V. (2001a) Vent field distribution and evolution along the Endeavour Segment, Juan de Fuca Ridge. *Eos* **82**, F612.

KELLEY D. S., KARSON J. A., BLACKMAN D. A., FRÜH-GREEN G. L., BUTTERFIELD D. A., LILLEY M. D., OLSON E. J., SCHRENK M. O., ROE K. K., LEBON G. T., RIVIZZIGNO P., and AT3-60 SHIPBOARD PARTY. (2001b) An off-axis hydrothermal vent field near the Mid-Atlantic Ridge at 30°N. *Nature* **412**, 145-149.

KIM K.-R., WELHAN J. A., and CRAIG H. (1984) The hydrothermal vent fields at 13°N and 11°N on the East Pacific Rise: *Alvin* 1984 results. *Eos* **65**, 973.

KINGSTON M. J. and DELANEY J. R. (1983) Sulfide deposits from the Endeavour Segment of the Juan de Fuca Ridge; comparison with other seafloor occurrences. *Eos* **64**, 723.

KROOPNICK P. M. (1985) The distribution of ^{13}C of ΣCO_2 in the world oceans. *Deep-Sea Res.* **32**, 57-84.

LILLEY M. D., BAROSS J. A., and GORDON L. I. (1983) Reduced gases and bacteria in hydrothermal fluids: The Galapagos spreading center and 21°N East Pacific Rise. In *Hydrothermal Processes at Seafloor Spreading Centers* (ed. P. A. Rona, K. Boström, L. Laubier, and K. L. Smith), pp. 411-449. Plenum.

LILLEY M. D., BUTTERFIELD D. A., OLSON E. J., LUPTON J. E., MACKO S. A., and MCDUFF R. E. (1993) Anomalous CH_4 and NH_4^+ concentrations at an unsedimented mid-ocean-ridge hydrothermal system. *Nature* **364**, 45-47.

MANGO F. D. (1997) The light hydrocarbons in petroluem: A critical review. *Org. Geochem.* **26**, 417-440.

MCCOLLOM T. M. and SEEWALD J. S. (2001) A reassessment of the potential for reduction of dissolved CO2 to hydrocarbons during serpentinization of olivine. *Geochim. Cosmochim. Acta* **65**, 3769-3778.

MCCOLLOM T. M., SEEWALD J. S., and SIMONEIT B. R. T. (2001) Reactivity of monocyclic aromatic compounds under hydrothermal conditions. *Geochim. Cosmochim. Acta* **65**, 455-468.

MERLIVAT L., PINEAU F., and JAVOY M. (1987) Hydrothermal vent waters at 13°N on the East Pacific Rise: Isotopic composition and gas concentration. *Earth Planet. Sci. Lett.* **84**, 100-108.

MICHARD G., ALBARÈDE F., MICHARD A., MINSTER J.-F., CHARLOU J.-L., and TAN N. (1984) Chemistry of solutions from the 13°N East Pacific Rise hydrothermal site. *Earth Planet. Sci. Lett.* **67**, 297-307.

MOTTL M. J. and HOLLAND H. D. (1978) Chemical exchange during hydrothermal alteration of basalt by seawater-I. Experimental results for major and minor components of seawater. *Geochim. Cosmochim. Acta* **42**, 1103-1115.

ROHR K. M. M. (1994) Increase of seismic velocities in upper oceanic crust and hydrothermal circulation in the Juan de Fuca plate. *Geophys. Res. Lett.* **21**, 2163-2166.

ROHR K. M. M., MILKEREIT B., and YORATH C. J. (1988) Asymmetric deep crustal structure across the Juan de Fuca Ridge. *Geology* **16**, 533-537.

SANSONE F. J., MOTTL M. J., OLSON E. J., WHEAT C. G., and LILLEY M. D. (1998) CO2-depleted fluids from mid-ocean ridge-flank hydrothermal springs. *Geochim. Cosmochim. Acta* **62**, 2247-2252.

SEEWALD J. S. (1994) Evidence for metastable equilibrium between hydrocarbons under hydrothermal conditions. *Nature* **370**, 285-287.

SEEWALD J. S. (1997) Mineral redox buffers and the stability of organic compounds under hydrothermal conditions. In *Aqueous Chemistry and Geochemistry of Oxides, Oxyhydroxides, and Related Materials*, Materials Research Society Symposium Proceedings **432** (ed. J. A. Voight, T. E. Wood, B. E. Bunker, W. H. Casey, and L. J. Crossey), pp. 317-331.

SEEWALD J. S. (2001) Aqueous geochemistry of low molecular weight hydrocarbons at elevated temperatures and pressures: Constraints from mineral buffered laboratory experiments. *Geochim. Cosmochim. Acta* **65**, 1641-1664.

SEEWALD J. S., CRUSE A. M., LILLEY M. D., and OLSON E. J. (1998) Hot-spring fluid chemistry at Guaymas Basin, Gulf of California: Temporal variations and volatile content. *Eos* **79**, F47.

SEEWALD J. S., CRUSE A. M., and SACCOCIA P. (2002a) Aqeous volatiles in hydrothermal fluids from the Main Endeavour Field, northern Juan de Fuca Ridge: Temporal variability following earthquake activity. *submitted to Earth and Planetary Science Letters.*

SEEWALD J. S., DOHERTY K. W., HAMMAR T. R., and LIBERATORE S. P. (2002b) A new gas-tight isobaric sampler for hydrothermal fluids. *Deep-Sea Res. I* **49**.

SEYFRIED W. E., JR. and BISCHOFF J. L. (1981) Experimental seawater-basalt interaction at 300°C, 500 bars: Chemical exchange, secondary mineral formation and implications for the transport of heavy metals. *Geochimica et Cosmochimica Acta* **45**, 135-149.

SEYFRIED W. E., JR., SEEWALD J. S., BERNDT M. E., DING K., and FOUSTOUKOS D. (2002) Chemistry of hydrothermal vent fluids from the Main Endeavour Field, Northern Juan de Fuca Ridge: Geochemical controls in the aftermath of June 1999 seismic events. *submitted to Journal of Geophysical Research.*

SHANKS W. C., III. (2001) Stable isotope systematics in seafloor hydrothermal systems: Vent fluids, hydrothermal deposits, hydrothermal alteration, and microbial

processes. In *Stable Isotope Geochemistry* (ed. J. W. Valley and D. R. Cole), pp. 469-525.

SHANKS W. C., III, BÖHLKE J. K., and SEAL R. R., II. (1995) Stable isotopes in mid-ocean ridge hyerothermal systems: Interactions between fluids, minerals and organisms. In *Seafloor Hydrothermal Systems: Physical, Chemical, Biological, and Geological Interactions*, Geophysical Monograph **91** (ed. S. E. Humphris, R. A. Zierenberg, L. S. Mullineaux, and R. E. Thomson), pp. 194-221.

SHERWOOD LOLLAR B., FRAPE S. K., WEISE S. M., FRITZ P., MACKO S. A., and WELHAN J. A. (1993) Abiogenic methanogenesis in crystalline rocks. *Geochim. Cosmochim. Acta* **57**, 5087-5097.

SHOCK E. (1990) Geochemical constraints on the origin of organic compounds in hydrothermal systems. *Origins of Life and the Evolution of the Biosphere* **25**, 119-140.

SHOCK E. L. and SCHULTE M. D. (1998) Organic synthesis during fluid mixing in hydrothermal systems. *J. Geophys. Res.* **103**, 28,513-28,527.

TISSOT B. and WELTE D. H. (1984) *Petroleum Formation and Occurrence*. Verlag.

TIVEY M. K. and DELANEY J. R. (1985) Sulfide deposits from the Endeavour Segment of the Juan de Fuca Ridge. *Marine Mining* **5**, 165-179.

TIVEY M. K. and DELANEY J. R. (1986) Growth of large sulfide structures on the Endeavour segment of the Juan de Fuca Ridge. *Earth Planet. Sci. Lett.* **77**, 303-317.

TIVEY M. K., STAKES D. S., COOK T. L., HANNINGTON M. D., and PETERSON S. (1999) A model for growth of steep-sided vent structures on the Endeavour Segment of the Juan de Fuca Ridge: Results of a petrologic and geochemical study. *J. Geophys. Res.* **104**, 22,859-22,883.

VOLPE A. M. and GOLDSTEIN S. J. (1990) Dating young MORB: ^{226}Ra-^{230}Th isotopic disequlibria measured by mass spectrometry. *Eos* **71**, 1702.

VON DAMM K. L. (1983) Chemistry of Submarine Hydrothermal Solutions at 21°N, East Pacific Rise and Guaymas Basin, Gulf of California. PhD., MIT/WHOI, WHOI-84-3. 240 p.

VON DAMM K. L. (1995) Controls on the chemistry and temporal variability of seafloor hydrothermal fluids. In *Seafloor Hydrothermal Systems: Physical, Chemical, Biological, and Geological Interactions*, Geophysical Monograph **91** (ed. S. E. Humphris, R. A. Zierenberg, L. S. Mullineaux, and R. E. Thomson), pp. 222-247.

VON DAMM K. L. and BISCHOFF J. L. (1987) Chemistry of hydrothermal solutions from the southern Juan de Fuca Ridge. *J. Geophys. Res.* **92**, 11,334-11,346.

VON DAMM K. L., EDMOND J. M., GRANT B., MEASURES C. I., WALDEN B., and WEISS R. F. (1985a) Chemistry of submarine hydrothermal solutions at 21°N, East Pacific Rise. *Geochim. Cosmochim. Acta* **49**, 2197-2220.

VON DAMM K. L., EDMOND J. M., MEASURES C. I., and GRANT B. (1985b) Chemistry of submarine hydrothermal solutions at Guaymas Basin, Gulf of California. *Geochim. Cosmochim. Acta* **49**, 2221-2237.

WAPLES D. W. (1984) Thermal models for oil generation. In *Advances in Petroleum Geochemistry* **1** (ed. J. Brooks and D. Welte), pp. 7-67.

WELHAN J. A. and CRAIG H. (1983) Methane, hydrogen and helium in hydrothermal fluids at 21°N on the East Pacific Rise. In *Hydrothermal Processes at Seafloor Spreading Centers* (ed. P. A. Rona, K. Boström, and L. Laubier), pp. 391-409. Plenum.

WHITE D. J. and CLOWES R. M. (1990) Shallow crustal structure beneath the Juan de Fuca Ridge from 2-D seismic refraction tomography. *Geophys. J. Int.* **100**, 349-367.

YOU C.-F., BUTTERFIELD D. A., SPIVACK A. J., GIESKES J. M., GAMO T., and CAMPBELL A. J. (1994) Boron and halide systematics in submarine hydrothermal systems: Effects of phase separation and sedimentary contributions. *Earth Planet. Sci. Lett.* **123**, 227-238.

ZHANG Q.-L. and WEN-JUN L. (1990) A calibrated measurement of the atomic weight of carbon. *Chinese Sci. Bull.* **35**, 290-296.

CHAPTER 6. CONCLUSIONS AND FUTURE WORK

6.1. GENERAL CONCLUSIONS

This thesis has constrained the abundance and distribution of a small number of organic compounds (saturated and unsaturated hydrocarbons, and aromatic compounds) in vent fluids from the northern Juan de Fuca Ridge. However, analysis of even this small number of compounds have provided powerful insights into the processes occurring in subsurface reaction zones at mid-ocean ridges. Secondary alteration processes within hydrothermal vent fluids reflect the influence of time and temperature on reaction kinetics. In some cases, reactions proceed at fast enough rates so that metastable equilibrium is attained in natural systems (e.g., alkane-alkene pairs). In others, kinetic barriers preclude the attainment of equilibrium, but hotter temperatures or longer reaction times in different environments cause greater extents of reaction progress (e.g., the differences in benzene-toluene ratios between the two Middle Valley vent fields). Equally important, a comparison of the organic geochemistry of fluids from Middle Valley and the Main Endeavour field (MEF) indicate that the redox state of the system also influences rate at which reactions can proceed and therefore the observed distributions of organic compounds. ODP Mound field, Middle Valley and the MEF differ in the relative distributions of organic compounds not necessarily because of hotter conditions at the MEF, as one might predict form the differences in measured exit temperatures, but because of differences in the redox state in the subsurface. Subsurface conditions at the MEF are more oxidizing, because of the regulation of fluid chemistry by basaltic rocks. In contrast, the presence of greater amounts of sediment-derived organic compounds in the ODP Mound fluids leads to more reducing conditions.

Vent fluids from Middle Valley indicate that both the inorganic chemistry of the fluid itself and the sulfide mineralogy of the overlying deposit are affected by the presence of aqueous organic compounds. That such a control is observed in these fluids when the organic compounds were derived from the alteration of relatively organic-lean sediment indicates that the potential role of organic compounds should not continue to be overlooked. This is especially true for places such as Guaymas Basin, where the

sediment overlying the ridge axis with which vent fluids interact contains up four to five times greater amounts of organic carbon than the Middle Valley sediments.

6.2. Future Work

This work, however, represents only the tip of the iceberg: there remain many other classes of compounds to be explored. For example, Seewald (2001) demonstrated that organic acids are derived from oxidation of hydrocarbons and produce specific distributions based on the initial hydrocarbon composition. The abundances of organic acids in these, and other vent fluids, may then provide insight into the ultimate source of the aqueous organic compounds (i.e., sedimentary kerogen versus dissolved organic matter). The analysis of organic acids in hydrothermal vent fluids and reaction intermediaries in their production could also be utilized as proxies for subsurface reaction zone redox conditions, complimenting the Fe/Cu proxy of Seyfried and Ding(1993).

Little is known about the reaction mechanisms by which organosulfur compounds are formed at elevated temperatures. Organosulfur compounds (OSC) have been proposed as important agents in ore deposition because the formation of metal-OSC complexes allows transport of both metals and reduced sulfur in a single fluid (Giordano, 1994). Given the high concentrations of other organic compounds in fluids from Middle Valley, and reducing conditions that should favor OSC stability, it is likely that the OSC's will also be found in high concentrations. The presence of such compounds may play a role in the transport of ore-forming metals by hydrothermal fluids—especially in fluids of low chlorinity. Middle Valley and the Main Endeavour Field represent ideal locations to investigate the role of such compounds in crustal alteration processes.

Additional analyses on Middle Valley vent fluids could provide answers to the questions that remain unanswered. For example, with this dataset, it is not possible to unequivocally differentiate between sedimentary kerogen and dissolved organic matter entrained from porewaters/bottom ocean water as the source of the low-molecular weight hydrocarbons analyzed in this thesis. However, analyses focusing on longer-chained alkanes and other diagnostic biomarkers could potentially distinguish between these

sources. An investigation of bulk dissolved organic carbon concentrations in hydrothermal fluids could also provide an important framework within which to investigate the high-temperature alteration reactions that control the distributions of organic compounds in hydrothermal vent fluids. At this point, limitations in sampler technology combined with the volatile and semi-volatile nature of many organic compounds, preclude an accurate measurement of bulk DOC concentrations. However, with such information, systems such as Middle Valley, where the sediments experience a high thermal gradient, could serve as natural laboratories at which to study the processes that control the formation of petroleum or natural gas accumulations.

The large changes in H_2 and H_2S concentrations observed in Spire vent fluids as compared to 1035H vent fluids at the ODP Mound field should also be accompanied by changes in the concentrations of transition metals. Analyses of transition metal concentrations are also required to determine if the presence of organic compounds in hydrothermal vent fluids affect metal concentrations as was observed in the laboratory experiments presented in Chapter 2. Based on temperature constraints alone, one would predict that the transition metal concentrations from Middle Valley fluids should be less than that observed at the MEF. However, if organic compounds are serving as ligands—especially in the ODP Mound fluids that have chloride concentrations that are less than seawater values—then metal concentrations from the ODP Mound field may exceed those in the MEF fluids.

Experimental work will also provide additional insight into the processes occurring in hydrothermal vent systems. For example, Horita (2001) achieved isotopic equilibrium between CO_2 and CH_4 by using Ni as a catalyst. The attainment of isotopic equilibrium between these compounds at Middle Valley might have been catalyzed by the presence of transition metals in sulfide minerals or basaltic rocks. A laboratory investigation of the kinetics for isotopic equilibration using these materials as catalysts could provide constraints on residence times of fluids in both the Middle Valley subsurface reaction zones, where isotopic equilibration was achieved, and at the MEF, where isotopic equilibration was not attained.

Sampling of fluids from other mid-ocean ridge systems could provide further insight into a variety of other processes. For example, fluids from cool fluids 18-51°C venting at Co-Axial contain hyperthermophilic organisms with optimal growth temperatures >80°C (DELANEY et al., 1998). Measurements of the concentrations of metabolic products from these microbes in Co-Axial fluids would provide further verification of the presence of a subsurface biosphere. Also, investigations of the organic geochemistry of vents from bare-rock mid-ocean ridges that are unaffected by a sediment source in the subsurface, such as 21°N on the East Pacific Rise or TAG on the Mid-Atlantic Ridge, could provide insight into the abiotic formation of organic compounds that may have been precursor compounds for the origins of life on this and other planets. The work in this thesis represents an important first step in the study of the high-temperature geochemistry of organic compounds, which have great potential for enhancing our understanding of a range of processes occurring on Earth.

6.3. REFERENCES

DELANEY J. R., KELLEY D. S., LILLEY M. D., BUTTERFIELD D. A., BAROSS J. A., WILCOCK W. S. D., EMBLEY R. W., and SUMMIT M. (1998) The quantum event of oceanic crustal accretion: Impacts of diking at mid-ocean ridges. *Science* **281**, 222-230.

GIORDANO T. H. (1994) Metal transport in ore fluids by organic ligand complexes. In *Organic Acids in Geological Processs* (ed. E. D. Pittman and M. D. Lewan), pp. 319-354. Springer-Verlag.

HORITA J. (2001) Carbon isotope exchange in the system CO2-CH4 at elevated temperatures. *Geochim. Cosmochim. Acta* **65**, 1907-1919.

SEEWALD J. S. (2001) Model for the origin of carboxylic acids in basinal brines. *Geochim. Cosmochim. Acta* **65**, 3779-3789.

SEYFRIED W. E., JR. and DING K. (1993) The effect of redox on the relative mobilities of Cu and Fe in Cl bearing aqueous fluids at elevated temperatures and pressures: An experimental study with application to subseafloor hydrothermal systems. *Geochim. Cosmochim. Acta* **57**, 1905-1917.

APPENDIX 1. GC-IRMS ANALYSIS OF VENT FLUIDS

A new method utilizing purge-and-trap injection was developed to analyze aqueous low-molecular weight hydrocarbons and carbon dioxide in vent fluid samples. One concern in the analysis was the need to analyze very high concentrations of CO_2 and CH_4 and orders-of-magnitude lower concentrations of the C_2-C_6 hydrocarbons, benzene and toluene. This difficulty was overcome by analyzing the fluids using two different injection techniques: direct injections of very small amounts of gas for CO_2 and CH_4, followed by purge-and-trap injection of large volumes of headspace gas for the longer-chained hydrocarbons. The methods developed here can be applied to analysis of hydrocarbon gas samples that are dominated by methane, as well as for gas-chromatographic analysis of any other aqueous volatiles of interest.

In order to accomplish the analyses, the hydrothermal fluid and headspace gas was first be transferred from the glass, gas-tight, valved tube utilized to hold subsamples until the time of their analysis. A 100-mL gas-tight syringe was used as the secondary storage container during GC-IRMS analysis. The methods used to accomplish the transfer are detailed in Section 1. Section 2 contains the method for GC-IRMS analysis of CO_2 and CH_4 in small (< 1 mL) subsamples of headspace gas. Section 3 contains the method for analysis of large-volume samples of the remaining gas via a purge and trap method for C_2-C_7 hydrocarbons. Section 4 details the GC configuration.

SECTION 1. TRANSFER OF HYDROTHERMAL FLUID AND HEADSPACE GAS TO SECONDARY SYRINGE

A schematic of the subsample tube, syringe and valves used in the transfer are contained in Figure A-1 below.

1. Turn on He to prime/purge (P/P) valve #1. Open P/P #1 and #2 to ensure all lines are flushing with He.

2. Attach vacutainer tube to Swagelock fitting.

3. Attach 10 mL syringe. Flush syringe with He by pulling back and depressing plunger several times. Do this at a slow enough rate to ensure that atmosphere is not drawn into system. After flushing all air out, fill syringe with 10 mL He and close syringe valve.

4. Fill 100 mL with 3-5 mL 25% H_3PO_4. Pull back on plunger so that when syringe is horizontal, the level of the acid is below the opening. Attach syringe and rinse dead volume with He as with the 10 mL syringe, ensuring that the acid is not injected through the lines. When all air is flushed out with He, depress plunger as far as possible, keeping the level of the acid below the opening. Close the 100 mL syringe valve.

5. Close P/P #1. Wait momentarily to allow backpressure to diminish and slide Teflon sleeve over opening on vacutainer piston.

6. Depress vacutainer onto piston.

7. Open 100 mL syringe valve, and pull back on plunger as far as possible (>80 mL). This will create a sufficient vacuum to pull all fluid into the syringe. Keep plunger pulled back.

8. Wait 15 seconds. Close P/P #2.

9. Open 10 mL syringe valve. Transfer He to 100 mL syringe. Close 10 mL syringe valve.

10. Close 100 mL syringe valve. Allow plunger to settle to natural position. Remove 100 mL syringe from apparatus and place in ring stand in a vertical position.

11. Close vacutainer by pulling tube upwards so that the piston hole is external to the Swagelock fitting. Remove tube from system.

SECTION 2: CH_4/CO_2 ANALYSES VIA DIRECT INJECTION

1. Attach a septum to the end of the 100 mL syringe using a Hamilton female luer-tip septum adaptor and a male luer-lock to RN adaptor.

2. Start IRMS acquisition.

3. Remove appropriate aliquots from 100 mL syringe using the gas-tight SGE syringes with integral valve. Allow 60 sec. for gases to equilibrate between the two syringes before closing valves. Always close the SampleLock syringe before closing the SGE syringe valve to avoid damaging the SGE needle tip. Keep SampleLock valve closed unless taking a sample.

3. Introduce samples to the GC though injector, after IRMS software shows "Wait for GC Trigger" prompt. Hole finger over needle tip to avoid gas loss during transfer to injector.

4. Replace septum with each sample.

SECTION 3: C_2-C_7 HYDROCARBON ANALYSES VIA PURGE AND TRAP

1. Fill 5 mL SampleLock syringe with 3-5 mL of ~50% NaOH solution.

2. Attach NaOH-filled syringe to 100 mL syringe using appropriate RN-luer tip adaptors.

3. Add NaOH to 100 mL syringe.

4. Shake 100 mL syringe to ensure NaOH and fluid are well mixed.

5. Using a clean set of RN-luer tip adaptors, extract the remaining headspace gas into a clean 10 mL SampleLock syringe. Before use with another sample, clean 100 mL syringe, adaptors, 10 mL sample syringe with acid (25% H_3PO_4 or 10% HCl and Milli-Q water to ensure all traces of base are gone. If all base is not removed, subsequent CO_2 analyses will be compromised.

6. Attach the 10 mL syringe to the P/P valve on the 8-port sample selection valve (Fig. A-2). Open P/P valve to flush appropriate sample loop with He.

7. After loop is flushed, close P/P valve to stop He flow. Make sure P/P valve is not leaking by checking to make sure all flow has stopped into the vent water. If using a 5 or 10 mL sample loop, depress plunger slightly to ensure there is positive pressure in the sample syringe. Open SampleLock valve and inject the appropriate volume of gas. Close SampleLock valve.

8. Place LN_2 on chill loop. Check to make sure chill loop valve is in the LOAD position. Wait for LN_2 to stop boiling. Inject gas onto chill loop. Allow gas to purge onto chill loop for 1 minute per 1 mL of gas. After purge time, switch injection valve to INJECT.

9. Ensure GC oven is ready at –30°C. Ensure that the IRMS backflush valve is open. Set the column flow to 10 mL/min.

10. Close septum purge vent using a Swagelock nut or cap. Hit PREP RUN on GC keypad. Wait for PRE-RUN light to stop blinking.

11. Place chill loop in boiling water. Purge onto column head for 5 minutes.

12. After purge time is complete, switch chill loop valve back to LOAD. Set column flow rate to 2.0 mL/min. Open septum purge vent.

13. When column flow has stabilized, start IRMS acquisition program. Make sure the method selected is "alkanes".

SECTION 4: GC CONFIGURATION

Column: AT-Q, 30 m long
Injector: Gerstul PTV; set to 150°C in split mode for CO_2/CH_4 direct injection analyses; in splitless mode for purge and trap analyses.
Furnace: 940°C; 1 Pt, 1 Ni, 1 Cu wire
Temperature programs:
Direct injection for CO_2/CH_4:
Initial setpoint: 40°C. Hold for 4.5 minutes
Ramp 1: 75°C/min to 240°C. Hold for 5.84 minutes.
Standards: ~1 mL aliquots of 1% tanks; 10:1 split ratio; GC held isothermal at 40 or 50°C.
Purge and trap for C_2-C_7 hydrocarbons
Initial setpoint: -30°C during transfer onto column head. Hold for 0 minutes in GC method.
Ramp 1: 50°C/min to 40°C. Hold for 3 minutes.
Ramp 2: 10°C/min to 240°C. Hold for 2 minutes.
Standards: 100 uL of 1000 ppm n-alkane tank; splitless; purge and trap.

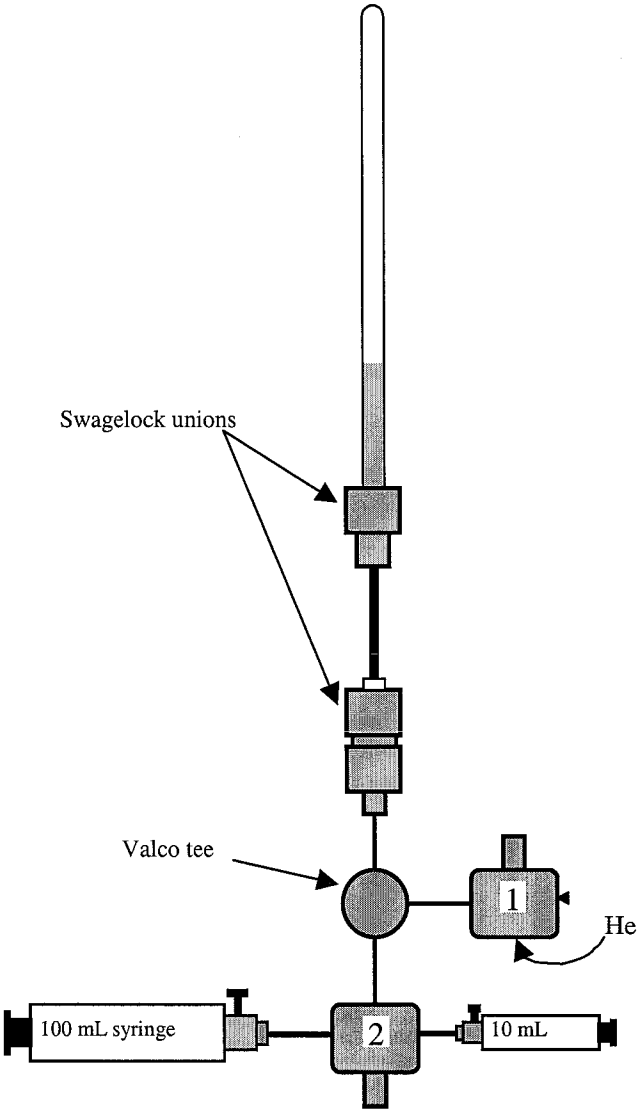

Figure A-1. Schematic of system used to transfer hydrothermal fluid and headspace gas from subsampling tube to 100 mL gas-tight syringe for GC-IRMS analysis.

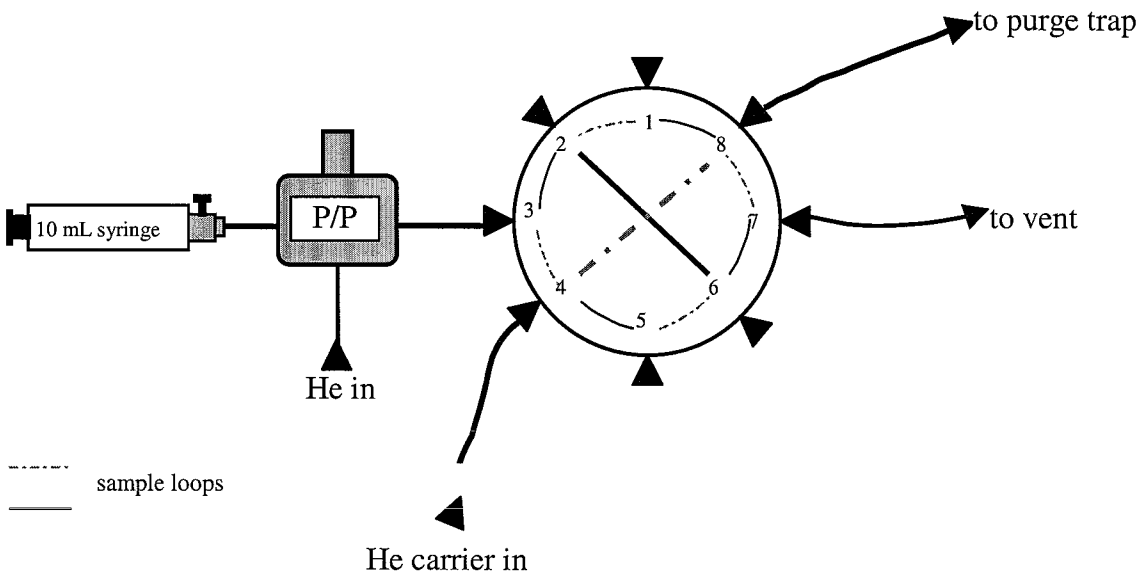

Figure A-2. Schematic diagram of 8-port valve used to send large volume samples (1-10 mL) of headspace gas to purge trap.